Root-zone Soil Moisture Redistribution in Cropping Systems under Freeze-Thaw Conditions

By

Frederick Cassian Kahimba

M.Sc. Eng. (WRE)

A Thesis submitted to the Faculty of Graduate Studies of
The University of Manitoba
In partial fulfilment of the requirements of the degree of

DOCTOR OF PHILOSOPHY

Department of Biosystems Engineering
University of Manitoba
Winnipeg, Manitoba, CANADA

THE UNIVERSITY OF MANITOBA
FACULTY OF GRADUATE STUDIES
*****
COPYRIGHT PERMISSION

Root-zone Soil Moisture Redistribution in Cropping Systems under Freeze-Thaw Conditions

By

Frederick Cassian Kahimba

A Thesis/Practicum submitted to the Faculty of Graduate Studies of The University of Manitoba in partial fulfilment of the requirements of the degree

of

DOCTOR OF PHILOSOPHY

ABSTRACT

The availability and distribution of soil moisture within the root zone is a key factor in ensuring better crop growth performance and attaining improved yield. The soil moisture is influenced by farm management practices such as cover cropping that affect the freeze-thaw processes during the fall. This in turn may influence accumulation and redistribution of soil moisture during the winter, and thereafter, the soil's response to thawing during spring, and availability of soil moisture for the subsequent season. The impact of cover cropping systems on soil temperature, infiltration, and soil moisture redistribution due to soil freezing and thawing was investigated. In addition, the effect of cover crop on the within-season and subsequent-season crop performance and yield was also investigated. Time Domain Reflectometry (TDR) and Neutron Scattering (NS) methods were used to measure the unfrozen and total water contents, respectively. Soil temperature was measured using thermocouples embedded in the soil profile. Soil moisture and soil temperature data were collected from August 2005 to September 2007.

Laboratory calibration of the TDR miniprobes indicated the maximum cable length for the RG-58 50 Ω coaxial cable to be 40.0 m when 35 mm TDR miniprobes were used. Since the TDR was found to overestimate the liquid water content at soil temperatures below 25°C, a method to correct the field measured TDR soil moisture for temperature effects was developed.

During soil freeze-up, water from unfrozen soil layers below the freeze front migrated towards frozen layers above. Compared to non-cover crop treatment, the cover crop treatment did not freeze earlier during the fall, froze to a shallower depth during the

winter, and accumulated less total water content in the root zone by spring. This led to relatively warmer soil temperatures along the soil profile and earlier thawing during spring. During the growing season, the previously cover-cropped treatment had lower soil water content and poor crop growth performance that resulted in significantly lower yield of canola in 2006 (1.99 vs. 2.72 t ha^{-1}). A physically based Simultaneous Heat and Water (SHAW) model was modified for use during wintertime to simulate hydrologic processes in soils experiencing seasonal soil freezing and thawing.

The depletion of soil moisture by the presence of cover crop can be beneficial to the main crop in wetter seasons. However, for drier seasons the cover crop will compete for soil moisture with the main crop resulting in negative effects. Rotational management practices that include cover crops need to consider using crops that are less sensitive to lower soil moisture during the subsequent season if it is expected to be drier.

ACKNOWLEDGEMENTS

To the Almighty God for His blessings that has made possible all the things that have happened to me and my family during my study and our stay here in Canada.

I would like to express my sincere thanks to my advisor, Dr. Ramanathan Sri Ranjan (Professor, Department of Biosystems Engineering, University of Manitoba) for his advice, guidance, and support throughout the undertaking of this research. I am also very grateful to the contribution and encouragement of my advisory committee, Dr. Danny Mann (Professor and Associate Head, Department of Biosystems Engineering, University of Manitoba) and Dr. Martin Entz (Professor, Department of Plant science, University of Manitoba). My special thanks to Dr. Ramesh P. Rudra (Professor, School of Engineering, University of Guelph) for being my external examiner and for his valuable comments on my PhD thesis.

I would also like to thank the Canadian Commonwealth Fellowship Program (CCFP-CBIE) for awarding me the scholarship to undertake my PhD studies in Canada. Thanks to the National Sciences and Engineering Research Council of Canada (NSERC) and the Sustainable Development Innovations Fund (SDIF) for the financial support of the research. Conference travel awards provided by the University of Manitoba Alumni Association, University of Manitoba Students Union (UMSU and UMGSA), and the Faculty of Graduate Studies (FGS) are also much appreciated.

Thanks to Dr. Jane Froese for access to her field experimental plots to be used in this research, for the advice and support she gave during field work, and for the technical assistance on cropping systems at the Ian N. Morrison Research Farm. The assistance of

staff managing the Ian N. Morrison Research Farm of the University of Manitoba is also appreciated for the logistical supports during my field work at Carman, Manitoba.

I also thank my fellow students Vanathy Nalliah and Marcos Cordeiro who lent their hands during lab experiments and field work. The support and company of all students and staff of the Department of Biosystems Engineering is also greatly appreciated. The technicians, Messrs. Dale Bourns, Matt McDonald, and Gerry Woods did a great job in fabricating the TDR probes and other research equipment.

I would also like to thank the staff and students of the Department of Soil Science for their support during the execution of this work. Thanks to Dr. Paul Bullock for allowing his Neutron Moisture Meter to be used during data acquisition, and Dr. Don Flaten and Dr. Wole Akinremi for the reference materials and advise they gave.

I wish also to express my heartfelt thanks and appreciations to my family, my wife Agnes, our beloved son Derrick-Martin, and daughter Grace-Juliana. I extend my appreciations to all our families back home in Tanzania for their prayers, patience, encouragement, and help during our stay and study in Canada. Thank you all.

DEDICATION

To my families in Tanzania and here in Canada for their prayers, tireless support, encouragement, patience, and help throughout the execution of my Ph.D. studies in Canada.

TABLE OF CONTENTS

Item	Page
ABSTRACT	i
ACKNOWLEDGEMENTS	iii
DEDICATION	v
TABLE OF CONTENTS	xi
LIST OF TABLES	xi
LIST OF FIGURES	xiv
LIST OF APPENDICES	xx
ABBREVIATIONS	xxii
LIST OF COPYRIGHTED MATERIALS	xxiv
CHAPTER 1 INTRODUCTION	1
1.1 Overview	1
1.2 Scope	4
1.3 Objectives	5
1.4 Thesis Organization	6
CHAPTER 2 LITERATURE REVIEW	8
2.1 Soil Moisture Measurements	8
2.1.1 General	8
2.1.2 Field methods of soil moisture measurements	8
2.1.3 Effects of soil water content on soil thermal properties	9

2.2 Time Domain Reflectometry 11

2.2.1 Background 11

2.2.2 Theory of TDR measurements 12

2.2.3 Fabrication and calibration of TDR miniprobes 14

2.2.4 Commonly used TDR systems for water content measurements.. 17

2.2.5 Field installation of TDR miniprobes 18

2.2.6 Influence of extension cable lengths 20

2.3 Neutron Scattering Method 21

2.3.1 General 21

2.3.2 Theory of the NS technique 21

2.3.3 NMM calibration and field data collection 22

2.3.4 The neutron access tubes 24

2.3.5 NMM radiation hazard and safety precautions 25

2.4 Infiltration and Soil Moisture Redistribution 26

2.4.1 Infiltration process 26

2.4.2 Infiltration into frozen soil 28

2.4.3 Factors affecting infiltration 29

2.4.4 Soil moisture redistribution 31

2.4.5 Soil moisture redistribution in freezing soils 31

2.4.6 Soil freezing and thawing 33

2.5 Soil Temperature 34

2.5.1 General 34

2.5.2 Soil thermal properties 34

2.5.3 Determination of surface soil temperature from air temperatures 36

2.6 Cover Crops 41

2.6.1 Introduction 41

2.6.2 Use of cover crops in areas experiencing excess precipitation .. 42

2.6.3 Use of cover crops in areas receiving low precipitation 43

2.6.4 Influence of cover crops on soil freezing and thawing 44

2.7 Unsaturated Flow Models 45

2.7.1 General 45

2.7.2 Flow models for soil freezing and thawing 46

2.7.3 The Simultaneous Heat and Water (SHAW) model theory 47

2.7.4 The SHAW model input parameters 48

2.7.5 Estimation of solar radiation using limited weather data 49

2.8 Chapter Summary 52

CHAPTER 3 IMPACT OF CABLE LENGTHS ON THE ACCURACY OF DIELECTRIC CONSTANT MEASUREMENTS BY TIME DOMAIN REFLECTOMETRY 53

3.1 Abstract 53

3.2 Introduction 54

3.3 Materials and Methods 62

3.4 Results and Discussion 67

3.5 Summary and Conclusions 75

CHAPTER 4 SOIL TEMPERATURE CORRECTION OF FIELD TDR READINGS OBTAINED UNDER NEAR FREEZING CONDITIONS 77

4.1 Abstract 77

4.2 Introduction 77

4.3 Materials and Methods 83

4.4 Results and Discussion 89

4.5 Summary and Conclusions 96

CHAPTER 5 COVER CROP EFFECTS ON INFILTRATION, SOIL TEMPERATURE, AND SOIL MOISTURE DISTRIBUTION IN THE CANADIAN PRAIRIES 98

5.1 Abstract 98

5.2 Introduction 99

5.3 Materials and Methods 103

5.4 Results and Discussion 113

5.5 Summary and Conclusions 133

CHAPTER 6 PREVIOUS SEASON COVER CROP EFFECTS ON SUBSEQUENT SOIL MOISTURE DISTRIBUTION AND YIELD IN THE NORTHERN GREAT PLAINS 135

6.1 Abstract 135

6.2 Introduction 136

6.3 Materials and Methods 139

6.4 Results and Discussion 146

6.5 Summary and Conclusions 162

CHAPTER 7 MODELING SOIL TEMPERATURE, FROST DEPTH, AND SOIL MOISTURE REDISTRIBUTION IN SEASONALLY FROZEN AGRICULTURAL SOILS 164

7.1 Abstract 164

7.2 Introduction 165

7.3 The SHAW model 167

7.4 Materials and Methods 170

7.5 Results and Discussion 179

7.6 Summary and Conclusions 202

CHAPTER 8 CONCLUSIONS 204

CHAPTER 9 RECOMMENDATIONS FOR FUTURE RESEARCH 208

REFERENCES 211

APPENDICES 225

LIST OF TABLES

Table		Page
Table 2.1	Regression statistics of the cubic function (after Gupta et al. 1990)	37
Table 3.1	Summary of statistical analysis for the apparent dielectric constant (K_a)* of water measured using variable extension cable lengths at 20±0.3°C	67
Table 3.2	Paired comparison between the measured and the actual dielectric constant (K_a) of water for different cable lengths	70
Table 4.1	Soil temperature and unfrozen and total water contents at different depths along the soil profile in the cover-cropped treatment during December 13, 2005	93
Table 4.2	Soil temperature and unfrozen and total water contents at different depths along the soil profile in the non-cover-cropped treatment during December 13, 2005	94
Table 5.1	Oats biomass yield for the treatments with and without a berseem clover cover crop in the 2005 growing season at the Ian N. Morrison Research Farm in Carman, Manitoba	115
Table 5.2	Reduction of root zone water content in oats with a berseem clover cover crop compared to oats alone treatment during the growing season on August 16, 2005	117
Table 5.3	Unfrozen (TDR) water content in the 0.0- to 0.8-m soil profile for the four cropping systems from August 2005 to April 2006	118

LIST OF TABLES

Table		Page
Table 2.1	Regression statistics of the cubic function (after Gupta et al. 1990)	37
Table 3.1	Summary of statistical analysis for the apparent dielectric constant (K_a)* of water measured using variable extension cable lengths at 20±0.3°C	67
Table 3.2	Paired comparison between the measured and the actual dielectric constant (K_a) of water for different cable lengths	70
Table 4.1	Soil temperature and unfrozen and total water contents at different depths along the soil profile in the cover-cropped treatment during December 13, 2005	93
Table 4.2	Soil temperature and unfrozen and total water contents at different depths along the soil profile in the non-cover-cropped treatment during December 13, 2005	94
Table 5.1	Oats biomass yield for the treatments with and without a berseem clover cover crop in the 2005 growing season at the Ian N. Morrison Research Farm in Carman, Manitoba	115
Table 5.2	Reduction of root zone water content in oats with a berseem clover cover crop compared to oats alone treatment during the growing season on August 16, 2005	117
Table 5.3	Unfrozen (TDR) water content in the 0.0- to 0.8-m soil profile for the four cropping systems from August 2005 to April 2006	118

Table 5.4 Comparison of accumulation of total soil water content in the root zone for oats with a berseem clover cover crop and oats alone treatments from the fall in November 2005 to spring in April 2006 120

Table 5.5 Comparison of accumulation of total soil water content in the 0.1- to 0.9-m depth for the fallow and native prairie grass treatments from the late fall in December 2005 to early spring in April 2006 129

Table 6.1 Total water content in the 0.1- to 0.9-m soil profile for two cropping systems from March 2006 to July 2007 147

Table 6.2 Soil temperature in the 0.2- to 0.8-m soil profile for two cropping systems from March 2006 to July 2007 153

Table 6.3 Effects of previous season (2005) cover crop management system on canola yield in the subsequent (2006) season 159

Table 6.4 Analysis of variance showing the effects of previous season (2005) cover crop on subsequent canola yield in 2006 for the canola_CC and canola_NC treatments 160

Table 7.1 Soil characteristics used as input parameters for the SHAW model 173

Table 7.2 Plant characteristics used as input parameters for the SHAW model 173

Table 7.3 The SHAW model statistical analysis for the measured and predicted total soil moisture and soil temperature during the 2005-2007 seasons 181

Table 7.4 Comparison of the summer and winter SHAW model predictions of soil

moisture and soil temperature on vegetated plots and continuous fallow treatments in the 2005-2007 seasons 186

Table 7.5 Comparison of winter model predictions of soil moisture on vegetated plots and continuous fallow treatments using the original and the revised SHAW models in the 2005-2007 seasons 193

LIST OF FIGURES

Figure		Page
Fig. 2.1	Commonly used TDR probe rods configurations: (a) two-wire; (b) three-wire; (c) four wire; and (d) five-wire configuration	15
Fig. 2.2	A typical three-wire 35 mm TDR miniprobe for water content measurements	16
Fig. 2.3	The TDR cable testers commonly used for water content measurements: (a) Tektronix 1502B (Tektronix Inc., Beaverton, OR); (b) TRACE SYSTEM 6050X1 (Soil Moisture Equipment Corp., Goleta, CA; (c) TDR100 (Campbell Scientific Inc., Logan, UT; and (d) TRIME-FM (IMKO, Ettlingen, Germany)	17
Fig. 2.4	Angular insertion metal guide (60-degree angle) for field installation of TDR miniprobes	19
Fig. 2.5	A neutron moisture meter (Troxler model 4302, Troxler Electronic Laboratories Inc., Research Triangle Park, NC) in position on top of a 50-mm aluminium access tube	23
Fig. 2.6	Schematic diagram of infiltration rates in frozen soil for different moisture conditions prior to soil freezing: (A) saturated, (B) 70-80% saturated, (C) low moisture content & high temp, and (D) low moisture content & low temp (*Source: Fig. V.7 of Gray et al. 1973*)	28
Fig. 2.7	Ridge positions for determination of surface soil temperature (*Source: Gupta*	

et al. 1990) 38

Fig. 3.1 Typical waveform for a 35-mm TDR miniprobe immersed in pure water and attached to a 2.5-m coaxial cable. The difference between the first peak and the end reflection defines the apparent length, L_a of the waveguide 61

Fig. 3.2 TDR waveforms for different cable lengths produced using a 35-mm TDR miniprobe immersed in pure water at an average temperature of 20°C ... 68

Fig. 3.3 Comparison of the measured and the actual dielectric constants (K_a values) for water content measurement 71

Fig. 3.4 Variability of the measured dielectric constant of water with increase in cable length. Error bars represent standard errors of measurement 72

Fig. 3.5 Comparison of physical and apparent cable lengths for water content measurement 73

Fig. 4.1 Comparison of TDR and NMM soil moisture measurements on the cover-cropped treatment at temperature ranges 6.5 to 2.3°C on November 22, 2005: (a) before temperature correction and (b) after temperature correction. The TDR measurements were taken as average of three replicates 90

Fig. 4.2 Comparison of TDR and NMM soil moisture measurements on the non-cover-cropped treatment at temperature ranges 8.8 to 2.5°C on November 22, 2005: (a) before temperature correction and (b) after temperature correction. The TDR measurements were taken as average of three replicates 91

Fig. 4.3 Variation of liquid (unfrozen) and total water content with depth for the non-

cover-cropped treatment on January 30, 2006. Error bars indicate standard errors of measurements. 95

Fig. 5.1 Monthly precipitation (ppt) from May 2005 to May 2006 and fifteen-year mean monthly precipitation (1991 – 2005) for Carman, Manitoba 104

Fig. 5.2 Monthly mean temperature from May 2005 to May 2006 and fifteen-year average monthly temperature (1991 – 2005) for Carman, Manitoba 105

Fig. 5.3 Field layout showing three blocks, each with oats with berseem clover cover crop (O+B) and oats alone (O) in the 2005 growing season. Numbers at the bottom represent plot numbers. The C, W, and L are respectively canola, wheat, and linola (flax) in the four-year rotation along with O+B or O ... 107

Fig. 5.4 (a) Total water content (measured with NMM), (b) unfrozen water content (measured with TDR), and (c) soil temperature variation for the oats with berseem clover cover crop and oats alone treatments during: (1) the fall of 2005, and (2) winter and (3, 4) spring of 2006. Error bars for TDR measurements indicates standard errors of three replicate measurements for each soil depth 122

Fig. 5.5 Partitioning of total water content into frozen and unfrozen phases for the oats with berseem clover cover crop and oats alone treatments during: (a and c) fall freeze-up in December 2005, and (b and d) spring in April 2006. The difference between the two curves represents the amount of soil moisture in the frozen state. Error bars indicate standard errors of measurement for three TDR replicates 124

Fig. 5.6 Variation of total water content with depth within each treatment for: (a) native prairie grass, (b) continuous fallow, (c) oats with berseem clover, and (d) oats alone, from September 2005 to April 2006. One measurement value was taken for each treatment at each depth on each date using NMM 128

Fig. 5.7 Soil temperature variations with depth for the fallow and native prairie grass treatments during: (a) early winter on December 21, 2005 and (b) early spring on March 29, 2006 130

Fig. 6.1 Mean monthly precipitation at the Ian N. Morrison Research Farm during year 2005 to 2007 as compared to the 15-year average monthly precipitation 140

Fig. 6.2 Monthly mean temperature at the Ian N. Morrison Research Farm during year 2005 to 2007 as compared to the 15-year average monthly mean temperatures 140

Fig. 6.3 Variations of total soil water content in the 0.1- to 0.9-m soil depth for the oats + berseem clover and oats alone treatments in the 2005/2006 season; and for canola_CC and canola_NC treatments in the 2006/2007 season. Measurements were taken using NMM 151

Fig. 6.4 Soil temperature variation with depth for the canola_CC and canola_NC treatments in the 2006 growing season during: (a) flowering stage and (b) maturity stage 154

Fig. 6.5 Comparison of growth performance of canola on June 26, 2006 for: (a) canola_NC and (b) canola _CC treatments 154

Fig. 6.6 Variations of total soil water content on the canola_CC and canola_NC treatments in the growing season during: (a) flowering stage in July 2006 and (b) maturity stage in August 2006 156

Fig. 6.7 (a) Total (NMM) water content, (b) unfrozen (TDR) water content, and (c) soil temperature variations with depth for the canola_CC and canola_NC treatments during the winter and spring of 2007. Rows 1 to 4 in the figure indicate different sampling dates 157

Fig. 6.8 Comparison of crop yields for oats with and without a berseem clover cover crop in the 2005 growing season, and canola alone in the 2006 growing season. Error bars indicate standard errors of measurement 159

Fig. 7.1 Measured and predicted total soil water contents at different soil depths in the oats + berseem clover cover crop treatment during: (a and b) the fall in 2005 and (c and d) winter and spring in 2006 182

Fig. 7.2 Measured and predicted total soil water contents at different soil depths in the fallow during: (a) winter on February 24, 2006 and (b) early spring on March 29, 2006. The measured total water contents (WC) were taken using NMM method 183

Fig. 7.3 Measured and predicted soil temperature at different soil depths: (a) in the oats + berseem clover cover crop and (b) in the fallow treatment. The measurements on (a1) and (b1) were during the fall; (a2) and (b2) during winter; and (a3) and (b3) during spring 184

Fig. 7.4 Scatter plots of estimated versus measured total soil moisture during the

summer of 2005 and winter 2006 for: (a) vegetated fields (oats with berseem clover cover crop) and (b) continuous fallow treatments 188

Fig. 7.5 Scatter plots of estimated versus measured soil temperature profile during the summer of 2005 and winter 2006 for: (a) vegetated fields (oats with berseem clover cover crop) and (b) continuous fallow 190

Fig. 7.6 Scatter plots of the measured vs. estimated soil moisture, predicted using the revised SHAW model during the winter of 2006 and 2007 for: (a) vegetated fields (oats with berseem clover cover crop) and (b) continuous fallow .. 194

Fig. 7.7 Comparison of predicted soil water content from the original and revised (rev) SHAW model for: (a) vegetated fields (oats with berseem clover cover crop) and (b) continuous fallow treatments on March 29, 2006 195

Fig. 7.8 Comparison of the measured and simulated frost depths from the original and revised SHAW models for: (a) vegetated fields (oats with berseem clover cover crop) and (b) continuous fallow treatments in the 2005-2006 seasons. The TDR measurements were used to determine the measured frost depth 199

Fig. 7.9 Revised SHAW model predictions of total soil moisture at 0.2- to 0.8-m soil depths in: (a) oats with berseem clover cover crop and (b) oats alone treatments during the 2005-2006 season 200

LIST OF APPENDICES

Appendix **Page**

Appendix A: Raw data used for laboratory water calibration of TDR miniprobes that were used for field installation and data collection at the Ian N. Morrison research farm in Carman, Manitoba 226

Appendix B: Calibration of TDR miniprobes for water content measurements using laboratory soil columns 229

Appendix C: Measured and actual dielectric constant (K_a) of water for different extension cable lengths. The data were used for determining the influence of cable lengths on the accuracy of TDR measurements ... 231

Appendix D: The SHAW model input data files on the continuous fallow treatment for the 2005-2006 seasons at the Ian N. Morrison research farm in Carman, Manitoba (data for one out of four treatments on one season have been taken as example of the SHAW input data files) 233

Table D-1: List of the SHAW model input/output files for the continuous fallow treatment 233

Table D-2: Total soil moisture at depths from 0.0 to 1.8 m 234

Table D-3: Soil temperature at depths from 0.0 to 1.8 m 235

Table D-4: Site characteristics of the experimental fields 236

Table D-5: Weather data 237

Appendix E: The SHAW model source code modifications to account for solar azimuth angle calculations and reduced soil saturation due to ice content in freezing soils 239

Code E-1 Modified subroutine SOLAR that calculates the solar azimuth angle based on the inverse cosine function. (The additions are presented in BOLD, and deletion of the original code have been written as comments in italic fonts preceded with C*) 239

Code E-2 Modified subroutine MATVLC that relates volumetric liquid water content and matric potential, taking into account the ice content of freezing soil. (The corrections to the original code are presented in BOLD fonts) 242

ABBREVIATIONS

ASABE	=	American Society for Agricultural and Biological Engineering
BNC	=	Bayonet Nelson Connector
CBIE	=	Canadian Bureau for International Education
CC	=	Cover crop
CCFP	=	Canadian Commonwealth Fellowship Program
CR	=	Count Ratio
CSBE	=	Canadian Society for Bioengineering
CV	=	Coefficient of variation
EM	=	Electromagnetic wave
FC	=	Field capacity
FDR	=	Frequency Domain Reflectometry
FFC	=	Farming with Fewer Chemicals
MAE	=	Mean absolute error
MASC	=	Manitoba Agricultural Services Corporation
MBE	=	Mean bias error
mCi	=	Millicurie (solar radiation units)
ME	=	Maximum error
MeV	=	Megaelectronvolt (radiation unit)

NC	=	No cover crop
NMM	=	Neutron moisture meter
NS	=	Neutron scattering method
NSERC	=	National Sciences and Engineering Research Council
O	=	Oats alone
O+B	=	Oats + berseem clover cover crop
PPT	=	Precipitation
PWP	=	Permanent wilting point
RMSE	=	Root mean square error
SD	=	Standard deviation
SDIF	=	Sustainable Development Innovations Fund
SEM	=	Standard error of measurement
SHAW	=	Simultaneous Heat and Water model
TDR	=	Time Domain Reflectometry
USDA-ARS	=	United States Department of Agriculture, Agricultural Research Service

LIST OF COPYRIGHTED MATERIALS

1. Gray, D.M., D.I. Norum and J.M. Wigham. 1973. Infiltration and the physics of flow of water through porous media. In *Handbook on the Principles of Hydrology*, ed. D.M. Gray, 5.1-5.58. Port Washington, NY: Water Information Centre, Inc. **Copyright source**: NRC Research Press, Canada.

   Fig. 2.6 28

2. Gupta, S.C., J.K. Radke, J.B. Swan and J.F. Moncrief. 1990. Predicting soil temperatures under a ridge-furrow system in the U.S. Corn Belt. *Soil & Tillage Research* 18(2): 145-165. **Copyright source**: Elsevier Limited.

   (a) Table 2.1 37

   (b) Fig. 2.7 38

3. Kahimba, F.C., R. Sri Ranjan and M. Krishnapllai. 2007. Impact of cable lengths on the accuracy of dielectric constant measurements by time domain reflectometry. *Canadian Biosystems Engineering* 49: 1.11-1.18. **Copyright source**: The Canadian Society for Bioengineering.

   Thesis chapter three 53

2. Kahimba, F.C. and R. Sri Ranjan. 2007. Soil temperature correction of field TDR readings obtained under near freezing conditions. *Canadian Biosystems Engineering* 49: 1.19-1.26 **Copyright source**: The Canadian Society for Bioengineering.

   Thesis chapter four 75

5. Kahimba, F.C., R. Sri Ranjan, J. Froese, M. Entz and R. Nason. 2008. Cover crop

effects on infiltration, soil temperature and soil moisture distribution in the Canadian prairies. *Applied Engineering in Agriculture* 3(2): 321-333. **Copyright source:** The American Society for Agricultural and Biological Engineering (ASABE).

Thesis chapter five 97

1. INTRODUCTION

1.1 Overview

The quantity of spring snowmelt infiltration, soil moisture redistribution in the soil profile, and the response of the soil to thawing, depends on the antecedent soil moisture conditions at the time of soil freezing (Luo et al. 2002). The freeze-thaw processes during the fall can be influenced by farming practices such as cover cropping from the previous growing season (Cruse et al. 2001). Determining the soil moisture status during the fall through spring freeze-thaw processes requires an understanding of vertical distribution of the unfrozen and total water content within the soil profile. During these periods, the soil is partly frozen, with unfrozen and frozen water existing simultaneously.

There are various methods for measuring soil moisture (Seyfried 2001; Warrick 2002; Evett 2000a and 2003a; Evett et al. 2002). However, most of these methods can measure either the total water content, or the unfrozen water content. There is no single method that can give the frozen, unfrozen, and total water contents simultaneously. In this study, two methods: Time Domain Reflectometry (TDR) and Neutron Scattering (NS) using neutron moisture meter (NMM), were used together in the field to measure simultaneously the unfrozen and total water contents, respectively.

The TDR measurements involve measuring travel time of electromagnetic wave (EM) along wave-guides of known length placed in the soil (Topp et al. 1980). The measured travel time is dependent on the dielectric constant of the medium in which the wave-guide is embedded. Since the change in volumetric water content (θ_v) is directly

related to the change in dielectric constant (K_a) based on dielectric mixture theories, the volumetric liquid water content (θ_v) can be determined from the dielectric constant (K_a) (Topp et al. 1980; Evett 2000).

The NS technique on the other hand, measures total water content (frozen and unfrozen) using neutron moisture meter (NMM). It uses a radioactive source emitting fast neutrons, and a counter for detecting slow neutrons thermalized by hydrogen ions in the soil water (Evett 2000, 2003a). The loss in kinetic energy of the neutrons varies depending on type of soil constituents they collide with. When neutrons collide with hydrogen atoms of approximately equal weight, their kinetic energy is significantly reduced by thermalization (Evett 2003a). The concentration of the thermalized neutrons is a measure of the number of hydrogen atoms, which is related to the total volumetric water content (Evett 2003a). The relationship between thermalized neutron counts and the volumetric moisture content depends on field calibration for a specific soil.

Previous studies have described the potential for using TDR and NMM in partitioning the total water content into frozen and unfrozen water (Baker and Allmaras 1990; Herkelrath and Delin 1999). However, very little has been documented on the freeze-thaw processes during the fall as the soil starts to freeze. In addition, the accuracy of TDR soil moisture measurements in the field at varying soil temperatures along the soil profile needs more attention. Spaans and Baker (1995) observed that calibration of TDR probes using water and soil in the laboratory does not give accurate results in the field when the temperature is low and the soil is partly frozen.

Considering soil moisture redistribution in crop fields, the influence of soil

moisture stress to the crop performance and yield within the season is well documented (Aspinall et al. 1964; Calvino et al. 2003; Osborne et al. 2003a). For example, Osborne et al. (2003a) observed that scarcity or excess moisture at different stages of plant growth affects soil processes such as root respiration, plant water uptake, and redox potential, which in turn, lower the crop yield potential. Cover crops are normally grown within the main crop for purposes such as suppressing crop weeds, minimizing soil erosion, and reducing excess soil moisture. The influence of a cover crop of one growing season to the soil moisture distribution during the fall to spring, and its residual effects on the moisture availability and crop performance of the subsequent season is less documented. Studies on soil temperature and moisture availability during the fall freeze-up, and how it influences the soil's response during spring snowmelt are also less documented in the literature.

Soil moisture stress in crops can be a result of low or excess precipitation accompanied by poor farm management practices or soil moisture conservation. The use of cover crops for example has been linked with reduction of available soil moisture within the growing season (Calvino et al. 2003; Osborne et al. 2003a). Cover crops in intercropping systems provide a protective cover that reduces runoff, erosion and nutrient losses, thereby facilitating more infiltration (Bargar et al. 1999). In the case of excess soil moisture, cover crops utilize the soil moisture within the rootzone. Osborne et al. (2003b) found that this assists in reducing the excess soil moisture that could affect the performance and yield of the main crop. In case of less precipitation however, the cover crop will compete with the main crop for the available soil moisture. While the cover crop is advantageous to existing crops, the residual effect can influence the fall

freeze/thaw behavior of the soil, and thereafter its response to spring snowmelt.

Hence, this study used two methods of soil moisture measurement to explore soil moisture for all the four seasons of the year, and its relation to crop management practices and crop performance. The cover crop effects on soil freeze-thaw processes and its residual effects to the subsequent growing season have also been addressed. Laboratory calibration was performed for the TDR miniprobes, and comparison was made for the field measurements using the TDR and NMM. The soil temperature, frost depth, and moisture redistribution due to soil freezing and thawing was modeled using the Simultaneous Heat and Water (SHAW) model. The model results were compared with three seasons of measured field data (2005-2007). Results from this work are expected to assist farmers to properly conserve soil moisture, and in decision-making for the type, timing, and management of rotational crops based on the available soil moisture. The knowledge will lead to effective utilization of soil moisture and better economic returns from agricultural fields.

1.2 Scope

Most research on soil moisture in agricultural soils concentrates on the availability and distribution of soil moisture within the growing season. Very little literature evidence exists on freeze-thaw processes from the fall through spring when the soil is frozen or partly frozen, and their effects on soil moisture availability and distribution during the subsequent growing season. While the influence of a cover crop on soil moisture distribution within the same season is well documented, the residual effects of the cover crop to the soil moisture availability, redistribution, and crop

performance of the subsequent season needs more attention. The information on frost depths, soil temperatures, and the quantity and redistribution of soil moisture as influenced by the soil freeze/thaw processes and farming practices, will assist farmers in planning various crop rotation strategies. This information will also assist in understanding the hydrology during the Spring.

1.3 Objectives

The main objective of the study was to determine the effects of cropping systems on soil temperature and soil moisture redistribution in seasonally frozen agricultural soils. Since the TDR equipment needed to be calibrated for use under low temperature conditions, laboratory experiments had to be completed prior to the commencement of the fieldwork.

The specific objectives were:

1. To study the influence of cable length on the accuracy of dielectric constant measurements by Time Domain Reflectometry.
2. To study the soil temperature and soil freeze-thaw effects on the accuracy of field TDR readings.
3. To determine the within-season cover crop effects on crop performance, and soil temperature and soil moisture redistribution during the fall, winter, and spring seasons.
4. To study the residual effects of one season's cover crop on soil moisture redistribution, crop performance, and yield in the subsequent season.

5. To model soil temperature, frost depth, and soil moisture redistribution in the root zone under soil freezing and thawing conditions.

1.4 Thesis Organisation

This thesis has been written according to the manuscript style outlined by the Department of Biosystems Engineering, University of Manitoba. The main topics of the thesis consist of five manuscripts, each having an abstract, introduction, materials and methods, results and discussion, and conclusions. The main manuscript topics have been preceded by the general introduction and literature review, and succeeded by the general discussion, conclusions, and recommendations for future research.

The first introductory chapter covered the general research overview, scope, main objectives of the research, and the organization of the thesis. Chapter two covers a review of literature on soil moisture measurement principles and techniques; the infiltration, soil temperature, and soil moisture movements in frozen soils; a review on cover crop farm management practices; and the unsaturated flow models. Chapter three, which addresses the first objective deals with laboratory experiments on the calibration of TDR miniprobes and cables, and determination of optimum cable lengths suitable for field TDR measurements.

Chapter four presents research findings that cover objective two explaining the use of TDR for field measurements during soil freezing, and the necessary corrections for temperature effects. The research findings on the within-season cover crop effects on soil moisture and soil temperature, outlined as objective three, are presented in chapter five. Chapter six addresses the fourth objective on the residual effects of one season's cover

crop on soil moisture redistribution and yield in the subsequent season. The fifth objective is addressed in chapter seven by the use of the SHAW model to predict the soil response to freeze-thaw processes. Comparison was made for the model performance during different seasons of the year. Recommendations have been made on areas of the model that need further improvement to better simulate the fall through spring hydrologic conditions in seasonally frozen agricultural soils. Chapter eight covers the general discussion, conclusions, and recommendations for future research.

The 'Materials and Methods' section is incorporated into the manuscript-style chapters of this thesis. References for all the manuscripts included in the chapters have been provided after chapter eight, and they have been combined together to avoid repetition. The list of appendices at the end provides some of the data used in preparing the thesis chapters.

2. LITERATURE REVIEW

2.1 Soil Moisture Measurements

2.1.1 General

Measurements of soil moisture have wide applications in the fields of agriculture, engineering, meteorology, and environment. When dealing with soil moisture measurements in frozen or partly frozen soils, some methods of soil moisture measurement may have shortcomings that can be overcome by a combination of more than one method. Time Domain Reflectometry (TDR) method measures the unfrozen water content (Herkelrath and Delin 1999; Evett 2000a). However, it does not measure frozen water content. Neutron Scattering (NS) method measures both liquid and solid (total) water content, but it does not distinguish between frozen and unfrozen water content (Evett 2003a). A combination of both TDR and NS can enable the determination of both the unfrozen and frozen water contents in the soil. This combination allows for study of soil moisture year-round in seasonally frozen soils in which both the frozen and unfrozen water can exist at the same time.

2.1.2 Field methods of soil moisture measurement

Several methods can be used to measure soil moisture directly in the field. The methods can be categorized into two main groups; the classical methods and the modern sensor methods (Warrick 2002). Examples of the classical methods are neutron scattering, electrical conductivity, and gravimetric (oven drying) methods (Jury et al. 1991; Evett 2000a; Warrick 2002). The modern sensor methods are such as Time Domain

Reflectometry (TDR), Frequency Domain Reflectometry (FDR), Water Content Reflectometry (WCR), and Capacitance methods (Seyfried and Murdock 2001; Warrick 2002). Despite the innovations on the new sensor methods, which are non-destructive with high precision, both the classical and new methods encounter particular problems related to the physics of the methods. Examples of the problems are accuracy and precision of the measurements, coverage and volume of measurements, data interpretations, and calibration according to varying soil conditions (Evett 2000b; Seyfried and Murdock 2001). During soil freezing, a combination of more than one method is needed to better understand the soil moisture patterns in the freezing or thawing soils (Herkelrath and Delin 1999).

Examples of practical applications of soil moisture measurements are determination of optimum moisture for operation of farm machinery, applications of farm manure, and maximum compaction of embankments and foundations. Other examples are irrigation scheduling, water balance studies, seed germinations, plant water uptakes, and movements of nutrients in agricultural soils (Evett 2000a; Warrick 2002).

2.1.3 Effects of soil water content on soil thermal properties

The response of the soil to freezing or thawing varies depending on the amount of initial soil water content in the soil profile at the onset of freezing or thawing. The soil moisture status in a freezing soil influences the soil's response by affecting the soil thermal properties (Jury et al. 1991). The amount of soil moisture affects the soil thermal conductivity, (k_s), heat capacity (C_v), and thermal diffusivity (κ_s). The soil thermal conductivity measures the ability of the soil to conduct heat. It is defined as the ratio of

the heat flux density to the temperature gradient (W m^{-1} K^{-1}).

The soil volumetric heat capacity refers to the energy required to raise the temperature of a unit volume of the soil by 1°C (units J m^{-3} K^{-1}). The soil heat capacity increases with an increase in moisture content (Jury et al. 1991; Warrick 2002). Hence, drier soils have lower heat capacity while wetter soils have higher heat capacity. The soil thermal diffusivity is its ability to diffuse the thermal influences. It is directly proportional to thermal conductivity and inversely proportional to heat capacity.

$$K_s = \frac{k_s}{C_v} \tag{2.1}$$

where

κ_s = soil thermal diffusivity (m^2 s^{-1}),

k_s = soil thermal conductivity (W m^{-1} K^{-1}), and

C_v = volumetric heat capacity (J m^{-3} K^{-1}).

The κ_s of a dry soil initially increases with the increase in soil moisture content due to the increase in soil thermal conductivity (k_s) at lower water content. The thermal conductivity increases with an increase in volumetric water content. At higher moisture contents, the soil thermal conductivity becomes constant with any further increase in moisture content (Jury et al. 1991; Warrick 2002). The heat capacity on the other hand, increases continuously with the increase in moisture content. Hence, at higher moisture content the C_v becomes a dominant factor. The κ_s will decrease since k_s become constant while the denominator, C_v, continues to increase (Warrick 2002; Miyazaki 2006). The thermal diffusivity, therefore, determines how fast the temperature of a soil layer will

change. This implies that during soil freezing, drier soils with low thermal diffusivity will freeze later compared to wetter soils with moisture content less than saturation due to dominance of the thermal conductivity effect. Similarly, saturated soils will freeze later compared to soils with relatively lower moisture due to dominance of the heat capacity effects at very high moisture contents. Therefore, the amount of water content in the soil affects the soil thermal properties that in turn, affect the response of the soil to freezing and thawing.

2.2 Time Domain Reflectometry

2.2.1 Background

Time Domain Reflectometry has become a popular method for measuring soil moisture since its introduction by Canadian scientists (Topp et al. 1980). Its importance over other electronic means of measuring volumetric moisture content is due to its lower sensitivity to variations in soil properties, and a better measurement accuracy of up to 1% to 2% of volumetric water content (Jones et al. 2002). The method is insensitive to soil composition and texture, can be automated, and has no radioactive hazard. Hence, it does not require soil specific calibration, and can be used to take continuous measurements in unattended areas (Topp et al. 1980; Evett 2000a; Brendan 2003). The ability of the TDR technique to measure water content and electrical conductivity simultaneously makes it a very important method for studying soil moisture and nutrients movement in agricultural soils (Vanclooster et al. 1994). The TDR method has been used in various research to measure water content and electrical conductivity (e.g. Topp et al. 1982; Vanclooster et al. 1994; Lane et al. 1995; Sri Ranjan and Domytrak 1997; Herkelrath and Delin 1999;

Logsdon 2000). The main principle of the TDR measurements involves relating the dielectric property of the soil medium with the soil water content. A third order polynomial equation (Topp et al. 1980) that is commonly used to relate dielectric constant of the medium with water content is presented as shown in Eq. 2.2 below:

$$\theta_v = -5.3\times10^{-2} + 2.92\times10^{-2}\varepsilon_b - 5.5\times10^{-4}\varepsilon_b^{\,2} + 4.3\times10^{-6}\varepsilon_b^{\,3} \qquad (2.2)$$

where:

θ_v = volumetric moisture content, and

ε_b = bulk electrical conductivity of the porous medium.

Main problems of using the TDR method are its sensitivity to air gaps when there is poor contact between soil and the probes, hence it is not suitable for use in stony soils; and limited application when the soil has high salinity. Other limitations are its sensitivity to organic matter and soils high in clay. Hence, it requires site-specific calibration on those soils (Herkelrath and Delin 1999; Seyfried and Murdock 2001; Brendan 2003). The method is also limited to near surface measurements due to difficulty in installing probes at greater depths (Evett 2000a, 2000b; Brendan 2003; Seyfried 2004).

2.2.2 Theory of TDR measurements

The TDR measurements involve measuring travel time of electromagnetic wave (EM) along wave-guides of known length placed in a porous medium. The measured travel time is related to the dielectric constant (K_a) of the medium in which the wave is moving. The K_a is then related to volumetric moisture content, (θ_v) since change in θ_v is directly related to the change in K_a (Topp et al. 1980). This is attributed to significant

difference between the dielectric constant of water and that of other soil materials (K_{water} = 80.4 at 20°C, K_{ice} = 3.2, K_{air} = 1.0, and K_{soil} = 3.0-7.0 depending on soil composition and texture) (Warrick 2002; Tardif 2002; Evett 2003b). As the soil freezes, the dielectric constant of frozen water changes significantly from that of unfrozen water. This allows for the unfrozen part of water content to be determined.

The velocity (v) of the electromagnetic (EM) wave in a dielectric material depends on the relative permeability (ε_r) and magnetic permeability (μ_r) of the material as follows:

$$v = \frac{c}{\sqrt{\mu_r \varepsilon_r}} \tag{2.3}$$

where, c is the velocity of EM wave in free space (= 2.998 x 10^8 m s^{-1}).

For non-magnetic soils, the magnetic permeability is assumed to be unity, and the permittivity of soil is taken as the apparent permittivity or dielectric constant K_a. Hence, K_a can be calculated from the propagation velocity along a known probe length L as follows:

$$v = \frac{c}{\sqrt{K_a}} \tag{2.4}$$

The travel time of the electromagnetic wave is given as

$$t = \frac{2L}{v} \tag{2.5}$$

where:

t = measured two way travel time (s), and

L = probe length (m).

Combining Eqs. 2.4 and 2.5, the value of K_a can then be calculated as

$$K_a = \left(\frac{ct}{2L}\right)^2 \tag{2.6}$$

Various calibration equations have been developed that relate K_a with θ_v. They range from empirical approximations to physically based models. Results from one model are normally compared with another model, or with the standard gravimetric method to ascertain their accuracy. Lane et al. (1995) used the physically based Topp model and suggested that the Topp equation (Eq. 2.2) gives a good approximation of TDR moisture content to gravimetric, with slight underestimation. Herkelrath and Delin (1999) and Jones et al. (2002) also compared moisture measurements by TDR using Topp model with the gravimetric method. They found that TDR probes were accurate within 0.01 to 0.02 $m^3 m^{-3}$. In this study, the physically based Topp model (Eq. 2.2) was used to relate the bulk electrical conductivity ε_b with the volumetric moisture content θ_v for the TDR water content measurements.

2.2.3 Fabrication and calibration of TDR miniprobes

Time domain reflectometry probes are normally used as waveguides along with the cable tester for measuring water content and solute concentrations in the soil. Ready-made industrial TDR probes are available with minimum sizes of 150 mm (Campbell Scientific, Inc. 2001; Brendan 2003). The TDR miniprobes (probe lengths less than 150

mm) need to be fabricated locally in the lab using materials such as stainless steel rods, Bayonet Nelson Connectors (BNC) and plastic insulators. The miniprobes can be made using different configurations such as two-wire, three-wire, four-wire, or five-wire configuration as shown in Fig. 2.1 (Zengelin et al. 1992; Jones et al. 2002; Brendan 2003). Considering the 3-wire configuration (Figs. 2.1b and 2.2), it is recommended that the critical wire spacing should be greater than three times the diameter of the central rods to avoid the "skin effect" (Zengelin et al. 1992). It is also suggested that when performing laboratory calibration of the probes, no part of the probe should be within 40 mm of the container used for calibration (Campbell Scientific, Inc. 2001). Procedures for making the TDR miniprobes have also been described by Heimovaara (1993), and Sri Ranjan and Domytrak (1997).

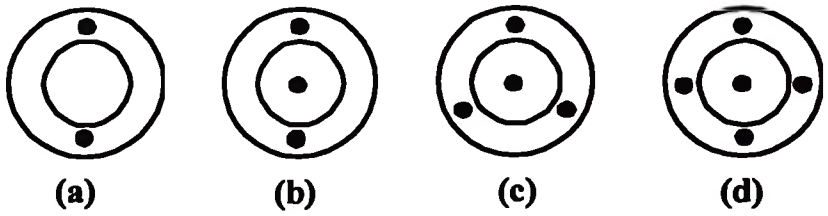

Fig. 2.1 Commonly used TDR probe rods configurations: (a) two-wire; (b) three-wire; (c) four-wire; and (d) five-wire configuration.

In measuring the dielectric constant of water, the physical length of the probe (the beginning and the end of the steel rods), is related to its apparent length (the length between the beginning and the end points of the waveform (Evett 2000a, 2000b).

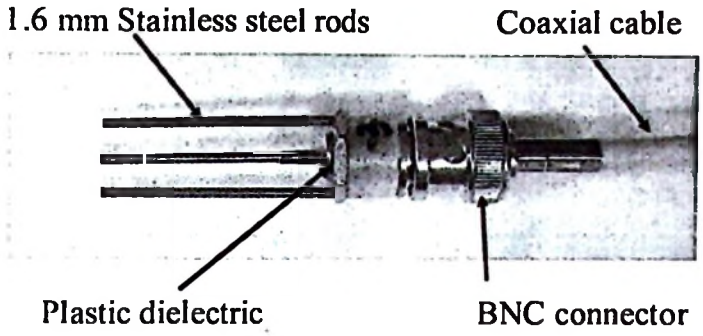

Fig. 2.2 A typical three-wire 35 mm TDR miniprobe for water content measurements.

The length of TDR probes influence the accuracy of TDR measurements. Mojid (2002) compared measurement accuracy of nine TDR miniprobes from 20 to 100 mm. The accuracy of measurement decreased with decreasing probe lengths. Specifically, probes less than 25 mm were found to be inaccurate. The measured pulse travel time for the shorter miniprobes had greater variation compared to the predicted pulse travel time. The sharpness of the pulse reflection increased with increase in probe length and moisture contents (Mojid 2002).

Laboratory calibration of TDR probes can be done using various fluid layers such as air, oil, water, acetone, and moist soil (Vanclooster et al. 1998; Robinson et al. 2003b). Errors in moisture measurements with TDR probes can be caused by varying moisture contents near the probes, non-uniform soil wetting, presence of air gaps caused by drying of the soil sample, and use of very short probe lengths (Heimovaara 1993). Another source of error is the use of longer extension cables for a specific type and size of probe (Pierce et al. 1994; Robinson et al. 2003a).

2.2.4 Commonly used TDR systems for water content measurements

Various TDR systems are currently available for water content measurements. Examples are the Tektronix 150X (Tektronix Inc., Beaverton, OR); TRACE SYSTEM (Soil Moisture Equipment Corp., Goleta, CA; TDR100 (Campbell Scientific Inc., Logan, UT; and TRIME-FM (IMKO, Ettlingen, Germany) (Fig. 2.3). The TDR systems were originally developed for detecting faults in electric transmission cables (Mojid et al. 2003).

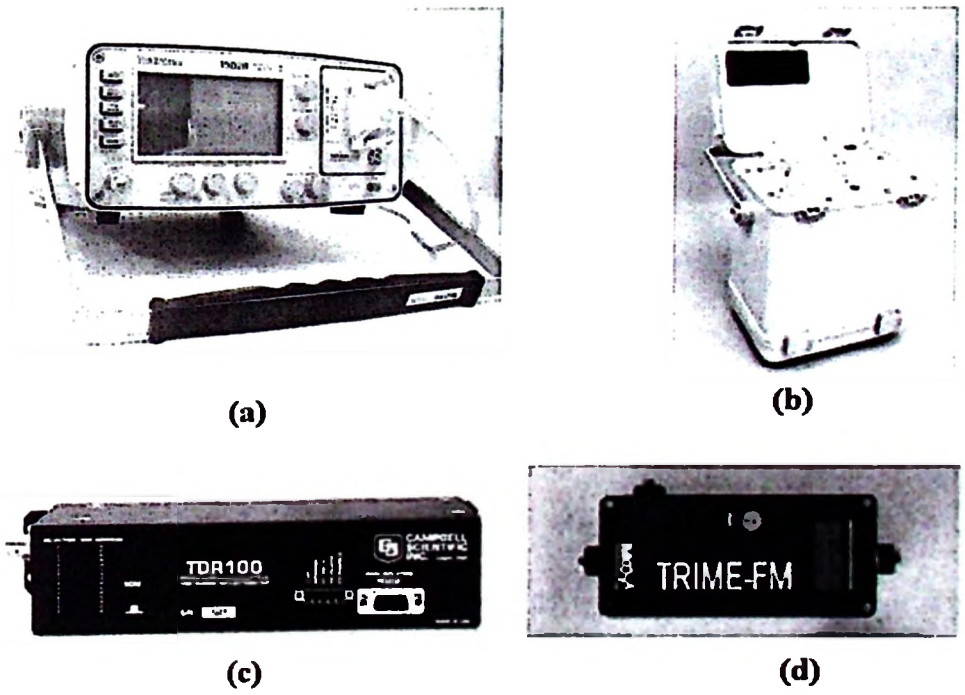

Fig. 2.3 The TDR cable testers commonly used for water content measurements: (a) Tektronix 1502B (Tektronix Inc., Beaverton, OR); (b) TRACE SYSTEM 6050X1 (Soil Moisture Equipment Corp., Goleta, CA; (c) TDR100 (Campbell Scientific Inc., Logan, UT; and (d) TRIME-FM (IMKO, Ettlingen, Germany).

The use of cable testers specifically for soil moisture measurements started in the early 1980s (e.g. Topp et al. 1980). At the moment, with the advances in computer technology and development of various software for analyzing the TDR waveforms, TDR systems have gained wide applicability for both soil water content and electrical conductivity measurements (e.g. Baker and Allmaras 1990; Hubscher et al. 1996; Brendan 2003; Or et al. 2004).

In the current study, a Tektronix 1502B cable tester (Fig. 2.3a) was used. During the calibration stage both water and soil calibration methods were used. Water calibration was performed to ascertain the uniformity of hand-made TDR miniprobes, and the effect of varying cable lengths and probe lengths on the accuracy of moisture measurements. Soil calibration was performed to compare the TDR measurements against the gravimetric method for probes with different cable lengths. For locally fabricated TDR miniprobes, calibrations need to be done for each individual probe along with the type of the extension cable that will be used for the field soil moisture measurements.

2.2.5 Field installation of TDR miniprobes

TDR probes can be installed in the soil profile horizontally, vertically, or at an angle. Vertical installation of the TDR probes is the easiest due to ease in making vertical holes in the soil profile. However, it has a disadvantage of allowing preferential flow along the cable, which may be a source of air gaps between the probes and the soil (Dahan et al. 2003). In addition, if longer probes (> 150 mm) are used, it is not possible to measure the variation in soil moisture at smaller depth intervals such as 100 mm or less. Angular installation is done to capture both vertical and horizontal movements of

soil moisture, and to minimize preferential vertical flow through the insertion holes. To maintain uniformity of the angle of installation, a metal guide (e.g. Fig. 2.4) can be used to guide the probe and ensure that all the probes are installed at the same angle. Field lines from TDR sensors are concentrated near probe surfaces. Hence poor contact between probe and the soil (air gaps) may affect accuracy of the TDR measurement.

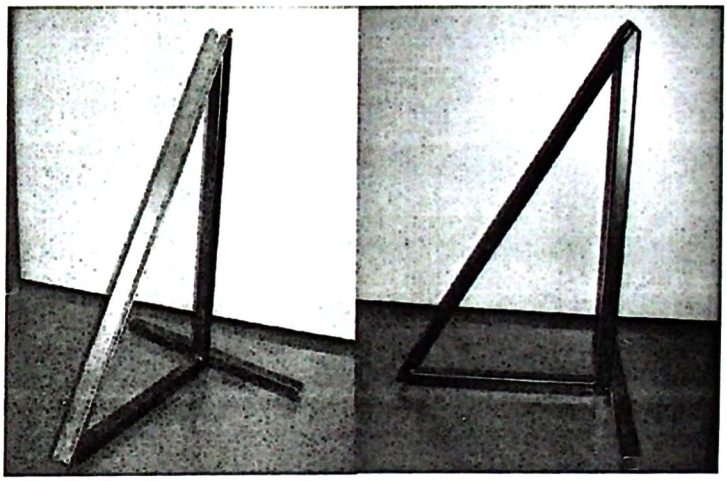

Fig. 2.4 Angular insertion metal guide (60-degree angle) for field installation of TDR miniprobes.

The angular installation of TDR probes has also been described by Dahan et al. (2003). During angular or horizontal installation, the steel rods of each probe are arranged in the same plane so that each leg would be at the same distance from the ground surface. Proper control of the angle of installation and the rod penetration depth will ensure that all the probes are positioned at the respective vertical depth from the ground surface.

2.2.6 Influence of extension cable lengths

Extension cables in TDR measurements are normally used in the field to extend the length of shorter cables (e.g. 2.5 m) attached to the probes embedded in the field. Ideally, shorter cables have been used for connecting individual probes when measuring soil moisture. Due to the narrow temperature range in which the TDR cable tester works (the operating temperature range for the 1502B TDR cable tester is -10 to 55°C, Tektronix, Inc., Beaverton, OR), the cable tester can not be taken to individual probes during the winter when the temperatures are much below -10°C. Therefore, extension cables can be used whereby the stationary TDR instrument is housed in a warmer compartment and connected to the probes in the field using extension cables (Hook and Livingston 1996; Logsdon 2000; Kahimba and Sri Ranjan 2007).

Other researchers have also used extension cables for taking TDR measurement with multiple probes (e.g. Logsdon 2000). Studies have also been made to simplify further the measurement of several sets of TDR probes by taking simultaneous measurements using automated multiplexers and the extension cables (Heimovaara 1993; Herkelrath and Delin 1999).

The use of extension cables, however, affects the accuracy of TDR measurements depending on the type and size of the cable used and the length extended. The length of the extension cable is also dependent on the temperature, and the type and size of the probes to be used (Deutsch et al. 1994; Kahimba et al. 2007). Therefore, if extension cables are to be used, calibration needs to be done to determine the optimum extension cable lengths depending on the type of the probes and cables to be used.

2.3 Neutron Scattering Method

2.3.1 General

Neutron Scattering (NS) technique is a classical non-destructive method of measuring soil water that allows repeated measurement of total water content. Unlike most other sensor techniques, NS is less sensitive to soil-probe contact (Brendan 2003). The method can be calibrated in the field with high precision, and it works better than the modern sensor methods in stony, cracking, and deeper soil profiles. Hence, NS technique is considered as among the best methods for repeated monitoring of total soil water content (Evett 2003a).

The main problem with the use of NS technique is the risk of radiation hazard, hence it requires licensing and training of the attendants, and it cannot be left unattended in the field. The method does not give spatial variation of moisture content, and it is less accurate for near surface measurements due to the possibility of neutrons escaping to the atmosphere. The NS technique also requires soil specific calibrations, and it uses a radioactive source that is expensive to store and dispose (Evett et al. 2002; Evett 2003a; Brendan 2003). Since the TDR method measures liquid water content and the NS measures total water content, a combination of the two methods can be used to partition the soil moisture into liquid and frozen water content when the soil is frozen or partly frozen during the fall, winter, and spring seasons.

2.3.2 Theory of the NS technique

Neutron scattering technique uses a radioactive source emitting fast neutrons, and

a detector source detecting slow neutrons thermalized and deflected back by soil constituents (Evett 2003a). A radioactive source produces high-energy fast neutrons in the soil at a rate approximately equal to 10^9 neutrons/s, with mean energy of 5 MeV. The high energy and fast neutrons emitted by the source can either collide with nuclei of larger soil constituent atoms and be absorbed, or collide with the larger nuclei and be deflected back to the detector with little energy loss. The neutrons can also collide with hydrogen atoms of approximately equal weight, which will cause them to be slowed due to reduced thermal energy level. The slowed neutrons will be deflected back to the detector with their kinetic energy significantly reduced and some of them absorbed by the hydrogen molecule (Evett et al. 2002; Evett 2003a). The concentration of the thermalized neutrons is directly proportional to the number of hydrogen atoms colliding with them. Since the main source of hydrogen in the soil is from water molecules, it can be related to the total volumetric soil moisture content (Evett 2003a). Calibrations are normally done to account for sources of hydrogen in the soil other than water, such as humus and organic matter, and other efficient nutrient thermalizers (e.g. Carbon, Nitrogen, and Oxygen).

2.3.3 NMM calibration and field data collection

The neutron moisture meter (NMM) used in the NS technique requires site-specific calibration. The NMM calibration involves correlation between neutron counts taken by the meter and volumetric water contents ($m^3\ m^{-3}$) taken using another method such as gravimetric method (Brendan 2003; Evett 2003a). During field calibration, neutron counts on a given soil are taken in a saturated, partially saturated, and air dry soil

condition. Thereafter, soil samples are taken at the same time and the corresponding moisture contents are determined using the gravimetric method. The calibration equation is established relating volumetric moisture contents with counts ratio (Evett, et al. 2002). To minimize measurement errors, it is recommended that the NMM has to be calibrated seasonally in the respective fields in which measurements are to be taken (Evett and Steiner 1995; Evett et al. 2002).

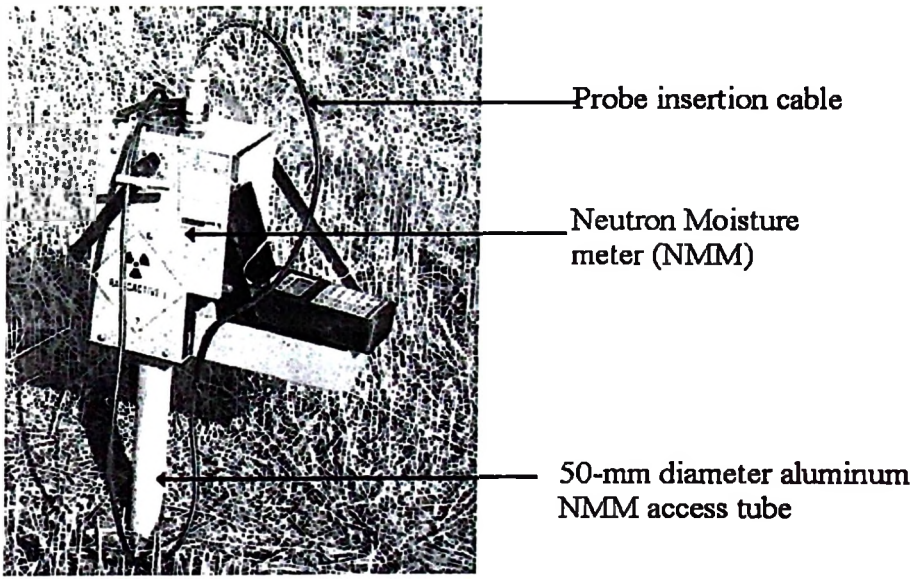

Fig. 2.5 A neutron moisture meter (Troxler model 4302, Troxler Electronic Laboratories Inc., Research Triangle Park, NC) in position on top of a 50-mm aluminum access tube.

The relationship between thermalized neutron counts and volumetric moisture content depends on field calibration for each specific soil. An empirical equation that relates volumetric moisture content with neutron counts ratio is given as:

$$\theta_v = a + b(CR) \tag{2.7}$$

where:

θ_v = volumetric moisture content,

CR = count ratio (ratio of slow neutron count at a specific location to standard count obtained when the NMM probe is in its shield), and

a, b = calibration coefficients depending on soil properties.

Once the calibration equation has been established for a specific soil, field measurements of the neutron counts at each depth can be converted to volumetric water content using this equation. The sphere of influence of measurements for the NMM, in which about 98% of the counted thermalized neutrons pass to reach the detector, is governed by a radius defined by Eq. 2.8 below (Troxler 2001):

$$R = 280 - 0.27M \tag{2.8}$$

where:

R = sphere radius of influence in the soil (mm), and

M = soil moisture content (kg/m^3).

The maximum radius of influence from the centre of a neutron access tube is 280 mm when the soil is completely dry. Hence, to avoid interference of the NMM measurements, any other installation in the field should be at least 0.3 m away from the neutron access tubes. In this study, the TDR miniprobes were installed at a minimum distance of 0.5 m away from the centre of the access tubes to avoid any interference between the TDR and the NMM measurements.

2.3.4 The neutron access tubes

During field data collection an access tube is normally inserted into the ground to

allow the NMM probe to be lowered into the soil profile. A plug is put at the bottom end to avoid water seepage into the access tube. The tube dimensions vary depending on diameter of probes from different manufacturers. A 50-mm diameter tube is normally used for Troxler moisture meters (Troxler Electronics Laboratories, Inc., Research Triangle Park, NC, USA). Materials commonly used for the access tubes are aluminum; polyvinylchloride (PVC); polycarbonate and polyethylene plastics; and mild and stainless steel. Plastic tubes are normally not preferred due to interference of the hydrogen molecules present in the plastic materials (Evett and Steiner 1995). Aluminum tubes are expensive, but they are the most preferable materials since they are transparent to the neutrons (Evett and Steiner 1995; Evett 2003a). However, irrespective of the tubing material used, it is recommended that the same type of material used during calibration should also be used in the field measurement in order to minimize calibration errors (Evett 2003a).

2.3.5 NMM radiation hazard and safety precautions

While the NS method is one of the most accurate techniques for determining field moisture content, the radiation emissions from the NMM can be a potential health hazard (Warrick 2002). The use of NMM requires special training on radiation hazards and safe handling procedures. The activity levels in most commercially available neutron meters range between 10 and 100 mCi (Brendan 2003). Safety precautions recommended while transporting and handling the neutron meters are: (1) maintain safe distance from the radiation source, (2) reduce the time that you are to be close to the meter, (3) use the recommended shielding, and (4) avoid physical damage to the instrument (Troxler 2001;

Evett 2003a; Brendan 2003). Due to the radiation hazard associated with a neutron moisture meter, it requires special certification to store, transport, and use. However, if the neutron meter is properly handled, the exposure to the radiation is normally within the permissible limits (Troxler 2001).

2.4 Infiltration and Soil Moisture Redistribution

2.4.1 Infiltration process

Infiltration can be defined as the process of water entering the soil profile from the soil surface (Marshall and Holmes 1988; Jury et al. 1991). Main forces contributing to infiltration are gravity and capillarity (Warrick 2002). The rate at which water enters the surface layer of the soil is called infiltration rate (f). However, the infiltration rate is initially high and declines to a constant rate called the basic infiltration rate (I_b). If the rainfall intensity is greater than the basic infiltration rate I_b, then infiltration rate equals I_b. If the intensity is less than I_b, then infiltration rate equals rainfall intensity (Gray et al. 1973; Warrick 2002).

When water infiltrates into a dry soil and percolates below, four main flow regions can be identified within the soil profile. They are the saturation zone, transmission zone, wetting zone, and the wetting front. The saturation zone is near the soil surface where soil pores are filled with water. The transmission zone below the saturation zone is the region where the soil is unsaturated, and some of the water moves by gravity. The wetting zone is the region in which moisture content increases as infiltration continues. It connects the transmission zone and the wetting front. The

wetting front forms the boundary between wet and dry soils below (Gray et al. 1973).

Various expressions are used to describe the process of infiltration into the soil. Examples are the Green & Ampt equation, Richard's equation (Flerchinger 2000; Warrick 2002), and Gardner & Wilstoe (1921). The Green & Ampt equation for infiltration is a finite difference approximation of the Richard's equation. The expression for Green & Ampt equation for infiltration rate, f (Marshall and Holmes 1988; Jury et al. 1991) can be written as:

$$f(t) = K_s + K_s \frac{\psi_{mf}(\theta_s - \theta_i)}{F} \quad \text{for } t > t_p \qquad [\text{cm}^3\ \text{s}^{-1}\ \text{cm}^{-2}] \tag{2.9}$$

$$f(t) = P \quad \text{for } t \le t_p \qquad [\text{cm}^3\ \text{s}^{-1}\ \text{cm}^{-2}] \tag{2.9a}$$

where:

P = precipitation rate (cm h^{-1}),

t_p = time when water begins to pond on the surface (h),

Ψ_{mf} = matric suction at the wetting front (cm of water),

K_s = saturated hydraulic conductivity (cm h^{-1}),

θ_s = saturated moisture content (cm^3 cm^{-3}),

θ_i = initial moisture content before infiltration began (cm^3 cm^{-3}), and

F = total volume (depth) of water infiltrated (cm).

When the soil is dry, the vertical infiltration rate is initially high, but it decreases with time to a constant value equal to the saturated vertical hydraulic conductivity of the soil medium (Marshall and Holmes 1988; Jury et al. 1991). The infiltration process is important since it controls the water balance within the soil (Warrick 2002; Miyazaki

2006). A better understanding of the infiltration and soil water movement in the soil are important for understanding the amount of water that is entering the soil, being stored, and the water leaving different layers of the soil profile.

2.4.2 Infiltration into frozen soil

The existence of water in three different phases has a great influence on its movements in frozen soils. Water can exist in frozen soils both in gaseous, liquid, and solid states. The main factors which govern the infiltration rate in frozen soils are the soil moisture content at the time of freezing and size of the ice-free pores (Gray et al. 1973; Baker 2001). Based on the initial water content before the soil freezes and the soil temperature during thawing, the infiltration process in frozen soil can be grouped into four main categories as shown in Fig. 2.6 below:

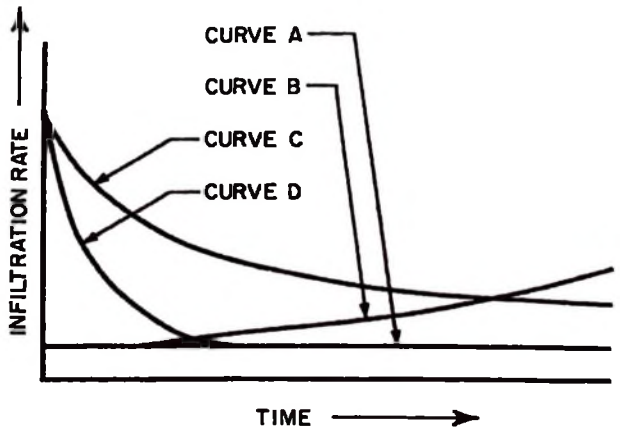

Fig. 2.6 Schematic diagram of infiltration rates in frozen soil for different moisture conditions prior to soil freezing: (A) saturated, (B) 70-80% saturated, (C) low moisture content & high temp, and (D) low moisture content & low temp *(Source: Fig. V.7 of Gray et al. 1973).*

From Fig. 2.6, if the soil is saturated during the fall when it starts to freeze, it will have a very small rate of infiltration and more precipitation will be converted to runoff (curve A). If the soil is frozen with high moisture content but not saturated (e.g. 70 – 80% of field capacity), some melting water from precipitation will infiltrate into the soil and will transfer heat through the pores, melting the frozen water within the soil profile. Hence, infiltration rate will increase with time (curve B). When the temperature is near or above freezing during thawing infiltration will proceed as in normal dry soil, decreasing with time, for soils that froze at low moisture content (curve C). When the soil is frozen at low moisture content and when snowmelt occurs at soil temperature below freezing point, water from snowmelt that infiltrates into the open pores will be frozen, blocking the pores, hence limiting further infiltration (curve D) (Gray et al. 1973). Therefore, the soil moisture status at the time of freezing during the fall greatly affects the infiltration process during the fall freeze-up and spring snowmelt.

2.4.3 Factors affecting infiltration

As the soil freezes and the freezing front advance downwards, the unfrozen soil moisture below the freezing front migrates upward towards the freezing front. Partly saturated frozen soils act like dry soil, pulling unfrozen water upwards from the lower layers because the water above the freezing front is already immobilized due to freeze-up (Flerchinger 2000).

Factors that affect infiltration are soil surface conditions, vegetation cover, soil physical properties, temperature, and chemical composition of the water (Marshall and Holmes 1988; Jury et al. 1991). Other factors are the hydraulic conductivity, soil

saturation, snow cover, and frost depth (Warrick 2002; Hillel 2004).

When soils warm up during spring, relatively drier soil requires lesser solar heat to warm up compared to the wetter soil due to the lower heat capacity of drier soil compared to wetter soil (as explained in section 2.1.3). The drier soil will have a higher infiltration rate during spring snowmelt due to the increased capillary gradient resulting from a shallower frozen layer. Generally, the flow of water in the soil under unsaturated conditions can be expressed using Darcy's law (Marshall and Holmes 1988; Jury et al. 1991; Hillel 2004) as shown in Eq. 2.10 below:

$$q = -K(\theta)\frac{dh}{dl} \tag{2.10}$$

where:

q = water flux or specific discharge (m s^{-1}),

$K(\theta)$ = unsaturated hydraulic conductivity (m s^{-1}),

dh/dl = hydraulic gradient,

h = total hydraulic head (m) ($h = p/\rho g + z$), and

l = distance (m).

According to the Darcy's law, the water flux in the soil profile depends on the hydraulic conductivity $K(\theta)$ and the hydraulic gradient dh/dl, (where dh is the difference in total head between two points, and dl is the distance between the two points). Drier soil with shallower depth of frozen soil layer will have smaller depth (dl) of the frozen soil layer due to earlier thawing of the upper soil layers. The shallower depth of frozen soil layer will lead to higher hydraulic gradient in drier soils compared to wetter soils. The smaller depth of frozen soil layer causes the component of the hydraulic gradient (dh/dl)

to be larger, hence making the water flux, q in the soil profile to be larger (Hillel 2004; Miyazaki 2006). Even though the initial lower soil moisture will lead to a lower unsaturated hydraulic conductivity, the increase in melt water infiltration into the upper soil layers will cause an increase in the unsaturated hydraulic conductivity of drier soils.

2.4.4 Soil moisture redistribution

The infiltration process ceases when the water supply (e.g. from precipitation or ponded water) has stopped and the ponded water has been depleted. The infiltrated water will continue to percolate and redistribute itself from regions of high water to low water contents (Marshall and Holmes 1988; Jury et al. 1991; Hillel 2004; Miyazaki 2006). Soil moisture redistribution can therefore be defined as the movement of infiltrated water in the soil profile (Jury et al. 1991; Charbeneau 2000). Part of the infiltrated water may be lost by evaporation and transpiration at the surface, while some will be moving downwards by gravitational and capillary forces. The redistribution of soil moisture in the soil profile determines the amount of water that can be retained by each layer, and the available soil moisture at the start of the next infiltration process (Charbeneau 2000; Hillel 2004).

2.4.5 Soil moisture redistribution in freezing soils

Soil freezing and thawing processes affect the migration of water in frozen soils. When the soil freezes from the top, the amount of unfrozen moisture in the top layers is reduced since some of the water will be converted into solid state (ice), thereby increasing the capillary gradient towards the freezing soil layer. Water will redistribute

from the bottom unfrozen layers that are at higher soil water potential to the upper frozen layers with low water potential (Xiaozu et al. 1987; Stahli et al. 1999). The redistribution of soil moisture in a freezing soil is assumed to be analogous to the redistribution in a drying soil (Flerchinger 2002). Hence, for modeling purposes the hydraulic conductivity and matric potential equations that define the soil moisture characteristic of a particular soil (Eq. 2.11) are assumed to be applicable to both frozen soils and unsaturated soils (Flerchinger and Hanson 1989; Flerchinger 2000).

$$\psi = \psi_e \left(\frac{\theta_l}{\theta_s}\right)^{(-b)} \tag{2.11}$$

where:

ψ = soil matric potential (m),

ψ_e = air entry potential (m),

θ_l = water content at a given time ($m^3\ m^{-3}$),

θ_s = saturated water content ($m^3\ m^{-3}$), and

b = pore size distribution index.

Studies however have indicated that, in a freezing soil, the part of soil water that freezes at low temperatures (ice) affects the effective porosity of the freezing soil, hence affecting its hydraulic conductivity (Xiaozu et al. 1987). Janowicz et al. (2003) observed that frozen water in the soil matrix increases the water flow path, and decreases the hydraulic conductivity by blocking the soil pores and increasing the tortuosity. The soil temperature, soil type, amount of initial water content, and dry density of the soil are among other factors that influence the movement of water in frozen soils (Xiaozu et al. 1987, Lunardini 1988). Hence, it is crucial to understand the hydrological processes

occurring during soil freezing and thawing to be able to properly predict the amount and redistribution of soil moisture in frozen soils.

2.4.6 Soil freezing and thawing

Soils can exist in frozen condition at low temperatures. Freezing of soil depends on its physical and chemical properties. It is mainly caused by fluctuations in soil temperature (Luo et al. 2002). The frost depth depends on factors such as snow depth, soil temperature, soil cover, and soil physical properties (Baker 2001; Hillel 2004). The freezing and thawing of soil cause changes in its physical properties. When the soil freezes, water in the pores also freezes causing the soil to expand, thereby reducing its bulk density. The infiltration rate of the soil is reduced when the frozen water creates ice lenses, which prevent further entrance of water (Baker 2001). Formation of cracks in frozen soil causes random macro pores that cause random water flow after thawing. Other problems associated with freezing and thawing of soils are migrations of hazardous compounds and agrochemicals in the soil, hill slopes stability, and frost heaving in structures (Jury et al. 1991; Hillel 2004). Therefore, the soil freeze-thaw processes affects the soil properties, hence the hydrological processes happening within the soil, and the whole soil-plant-atmosphere ecosystem's energy and water balance.

2.5 Soil Temperature

2.5.1 General

Soil temperature is among important factors that influence the soil freezing and thawing. It has a great influence on the distribution and movement of water within the soil. The soil temperature also controls microbial activities and other processes responsible for plant growth (Gupta et al. 1982, 1984; Spokas and Forcella 2006). Soil temperature constantly varies both diurnally and seasonally, with solar radiation being the main heat source that influences soil temperature changes (Winslow et al. 2001; Hillel 2004). For the diurnal case, variations are more pronounced at the top with maximum temperature during the day and minimum at night. The amplitude of variations are extreme at the soil surface and decrease with depth to a constant value equal to average annual temperature at approximately 4.0 m from the soil surface (Flerchinger 2000). The amplitude of maximum and minimum temperatures has a time-lag at each depth, with the lag increasing with depth (Gupta et al. 1984; Warrick 2002).

During soil freezing, the temperature profile in a frozen soil increases from the soil surface through frozen layers to unfrozen layers below. At low temperatures, soil moisture migrates from regions of higher temperature to low temperature. Therefore, when frozen and unfrozen or partly frozen soil layers exist, the soil temperature will influence the redistribution of soil moisture between different layers within the soil profile.

2.5.2 Soil thermal properties

The response of the soil to temperature change is dependent on the soil moisture status, its bulk density, and the main soil thermal properties: volumetric heat capacity, thermal conductivity, and thermal diffusivity (Marshall and Holmes 1988; Lunardini 1988; Jury et al. 1991; Hillel 2004). Details of the relationships between the thermal properties and water content have been discussed before (see section 2.1.3). The movement of heat energy from higher to lower temperatures within the soil occurs by conduction, convection, and thermal radiation, with the thermal conduction being the dominant mechanism (Jury et al. 1991). The Fourier's law for heat flow by thermal conduction (Flerchinger 2000; Warrick 2002) is given as:

$$\frac{dQ}{dt} = -kA\frac{dT}{dx} \tag{2.12}$$

where:

Q = amount of heat transferred (W),

t = time (s),

k = thermal conductivity (W m^{-1} K^{-1}),

T = temperature (K),

x = distance between two ends (m), and

A = cross-sectional area (m^2).

The heat transfer between different layers will therefore be controlled by the difference in temperatures between the soil layers, thickness of the soil layers, and the soil thermal properties of each individual layer. In-situ soil temperature measurements

using thermal probes such as thermocouples are taken at depths such as 50, 100, 200, and 400 mm from the soil surface (Gupta et al. 1982, 1984, 1990; Guaraglia et al. 2001). Soil temperature at the surface of the soil is difficult to measure by these probes due to the difficulty in establishing soil probe-surface contact without affecting the microclimate characteristics at the soil surface (Gupta et al. 1982).

Despite the difficulty in the physical measurement of the temperature at the soil surface, surface soil temperature is needed for modeling purposes such as using the Simultaneous Heat and Water (SHAW) model (described in section 2.8.3). Hence, for modeling purposes, it is important to determine a method for estimating the surface soil temperature. Models for estimating the surface soil temperature use either observed soil temperatures near the soil surface, or air temperatures normalized based on daily maximum and minimum air temperatures (Gupta et al. 1982; Guaraglia 2001). Estimation of surface soil temperature based on air temperature is commonly preferred due to the ease in getting hourly or daily weather parameters from automatic stations.

2.5.3 Determination of surface soil temperature from air temperatures

Soil surface temperature can be obtained by either determining surface energy balance, interpolating with observed temperatures below the soil surface, or by estimating it from maximum and minimum air temperatures (Gupta et al. 1982, 1984; Guaraglia et al. 2001). Gupta et al. (1990) presents one of the methodologies for predicting surface soil temperature using thermal diffusivity calculations and the recorded air temperatures.

During field data collection in this study, the temperature probes were installed at 0.1, 0.2, 0.4, 0.6, and 0.8 m depths from the ground surface. Since surface temperature

was required as an input in the model simulations, the surface temperature was estimated using air temperatures. Soil temperature at 4.0 m depth is normally assumed to be constant and equal to average annual temperature of the location (Flerchinger 2000; Warrick 2002). Procedures for determining surface temperature from air temperature as presented by Gupta et al. (1990) are briefly summarized as outlined below:

Table 2.1 Regression statistics of the cubic function (after Gupta et al. 1990)

	Regression statistics*					
Position**	a	b x 10^2	c x 10^3	d x 10^4	R^2	SE***
Bare ridge						
F	11.97	-76.56	109.62	-18.10	0.83	4.01
1/3NF	11.46	-124.58	169.08	-31.30	0.80	5.31
2/3NF	8.56	-117.87	184.17	-35.25	0.79	6.12
P	4.12	-49.25	137.30	-26.61	0.87	4.43
1/3NP	5.69	19.57	55.83	-9.56	0.91	2.64
2/3NP	7.62	-4.28	65.64	-10.90	0.90	2.72
Residue plus plant-cover ridge						
F	8.93	46.65	4.92	0.68	0.77	2.81
1/3NF	9.75	1.66	42.02	-5.01	0.76	4.05
2/3NF	8.98	-29.86	72.79	-9.83	0.76	5.12
P	6.12	1.16	59.33	-8.84	0.78	4.61
1/3NP	7.62	28.23	26.42	-3.19	0.85	1.71
2/3NP	8.68	38.04	12.03	-0.47	0.83	2.44

* a, b, c, d are the regression statistics parameters used in the cubic fit (Eq. 2.13)

** Various positions in the ridge (as defined in Fig. 2.7).

*** SE is the standard error of measurement.

The maximum and minimum air temperatures at 2.0 m height are determined for each day from a nearby weather station. The regression statistics for the cubic function (Eq. 2.13) are obtained from the Table 2.1, which relates the maximum and minimum soil surface temperature with maximum and minimum air temperature for a bare ridge or vegetation-covered ridge. The various positions in the ridge for both the bare and vegetation-covered ridge are shown in Fig. 2.7 below:

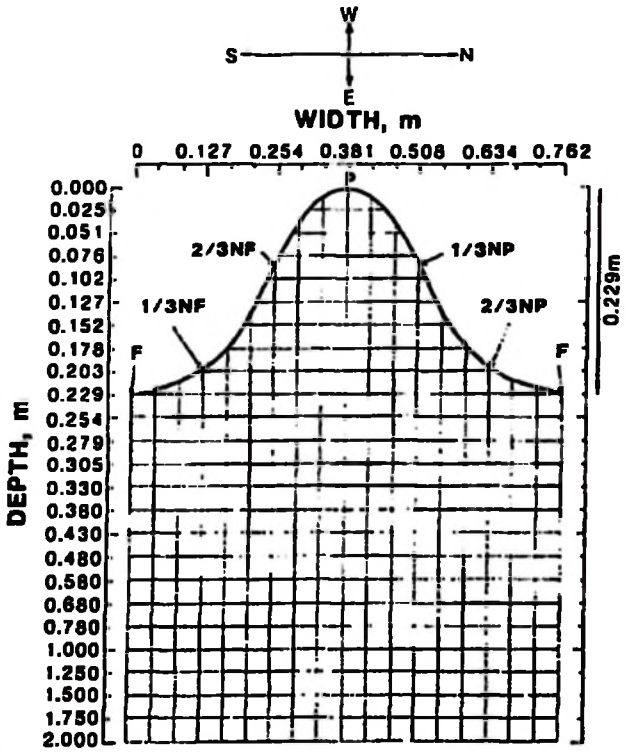

Fig. 2.7 Ridge positions for the determination of surface soil temperature (*Source: Gupta. et al. 1990*).

The position *P* in Fig. 2.7 indicates the top of the ridge and *F* the bottom of the ridge. On high latitude regions such as the Canadian prairies, the ridge surfaces may warm differently depending on whether the surface is facing North or South (Spokas and

Forcella 2006). However, the top of the ridge that is fully exposed to the incoming solar radiation may not be affected by the ridge aspect effect. Hence, it can be taken as a better approximation of the radiation reaching a flat surface.

The regression statistics for the selected location in the ridge and the maximum or minimum air temperature are used to determine the maximum or minimum surface temperature at a given position in the ridge using the following cubic fit (Gupta et al. 1990):

$$y = a + bx + cx^2 + dx^3 \tag{2.13}$$

where:

y = maximum or minimum surface temperature at a given position in the ridge, and

x = maximum or minimum air temperature at 2.0 m height.

For each hour of the day, the average normalized hourly soil surface temperature curve is described using a Fourier series (Gupta et al. 1990) as follows:

(a) $$\Gamma_{0t} = 0.421 + 0.434\sin(\omega t + 4.09) + 0.101\sin(2\omega t + 0.83) \tag{2.14}$$

where:

Γ_{0t} = average normalized hourly soil surface temperature for a bare ridge

ω = $2\pi/P$ where, P is the period (24 h or 86,400 s), and

t = hour of the day (0, 1, 2, 3 ...23).

(b) $$\Gamma_{0t} = 0.445 + 0.424\sin(\omega t + 3.98) + 0.097\sin(2\omega t + 0.77) \tag{2.15}$$

where:

Γ_{0t} = average normalized hourly soil surface temperature for a residue

and plant-coverage ridge.

The estimated hourly soil temperature series is then estimated using the normalized hourly values and the maximum and minimum soil surface temperature as follows:

$$T_{ot} = \Gamma_{ot}(T_{o\max} - T_{o\min}) + T_{o\min} \tag{2.16}$$

where:

T_{ot} = the estimated soil surface temperature at time t,

Γ_{ot} = average normalized hourly soil surface temperature,

T_{omax} = estimated maximum soil surface temperature, and

T_{omin} = estimated minimum soil surface temperature.

The values of soil surface temperature obtained from Eq. 2.16 can be used as input parameters for the surface node in models such as the SHAW model that require surface soil temperature as one of the input parameters.

However, it is important to note that estimation of surface soil temperature from air temperature as proposed by Gupta et al. (1990) may not be accurate when the ground is covered with a layer of snow, since the snow provides insulation of the soil surface (Xiaozu et al. 1987; Lunardini 1988; Hillel 2002). Hence if actual soil measurements are available for other soil layers close to the soil surface, a better approximation of the surface soil temperature on snow-covered grounds could be obtained by interpolation with measured near-surface soil temperature profiles rather than using the models that use air temperature such as the one proposed by Gupta et al. (1990).

2.6 Cover Crops

2.6.1 Introduction

Cover crops are annual, biennial, or perennial plants grown in the fields alone (monoculture) or within other main crops (intercropping production system). They are normally grown for the purpose of covering the soil to protect it from erosion and to prevent plant nutrient losses by surface runoff and leaching (Dabney et al. 2001). Other purposes of growing cover crops are to control weeds, pests, and plant diseases (Sainju 2005); to improve water quality by reducing sediment losses towards streams and rivers (Dabney et al. 2001); and to facilitate infiltration by reducing precipitation runoff (Nielsen et al. 2002). Cover crops also reduce evaporation by covering the ground and minimizing convective exchange of soil water vapor at the soil surface. When the cover crops are incorporated into the soil, they improve the soil quality by increasing organic matter concentration, and recycling nutrients (Sainju 2005).

Cover crops can be grouped into two main groups: leguminous and non-leguminous. Examples of non-leguminous cover crops are winter wheat (*Triticum aestivum L.*), rye (*Secale cereale*), and ryegrass (*Lolium perenne L.*) (Dabney et al. 2001; Boquet et al. 2004). Advantages of non-leguminous cover crops are low cost of establishment, fibrous root system that provides longer and better erosion protection, and more winter growth resistance (Dabney et al. 2001). The non-leguminous cover crops have disadvantages of not being able to fix nitrogen (N), hence they are prone to N depletion, and they may require additional N fertilizer (Bonfil et al. 1999; Joyce et al. 2002).

Examples of leguminous cover crops are alfalfa (*Medicago sativa L.*), hairy vetch (*Vicia villosa Roth*), various species of clover (*Trifolium spp.*), and winter peas (*Pisum sativum L.*) (Entz et al. 2002; Joyce et al. 2002). The main advantage of leguminous cover crops such as berseem clover (*Trifolium alexandrium* L.) is their ability to fix nitrogen in the soil, hence minimizing the nitrogen N fertilizer and energy requirements (Dabney et al. 2001; Entz et al. 2002; Boquet et al. 2004). Studies have also shown yield increase of cereal crops planted following leguminous cover crops (e.g. Boquet et al. 2004). In general, all types of cover crop have the additional potential of being used as rotational or cash crops, and for forage harvest.

The use of cover crops has some shortcomings. Examples of disadvantages associated with cover crop are additional costs of seeds, planting and termination of the cover crop; increase in risks of diseases and pests; and reduction of soil moisture (Joyce et al. 2001; Sainju 2005). Hence, the decision on whether to adopt a cover cropping system and the choice of the cover crop to be used will depend on evaluations of the agronomic and economic merits and demerits of different options of the cover cropping and other rotational management systems.

2.6.2 Use of cover crops in areas experiencing excess precipitation

The presence of excess soil moisture in the root zone can cause soil moisture stress to the plants in areas receiving excess precipitation. The excess water in the root zone causes oxygen depletion, resulting in poor root respiration and accumulation of phyto-toxic compounds (Cavers and Heard 2001). The waterlogged conditions also cause loss of nitrogen in the soil by changing the redox potential of the soil (Cavers and Heard

2001). A combination of these factors can lead to yield losses associated with excess soil moisture.

The severity of the impact of excess soil moisture on crop yield depends on factors such as the stage of plant growth, soil type, duration of water logging, and plant species (Cavers and Heard 2001). Cavers and Heard (2001) noted that, in clay soils, the presence of excess soil moisture during anthesis (flowering) stage had the largest negative impact on crop yields compared to other types of soil and other stages of plant growth. Cover crops can reduce excess soil moisture, thereby minimizing the soil water stress to the main crop. They can also facilitate reduction of water in the root zone by increasing the evapotranspiration (Sainju 2005). The cover crops also improve the field trafficability and increases the population of beneficial insects (Ess et al. 1998; Dabney et al. 2001; Entz et al. 2002). Hence, using cover crop can potentially be a better farm management alternative in agricultural soils that are located in wetter areas.

2.6.3 Use of cover crops in areas receiving low precipitation

The presence of a cover crop may cause soil moisture competition with the main crop in areas receiving low precipitation during the growing season. The within-season effects can occur especially if the cover crop is planted early in the growing season (Sainju 2005). The presence of a cover crop has been shown to increase the evaporative demand, thereby depleting soil water storage for the subsequent crops (Joyce et al. 2001). The same study also suggested that soil water storage for the subsequent season could be improved if the cover crop is destroyed early to reduce water losses by evapotranspiration. Bonfil et al. (1999) observed increased yield when a wheat-fallow

cropping system was used compared to continuous wheat. The higher yield in the wheat-fallow system was associated with soil moisture storage in the absence of crop growth during the fallow season. Hence, when cover crops have to be used in drier soils, consideration has to be made on soil moisture competition between main crop and the cover crop, and the soil moisture storage for the following growing season.

2.6.4 Influence of cover crops on soil freezing and thawing

Cover crops planted during the fall can be advantageous during the winter and next spring season. Winter cover crop can reduce winter weed growth and prevent deep penetration of frost, thereby allowing earlier thawing of the soil (Dabney et al. 2001; Joyce et al. 2002; Kahimba and Sri Ranjan 2007). The crop residues from the winter cover crop will increase organic matter early in the next growing season. Cover crops that are planted as living mulch with the main crop in the summer continue to grow during the fall after harvest of the main crop and deplete the soil moisture prior to soil freezing. At the onset of fall freeze-up, the soils that had cover crop will freeze with lower soil moisture compared to the soils that had no cover crop (Boquet et al. 2004; Kahimba and Sri Ranjan 2007). The amount of initial soil moisture prior to soil freezing can influence the depth and timing of freezing as explained in sections 2.1.3 and 2.4.2 above. Hence, the presence of cover crop is expected to influence the response of the soil to freezing during the fall and winter, and the thawing response in the following spring.

2.7 Unsaturated Flow Models

2.7.1 General

The physical and hydrological processes that occur in the soil, snow, plant, and atmosphere ecosystem can be measured either directly, or predicted using numerical models. The direct methods that can be used to measure soil moisture in the field (e.g. gravimetric method, TDR, NS, and FDR) have problems of being tedious, expensive and time consuming for wider coverage (Hymer et al. 2000). The direct methods are also limited to discrete measurements and they cannot be used to determine spatial and temporal distributions at a regional scale. The methods also cannot be used to predict the future distribution of moisture and other hydrologic parameters (Flerchinger 1991; Flerchinger and Hanson 1989; Amer et al.1994). The problems associated with direct moisture measurement can be accounted for by the use of numerical models.

The modeling approach can be used to simulate processes happening in the soil and predict the future performance for given initial and boundary conditions. The main challenge of the modeling approach is accurate representation of the modeled processes, and proper solution of mathematical equations that represent the mechanisms (Vanderborght et al. 2005). Hence, better simulation models can accurately represent complex boundary conditions and non-linear processes with mathematical equations, and provide accurate solutions of the associated flow and transport equations (Ross 2003; Vanderborght et al. 2005).

Advantages of using numerical models are prediction of present and future events,

study of water and nutrient movement over a wider coverage (e.g. regional scale), and accurate simulation of field conditions (Vanderborght et al. 2005). The modeling approach has its own shortcomings: Most of the models are data intensive, they are general and not specific, inaccurate for field conditions, time consuming (to develop), and expensive (Flerchinger and Hanson 1989; Gronsten 2001). Models may also fail due to complications associated with winter hydrology, and they may be specific depending on the conditions of the soil where the model was developed. With the advancement in computing technology and development of faster processors, detailed models are now available that can accurately represent the physical conditions with more input parameters, yet minimizing the computing time (Ross 2003).

2.7.2 Flow models for soil freezing and thawing

Models for water and solute transport range from one-dimensional (1-D) seepage flows to complex multiphase flow and multi species transport that consider both conservative and non-conservative solutes. Examples of 1-D models are HELP (Warrick 2002), HYDRUS-1D (Vanderborght et al. 2005), CLASS (Verseghy et al. 1993), SHAW (Flerchinger 1991), and WEPP (Gronsten 2001). Most models dealing with water and solute transport do not account for soil freezing and thawing processes. This is due to complex nature of the soil associated with freezing and thawing. Examples of models that incorporate the component of soil freezing and thawing are the SOIL (simulation model for soil water movement and heat) by Jansson (1991), SHAW (Simultaneous Heat and Water) by Flerchinger and Saxton (1989a, 1989b), CLASS (Canadian Land Surface Scheme) by Verseghy et al. (1993), FROST (Kennedy and Sharratt 1988), and SEWAB (Surface Energy and Water Balance) (Warrach et al. 2001).

In this research, the SHAW model was used to predict frost depth, soil temperature, and soil moisture redistribution under freeze-thaw conditions. The SHAW model, originally developed by Flerchinger and Saxon (1989a), has been used in many other researches that deal with soil freezing and thawing (e.g. Flerchinger et al. 1996; Flerchinger 2000; Guaraglia et al. 2001; Lin and McCool 2006). The model performance has also been tested against other models. Kennedy and Sharratt (1998) compared SHAW, SOIL, Benoit, and Gusev models and concluded that the SHAW and SOIL models had better predictions of frost depth. The SHAW model is regarded as one of the most detailed models for simulating the soil freeze-thaw processes (Kennedy and Sharrat 1998; Flerchinger 2000). Hence, the SHAW model was selected for use in this study based on its accuracy and the inclusion of the soil freeze-thaw processes in detail.

2.7.3 The Simultaneous Heat and Water (SHAW) model theory

The SHAW model simulates a vertical one-dimensional profile of the soil, surface residue, vegetation cover, and snow cover. It incorporates simulation of heat, water, and solute transfer within the soil and plant ecosystem (Flerchinger 2000). Mathematical formulations in the model have been solved using implicit difference equations for each layer of the soil. Equations that relate the soil hydraulic properties (K, θ, and ψ) have been assumed as per Brooks and Corey (1966). Water flux through the soil, taking into account the soil freezing and thawing, is given in Eq. 2.17 below (Flerchinger 2000):

$$\frac{\partial \theta_l}{\partial t} + \frac{\rho_i}{\rho_l}\frac{\partial \theta_i}{\partial t} = \frac{\partial}{\partial z}\left\{K\left(\frac{\partial \varphi}{\partial z} + 1\right)\right\} + \frac{1}{\rho_l}\frac{\partial q_l}{\partial z} + U \qquad (2.17)$$

where:

θ_l = volumetric liquid water content ($m^3\ m^{-3}$),

θ_i = volumetric ice content ($m^3\ m^{-3}$),

K = saturated hydraulic conductivity ($m\ s^{-1}$),

t = time (s),

z = soil depth (m),

φ = soil matric potential (m), and

U = source/sink term ($m^3\ m^{-3}\ s^{-1}$).

From Eq. 2.17, change in volumetric liquid water content and change in volumetric ice content are determined by net liquid influx into a specified soil layer, net vapor influx, and water extraction by plant roots. Flerchinger and Pierson (1991), Flerchinger et al. (1996), and Flerchinger (2000) describe details of physical system of the model.

2.7.4 The SHAW model input parameters

The SHAW model uses input parameters that can be grouped into five main categories: 1) general input-output files; 2) initial profile soil moisture; 3) initial soil temperature profile; 4) weather data; and 5) description of site characteristics (Flerchinger 2000). The soil temperature profile and soil moisture data used in this study were obtained from field measurements done at the Ian N. Morrison Research Farm in Carman, Manitoba, from August 2005 to September 2007. Soil properties in the site characteristics input file were obtained from soil survey that was performed during establishment of the research farm (Mills and Haluschak 1993).

The weather data were obtained from an automatic weather station near the study site. The weather parameters needed in the SHAW model are air temperature, wind speed, relative humidity, precipitation, and daily or hourly incoming solar radiation.

However, most weather stations either do not record solar radiation data, or they record for a specific period of the year. On average for every 500 weather stations worldwide, only one station measures solar radiation (Spokas and Forcella 2006). At the Carman weather station for example, the average solar radiation (W/m^2) is only measured seasonally during the growing season (May to August). Hence, for year-round modeling purpose, alternative approach of estimating the incoming solar radiation from the commonly measured weather parameters had to be considered.

2.7.5 Estimation of solar radiation using limited weather data

2.7.5.1 Daily solar radiation. Solar radiation, R_s is measured directly in the field using solar radiation measuring devices such as pyranometer. It can also be estimated indirectly using weather data such as maximum and minimum air temperatures, duration of sunshine, and vapor pressure (Spokas and Forcella 2006). In the absence of detailed weather data, the solar radiation can be estimated either by interpolation using data from a nearby weather stations, or using a difference between maximum and minimum air temperatures. The difference in air temperature is directly related to the cloud cover, which also determines the amount of net radiation reaching the earth's surface for a given location and time (Allen et al. 2002; Spokas and Forcella 2006).

The shortwave solar radiation, R_s, is the solar radiation that actually reaches the surface of the earth at a given period. The R_s is estimated from extraterrestrial radiation R_a, which is the amount of radiation reaching the top of the atmosphere on a horizontal surface (Winslow et al. 2001; Allen et al. 2002). The daily extraterrestrial radiation (R_a) for a given location depends on solar constant, latitude of the area, day of the year, and

solar declination (Jury et al. 1991). When the sun rays are at right angles to the surface at the top of the atmosphere, the R_a becomes equal to the solar constant, G_{sc} (0.0820 MJ m^{-2} min^{-1}) (Winslow et al. 2001; Allen et al. 2002). Hence for a given location and time of the year, Allen et al. (2002) presents an equation for calculating the R_a as follows:

$$R_a = \frac{24 \times 60}{\pi} G_{sc} d_r [\varpi_s \sin\varphi \sin\delta + \cos\varphi \cos\delta \sin\varpi_s] \quad (2.18)$$

where:

R_a = extraterrestrial radiation (MJ m^{-2} d^{-1}),

G_{sc} = solar constant = 0.0820 (MJ m^{-2} min^{-1}),

d_r = inverse relative distance Earth-Sun,

ω_s = sunset hour angle (Eq. 25 or 26 of Allen et al. 2002) (radians),

φ = latitude of the area (radians) = [(π/180) x decimal degrees], and

δ = solar declination (radians).

$$d_r = 1 + 0.033 \cos\left[\frac{2\pi(J)}{365}\right] \quad (2.18a)$$

where:

J = Julian day of the year

$$\omega_s = \arccos[-\tan\varphi \tan\delta] \quad (2.18b)$$

$$\delta = 0.409 \sin\left[\frac{2\pi(J)}{365} - 1.39\right] \quad (2.18c)$$

The R_s can then be calculated from R_a and maximum and minimum air temperatures as follows (Allen et al. 2002):

$$R_s = R_a k_{Rs} \sqrt{(T_{max} - T_{min})} \quad (2.19)$$

where:

T_{max} = maximum air temperature (°C),

T_{min} = minimum air temperature (°C), and

k_{Rs} = adjustment coefficient ($°C^{-0.5}$), 0.16 for inlands areas and 0.19 for coastal areas.

The calculated R_s (MJ m^{-2} d^{-1}) can then be multiplied by a factor of 11.6 to convert it to the average daily solar radiation in W m^{-2}, the radiation units used in the SHAW model.

2.7.5.2 Hourly solar radiation. The SHAW model has another alternative of using hourly solar radiation as input parameters in the weather data. The hourly solar radiation for the missing data can also be calculated using models that use limited weather data as input parameters (Spokas and Forcella 2006; Kahimba et al. 2008a). The SolarCalc model developed by Spokas and Forcella (2006) is one such example. The input parameters in the SolarCalc model are total daily precipitation, daily maximum and minimum air temperatures, latitude and longitude of the area, and elevation. The SolarCalc model gives the hourly incoming solar radiation (W m^{-2}) as output. Details of estimating the hourly solar radiation using limited weather data are available in Spokas and Forcella (2006).

Hence, using the measured soil moisture and soil temperature data, and the weather and site characteristics of the study area, model simulations can be performed and

comparisons can be made between the measured and predicted soil physical processes in the respective study area.

2.8 Chapter Summary

Studies on physical and hydrological processes of the soil-plant-atmosphere ecosystem are complicated due to complex nature of the processes that happen in the soil. The complexity of soil physical processes is even magnified when they are associated with soil freezing and thawing (Flerchinger et al. 1996; Kennedy and Sharrat 1998). The presence of vegetation on the soil, such as cover crops, modifies the physical processes in the soil. The presence of cover crops in agricultural fields has both agronomic advantages and disadvantages. During their growth period, the cover crops consume both soil moisture and nutrients from the soil. Hence, depending on availability of soil moisture to the main crop, they may cause competition for moisture and nutrients with the main crop (Joyce et al. 2002).

The soil moisture reduction by cover crops during the summer growing season influences the response of the soil to freezing and thawing during the fall. The residual effects may also influence the soil moisture redistribution during the winter and the subsequent response of the soil to thawing during spring (Kahimba and Sri Ranjan 2007). Modeling approach can be a better alternative for understanding the complex processes happening in the soil and for predicting the future response of the soil.

3. IMPACT OF CABLE LENGTHS ON THE ACCURACY OF DIELECTRIC CONSTANT MEASUREMENTS BY TIME DOMAIN REFLECTOMETRY

3.1 Abstract

Time Domain Reflectometry (TDR) probes are usually connected with a 2-m long coaxial cable to the TDR instrument necessitating the instrument to be close to the point of measurement. However, during the wintertime, the TDR instrument has to be operated in a warm enclosure and connected with an extension cable to the probes embedded in the field. The varying length of the extension cable has an influence on the accuracy of measurement. This paper presents the influence of extension cable length on the accuracy of dielectric constant measurement. Measurements were made in pure water using eleven coaxial cables with lengths from 2.5 to 70.0 m. The TDR probes were made of stainless steel rods 1.6 mm diameter and 35-mm long (3-rod configuration). The dielectric constant of water calculated from the waveforms obtained with varying lengths was compared to the actual values of the dielectric constant at 20±0.3°C. The sensitivity of measurements decreased with increasing cable lengths. Cables from 2.5 to 40.0 m measured the dielectric constant accurately, with a variation in dielectric constant of ±0.05. In a moist sandy soil, only the water content influences the dielectric constant of the media. The maximum cable length for the RG-58 cable was found to be 40.0 m. A regression equation was derived relating physical and apparent cable lengths. This equation could be used to correct for the change in dielectric constant measurement arising from varying cable lengths. Results from this study can be used to develop calibration equations for different extension cable lengths.

3.2 Introduction

3.2.1 General

Time Domain Reflectometry (TDR) is a widely used method for measuring soil water content and electrical conductivity. The ability to measure non-destructively both water content and electrical conductivity simultaneously makes it a very important method for measuring water content and nutrient movement in porous media (Vanclooster et al. 1994; Robinson et al. 2003a). The accuracy of measurement with TDR instruments depends on factors such as cable length, probe length, calibration method, waveform analysis, and temperature (Zegelin et al. 1992; Logsdon 2000; Evett 2000c; Robinson et al. 2003b). In this study, the influence of cable length on the accuracy of the TDR method for dielectric constant measurements is presented. Calibrations of the extension cables were performed to determine the maximum length of the RG-58 50 Ω coaxial cable used in the experiment.

The TDR probes are usually connected with a 2-m long coaxial cable to the TDR instrument necessitating the instrument to be closer to the point of measurement in the field. However, because of the operating temperature range of -10 to 55°C for the 1502B cable tester as recommended by the manufacturer (Tektronix, Inc. 1998), field measurements during the winter under temperatures below the operating temperature range is not possible. Other researchers who used this instrument in the field have recommended a narrower range of 5 to 55°C (Jones et al. 2002; Jones and Or 2002; Blonquist et al. 2005). During wintertime soil moisture measurements, the TDR instrument has to be operated in a warm enclosure located away from the field where the probes are embedded. Therefore, another extension cable of varying length is used to

connect the TDR probe to the TDR instrument located in the warm enclosure (i.e., a truck cab). Normally the user has to set the relative dielectric constant for a given cable type and assume that the same length is used for all the different probe measurements. Thus, any change in dielectric constant is attributed to the material in which the TDR probe is embedded. However, it is impractical and expensive to have the same extension cable length for all the probes irrespective of the distance to the warm enclosure. The variable distances from the cable tester necessitates the use of extension cables of various lengths depending on the proximity between the probes in the field and the location of the cable tester in the warm enclosure. Extension cables are needed during other times of the year if the probes are multiplexed and measurements need to be taken simultaneously using a single cable tester.

Various studies have been conducted on the effects of cable lengths on the accuracy of TDR measurements. Logsdon (2000) observed that cable length affects the dielectric constant measurement in soils. Pierce et al. (1994) used a 22.2-mm diameter coaxial cable to investigate the effect of length, shear, and crimps on long cables to the reflection signatures measured by TDR. They used the coaxial cable with lengths from 90 to 530 m. Their results indicated that resolution of the reflection signatures decreased with increase in cable length. Shorter cables were more accurate in detecting the cable deformations compared to longer cables. When the cable length was increased from 94 to 268 m, the reflection amplitude reduced by 80%. For cables longer than 268 m, Pierce et al. (1994) commented that TDR measurement resolutions decrease non-linearly causing difficulty in getting accurate measurements. They concluded that the optimum length for the 22.2 mm coaxial cable was 268 m. The experiment however involved large diameter

cables (22.2 mm) that are not typical of the RG-58 cables used for soil moisture measurements.

Brendan (2003) investigated the RG-58 and RG-8 extension cables for multiple measurements. The extension cables were connected to shorter cables holding the TDR probes. A longer cable filtered high frequency electromagnetic waves causing a loss of resolution in the reflected wave. The decrease in the returning EM wave-energy caused a decline in the slope used for the automatic end-point determination. Brendan (2003) recommended the use of similar types of cables (the short cable holding the probe and the extension cable) when extension cables are to be used. While the author did not perform optimization to determine the maximum cable lengths, he recommended a maximum length of 35 m for the RG-58 cable depending on the manufacturer's recommendations. Brendan (2003) also noted that cables with heavier shield such as the RG-8 have lower signal loss; hence, they can be used for extensions up to 60 m. The RG-58 cable is 5 mm in diameter, has a single and thinner shielding, and is more flexible. On the other hand, the RG-8 cable is 10 mm in diameter, has a double insulation, and is less flexible. Both cables have the same 50 Ω impedance values (Logsdon 2000; Fuller and Blankenship 2002).

Other researchers have also used extension cables for automation and multiplexing the TDR measurement with multiple probes (Herkelrath and Delin 1999; Logsdon 2000). Despite these advances, studies also have shown that a combination of accessories such as extension cables and multiplexers greatly affect the accuracy of dielectric constant measurements (Logsdon 2000). The use of extension cables affects the accuracy of TDR measurements depending on type and size of the cable used, length

extended, temperature, and type and size of the probes used (Deutsch et al. 1994; Robinson et al. 2003a).

Many experiments with longer cables have been reported in the literature (Logsdon 2000; Fuller and Blankenship 2002). However, not much has been done to determine the optimum extension cable length that can still give accurate measurements of dielectric constant. The influence of a combination of materials used in the construction of the probe (i.e., probe head and probe rods) has not been explored. The relationship between physical cable length and its equivalent length is important for determining the dielectric constant.

The aim of this experiment was to determine the maximum length that the RG-58 50 Ω coaxial cable can be extended and still give accurate measurement of the dielectric constant. The results were used to develop a calibration equation that can be used to correct the data for the effect of extension cable lengths on the TDR water content measurements. Similar procedures could also be adopted to develop calibration equations for different probe-cable combinations, and for different non-lossy and lossy dielectric media.

3.2.2 The theory of TDR method

The principle of operation of the TDR for measuring the dielectric constant has been presented by a number of researchers (e.g. Topp et al. 1980 and 1982; Baker and Allmaras 1990; Evett 2000b; Jones et al. 2002; Or et al. 2004). It involves measurement of the propagation velocity of an electromagnetic (EM) wave generated by the TDR cable tester into a dielectric material such as water or soil solution. The length of the waveguide

embedded in the dielectric material and the propagation velocity of the EM wave determine the two-way travel time as:

$$t = \frac{2L}{v} \tag{3.1}$$

where:

L = length of waveguide (m),

v = propagation velocity of EM wave (m s^{-1}), and

t = time of travel (s).

The propagation velocity is related to the apparent dielectric constant of the medium as:

$$v = \frac{c}{\sqrt{\mu K_a}} \tag{3.2}$$

where:

μ = magnetic permeability of the medium (assumed to be 1.0 for non-magnetic dielectric material)

c = speed of light in free space or velocity of the EM wave in vacuum (3 x 10^8 m/s), and

K_a = apparent dielectric constant of the material.

Combining Eqs. 3.1 and 3.2 and setting $\mu = 1$ gives the apparent dielectric constant as:

$$K_a = \mu^{-1}\left(\frac{c}{v}\right)^2 = \mu^{-1}\left(\frac{ct}{2L}\right)^2 \tag{3.3}$$

During waveform analysis, the horizontal axis on the 1502B Tektronix cable tester is set in the equivalent length (L_a) units. The apparent length of the probe, L_a is therefore defined as:

$$L_a = \frac{ct}{2} \tag{3.4}$$

Hence the K_a can be expressed in terms of the ratio of apparent length of the waveguide to the physical length by Eq. 3.5.

$$K_a = \left(\frac{L_a}{L}\right)^2 \tag{3.5}$$

During soil moisture measurement, the TDR probe embedded in the soil measures the composite dielectric constant of the media. However, most materials in the soil have smaller dielectric constants compared to water, (K_{soil} = 3.0-7.0; K_{ice} = 3.2; K_{air} = 1.0; $K_{water} \approx$ 78.5 at 25°C) (Warrick 2002; Tardif 2002; Evett 2003b). This large contrast in dielectric constant can be used to determine the water content of the mixture.

The calculated apparent dielectric constant is related to the water content θ_b using either empirical models such as the model proposed by Topp et al. (1980), or physical (dielectric mixing) models. The empirical models are less accurate for water contents above 0.5 m^3 m^{-3}, and on soils with high organic matter and clay contents (Jones et al. 2002). The physical (dielectric mixing) models are more accurate for wider ranges of water contents and soil salinity since they consider the geometry of the medium in relation to the axial direction of the wave-guide, and the dielectric constant of various materials in the soil (Baker and Allmaras 1990; Jones et al. 2002; Warrick 2002). However, for most practical soil moisture measurement purposes the Topp model has

been accepted and used in various studies involving TDR measurements (e.g. Topp et al. 1982; Sri Ranjan and Domytrak 1997; Wraith and Or 1999; Blonquist et al. 2005). The model relates the apparent dielectric constant, K_a with volumetric water content, θ_v as:

$$\theta_v = -5.3\times10^{-2} + 2.92\times10^{-2}K_a - 5.5\times10^{-4}K_a^2 + 4.3\times10^{-6}K_a^3 \quad (3.6)$$

3.2.3 The TDR waveform analysis

Analysis of the waveform is another key factor in getting accurate measure of the dielectric constant. The analysis involves determination of the first peak of the wave at the base of the probe when the wave enters the dielectric medium and the end reflection when the wave encounters discontinuity at the end of the probe. Waveform interpretations can be done by manual graphical methods or by waveform analysis using software.

Using the graphical method (Baker and Allmaras 1990; Evett 2000c), the initial travel time, t_1 at the first peak is taken as the intersection between the tangent on the first descending limb and the horizontal line at the first peak (Fig. 3.1). This same point is also defined by Logsdon (2000) as 90% of the height of the first peak or rise time. The second reflection point at time t_2 is defined as the intersection between the tangent on the second rising limb and the tangent on the horizontal or sloping portion of the waveform at the 'global minimum' (Evett 2000c). The difference between the two times gives the travel time of the EM wave. These two key points can also be obtained using the first derivative of the waveform whereby the point corresponding to t_1 and t_2 are taken as the minimum of the first derivative and the second peak of the first derivative (Baker and Allmaras 1990; Evett 2000c; Jones et al. 2002; Or et al. 2004).

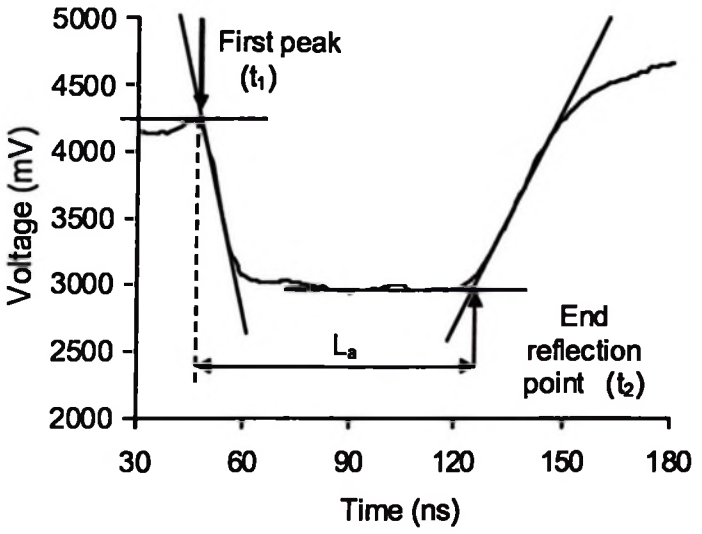

Fig. 3.1. Typical waveform for a 35-mm TDR miniprobe immersed in pure water and attached to a 2.5-m coaxial cable. The difference between the first peak and the end reflection defines the apparent length, L_a of the waveguide.

Owing to the inaccuracies associated with graphical interpretation of the waveforms, computer programs have been developed for the TDR waveform analysis. Some examples are the TACQ program developed by Evett (2000b), and the WinTDR developed by Hubscher et al. (1996) and revised by Or et al. (2004). Procedures for the automatic waveform analysis using the TACQ software are explained in detail in Evett (2000b and 2000c). The WinTDR program currently analyzes waveforms from Tektronix 150X (B/C) cable testers only (Or et al. 2004). Most computer programs for waveform analysis supplied by manufacturers are suitable for commercial TDR probes longer than 0.15 m. Heavy-duty commercial TDR probes are also made with lengths such as 0.6 to 1.0 m (Long et al. 2002). However, when shorter probes that are 0.04 m long are used with the Tektronix 150X (B/C), the waveforms have a lot of noise that needs to be

filtered. Therefore, the program that came along with the Tektronix 1502B cable tester used in this study was extensively modified to filter the noise associated with shorter probes for use in a study to determine the effective volume measured by miniprobes (Sri Ranjan and Domytrak 1997). This modified program has been used with our miniprobes in this research.

3.3 Materials and Methods

3.3.1 Instrumentation

The TDR miniprobes were made in the laboratory and individually calibrated. The 35-mm miniprobes used in this experiment were made using three 1.6 mm-diameter stainless steel rods (three- rod configuration). The three rods were connected using a Bayonet Nelson Connector (BNC) type KC-79-35 (King's Electronics Co. Inc., Rock Hill, SC). The probes were then connected to a 2.5-m coaxial cable type RG-58 50 Ω (Belden Electronics Division, Richmond, IN), which had BNC coaxial connector cable terminations on both ends. Since the impedance is inversely proportional to the diameter of the probes, smaller diameter probes have the advantage of producing high impedance and peak (Mojid et al. 2003). The three-rod TDR miniprobe construction is described in Sri Ranjan and Domytrak (1997). In the three-rod configuration, it is recommended that the critical rod spacing should be greater than three times the diameter of the central rod to avoid the "skin effect" (Zengelin et al. 1992). The rod spacing was 6 mm, which is 3.75 times the diameter of the rods; hence, the conditions for avoiding the skin effect were satisfied. It is also suggested that when performing laboratory calibration, no part of the probe should be within 40 mm of the edge of the container used for calibration

(Campbell Scientific, Inc. 2001). This also helps to prevent the energy field from extending outside the container. The TDR probe was inserted in a water column 250 mm deep and 280 mm in diameter leaving a minimum clearance of 130 mm from the sides of the container.

Various researchers have successfully used the TDR miniprobes for water content measurements. Mojid et al. (2003) used a 45 mm miniprobe and commented that longer probes cause continuous energy loss along the probe rod causing wave attenuation even at lower ranges. The miniprobes are also more accurate for point measurements of soil moisture on depth intervals of 0.10 m or less (Sri Ranjan and Domytrak 1997). Topp et al. (1980 and 1982), Sri Ranjan and Domytrak (1997), and Evett (2000b) successfully used 50 mm TDR miniprobes for soil moisture measurements.

The calibration of the miniprobe was done in pure water as a dielectric medium. The probe length, distance per division and peak were set in the Quick Basic program code. The probe's apparent length was altered in the program code until the probe was able to repeatedly measure the dielectric constant (K_a) value of 80.36 at a specified water temperature of 20°C. Calibration of TDR probes using dielectric fluids such as water, acetone, oil, and air have also been reported by Logsdon (2000), Robinson et al. (2003b), and Blonquist et al. (2005).

3.3.2 Measurement using different lengths of extension cables

Having calibrated the 35-mm TDR miniprobe with a 2.5-m cable, the length of coaxial cable was then altered. Eleven coaxial cables of type RG-58 50 Ω (Belden Electronics Division, Richmond, IN) and varying lengths (2.5, 4.5, 7.1, 9.6, 12.9, 17.4,

19.9, 30.0, 40.0, 50.4, and 70.0 m) were used to measure the dielectric constant of water in a constant temperature enclosure maintained at an average temperature of 20.0±0.3°C. The cables were uncoiled and stretched prior to taking the measurements. Since the TDR assumes a uniform velocity of propagation along the cable length as well as the miniprobe, any large variation in cable length in relation to the probe length will affect the dielectric constant reported by the TDR. Therefore, for longer extension cables, the physical cable length has to be modified to attain the prescribed dielectric constant for the media in which the probe is embedded. This was accomplished by modifying the cable length within the computer program until the cable was able to measure the prescribed dielectric constant of water at the specified temperature. After attaining a stable value, four measurements were taken for each cable, and were used for statistical analysis to determine the measurement accuracy of each extended length. The waveforms captured by Tektronix 1502B metallic cable tester (Tektronix Inc., Beaverton, OR) for each cable were recorded and analyzed. The waveforms obtained with varying cable lengths were then plotted on the same scale and compared.

3.3.3 Waveform analysis

Waveform analysis can be done both manually and by using the auto-analysis option. Using the manual method, the data file created by cable tester as a text file was downloaded and plotted using a spreadsheet program. The tangents corresponding to the first peak and end reflection were fitted manually (Fig. 3.1).

Figure 3.1 shows a waveform created by a 35-mm TDR probe immersed in pure water and attached to a 2.5-m coaxial cable. The distance between the first peak and the

end reflection point define the apparent length L_a of the waveguide. The procedure for determining the L_a is also reported in the literature (e.g. Jones et al. 2002; Or et al. 2004).

During the initial calibration, the 35-mm TDR miniprobe was attached to a 2.5-m coaxial cable and immersed in pure water at 20°C. The probe's information was entered into the Quick Basic program. The executable program was created and used to run the cable tester. A trace of the waveform was developed and tangent lines were drawn that gave the best fit while monitoring the K_a measured by the probe. The procedure was repeated to obtain an apparent length that gave K_a value of 80.36 at the recorded temperature of 20°C.

The auto analysis was used to analyze the waveforms generated when the cable lengths were altered from 2.5 m to 70.0 m. During this process, the probe specifications were unaltered. For each physical cable length, an apparent cable length was input into the computer program until the miniprobe with the extension cable was able to measure the K_a value at the specified temperature.

3.3.4 Comparison of measured and actual dielectric constants

Four readings of dielectric constant of water (K_a values) were taken for each cable length. The aim was to determine the extent to which the measured K_a values deviated from the known K_a value of water at a particular temperature as the cable length increased. The General Linear Model (GLM) procedure of the statistical analysis system (SAS) software version 9.1.2 (SAS Institute Inc. 2004) was used for the statistical analysis. Comparison of means was performed between the average of four measurements for each cable length and the actual K_a value. The difference between the

average of the measured K_a values and the actual K_a value were compared, and the maximum length with a dielectric constant difference of less than 0.05 was determined. Logsdon (2000) also performed the cable length experiment with cable lengths ranging from 6.4 to 49.5 m. He concluded that cable lengths significantly affected the dielectric constant measurements. However, no optimization was performed to determine the maximum length that the RG-58 and RG-8 cables could be extended and still obtain acceptable accuracy for water content measurement.

3.3.5 Comparison between the physical and apparent cable lengths

Comparison was made between the physical cable length and the equivalent length as interpreted by the cable tester (apparent cable length). The apparent cable length is a combination of the effects of the coaxial cable, BNC connectors and the wave-guide. Determination of the apparent length of the cable was performed after the apparent length of the probe had already been determined and fixed in the initial probe calibration with a fixed cable length of 2.5 m. This second stage of calibration involved changing the value of the equivalent length of each specific cable on the computer program. Ideally, the physical length of probe-cable combination differs from the length interpreted by the cable tester due to combination of more than one type of materials (coaxial cable, probe head, and probe rods). This experiment aimed at determining what the equivalent length should be whenever the physical cable length is to be changed to satisfy the cable extension requirements.

For a given physical cable length, the equivalent apparent length was iterated within the computer program until it gave the known dielectric constant (80.36) at a temperature of 20°C. The correlation between the two parameters was performed using

correlation procedure in the SAS analysis to ascertain how the physical cable length corresponded to its apparent length as the cable length was increased. A linear regression analysis was performed to establish an equation that could be used to calculate the apparent length for a given physical cable length.

3.4 Results and Discussion

3.4.1 Measurement of dielectric constant of water using variable extension cable lengths

Summary of the Univariate procedure of SAS statistical analysis for the dielectric constant of water measured at 20±0.3°C is presented in Table 3.1.

Table 3.1. Summary of statistical analysis for the apparent dielectric constant (K_a)* of water measured using variable extension cable lengths at 20±0.3°C.

Physical cable length (m)	Apparent cable length (m)	Statistical parameters for measured K_a values						
		N	Mean	SD	CV (%)	SEM	Variance	Range
2.50	3.00	4	80.48	0.21	0.26	0.11	0.04	0.49
4.50	5.61	4	80.29	0.19	0.24	0.09	0.04	0.40
7.05	8.74	4	80.20	0.25	0.31	0.13	0.06	0.60
9.55	11.95	4	80.37	0.76	0.95	0.38	0.58	1.50
12.85	16.16	4	80.53	0.60	0.74	0.30	0.36	1.37
17.40	21.52	4	80.57	0.61	0.76	0.31	0.38	1.38
19.90	24.91	4	80.73	0.33	0.41	0.17	0.11	0.77
30.00	37.79	4	80.39	0.77	0.96	0.39	0.60	1.72
40.00	49.95	4	80.37	0.62	0.77	0.31	0.38	1.36
50.35	62.86	4	79.61	2.01	2.52	1.01	4.04	4.64
70.00	87.91	4	77.91	3.84	4.47	1.74	12.11	7.50

* The actual dielectric constant of water (K_a value) at 20°C is 80.37.

Four measurements were taken for each cable length from 2.5 m to 70.0 m. The average K_a values ranged from 80.2 to 80.73 for cable lengths from 2.5 to 40.0 m, and from 79.51 to 77.91 for 50.4 to 70.0-m lengths, respectively. The standard deviation (SD) for the K_a values ranged from 0.21 to 0.77 for the cables from 2.5 to 40.0 m, and from 2.01 to 3.84 for the 50.4 to 70.0-m cables. The standard error of the mean was less than 0.40 for the lengths up to 40.0 m, and it increased by 3.3 times when the length was changed from 40.0 to 50.4 m. This indicated that the cables from 2.5 to 40.0 m were more accurate (CV = 0.26 – 0.77) compared to the cables beyond 40.0 m (CV = 2.52 – 4.47).

3.4.2 Waveform analysis for cable lengths from 2.5 m to 70.0 m

Waveforms for different extension cable lengths were plotted on the same graph (Fig. 3.2) showing changes in shapes of the waveform for the different cable lengths. The variation in TDR waveforms as a result of an increase in cable length from 2.5 to 70.0 m is shown (Fig. 3.2).

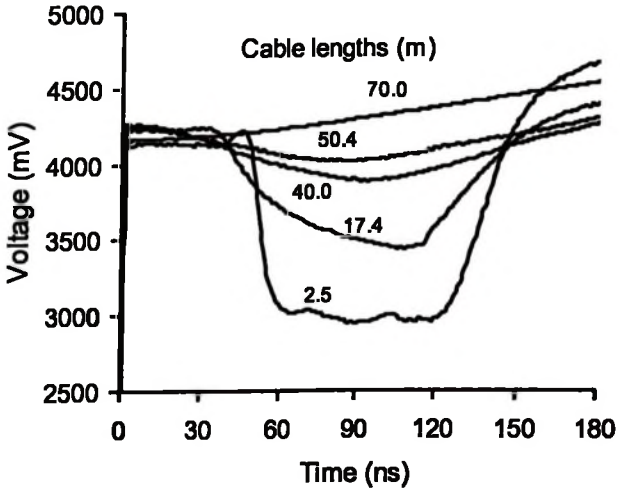

Fig. 3.2. TDR waveforms for different cable lengths produced using a 35-mm TDR miniprobe immersed in pure water at an average temperature of 20°C.

The apex corresponding to the first reflection at the base of the probe rods was approximately the same for the cable lengths from 2.5 m to 17.4 m. As the cable length increased, the height of the first peak decreased and the curve became more flat causing difficulty in identifying the inflection points for fitting the tangents associated with the determination of the first reflection point at the probe base.

Similarly, the shape of the waveform corresponding to the end of the waveguide became continuously wider and the minimum point corresponding to the end reflection could not be easily identified. There was no clear demarcation between the horizontal limb and the second rising limb for the longer cables beyond 40.0 m. The reflection depth of the waveforms also decreased with increase in cable length. This was an indication that the accuracy of fitting of the tangent lines to demarcate the first peak and end reflection points decreased with increase in cable length.

Ideally, for a given type and length of probe, the travel time of the EM wave through the probe should be the same regardless of the cable length (Evett 2000c). However, beyond a certain limit of cable length, a deviation occurs due to the inaccuracy of obtaining the peak points from the resulting shape of the waveform. Results on the effect of cable lengths on dielectric constant measurements were also obtained by Logsdon (2000), Brendan (2003), and Robinson et al. (2003b) as explained earlier.

3.4.3 Comparison of measured and actual dielectric constants

The accuracy of measurements was verified further by statistical comparison of the measured and the actual dielectric constant of water (Table 3.2) at a specific temperature for the different cable lengths. The measured dielectric constant of water (K_a

measured) and the actual value (K_a actual) were compared using paired comparison procedure of SAS statistical analysis for the various extension cable lengths (Table 3.2, Appendix C).

Table 3.2. Paired comparison between the measured and the actual dielectric constant (K_a) of water for different cable lengths.

Cable length (m)	Difference* (K_a measured – K_a actual)				Difference* ($\theta_{measured} - \theta_{actual}$)
	N	Mean diff	SD	SEM	$m^3\ m^{-3}$
2.50 – 40.0	9	0.05	0.17	0.06	0.001 – 0.007
50.4 – 70.0	2	-1.36	1.01	0.72	0.015 – 0.047
2.50 – 70.0	11	-0.20	0.67	0.20	

* The measured and estimated values of K_a and θ are presented in Appendix C.

From Table 3.2, cables from 2.5 to 40.0 m had a mean difference of 0.05 and standard deviation of 0.17. The cables from 50.4 to 70.0 m had a mean difference of minus 1.36 and standard deviation of 1.01. The range of accuracy for the water content determination was between 0.001 and 0.007 $m^3\ m^{-3}$ for cables from 2.5 to 40.0 m, and from 0.015 to 0.047 $m^3\ m^{-3}$ for the cables from 50.4 to 70.0 m. The range produced by the cables from 2.5 to 40.0 m is within the range of accuracy of TDR measurement reported in the literature (Topp et al. 1980; Baker and Allmaras 1990).

Figure 3.3 presents the deviations between the measured and the actual K_a values of water for the cable lengths from 2.5 to 70.0 m.

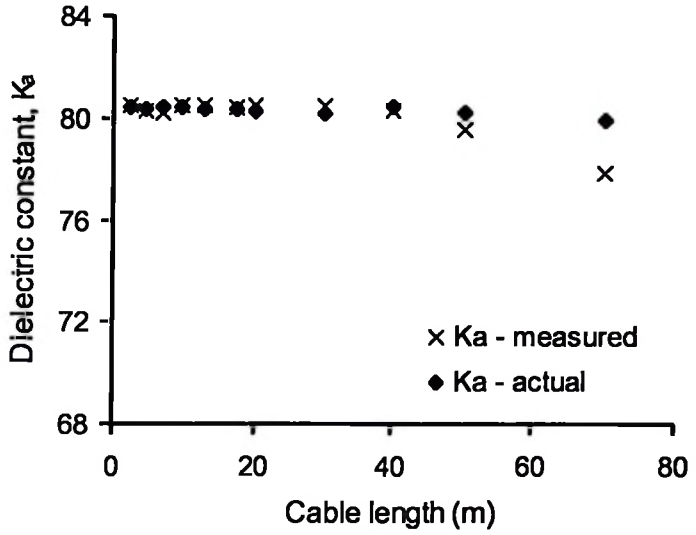

Fig. 3.3. Comparison of the measured and the actual dielectric constants (K_a values) for water content measurement.

The difference between the measured and actual dielectric constant increased with an increase in cable length (Fig. 3.3). Longer cables underestimated the K_a values. The increase in the deviation with cable length was also an indication of the decrease in accuracy of the TDR measurements with increased cable length. The deviations of the measurement within each individual length of cable are shown in Fig. 3.4.

The variation of K_a values with increase in cable lengths are presented for four replicates in each length (Fig. 3.4). Shorter cables were found to have a lower variability compared to the longer cables. This suggested that there was loss in signal response when longer cables were used causing the data generated by the longer cables to be more dispersed as indicated by an increase in length of the error bars. Hence for the RG-58 50 Ω coaxial cable used in this study, the cables gave an accurate measure of K_a values up to a length of 40.0 m. Similar responses on the effect of cable length on TDR measurement

accuracy were also observed by Pierce et al. (1994) and Brendan (2003) on larger diameter cables (22.2 mm and 10 mm, respectively). The optimum extension length for the RG-58 50 Ω cable to be used with 35-mm TDR probes was found to be 40 m. The extension cables calibrated in the laboratory using water as a dielectric medium were to be used for field soil moisture measurements. However, shapes of waveform are expected to be different due to the differences in the amount of water content in the soil.

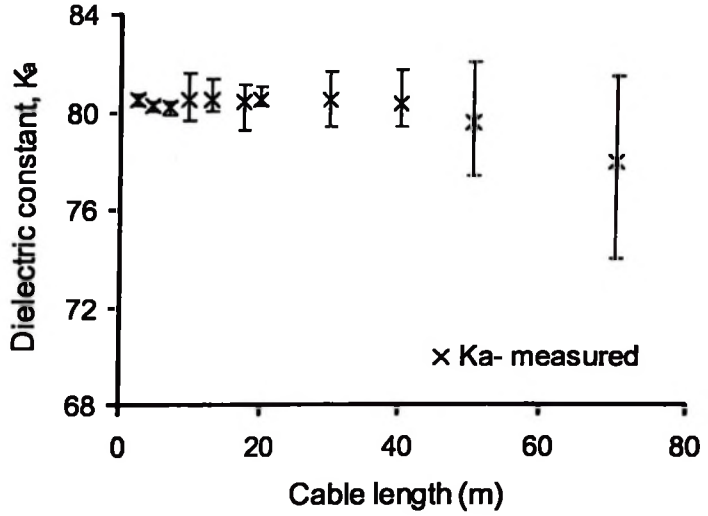

Fig. 3.4. Variability of the measured dielectric constant of water with increase in cable length. Error bars represent standard errors of measurement.

3.4.4 Comparison of physical and apparent cable lengths

Results from the SAS correlation procedure between the physical and its corresponding apparent length indicated that there was a good correlation between the physical and the apparent cable length (R^2 = 1.0). The percent increase of the apparent length from the physical length ranged from 20.0 to 25.6% with an average of 24.5%

(Table 3.1). The regression equation for determining the apparent length from a given physical cable length was derived (Fig. 3.5).

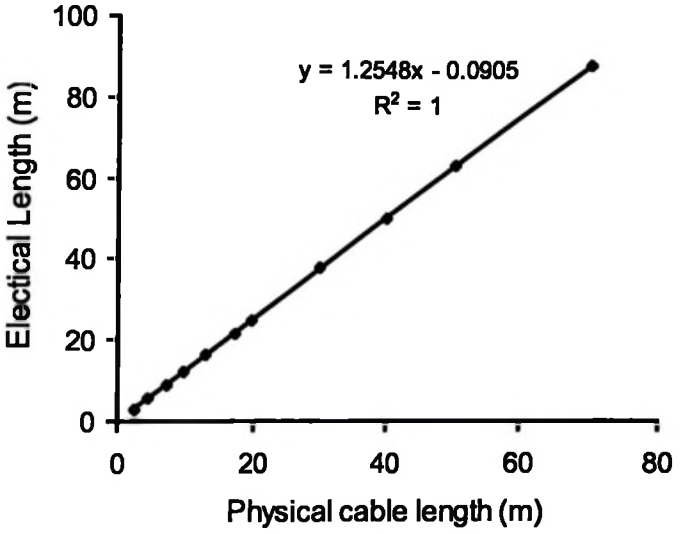

Fig. 3.5. Comparison of physical and apparent cable lengths for water content measurement.

The apparent length could therefore be obtained for any given physical length for the RG-58 50 Ω coaxial cable using Eq. 3.7 as follows:

$$y = 1.2548x - 0.0905 \tag{3.7}$$

where:

y = apparent cable length for water content measurement (m), and

x = physical cable length (m).

The established equation (Eq. 3.7) is useful especially during TDR calibrations with multiple extensions since the apparent lengths are needed in the TDR software programs to measure correctly the apparent dielectric constant of the media. Therefore, it eliminates the need for multiple iterations on the cable calibration once the waveguide

has already been calibrated with a shorter length of cable. The derived equation could also be used in other porous media containing water such as moist soils. However, the equation is specific to the type of TDR probe and type of the coaxial cable. For different kinds of probes and/or a different type of the coaxial cable, similar procedures could be followed to establish its corresponding regression equation that will eliminate the need for further calibrations with other similar probes and cables.

Procedures developed in this research that can be followed to calibrate extension cables along with the TDR probes to be used are as follows:

- Determine the physical length of extension cable depending on field requirements
- Decide on the type and size of TDR probes to be used.
- Calibrate the chosen probe size using a short coaxial cable, example 2.5 m. The probe should be able to read a known dielectric constant of the dielectric fluid used at a particular temperature.
- Connect the extension cable to the cable with the calibrated probe on one side, and to the cable tester on the other side.
- Perform iterations by changing the apparent length on the waveform analysis program code until the actual value of dielectric constant is obtained.
- Repeat the procedure for different extension cable lengths and develop a calibration equation relating the physical and apparent cable length.
- The developed equation can then be used to determine equivalent length for any length to be extended (to the proposed limit of 40.0 m if the RG-58 50 Ω coaxial cable is to be used) without the need for performing the iterations.

- For the RG-58 coaxial cable and 35-mm TDR miniprobes, Eq. 3.7 developed above can be used to determine the apparent lengths for any cable length without the need for performing the mentioned iterative procedures.

It should be noted that the diameter of the cable has great influence on the maximum length with which the cable can be extended. The optimum length is expected to increase with cable size as observed by other researchers (Pierce et al. 1994) who worked with large diameter cables and obtained TDR reflection up to 168 m using the 22.2-mm diameter coaxial cables.

3.5 Summary and Conclusions

A laboratory experiment was conducted to determine the influence of cable lengths on the accuracy of dielectric constant for TDR water content measurement. The RG-58 50 Ω coaxial cable used in this experiment ranged in length from 2.5 to 70.0 m. The TDR miniprobe was made with three 1.6-mm diameter and 35-mm-long stainless steel rods (3-rod configuration). Use of longer extension cables affected the accuracy of TDR measurement. Cables from 2.5 to 40.0 m measured the dielectric constant accurately within an accuracy range of ±0.05. Beyond 40.0 m, the measurement error increased to a range of ±1.36. The difference between the measured and the actual K_a values increased with an increase in cable length. Longer cables underestimated the K_a values. Therefore, shorter cables were more accurate than longer cables. The maximum cable length for the RG-58 50 Ω coaxial cable and 35 mm TDR miniprobe combination was found to be 40.0 m.

The physical cable lengths were compared with their corresponding apparent lengths and they showed a very good correlation ($R^2 = 1.0$). An equation was derived that could be used to determine the corresponding apparent length for each given physical cable length for water content measurement. The derived equation eliminates the need for multiple iterations during the calibration of extension cables once the waveguide has already been calibrated with a shorter cable length. If extension cables are to be used, the probes should also be calibrated along with the selected extension cables.

4. SOIL TEMPERATURE CORRECTION OF FIELD TDR READINGS OBTAINED UNDER NEAR FREEZING CONDITIONS

4.1 Abstract

The quantity of spring snowmelt infiltration and runoff depends on the antecedent soil moisture conditions at the time of soil freezing. Determining the soil moisture status at any particular time during the freezing process requires an understanding of vertical distribution of liquid and frozen water content within the soil profile. This study investigated the effects of soil freezing and thawing during the fall, on partitioning of soil water into the frozen and unfrozen components as a function of depth. Time Domain Reflectometry (TDR) with 35-mm miniprobes was used to determine the unfrozen water content. The total water content was determined using neutron scattering method. Comparison between the two methods was made, and a temperature calibration method was developed to account for the effect of change in soil temperature on the accuracy of TDR measurements. A combination of TDR and neutron scattering methods was also used to quantify the frozen and unfrozen soil water content within the soil profile as the soil freezing progressed with time. The temperature calibration method developed in this research could be used for adjusting field TDR readings taken at temperatures below or above the probes' laboratory calibration temperatures.

4.2 Introduction

4.2.1 General

Soil freezing and thawing processes play a major role in soil water movement in seasonally frozen soils. The quantity and distribution of soil water content during the fall,

when soil begins to freeze, influences the freeze-thaw behavior of the soil during the spring snowmelt (Luo et al. 2002). Understanding the soil moisture distribution during the fall and early winter requires measurement of both the frozen and unfrozen (liquid) parts of the total soil water content because the soil is partly frozen.

Methods for measuring soil water content can be grouped into classical and modern sensor methods. The classical methods are such as neutron scattering using a neutron moisture meter (NMM), electrical conductivity, and gravimetric. Examples of modern sensor methods that are based on capacitance are time domain reflectometry (TDR) and frequency domain reflectometry (FDR) (Seyfried and Murdock 2001; Warrick 2002; Evett 2000a and 2003b; Evett et al. 2002; Topp et al. 2003). Despite the innovations of these modern non-destructive and high precision methods, both the classical and the modern methods encounter particular problems related to the physics of the methods (i.e., accuracy and precision of the measurements, coverage and volume of measurements, and varying soil conditions) (Evett 2000a; Warrick 2002).

A study by Seyfried and Murdock (2001) showed that the sensitivity of the water content reflectometer (WCR) instrument varies with temperature, and the temperature effects also vary with water content and type of the soil. Soil moisture measurements in partly frozen soils in particular pose a challenge to many methods, such as TDR and WCR, due to the existence of water in both liquid and frozen conditions. Evett (2003b) noted that when the TDR method was used, the decrease in permittivity of water as it freezes hindered accurate measurement of frozen water content in the soil.

In this study, two methods of soil moisture measurements (TDR and NMM) were used to measure the unfrozen and total soil water content. The TDR, being dependent on

the dielectric constant of the medium in which the probe is embedded, measures only the unfrozen water content of the soil. The method involves measurement of travel time of the electromagnetic wave (EM) along wave-guides of known length placed in the soil. The measured travel time is related to the dielectric constant of the medium in which the wave is moving. The dielectric constant (K_a) is then related to the volumetric liquid water content (θ_v), since changes in θ_v are directly related to the changes in K_a (Evett 2000a). This is attributed to the significant difference between the dielectric constant of water and that of other soil materials (K_{water} = 78.5 at 25°C, K_{air} = 1.0, K_{ice} = 3.2, and K_{soil} = 3.0-7.0 depending on soil composition and texture) (Warrick 2002; Tardif 2002; Evett 2003b). As the soil freezes, the dielectric constant of frozen water decreases significantly from that of unfrozen water due to inability of the water molecules to rotate freely in the electromagnetic field used in the TDR measurement method. This allows for the unfrozen part of water content to be determined.

The neutron scattering technique, on the other hand, measures the total (frozen and unfrozen) soil water content using a neutron moisture meter (NMM). It uses a radioactive source emitting fast neutrons, and a counter for detecting slow neutrons thermalized by the hydrogen atoms in the soil water, whether in the frozen or unfrozen state (Evett 2000a, 2003a). The loss in the kinetic energy of the neutrons varies depending on type of soil constituents they collide with. When neutrons collide with hydrogen atoms that are similar in weight, they are thermalized leading to a reduction in their kinetic energy (Evett 2003a). The concentration of the thermalized neutrons is a measure of the number of hydrogen atoms, which is related to the total volumetric water content (Evett 2003a). Calibrations are normally performed to account for other sources

of hydrogen in the soil other than water, such as humus, organic matter, and other efficient neutron thermalizers (Carbon, Nitrogen, and Oxygen). The relationship between thermalized neutron counts and the volumetric water content depends on field calibration for each specific soil.

Studies have described the potential for the use of TDR and NMM in partitioning total water content into frozen and unfrozen water (Baker and Allmaras 1990; Herkelrath and Delin 1999). However little has been documented on the freeze thaw processes during the fall as the soil starts to freeze. In addition, the accuracy of TDR soil moisture measurements in the field at varying soil temperatures along the soil profile needs more attention.

Spaans and Baker (1995) studied the use of TDR in frozen soils and found that calibration of TDR probes using water and soil in the laboratory does not give accurate results in the field when the soil is partly frozen. Tardif (2002) suggested temperature correction on soil moisture sensors depending on manufacturers' recommendations. Seyfried (2004) also showed that field measurements made in partly frozen soils using TDR probes calibrated in the laboratory were not accurate.

4.2.2 Soil temperature and field TDR measurements

The accuracy of determining the apparent dielectric constant (K_a) of the soil is one of many other factors that affect the accuracy of measuring soil water content with TDR. In the early developments of TDR (Topp et al.1980), it was assumed that TDR method is less sensitive to temperature variations and soil factors with an accuracy of 0.013 $m^3 m^{-3}$. Further research on TDR measurements has shown that factors such as soil texture, bulk

density, soil water content, and soil temperature affect the accuracy of TDR measurements (Pepin et al. 1995; Or and Wrath 1999; Gong et al. 2003; Robinson et al. 2003a). Errors in applying the Topp's calibration equation (Topp et al. 1980) without any correction are more pronounced especially in soils with large specific surface area and high salinity (Persson and Berndtsson 1998; Gong et al. 2003). Persson and Berndtsson (1998) also suggested a temperature correction factor for water content measurement to range between -0.00253 and -0.00419. The same study also reported a decrease of K_a of pure water and wet soils with an increase in temperature, and an increase of K_a with an increase in temperature when the soil was dry. Seyfried and Murdock (1996) obtained similar results regarding the influence of total soil water content, especially in frozen soils, and concluded that the amount of liquid water in frozen soil depends on the amount of total water content.

The TDR measurements obtained in various types of soils such as sand, silt loam, and clays showed that the K_a is less affected by water content in coarse textured soil compared to fine textured soils, which have a large specific surface area (Pepin et al. 1995; Persson and Berndtsson 1998; Wrath and Or 1999; Gong et al. 2003). The impact of a combination of factors such as water content, soil texture, and soil temperature on the accuracy of TDR measurements has been reported in a contradictory manner (Or and Wrath 1999; Gong et al. 2003). In their studies, Or and Wrath (1999) and Wrath and Or (1999) have given a clear description on how these three factors interact with each other and hence, affect the accuracy of TDR measurements. In brief, they describe that for soils having higher moisture content, the TDR measured K_a decreases with an increase in temperature and an increase in the bound water content. The bound water is not detected

by the TDR and hence has less influence on the changes observed in the measured K_a with temperature. At very low moisture content, an increase in temperature causes the bound water to become free causing a net increase in K_a with an increase in temperature.

To account for these changes in K_a with temperature, the measured K_a needs to be adjusted to a standard temperature. The normal practice as reported in the literature is to adjust to a temperature that had been used during the calibration of the TDR probes. Weast (1986), as reported by Or and Wrath (1999), developed an equation relating K_a of free water with temperature, and normalizing the values to 25°C as follows:

$$\varepsilon_w(T) = 78.54\left[1 - 4.579\times10^{-3}(T-25) + 1.19\times10^{-5}(T-25)^2 - 2.8\times10^{-8}(T-25)^2\right] \quad (4.1)$$

where:

$\varepsilon_w(T)$ = dielectric permittivity of free water, and

T = temperature (°C).

Other studies that have used 25°C as a baseline for adjusting TDR measurements are Wrath and Or (1999), and Robinson et al. (2003b).

The objective of this research was to develop a temperature calibration method that could be used for adjusting field TDR measurements taken at different soil temperatures. A combination of TDR and NMM was used to partition the total water content into unfrozen and frozen states as the soil continued to freeze during the fall and winter.

4.3 Materials and Methods

4.3.1 Location of the study area

The field plots are located in Carman, Manitoba, at the Ian N. Morrison Research Farm of the University of Manitoba, about 90 km Southwest of Winnipeg, Manitoba. The plots are part of a long-term crop rotation study looking at the water use of different cropping systems: oats with berseem clover cover crop, oats alone, fallow, and native prairie grass. Soils in the selected experimental plots are well-drained Fine Sandy Loam soils (well-drained Hibson from sub group Orthic Black Chernozem). The average particle size distribution of the soil was 76% sand, 8% silt, and 16% clay, with average depth of 0.70 m to a clay layer (Mills and Haluschak 1993).

The water content at different depths within the soil profile was measured using two different methods (i.e., Time domain reflectometry (TDR) and neutron moisture meter (NMM)). The TDR measures only the unfrozen water content of the soil, while the NMM method measures the total water content. Multiple measurements over several days were taken after each snowfall event to track the movement and state of water within the vertical soil profile. The soil and atmospheric temperatures fluctuated much above and below 0°C during and after the different snowfall events during late fall. Late fall weather in Southern Manitoba is usually characterized by periods of snowfall followed by warmer weather before the onset of the winter snowfall. It is this period of temperature fluctuation under near freezing/thawing conditions that was investigated in this study. The soil temperature profile was measured using thermocouples. Milder temperatures following early snowfall events may result in snowmelt infiltration events prior to soil freezing with the arrival of winter weather.

4.3.2 TDR instrumentation

The TDR miniprobes used in this field study were calibrated in a laboratory experiment at an average temperature of 25±0.3°C using water and soil columns. The TDR used miniprobes that were 35-mm-long stainless steel rods (1.59 mm diameter) in a 3-rod configuration placed in a single plane at a spacing of 6 mm, centre to centre. The rods were connected to an outer conductor coaxial cable type RG-58 50 Ω, with different lengths 2.0, 2.5, and 3.0 m, depending on depth of installation within the soil profile. Procedures for making TDR miniprobes are described in Sri Ranjan and Domytrak (1997). Evett (1994) found that three-rod configuration gave better soil moisture measurement compared to two-rod probe. The need for the impedance matching transformer used in the two-rod configuration is also eliminated due to semi-coaxial nature of the three-rod configuration (Evett 1994).

4.3.3 Field installation

The TDR probes were installed in an existing long-term cropping systems trial established at the Ian N. Morrison Research Farm of the University of Manitoba. Two of the cropping systems' treatments used in this research were no-till farming of oats with berseem clover cover crop and oats alone. Three replicates of measurement locations were selected in each cropping system to minimize errors due to soil heterogeneity. At each measurement location, five TDR probes were installed at depths of 0.1, 0.2, 0.4, 0.6, and 0.8 m from the ground surface. The probes were installed at an angle of 60° from the horizontal to prevent any preferential flow in the vertical direction. A 19-mm diameter hole was made by pushing a metal rod, along a specially made guide, to a depth 50 mm shorter than the desired depth of installation of the probe. The TDR miniprobe was

inserted into this hole using a specially made insertion tool and the probe ends were pushed into the soil to attain better soil contact in the last 35 mm. The steel rods of each probe were arranged in the same plane so that each leg would be at the same distance from the ground surface. The hole was then back-filled with industrial bentonite to avoid preferential flow along the coaxial cable extending to the ground surface. Angled installations and sealing procedures have also been described by Dahan et al. (2003) for deeper soil layers. The installation in that study however involved large diameter holes up to 200 mm, drilled at an angle of 45° from the horizontal No pre-drilling was done in the current study. Topp et al. (2003) also used angular, vertical, and horizontal probe installations and commented that the installation at an angle gave more reliable data.

The maximum vertical depth of installation within the soil profile was 0.8 m. Of the 60 TDR miniprobes installed in the field, 20 probes had thermocouples attached to them for monitoring soil temperature. The temperature was monitored at the same depths used for TDR measurements. A digital thermocouple thermometer with a precision of 0.1°C (Fluke 51 II Digital Thermometer, Fluke Corporation, Everett, WA, USA) was used for the soil temperature measurements. Probes in the field were connected using a 17.5-m long extension cable (RG-58 50 Ω coaxial cable), to a Tektronix 1502B metallic cable tester (Tektronix, Inc., Redmond, OR, USA) located in a warm cubicle (tractor cab). Information recorded by the cable tester was then downloaded into a notebook for further analysis. Data from TDR measurements were analysed to determine the quantity of liquid water as a function of depth as the soil continued to freeze.

4.3.4 Measurements using neutron moisture meter (NMM)

A profiling neutron moisture meter (NMM) (Troxler Model 4300 Depth Moisture Gauge, Troxler Electronics Laboratories Inc., Research Triangle Park, NC, USA) was used to measure the total volumetric water content. Measurements were taken at a different position in the same plots in which TDR probes were installed. The NMM sphere of influence, in which about 98% of the counted thermalized neutrons pass to reach the detector, is governed by a radius defined by Eq. 4.2 (Troxler 2001):

$$R = 280 - 0.27M \tag{4.2}$$

where:

R = sphere radius of influence in the soil (mm), and

M = soil moisture content (kg/m^3).

Based on Eq. 4.2, the maximum radius of influence from the centre of the neutron access tube is 280 mm when the soil is completely dry ($M = 0.0$). Hence, to avoid interference of TDR probes with the NMM measurements, the TDR probes were installed at a distance of 500 mm from the NMM access tubes. This distance was considered far enough to avoid interference between the two methods (Troxler 2001), and close enough for comparison of the two methods under similar soil moisture states. Calibration of the NMM gauge was done by measuring soil moisture at an interval of 0.2 m from 0.2 to 1.8 m depth. The measurements were compared against the gravimetric method, along with bulk density measurements made on undisturbed soil samples obtained from the same field. Samples for the gravimetric method were taken at the same depth intervals within

500 mm distance from the access tubes. A calibration equation was then derived and used for subsequent field measurements.

Three sets of measurements were taken within the soil profile during each time of data collection event (TDR, NMM, and soil temperature profiles). The data collection started in August 2005 when the soil was still unfrozen, and progressed until January 2006 when the soil had already begun to freeze. Comparison was made between the TDR and NMM data before and after soil freezing. Before soil freezing, ideally the TDR liquid water content was expected to be equal to the NMM total water content, since both methods measured water in the liquid (unfrozen) state. Temperature measurements were used to determine how the variation in soil temperature affected the accuracy of TDR measurements as compared to the neutron moisture meter. The General Linear Model (GLM) and Means comparison procedures of the Statistical Analysis System (SAS) software version 9.1 (SAS, Inc., Cary, NC, USA) was used to compare the uncorrected and corrected values of TDR moisture content with the NMM measurements. Water content measurement using both methods progressed during the fall and winter when soil in the top layers had frozen.

4.3.5 Development of a temperature calibration method applicable to TDR measurements

The apparent dielectric constant (K_a) for water decreases from about 88 near freezing to about 70 at 50°C (Warrick 2002). A third-order polynomial regression equation (Eq. 4.3) was derived ($R^2 = 1.0$) using the relative permittivity of liquid water and the corresponding temperature at 0.1 MPa pressure (atmospheric pressure) using data obtained from Fernandez et al. (1997). The data were taken for the temperature ranges of

0°C (273 K) to 40°C (313 K), which are within the range of normal soil temperatures (Nadler 2007).

$$K_T = K_0 - 4.010\times10^{-1}T + 8.988\times10^{-4}T^2 - 1.414\times10^{-6}T^3 \quad (4.3)$$

where:

T = temperature of water (°C),

K_o = dielectric constant of liquid water at 0°C (K_o = 87.90), and

K_T = apparent dielectric constant of water at the desired temperature, T.

The probes used for this experiment were calibrated at a temperature of 25°C. This temperature has also been reported to be the base line temperature at which the TDR over-predicts the volumetric water content as the temperature decreases (Wrath and Or 1999). The temperature data from Fernandez et al. (1997) was adjusted by subtracting 25°C to establish a regression equation (Eq. 4.4) with a K_a value corresponding to the baseline temperature:

$$K_T = K_{25} - 3.572\times10^{-1}(T-25) + 8.250\times10^{-4}(T-25)^2 - 1.000\times10^{-6}(T-25)^3 \quad (4.4)$$

where:

K_{25} = dielectric constant of liquid water at 25°C and 0.1 MPa (K_{25} = 78.434). The field measured dielectric constant (K_{field}) was adjusted using the following equation (Eq. 4.5) to a K_a corresponding to 25°C (K_{adj}).

$$K_{adj} = K_{field} + 3.572\times10^{-1}(T_{soil} - 25) - 8.250\times10^{-4}(T_{soil} - 25)^2 + 1.000\times10^{-6}(T_{soil} - 25)^3 \quad (4.5)$$

where:

T_{soil} = actual field soil temperature at the depth of interest (°C).

The K_a values adjusted to a soil temperature of 25°C were used in Eq. 4.6 (Topp et al. 1980) to determine liquid water content.

$$\theta_v = -5.30\times10^{-2} + 2.92\times10^{-2} K_{adj} - 5.50\times10^{-4} K_{adj}^{\ 2} + 4.30\times10^{-6} K_{adj}^{\ 3} \quad (4.6)$$

where:

θ_v = volumetric soil water content ($m^3\ m^{-3}$).

4.4 Results and Discussion

Soil temperature affects the TDR measurement of dielectric constant and thus, a temperature correction had to be carried out to adjust the field-measured dielectric constant. Before the ground is frozen, water content measured by TDR miniprobes, adjusted for temperature, and the NMM readings should be identical since both methods measure the soil water in the liquid state. Therefore, the temperature corrected soil water content data obtained by the TDR miniprobes were compared to the total soil water content measured by NMM to verify the accuracy of the TDR readings.

4.4.1 Influence of soil temperature on TDR measurements

Soil moisture measurements using TDR and NMM were compared in the field at varying soil temperatures before soil freezing. The aim was to determine how the variation in soil temperature affects TDR readings. The readings were taken when the soil temperatures were below 25°C, the temperature used for laboratory calibration of the TDR probes. On November 22, 2005, the soil temperature in the cover crop treatment

varied from 6.5°C near the surface to 2.3°C at 0.8 m depth. For the treatment without a cover crop, the temperature was 8.8°C near the surface and 2.5°C at 0.8 m depth. The TDR and NMM soil moisture measurements were compared at soil temperatures lower than the probes' calibration temperature of 25°C (Figs. 4.1 and 4.2).

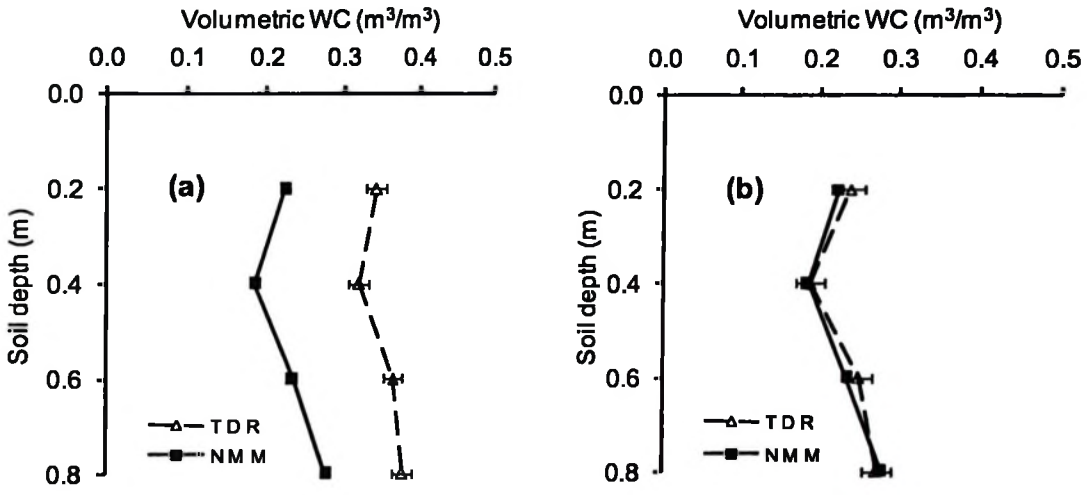

Fig. 4.1. Comparison of TDR and NMM soil moisture measurements on the cover-cropped treatment at temperature ranges 6.5°C to 2.3°C on November 22, 2005: (a) before temperature correction and (b) after temperature correction. The TDR measurements were taken as average of three replicates.

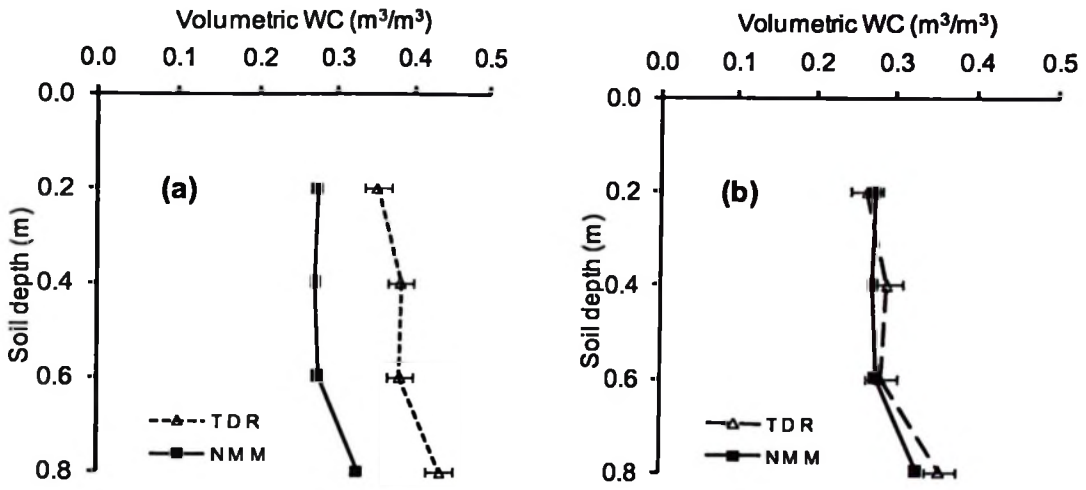

Fig. 4.2. Comparison of TDR and NMM soil moisture measurements on the non-cover-cropped treatment at temperature ranges 8.8°C to 2.5°C on November 22, 2005: (a) before temperature correction and (b) after temperature correction. The TDR measurements were taken as average of three replicates.

The uncorrected TDR moisture measurements for the two treatments before soil freezing were not comparable to the NMM measurements. The TDR method overestimated the amount of field soil moisture at lower soil temperatures (Figs. 4.1a and 4.2a). The overestimation of TDR measurement at lower soil temperatures is attributed to the fact that TDR measures dielectric constant of water (K_a value), which changes with temperature (Topp and Davis 1985; Tardif 2002). The K_a value of unfrozen water increases with decreasing temperature. Hence, there was a need to develop an equation for correcting the TDR dielectric constant measurement in the field to enable accurate measurement at any soil temperature range. The NMM method used for comparison is

not affected by temperature variations. The neutron moisture meter used in this study had been calibrated in the same field using gravimetric method.

4.4.2 Temperature correction of field TDR measurements

The equation derived for adjusting the field TDR measurements (Eq. 4.5) was used to determine the temperature-corrected dielectric constants, (K_{adj}). These adjusted K_a values were then used to obtain the volumetric soil moisture values using the Topp's model (Eq. 4.6). The soil moisture measurements obtained from the adjusted K_a values were compared with results obtained by NMM prior to soil freezing. A paired t-test was done using the SAS program to analyze data for the two different methods of measurement. In both the cover-cropped and the non-cover-cropped treatments, there was a significant difference between TDR and NMM measurements prior to temperature corrections ($P = 0.001$). After adjusting for the difference in temperature (Fig. 4.1b and 4.2b), the difference in water content measured by the two different methods was not significant ($P = 0.14$). The soil moisture content, prior to doing the temperature correction on the dielectric constant, was overestimated by an average of 0.10 m^3 m^{-3} above the NMM measured data. This difference disappeared after the temperature correction was done on field measured K_a values.

The temperature-corrected TDR measurements corresponded well with the NMM prior to soil freezing for both treatments (Figs. 4.1b and 4.2b). This was because the total soil moisture measured by NMM was the same as liquid moisture content measured by TDR when the water in the soil remained unfrozen. Brendan (2003) has also done comparison of the two methods. However, his study did not account for field variation of the soil temperature during the fall and winter when the soil is frozen or partly frozen.

4.4.3 Using TDR and NMM for soil moisture partitioning during soil freezing

As the soil started to freeze, the liquid and total soil water contents started to diverge. During late fall and early winter in December, water content measured by the TDR method was found to be less than that measured by the NMM method. The difference between the two measurements indicated the amount of soil moisture content in the frozen state (Tables 4.1 and 4.2).

Table 4.1. Soil temperature and unfrozen and total water contents at different depths along the soil profile in the cover-cropped treatment during December 13, 2005.

	Soil measurements				
		Unfrozen		Frozen	
Soil Depth (m)	Soil Temperature (°C)	water content ($m^3\ m^{-3}$)	Total water content ($m^3\ m^{-3}$)	water content* ($m^3\ m^{-3}$)	Percentage freezing (%)
0.20	-0.3	0.00	0.34	0.34	100.00
0.40	0.6	0.06	0.20	0.14	70.00
0.60	1.6	0.14	0.19	0.05	26.31
0.80	2.8	0.22	0.25	0.03	12.00

* The frozen water content was calculated as the difference between NMM (total) and TDR (unfrozen) water contents.

By December 13, 2005, soil layers on the treatment that had oats with berseem clover cover crop had completely frozen to a depth of 0.2 m. At 0.8 m depth, only 12% was frozen (Table 4.1). On the treatment with oats alone, the soil had completely frozen

to a depth of 0.4 m, and it was 52% frozen at 0.8 m depth (Table 4.2). The total water content in the 0.2- to 0.8-m soil depth was uniform. There was no influence of water table because during the fall and winter the water table drops to 1.5 to 2.0 m (Mills and Haluschak 1993).

Table 4.2. Soil temperature and unfrozen and total water contents at different depths along the soil profile in the non-cover-cropped treatment during December 13, 2005.

	Soil measurements				
		Unfrozen		Frozen	
Soil Depth (m)	Soil Temperature (°C)	water content ($m^3\ m^{-3}$)	Total water content ($m^3\ m^{-3}$)	water content* ($m^3\ m^{-3}$)	Percentage freezing (%)
0.20	-0.5	0.00	0.38	0.38	100.00
0.40	0.4	0.00	0.26	0.26	100.00
0.60	1.5	0.10	0.27	0.17	62.96
0.80	2.5	0.15	0.31	0.16	51.61

* The frozen water content was calculated as the difference between NMM (total) and TDR (unfrozen) water contents.

There is no unfrozen water content at 0.4 m depth despite the soil temperature being above 0.0°C. This can be a result of resistance of the soil to thawing at low temperatures (freeze-thaw hysteresis) once it has completely frozen during the nighttime. Soil moisture and soil temperature measurements were taken during the daytime at around 10:00 am to 11:00 am.

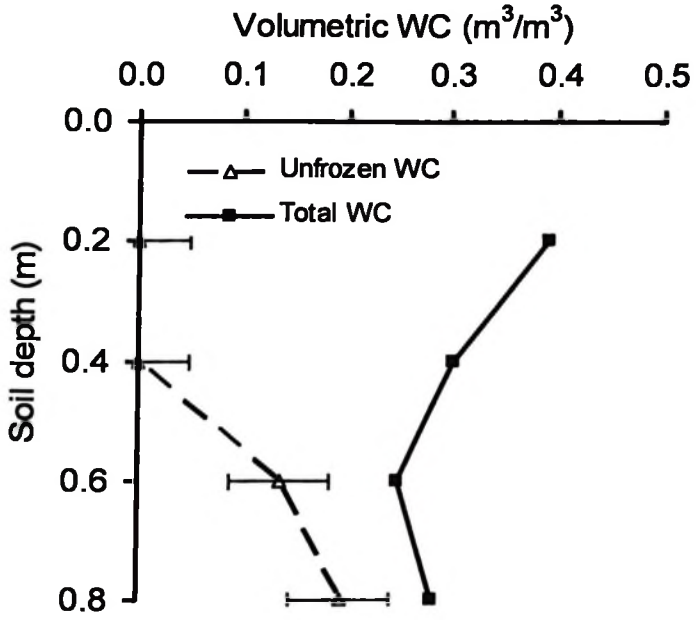

Fig. 4.3. Variation of liquid (unfrozen) and total water content with depth for the non-cover-cropped treatment on January 30, 2006. Error bars indicate standard errors of measurements.

The TDR liquid water content and NMM total water content taken on January 30, 2006, at different depths within the soil profile, for the treatment that had oats alone during the summer, are presented (Fig. 4.3). The soil temperatures were 0.2, 0.4, 1.0, and 1.6°C at 0.2, 0.4, 0.6, and 0.8 m depths, respectively. The ground had frozen to a depth of 0.4 m by January 30, 2006. Below that depth, the soil water was still unfrozen/partly frozen, signified by the presence of some liquid water content less than the total water content and soil temperatures of 1°C and above. At a depth of 0.6 m, for example, the total water content was 0.25 $m^3 m^{-3}$ and the liquid water content was 0.14 $m^3 m^{-3}$. The difference between the two values gave the amount of frozen water content as 0.11 $m^3 m^{-3}$ at that depth. Baker and Allmaras (1990) also demonstrated the possibility for using

TDR and NMM to partition liquid and frozen water content in the soil during spring snowmelt. Hence, a combination of TDR and NMM methods could be used as a means for studying the amounts and redistribution of soil water content especially during the fall to spring seasons when the soil water may exist in both the frozen and unfrozen states.

4.5 Summary and Conclusions

Time Domain Reflectometry (TDR) and Neutron scattering methods using neutron moisture meter (NMM) were used to measure soil water content in partly frozen agricultural soils. Laboratory-calibrated TDR miniprobes (35 mm long) were installed in the field, and water content measurements were taken under actual field conditions. The influence of soil varying temperature on the accuracy of TDR measurement was investigated. The TDR method overestimated the actual field soil moisture content at lower soil temperatures below 25°C ($\alpha = 0.05$). Therefore, a temperature calibration method was developed and used for adjusting the measured field dielectric constant of the soil. The adjusted dielectric constant was used to determine the soil water content at different soil temperatures. There was no significant difference ($\alpha = 0.05$) between the TDR and NMM readings after adjusting the TDR readings for temperature. After adjustment, the mean difference between the two methods was 0.01 $m^3 m^{-3}$. The calibration method developed in this study can be used for adjusting field TDR readings taken at temperatures below or above the probes' laboratory calibration temperatures.

A combination of both TDR and NMM measurements have been used to partition total soil water content into unfrozen and frozen amounts. The soil in the oats alone treatment had frozen to a depth of 0.4 m by January 30, 2006. Bellow 0.4 m, the soil was partly frozen, with the frozen and unfrozen water existing simultaneously. In addition to

determining the depth of frozen soil layer, a combination of the two methods can be used to partition the total water content into frozen and unfrozen states at different depths within the soil profile. Simultaneous use of both the TDR and NMM methods can be a valuable tool for studying soil moisture distribution and free water migration within the soil profile during the fall, winter, and spring in seasonally frozen agricultural soils.

5. COVER CROP EFFECTS ON INFILTRATION, SOIL TEMPERATURE, AND SOIL MOISTURE DISTRIBUTION IN THE CANADIAN PRAIRIES

5.1 Abstract

Excess soil moisture in the root zone resulting from annual precipitation in excess of crop water requirements negatively affects crop yields. A field study was conducted in the 2005 and 2006 seasons on sandy loam soils to investigate the influence of berseem clover *(Trifolium alexandrium* L.*)* cover crop in oats *(Avena sativa* L.*)* on soil temperature, infiltration, and soil moisture redistribution within the growing season, and during the fall to spring seasons. A four-year crop rotation experiment to investigate farming with fewer chemicals was used to grow oats in a no-till farming system with and without the cover crop. The total and unfrozen water contents were measured in the field using a neutron moisture meter and time domain reflectometry, respectively, at 0.2 m intervals from the surface to 1.8 m deep, plus a 0.1-m measurement depth. The cover crop significantly reduced soil moisture during the growing season resulting in significantly lower biomass yields (6146 kg ha^{-1} combined biomass for oats and berseem clover, vs. 7327 kg ha^{-1} for oats alone). By mid-August 2005, the cover crop treatment had 34.6% lower water content (0.17 vs. 0.26 m^3 m^{-3}) within the 0.0- to 0.7-m root zone depth compared to the non-cover crop treatment. However, the presence of berseem clover within the same season did not significantly affect the final oats yield (1671 kg ha^{-1} for oats with cover crop against 1844 kg ha^{-1} for oats alone). During the fall, the soil profile in the cover crop treatment was 3°C warmer, thus delaying soil freezing and leading to a shallower depth of the frozen soil layer (0.4 m vs. 0.6 m) in March 2006. During the spring, the cover crop treatment warmed and thawed earlier enabling more

snowmelt infiltration and deep percolation. Areas experiencing excess soil moisture could use annual cover crops as a means for reducing excess soil moisture during the summer growing season and avoiding accumulation of soil moisture during the fall, winter, and spring seasons.

5.2 Introduction

The quantity and distribution of soil moisture in seasonally frozen soils such as in the Prairies in Canada plays a significant role in ensuring optimum crop yield from agricultural lands. Among the primary factors contributing to crop failure and hence low yield is the presence of excess soil moisture within the root zone for an extended period of time during the growing season (Cavers and Heard 2001). Conservation practices involving cover crop have long been used as a means of reducing the excess soil moisture during the growing season by improving soil physical properties, and increasing the plant water uptake (Dabney 1998; Bargar et al. 1999; Boquet et al. 2004). The use of cover crops combined with no-till conservation practice has been reported to prevent soil erosion and nutrient leaching, increase organic carbon, and modify soil temperature. The combined practice has also been reported to increase water holding capacity, improve soil trafficability, and reduce compaction by machine (Unger and Vigil 1998; Dabney et al. 2001; Boquet et al. 2004). However, little has been reported on the influence of the cover crop on the redistribution of soil moisture within the soil profile during the fall and early winter, and its effect on the response of the soil to thawing during the following spring season. In addition, the existence of soil moisture in both frozen and unfrozen states during the fall through spring seasons provides a challenge in predicting the soil's

response to previous farm management practices (Flerchinger et al. 2000). Data collection under Canadian winter and spring conditions also has been a challenge.

Annual cover crops such as berseem clover (*Trifolium alexandrium* L.) planted in spring influence the availability and redistribution of soil moisture within the growing season, during the winter, and in the following spring. Previous studies on the effect of cover crops during winter have mainly focused on the winter cover crops grown during the fall after the harvest of summer crops (Raper et al. 2000; Dabney et al. 2001; Joyce et al. 2002). The effect of the within-season cover crop on the soil's response to freeze-up and meltdown in the fall, winter, and spring seasons as reported in the present study is sparse in the literature. Joyce et al. (2002) investigated the influence of common vetch (*Vicia sativa* L.) winter cover crop on the availability of soil moisture for the subsequent growing season. They concluded that winter cover crop could potentially improve water storage for the next crop if the cover crop is destroyed early, thereby reducing water loss by evapotranspiration. The use of continuous cropping instead of fallow before winter wheat has also been reported to cause soil moisture depletion and low yield of winter wheat (*Triticum aestivum* L.) (Nielsen et al. 2002).

Excess soil moisture affects several processes in the soil, which in turn, influences the crop yield potential. Cavers and Heard (2001) studied processes affected by excess soil moisture and found that problems associated with excess moisture are poor aeration, reduced root respiration, changes in soil redox potential, and production of phytotoxic compounds within the root zone. When the excess moisture occur during the middle of the growing season (i.e., during the time of flowering and seed set), the negative effect on crop yield is even more magnified.

The excess soil moisture problem is especially important in parts of the Canadian prairies, such as that of southern Manitoba, which includes the study site, the Ian N. Morrison Research Farm (formerly Carman Research Station) of the University of Manitoba (Carman, Manitoba), which receives excess precipitation in the form of both rainfall and snowmelt. Average annual precipitation of the Carman area is 588.8 mm (15 years average from 1991-2005, Environment Canada 2007). The average seasonal crop moisture requirement for the crops grown in this area (estimated as total evapotranspiration) ranges from 250 to 350 mm (Entz et al. 2002). The extent of crop failure due to excess soil moisture within the growing season depends on soil type, plant species, stage of plant growth, temperature, and day length (Cavers and Heard 2001; Osborne et al. 2003a). Cavers and Heard (2001) found that water logging over five days during flowering stage of peas (*Astragalus nuttallianus* DC) reduced the yield to 25% compared to the control (non-flooded), while two days of water logging had insignificant effect on yield.

Currently, surface drainage (i.e., field ditches) and subsurface drainage (i.e., drains) are the most widely used technique to reduce excess soil moisture in the area around Carman, Manitoba. With these drainage techniques, the potential for pollution from agricultural chemicals and sediments discharged along with the drained water from agricultural fields is also a major concern. Therefore, to minimize the loading, long-term experiments have been conducted from year 2000 at the Ian N. Morrison Research Farm on a site managed with no-till farming to investigate how various crop rotation options can best be adopted in "farming with fewer chemicals, (FFC)" (Schoofs et al. 2005). Berseem clover, an annual legume, has also been included as a cover crop in the four-

year-rotation to determine its suitability under Manitoba's soil and environmental conditions. However, the influence of the cover crop management practice on the availability and distribution of soil moisture has not been fully investigated. The effect of the presence of a cover crop on soil freezing and thawing characteristics during the fall, and its impact on soil moisture redistribution during the following spring snowmelt also needs further investigation.

The use of a cover crop, such as in an intercropping system, provides a protective cover that reduces runoff, erosion and nutrient losses, thereby facilitating more infiltration (Bargar et al. 1999). In the case of excess soil moisture, cover crop work with the main crop to uptake more water from within the root zone. Osborne et al. (2003b) found that the addition of a cover crop assists in reducing the excess moisture that could otherwise negatively affect the main crop yield potentials. The same study reported that no-till farming delayed soil warming in the spring and resulted in excess soil moisture during the spring growing season. They further noted that the use of cover crop with a no-till system helped to reduce the excess soil moisture.

Considering the agronomic advantages of cover crop, Boquet et al. (2004) reported that compared to conventional tillage with a cover crop, the no-till cover crop led to lower yield if no nitrogen fertilizer was used. Higher yields were obtained when N-fertilizer was added. However, the no-till cover crop needed more fertilizer to attain the optimum yield than conventional tillage with cover crop. The main problems with the use of cover crop are: (1) excessive consumption of water that could otherwise be available for the subsequent growing season if it were drier; (2) competition of crop nutrients with the main crop resulting in decreased crop yield if less fertilizer is applied; (3) additional

costs of seed, planting, and chemicals; and (4) water deficit at the time of the subsequent planting time (Unger and Vigil 1998; Dabney et al. 2001; Sainju and Singh 2001; Boquet et al. 2004).

Soil moisture status during the spring and summer season can be attributed to the soil conditions during the fall before soil freezing. The freeze-thaw processes and the presence of a crop cover on the ground prior to soil freezing affects infiltration, soil temperature, and soil water movement (Zuzel and Pikul 1987; Kane and Chacho 1990; Spaans and Baker 1995). Therefore, the objectives of this study were to: (1) determine the influence of an annual berseem clover cover crop in oats on infiltration, soil temperature, and soil moisture redistribution during the fall through spring; (2) determine the influence of within season berseem clover cover crop on the crop performance and yield; and (3) determine the potential of berseem clover cover crop and native prairie grass to reduce excess soil moisture within the growing season, and to reduce the accumulation of total soil moisture in the root zone during the fall through spring.

5.3 Materials and Methods

5.3.1 Site description

A field study was conducted from May 2005 to April 2006 at the Ian N. Morrison Research Farm of the University of Manitoba (Carman, Manitoba) located 90 km west of Winnipeg, Manitoba (49° 30' N, 98° 02' W, 262 m elevation). The Carman region is at the eastern edge of the Canadian prairies and experiences seasonal soil freezing and thawing during the fall, winter, and spring seasons, with the frost-free season ranging from 119 to 126 days. The frost-free season starts from May 15 to September 26 (Nadler

2007). The 588.8 mm per year average annual precipitation that the area receives is in the form of rain (477.5 mm) and snow (111.3 mm) (Environment Canada 2007). Year 2005 was wetter than normal, especially in the months of May and June. The annual precipitation for the year 2005 was 637.4 mm, of which 71% (450.6 mm) was rain between May and September, and 20% (127.6 mm) was in the form of snow between December and March. The annual mean temperature for the same year (2005) was 4.1°C (Fig. 5.1 & 5.2; Nadler 2007). The monthly mean temperature over the area (15 years average) ranges from -16.2°C in January to +19.1°C in July. The 15-year mean annual temperature was 3.4°C (Fig. 5.2). Topography of the area is relatively flat with ground slopes ranging from 0.0 to 0.5%.

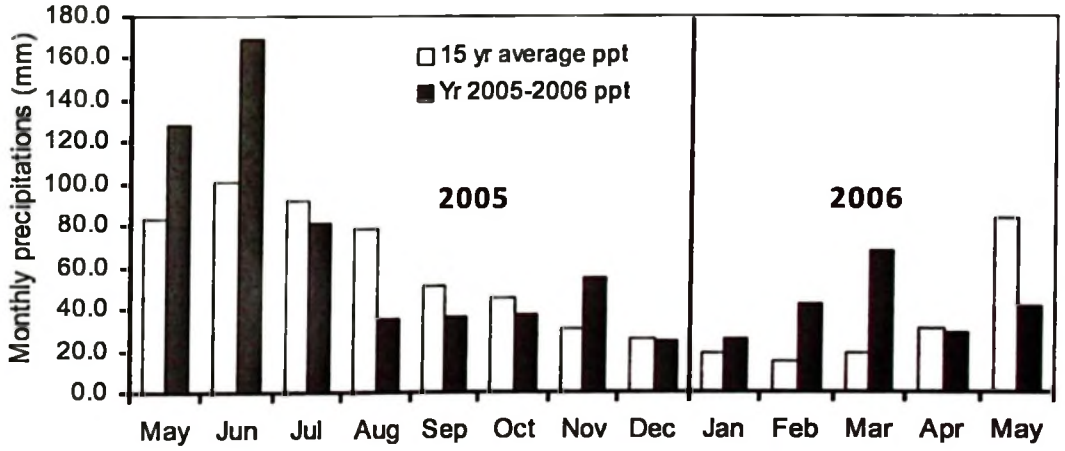

Fig. 5.1. Monthly precipitation (ppt) from May 2005 to May 2006 and fifteen-year mean monthly precipitation (1991 - 2005) for Carman, Manitoba.

The surface texture of the soil at the experimental site was classified as a well-drained Hibson, with a texture class of very fine sandy loam from the sub group Orthic Black Chernozem (Mills and Haluschak 1993) or Mollisol (very fine sandy loam) in the

USDA Soil Taxonomy. The soil particle size distribution was 76% sand, 8% silt, 16% clay, and 4% organic matter in the top 0.16 m. The average depth to the clay layer was 0.70 m. The bottom layers from 0.7 to 1.2 m had 4% sand, 44% silt, and 52% clay (Mills and Haluschak 1993). Detailed soil survey carried out by the Canada-Manitoba Soil Survey Unit (Mills and Haluschak 1993) indicated uniform soil profiles within the selected site with the depth to clay layer on an area 500 by 800 m across the experimental plots as being between 0.70 and 0.75 m (Mills and Haluschak 1993).

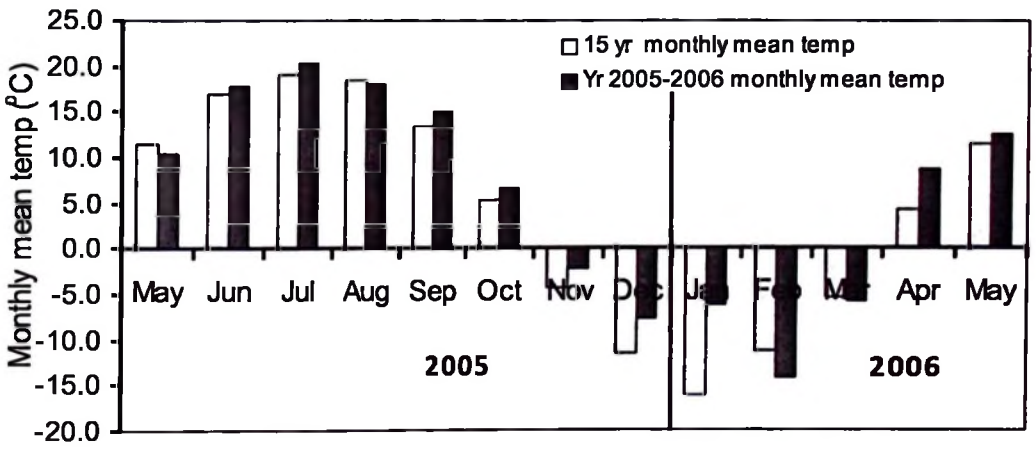

Fig. 5.2. Monthly mean temperature from May 2005 to May 2006 and fifteen-year average monthly temperature (1991 – 2005) for Carman, Manitoba.

The very fine sandy loam soils in the study area are generally well drained with the water table within one meter of the soil surface during the spring and early summer, and dropping to 1.5 to 2.0 m during the fall and winter (Mills and Haluschak 1993). The soils at the selected site had a field capacity (FC) ranging from 0.22 to 0.25 m^3 m^{-3}, and a permanent wilting point (PWP) of 0.064 to 0.082 m^3 m^{-3} (Mills and Haluschak 1993). The bottom layers from 0.7 to 1.2 m had 0.30 m^3 m^{-3} FC, and 0.13 m^3 m^{-3} PWP. The

available water (% volume) ranged between 15 and 17% on the top 0.0- to 0.7-m soil layers, and 21% between 0.7 and 1.2-m depth. The average saturated hydraulic conductivity of the top soil layers was 29 mm per day (0.336×10^{-6} m sec^{-1}) (Mills and Haluschak 1993).

5.3.2 Experimental design

The experimental site selected was within a long-term no-till, four-year crop rotation trial for investigating the concept of farming with fewer chemicals (FFC). The FFC trial, which started in year 2000, examines the growing of crops under no-till farming and the absence of in-crop pesticides application during the growing season (Schoofs et al. 2005). The trial rotations include wheat (*Triticum spp.*), canola (*Brassica napus*), oats (*Avena sativa* L.), linola /flax (*Linum usitatissimum*), and alfalfa (*Medicago sativa* L.), with native prairie and continuous fallow for comparison. Of these, only four treatments consisting of oats alone, oats with berseem clover, native prairie grass, and continuous fallow plots (Fig. 5.3) were instrumented for detailed soil moisture and temperature measurements.

The total soil moisture and soil temperature monitoring was carried out in one individual plot for each of the four treatments (plots 46, 48, 18, and 52 for oats with berseem clover, oats alone, native prairie grass, and fallow, respectively) (Fig. 5.3). Within each of these four plots one replicate of neutron access tube, one replicate of soil temperature probes, and three replicates of TDR probes were installed. Therefore, for the soil temperature and total soil moisture measured by NMM, one measurement value was taken per depth for each treatment and each time of data collection.

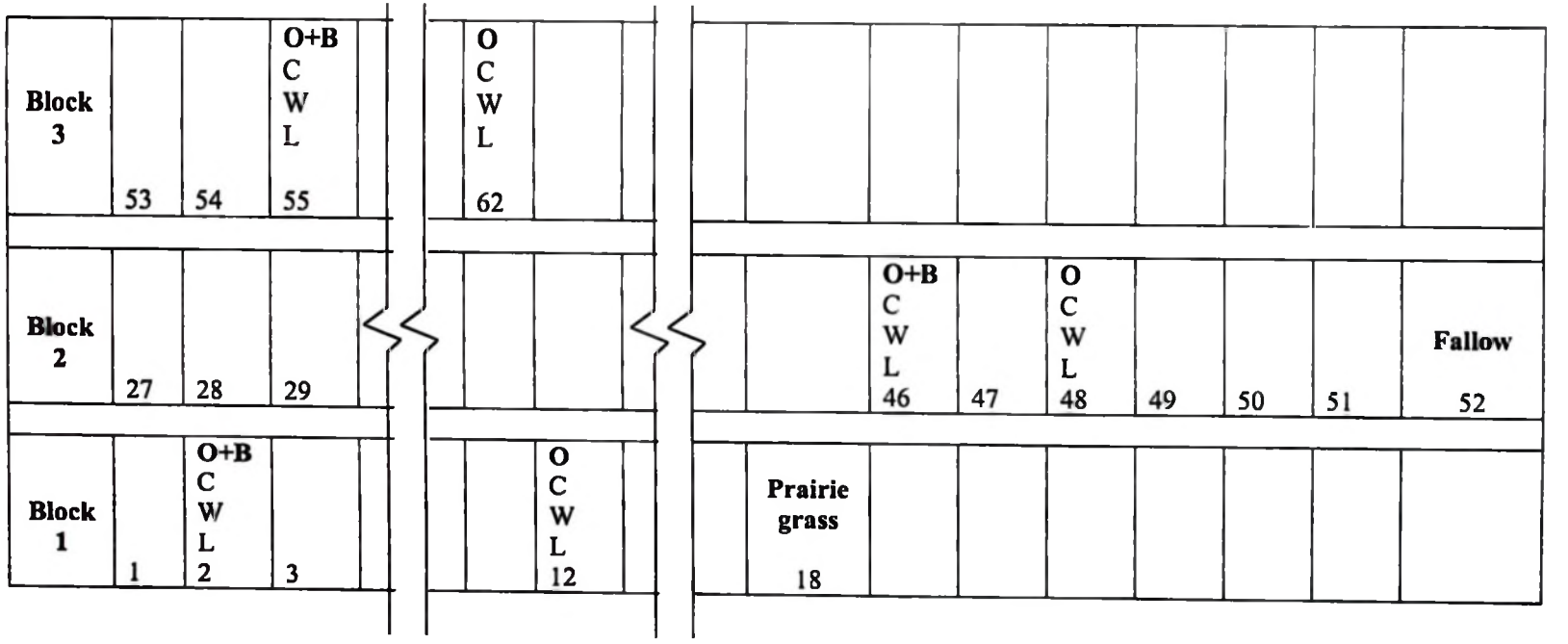

Fig. 5.3. **Field layout showing three blocks, each with oats with berseem clover cover crop (O+B) and oats alone (O) in the 2005 growing season. Numbers at the bottom represent plot numbers. The C, W, and L are respectively canola, wheat, and linola (flax) in the four-year rotation along with O+B or O.**

For the unfrozen water content measured by TDR, three measurement values per depth were taken for each treatment each time. The continuous fallow and native prairie grass were included in the study as two opposite extremes of continual bare-ground and vegetated conditions, respectively. Measurements during the winter were limited to four plots (plot 18, 46, 48, and 52) that were located near the main access road due to the narrow operational temperature range of TDR, limitation of extension cable length (40.0 m) and winter field accessibility.

Nason (2007) investigated water use efficiency of various cropping systems in experimental plots within the same study area during the growing seasons in 2005 and 2006. Mean differences between treatments as low as 0.02 $m^3 m^{-3}$ were found to be significantly different ($\alpha = 0.05$) based on NMM soil moisture data obtained from plots located in three different blocks for each treatment. This is an indication of the uniformity of the soil profile within the long-term experimental plots. The maximum length of the TDR coaxial cable that will allow us to make accurate soil moisture measurements was found to be 40 m (Kahimba et al. 2007a). This limitation in length and the inaccessibility to the entire experimental area during the winter prevented the installation of TDR miniprobes in all individual plots.

For the crop performance data, which were collected during the summer growing season, a randomized complete block design was used with three replicate blocks of the oats with berseem clover cover crop (plots 2, 46, and 55) and the oats alone (plots 12, 48, and 62) treatments (Fig. 5.3, Nason 2007). No yield measurements were taken on the fallow and native prairie grass treatments, hence one plot was used for the soil moisture and soil temperature measurements on the fallow (plot 52) and prairie (plot 18), as stated

earlier. To minimize measurement variations due to soil heterogeneity and management practices for the cover crop and non-cover crop treatments, the plots were selected within the same block (plot 46 and 48) that were fairly close (6 m gap). The crop planting date was the same and the two treatments received the same farm management practices. The repetition of total soil moisture and soil temperature monitoring at the same depth over several days within the year also assisted to confirm the soil moisture and soil temperature trends over time.

5.3.3 Field installations

Time domain reflectometry (TDR) cable tester (Tektronix model 1502B, Tektronix Inc., Beaverton, OR, USA) and TDR miniprobes with probe rods 35 mm long and 1.6 mm diameter (three-wire configuration) were used for measuring the unfrozen water content. The measurement precision for the down-sized TDR probe lengths ranging from 25 to 75 mm is 0.035 to 0.015 $m^3 m^{-3}$, respectively (Kelly et al. 1995; Persson and Haridy 2003). Sri Ranjan and Domytrak (1997), using a wave-form noise reduction algorithm to determine the effective volume of 50-mm miniprobes, reported a precision of 0.01 $m^3 m^{-3}$. To minimize the effect of soil variability and plot disturbance due to access during the winter months, three replications of the TDR probes were installed within each treatment. The TDR miniprobes were installed in the field at depths of 0.1, 0.2, 0.4, 0.6, and 0.8 m from the ground surface for each of the three replicates in a treatment. The probes were attached to RG-58 50 Ω coaxial cables that were brought above the ground surface for connection to the TDR.

The installation of the miniprobes was done at a 30° angle to the vertical to avoid preferential water flow through the installation holes. One replicate of thermocouples for

recording soil temperature were installed along with the TDR probes at the same depths. A combination of soil temperature profile and the TDR unfrozen soil moisture measurements assisted in determining the soil freezing depth during the fall to spring seasons. The advantage of TDR miniprobes (35 mm) compared to commercial probes (>150 mm long) is that they can be used to accurately measure soil water content at depth intervals of 100 mm or less. The applications and effectiveness of downsized TDR miniprobes are described in Sri Ranjan and Domytrak (1997), Persson and Haridy (2003), and Kahimba and Sri Ranjan (2007).

Aluminium access tubes (50 mm diameter) were installed, one tube in each treatment to a depth of 2.0 m from the ground surface for use with the neutron moisture meter, (NMM, Troxler model 4302, Troxler Electronic Laboratories, Inc., Research Triangle Park, NC, USA). One NMM access tube was installed for each treatment close to the centre of the three TDR replicates on plots 18, 46, 48, and 52 (Fig. 5.3). The NMM was used to measure total water content along the vertical soil profile at 0.2 m intervals from 0.2 m to a depth of 1.8 m. Prior to data collection, the NMM was calibrated in the field by taking both NMM data and volumetric water content data obtained from core samples using gravimetric method. A calibration equation was established (Eq. 5.1) that was used for interpretation of the NMM field data.

$$Y(\%) = \frac{CR}{0.022} - \frac{22.3}{2.2} \qquad (5.1)$$

where:

Y = total volumetric water content (%), and

CR = count ratio.

The NMM measurement precision for measuring water content is ±0.01 $m^3 m^{-3}$ (Evett and Steiner 1995). Due to its high precision and extensive references in the literature, the NMM has been used as a standard measurement technique to compare with other methods of water content measurement (Evett 2003a). In this experiment, one replicate of NMM measurement was used as the standard for each treatment, along with the three replicates of TDR measurements that were also installed in each treatment.

5.3.4 Field data collection and analysis

One of the challenges in studying soil moisture availability and redistribution during the fall and winter seasons is the ability to quantify soil water in the frozen and unfrozen states. As the soil transforms from the unfrozen to frozen state, physical measurement of the depth of freezing front and the available unfrozen and frozen water content, requires the combination of soil moisture measuring methods that can partition total moisture into frozen and unfrozen states. In this study, total soil water content was measured using NMM because this method is only influenced by the presence of hydrogen atoms irrespective of its state. The TDR was used to measure unfrozen (liquid) water content because this method measures dielectric constant of water in the liquid state (Topp et al. 1980; Seyfried 2004). A single soil moisture measurement technique can not give both the frozen, unfrozen, and total water contents, simultaneously (Kahimba and Sri Ranjan 2007). A combination of the two methods allowed partitioning of the total water content into the frozen and unfrozen components. Detailed procedures on principles of NMM measurements are described in Evett (2000a).

Both the TDR and NMM measurements and the soil temperature within the soil profile were taken on the same day within one hour of each other to allow comparison of

the two methods. The one-hour range of time for data collection assisted to minimize measurement errors from evaporative losses and temperature variability that could affect the TDR water content measurements. Measurements were taken once every month from August 2005 to April 2006. The Topp model (Topp et al. 1980), used to relate the dielectric constant with volumetric water content, is as follows:

$$\theta_v = -5.3\times10^{-2} + 2.92\times10^{-2}\varepsilon_b - 5.5\times10^{-4}\varepsilon_b^{\,2} + 4.3\times10^{-6}\varepsilon_b^{\,3} \qquad (5.2)$$

where:

θ_v = volumetric water content ($m^3\ m^{-3}$), and

ε_b = composite dielectric constant of the medium corrected for temperature.

As the soil started to freeze, and throughout the winter, the two methods of soil water content measurements were used simultaneously to track the depth of freezing front, and the partition of frozen and unfrozen water within the soil profile. Details on the combination of TDR and NMM methods to determine the soil freezing and thawing patterns are given in Kahimba and Sri Ranjan (2007). Soil temperature was measured using a digital thermocouple thermometer with a precision of ±0.1°C at the same depths as the TDR soil water content measurements. Analysis was performed to determine the influence of the crop cover on soil temperature and soil moisture redistribution, as well as the soil freezing-thawing response during the fall through spring seasons for different ground cover conditions.

In the year 2005, the maximum daily air temperature at the Carman automatic meteorological station started to be below zero (-0.2°C) on November 14, and by November 30 it was -8.7°C (Nadler 2007). This was an indication that the fall freeze-up started in late November. During spring, the soil started to thaw between April 4 and 9,

2006 (Nadler 2007). The 2005-2006 was a wetter season compared to the 15-year average as recorded at the Carman meteorological station. During the growing season from May to August 2005, the total precipitation was 414.2 mm compared to the 15-year average of 354.1 mm in the same period (Environment Canada 2007, Fig. 5.1). During the fall to spring season from November 2005 to April 2006 the total precipitation (rain and/or snow) was 241.8 mm compared to a 15-year average of 138.7 mm (and Fig. 5.1). The snow depth was measured once using a meter rule at the end of the winter on February 24, 2006. Three replicates of the snow depth were taken at three different locations surrounding the neutron access tube within each treatment.

Measurements of the crop performance (above ground biomass) in the cover crop and non-cover crop treatments were taken during the growing season from May to October 2005. The oats were seeded on May 12, 2005 and harvested on August 08, 2005. The berseem clover in the cover crop treatment was also seeded on May 12, 2005, and continued to grow after the main crop had already been harvested in August 2005 (Nason 2007). The oats yield measurements were taken at the end of the growing season in August 2005. During the harvest, a strip of 1.0 m by 2.0 m (2.0 m^2 area) was harvested close to the centre of the plots and used for the yield measurements. The yield was taken by averaging data from three replicates, each having the same four-year rotational strategy and receiving the same crop management practice. After harvest of the rest of the main crops, 200 mm of oats stubbles were left along with the berseem clover cover crop. The cover crop continued to grow (Table 5.1) until late November when the fields were covered with snow and the soil started to freeze.

5.3.5 Statistical analysis

The soil moisture and soil temperature data within the soil profile were compared for different treatments and different times of the year. The general linear model (GLM) procedure of the SAS statistical analysis software (SAS Inc. 2004) was used to determine variations of total soil moisture in the root zone to a depth of 0.8 m, with a null hypothesis that there was no difference between the crop-covered and the non crop-covered treatments at $\alpha = 0.05$. The Least Significant Difference (LSD) multiple comparisons test with $\alpha = 0.05$ was used to determine the means that had no significant difference at similar depths. The means procedure of the SAS was also used to compare the total and the unfrozen water content, and to determine the differences in the soil temperature along the soil profile as a function of time.

5.4 Results and Discussion

5.4.5 Influence of berseem clover cover crop on the main crop performance and yield

While cover crops help to reduce excess soil moisture during the growing season, the competition with the main crop in terms of nutrient and water availability at later stages of the growing season may affect the performance and hence, the yield of the main crop. A paired two-sample test for means analysis was performed to assess the growth performance of oats on two treatments of oats alone and oats with berseem clover cover crop at different stages of plant growth (Table 5.1).

Considering the growth performance for the two management systems (Nason, 2007; Table 5.1), both treatments had no significant difference in biomass yield at early stages of the growth from May to July 2005 when the cover crop had not yet fully established.

However, towards the end of the season on August 05, 2005, the biomass yield in oats alone (7327 kg ha^{-1}) was significantly higher ($\alpha = 0.05$) compared to the combined biomass yield of oats and berseem clover (6146 kg ha^{-1}) (Table 5.1; Nason 2007).

Table 5.1. Oats biomass yield for the treatments with and without a berseem clover cover crop in the 2005 growing season at the Ian N. Morrison Research Farm in Carman, Manitoba.

	Above ground biomass yield (kg ha^{-1})				
	Crop specific biomass			Total biomass	
Date	Oats alone	Oats in cover crop	Berseem clover cover crop	Oats alone	Oats plus berseem clover
May26, 2005	12 a*	13 a	0	12	13
June 17, 2005	959 a	975 a	77	959	1052
July 12, 2005	5949 a	5304 a	66	5949	5370
Aug 05, 2005	7327 a	6080 b	66	7327	6146
Sept 06, 2005	0	0	241	0	241
Sept 30, 2005	0	0	399	0	399
Oct 25, 2005	0	0	640	0	640

* Means followed by the same letter on each date are not significantly different ($\alpha = 0.05$).

The competition for soil moisture between the cover crop and the main crop at later stages of plant growth (Table 5.1, Nason 2007) did not give a significant difference ($\alpha = 0.05$) in the final oats yield (1844 kg ha^{-1} for oats alone and 1671 kg ha^{-1} for oats with berseem clover, Nason 2007). Results on low yields of the main crop due to moisture competition with the cover crop were also obtained by Reddy (2001). Although cover crops could be helpful in reducing the excess soil moisture, the cover crop can lead to soil moisture competition at later stages of plant growth when the precipitation

becomes low in August and September (Fig. 5.1). Hence, for farm management systems involving both no-till and a berseem clover cover crop, consideration has to be given on soil moisture competition between the main crop and the cover crop, which may affect the performance of the main crop if there is less soil moisture available at later stages in the growing season.

5.4.2 Influence of cover crop within the growing season on soil moisture redistribution

During the growing season, the cover crop helped to reduce excess soil moisture that could otherwise cause stress to the main crop, especially at the early stages of the plant growth. However, during the later stages of plant growth when both the main crop and the cover crop need a lot of soil moisture, the cover crop may cause a soil moisture deficit to the main crop leading to lower crop yields.

Table 5.2 presents the root zone water content in the oats with berseem clover cover crop compared to oats alone during the growing season on August 16, 2005. During maturity stage in August 2005, the total volumetric water content within the root zone (0.0 to 0.7 m depth) was 34.6% lower in the cover crop treatment (0.17 m^3 m^{-3}) compared to the oats alone treatment (0.26 m^3 m^{-3}).

Table 5.2. Reduction of root zone water content in oats with berseem clover cover crop compared to oats alone treatment during the growing season on August 16, 2005.

Soil depth (m)	Root zone water content on August 16, 2005*		
	Oats alone** ($m^3\ m^{-3}$)	Oats + Berseem** ($m^3\ m^{-3}$)	Reduction*** (%)
0.10	0.23	0.15	34.8
0.20	0.25	0.17	32.0
0.40	0.31	0.19	38.7
0.60	0.27	0.18	33.3
Total ****	0.26	0.17	34.6

* Water content measurements taken using time domain reflectometry (TDR) method

** TDR measurements at each depth on each treatment are averages of three replicates

*** The percentage reduction is relative to the oats alone as the denominator

**** Total soil water content in the depth from 0.05 m to 0.7 m.

Table 5.3 presents the unfrozen water content in the 0.1- to 0.9-m soil profile for the four cropping systems (oats with berseem clover, oats alone, fallow, and native prairie grass) from August 2005 to April 2006. The unfrozen (TDR) water content at each depth from 0.2 to 0.8 m in the oats with berseem clover cover crop treatment was significantly lower ($\alpha = 0.05$) compared to the water content in the oats alone treatment on August 16, 2005 (Table 5.3). Similar results were also observed for the native prairie grass and fallow, whereby the native prairie grass had significantly lower water content at each depth ($\alpha = 0.05$) compared to the fallow treatment.

Table 5.3. Unfrozen (TDR) water content in the 0.0- to 0.8-m soil profile for the four cropping systems from August 2005 to April 2006.

Soil depth (m)	Management system	Unfrozen soil water content (measured by TDR) (m^3 m^{-3})* Aug 16 2005	Sept 07 2005	Oct 11 2005	Nov 24 2005	Dec 21 2005	Jan 30 2006	Mar 29 2006	Apr 04 2006
0.2	Oats + Berseem clover	0.17 a**	0.25 a	0.32 a	0.24 a	0.0 a	0.0 a	0.0 a	0.0 a
	Oats alone	0.25 b	0.26 a	0.31 a	0.19 b	0.0 a	0.0 a	0.0 a	0.0 a
	Continuous fallow	0.31 c	0.30 b	0.33 a	0.25 a	0.0 a	0.0 a	0.0 a	0.0 a
	Native prairie grass	0.17 a	0.26 a	0.32 a	0.24 a	0.17 b	0.15 b	0.14 b	0.327 b
0.4	Oats + Berseem clover	0.19 a	0.18 a	0.34 a	0.25 a	0.08 b	0.08 b	0.0 a	0.0 a
	Oats alone	0.31 c	0.29 b	0.37 b	0.26 a	0.0 a	0.0 a	0.0 a	0.0 a
	Continuous fallow	0.34 d	0.24 c	0.31 a	0.25 a	0.0 a	0.0 a	0.0 a	0.0 a
	Native prairie grass	0.24 b	0.23 c	0.37 b	0.29 b	0.22 c	0.28 c	0.29 b	0.36 b
0.6	Oats + Berseem clover	0.18 a	0.33 c	0.32 a	0.27 a	0.09 b	0.14 b	0.1 b	0.12 b
	Oats alone	0.27 b	0.28 b	0.35 ab	0.30 b	0.08 b	0.14 b	0.0 a	0.0 a
	Continuous fallow	0.34 c	0.31 bc	0.38 bc	0.32 b	0.0 a	0.0 a	0.0 a	0.0 a
	Native prairie grass	0.25 b	0.21 a	0.39 c	0.27 a	0.30 c	0.28 c	0.30 c	0.31 c
0.8	Oats + Berseem clover	0.26 a	0.32 c	0.37 a	0.31 a	0.18 b	0.16 b	0.11 c	0.17 c
	Oats alone	0.29 bc	0.29 b	0.37 a	0.35 b	0.21 c	0.20 c	0.07 b	0.07 b
	Continuous fallow	0.32 c	0.31 bc	0.37 a	0.35 b	0.09 a	0.04 a	0.0 a	0.0 a
	Native prairie grass	0.28 ab	0.25 a	0.43 b	0.36 b	0.34 d	0.37 d	0.33 d	0.34 d

* Data were taken as average of three replicate TDR measurements.

** Means followed by a different letter in the same column at the same soil depth are significantly different ($\alpha = 0.05$).

5.4.3 Variation of water content within the root zone from fall through spring

In the 2005 - 2006 seasons, snow started to accumulate in late November 2005. During spring of 2006, the maximum daily temperatures started to be above zero (0.8°C) on March 24, and the minimum temperature was above zero (0.9°C) on April 09 (Environment Canada 2007; Nadler 2007). The spring snowmelt started on March 30, 2006. Towards the end of the winter on February 24, 2006 there was no significant

difference in snow depth ($\alpha = 0.05$) between the oats with berseem clover cover crop treatment (0.31 m) and the oats alone (0.29 m). This was partly because by the beginning of the snow accumulation in late November 2005, the oats stubble remaining in the plots were similar in height (200 mm) to berseem clover. However, the native prairie grass treatment had significantly deeper layer of snow pack (0.68 m) compared to the fallow treatment (0.21 m). The native prairie grass accumulated more snow pack since it had dense grass stands of about 0.7 m by November 2005 that helped to trap snow throughout the winter. The insulation in the native prairie grass caused the treatment to continue having unfrozen water contents throughout the fall through spring seasons (Table 5.3).

As the soil began to freeze in late November 2005, the oats alone and oats with berseem clover treatments accumulated soil moisture due to fall snowmelt and rain infiltration from early snowfall (Table 5.4). By December 21, the average total water content in the top 0.8 m was 0.24 $m^3 m^{-3}$ for the cover crop treatment and 0.31 $m^3 m^{-3}$ for the treatment without a cover crop (Table 5.4). This indicated that the cover crop treatment accumulated less total water content than the non-cover crop treatment.

Table 5.4 presents the total soil water content within the root zone at 0.2 m intervals from 0.2 to 0.8 m depths for two treatments shown as a function of time from the fall (November 2005) through spring (April 2006). The soil water content at each depth in the 0.1- to 0.9-m depth was consistently lower in oats with berseem clover cover crop treatment compared to oats alone during the fall and winter from November 2005 to March 2006 (Table 5.4).

Table 5.4. Comparison of accumulation of total soil water content in the root zone for oats with berseem clover cover crop and oats alone treatments from the fall in November 2005 to spring in April 2006.

Date	Soil depth (m)	Total water content measured by NMM*		
		Oats alone ($m^3\ m^{-3}$)	Oats + berseem ($m^3\ m^{-3}$)	Reduction** (%)
Nov 24, 2005	0.20	0.30	0.25	16.7
	0.40	0.30	0.21	30.0
	0.60	0.31	0.25	19.4
	0.80	0.37	0.31	16.2
	Total ***	0.32	0.26	18.8
Dec 13, 2005	0.20	0.38	0.34	10.5
	0.40	0.26	0.20	23.1
	0.60	0.27	0.19	29.6
	0.80	0.31	0.25	19.4
	Total	0.31	0.25	19.4
Dec 21, 2005	0.20	0.39	0.34	12.8
	0.40	0.29	0.22	24.1
	0.60	0.26	0.19	26.9
	0.80	0.29	0.22	24.1
	Total	0.31	0.24	22.6
Jan 30, 2006	0.20	0.38	0.34	10.5
	0.40	0.29	0.22	24.1
	0.60	0.24	0.20	16.7
	0.80	0.28	0.22	21.4
	Total	0.30	0.25	16.7
Mar 29, 2006	0.20	0.39	0.34	12.8
	0.40	0.40	0.35	12.5
	0.60	0.31	0.26	16.1
	0.80	0.22	0.13	40.9
	Total	0.33	0.27	18.2
Apr 04, 2006	0.20	0.39	0.39	0.0
	0.40	0.41	0.40	3.5
	0.60	0.34	0.32	5.1
	0.80	0.32	0.30	5.5
	Total	0.37	0.35	5.4

* For each treatment, one measurement value was taken using NMM on each date and at each soil depth.

** The percentage reduction is relative to the oats alone as the denominator.

*** Total soil water content in the depth from 0.1 m to 0.9 m.

The lower soil water content in oats with berseem clover cover crop treatment is attributed to more consumption of the soil moisture by both the oats main crop and the berseem clover cover crop during the growing season and early fall. During the winter, by March 29, 2006 there was an 18% lower accumulation of total water within the top 0.8 m in the oats with berseem clover cover crop treatment compared to the treatment containing oats alone.

The cover crop treatment had 22.6% lower total soil water content compared to the non-cover crop treatment on December 21, 2005. This was largely due to the greater reduction of the soil moisture in the root zone by the remaining cover crop vegetation that continued to grow after the harvest of the main crop and consumed the remaining available soil moisture in the root zone before the fall freeze-up.

In both treatments, the soil started to freeze in late November 2005, and by January 30, 2006 the top 0.2 m had completely frozen (Table 5.3, Fig. 5.4 b2) limiting any further infiltration from the surface. However, as the winter progressed between January and March 2006 there was an increase in total soil water content in the layers 0.4 to 0.6 m (Table 5.4, Fig. 5.4 a2 and a3). At the end of winter in March 2006, the total water content at 0.8 m-depth was the lowest (Table 5.4, Fig. 5.4 a3), indicating upward migration of water towards the freeze-front from the partly frozen soil layers below. In general, compared to the treatments that had less vegetation (oats only) or did not have vegetation (fallow), the treatments with more vegetation (native prairie grass and oats with berseem clover) had lower soil water contents during the summer and accumulated less total water content during the winter (Table 5.3, Table 5.4, Fig. 5.4).

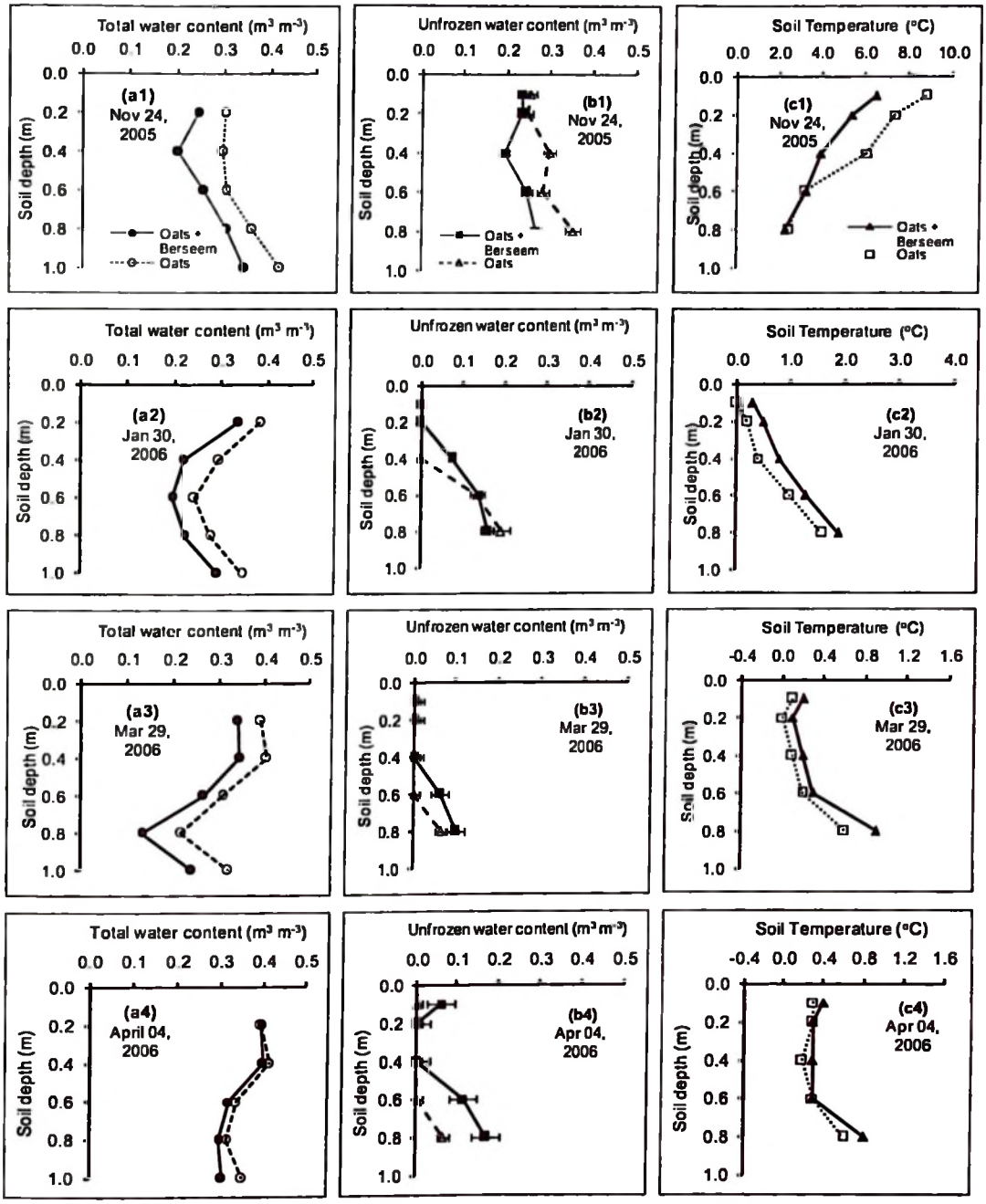

Fig. 5.4. **(a) Total water content (measured with NMM), (b) unfrozen water content (measured with TDR), and (c) soil temperature variation for the oats with berseem clover cover crop and oats alone treatments during: (1) the fall of 2005, and (2) winter and (3, 4) spring of 2006. Error bars for TDR measurements indicates standard errors of three replicate measurements for each soil depth.**

The presence of vegetation (such as the residual cover crop) after the summer harvest period, contributed to the reduction of soil moisture for the oats with berseem clover compared to oats alone at each depth in the root zone between the fall (November 24, 2005) and the following spring (March 29, 2006) (Table 5.4). This reduction is expected to lower the soil moisture available at the beginning of the next growing season. Nielsen et al. (2002) who studied the influence of a winter wheat cover crop on soil moisture availability also observed reduced soil moisture at the beginning of the next growing season due to previous cover crop.

The total water content, unfrozen water content and soil temperature as a function of depth for the treatments with and without a berseem clover cover crop from the fall 2005 through spring of 2006 are shown in Fig. 5.4. Compared to the treatment that had a cover crop, the treatment containing oats alone had consistently higher total soil moisture within the 0.1- to 0.9-m soil depth throughout the fall, winter and spring (Fig. 5.4 a1- a3). However, as snow started to melt in early April, the top soil layers in the oats with berseem clover cover crop treatment started to thaw earlier (Fig. 5.4 b4). The earlier thawing allowed snowmelt infiltration into the top layers (0.0 – 0.6 m) causing its total water content to temporarily increase and be approximately equal to the treatment with no cover crop. This was signified by the presence of unfrozen water in the top 0.2 m as measured by TDR, on the treatment with a berseem clover cover crop (Fig. 5.4 b4). The treatment containing oats alone had greater depths of frozen layer throughout the winter and early spring as determined by TDR (Fig. 5.4b). The treatment also had consistently cooler soil temperatures during the winter and spring (Fig. 5.4c). Sainju and Singh (2001) have also reported results of lower soil moisture during spring due to the presence of

cover crops. The presence of the cover crop provided insulation at the ground surface causing a delay in fall freeze-up that led to a shallower depth of the frozen soil layer.

5.4.4 Soil moisture partitioning and determination of the depth of freezing front

A combination of two soil moisture measurement techniques helped to partition the total soil moisture into frozen and unfrozen states and track the frost depth (Fig. 5.5).

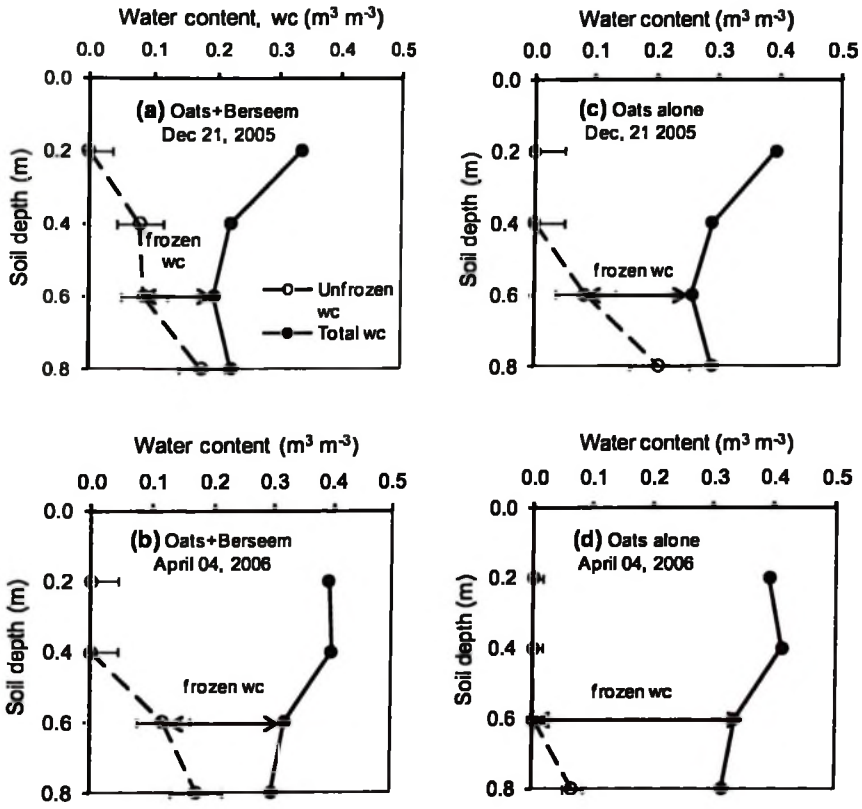

Fig. 5.5. Partitioning of total water content into frozen and unfrozen phases for the oats with berseem clover cover crop and oats alone treatments during: (a and c) fall freeze-up in December 2005, and (b and d) spring in April 2006. The difference between the two curves represents the amount of soil moisture in the frozen state. Error bars indicate standard errors of measurement for three TDR replicates.

The depth to which the TDR measured zero or close to zero unfrozen soil water content was an indication of the depth of the soil profile in which the soil moisture had completely frozen or partly frozen at temperatures very close to zero.

Considering the treatments with and without berseem clover during fall freeze-up, by December 21, 2005 the non-cover crop treatment had frozen to a depth of 0.4 m while the cover crop treatment had frozen only to a depth of 0.2 m (Fig. 5.5 a and c). During spring (April 04, 2006), the freezing front had advanced to 0.6 and 0.4 m depths for the non-cover crop treatment and cover crop treatment, respectively (Fig. 5.5 b and d). Hence, the presence of a cover crop during the previous season delayed soil freezing during the winter and led to a shallower depth of the frozen soil layer. For both the cover crop and non-cover crop treatments, deeper layers were partly frozen with unfrozen water content increasing with depth and approaching the amount of total water content at 0.8 m depth. Compared to using one soil moisture measurement technique, the two techniques, TDR and NMM, combined together gave a better indication of how the freezing front was advancing downwards with time as the winter progressed.

5.4.5 Soil moisture redistribution during the winter and spring

From January 2006 to March 2006, the total soil moisture decreased with time at the 0.6 and 0.8 m depth, and increased with time at the 0.2 and 0.4 m depth (Fig. 5.4 a2 and a3). This data indicates that as the soil continued to freeze and the freezing front advanced downwards, the unfrozen soil moisture from the soil layers below the freezing front migrated upwards towards the freezing front. Partly saturated frozen soils act like

dry soil, pulling unfrozen water upwards from the lower layers because the water above the freezing front is already immobilized due to freeze-up. The March 29 was a date just before the start of spring snowmelt, while April 4 was a date five days after the start of spring snowmelt. The snowmelt started on March 30 as explained earlier. Therefore, compared to the soil moisture status when the soil started to freeze in the fall, the soil layers below the freezing front had a net decrease in water content at the end of winter, while the soils above the freezing front had a net increase. As a result, the non-cover crop treatment with higher soil water content during the fall led to greater accumulation of total soil water at the end of the winter season. Compared to the non-cover crop treatment of oats alone, the cover crop treatment warmed and thawed earlier, with soil profile temperatures being 0.1°C to 0.3°C warmer during the spring (Fig. 5.4 c3 and c4).

Based on a precision of 0.2% for the temperature measurement, the non-cover crop treatment had 2.3°C, 2.0°C, and 2.1°C higher soil temperature at 0.1-, 0.2- and 0.4-m depths of the soil profile during the fall (November 24, 2005) compared to the cover crop treatment (Fig. 5.4 c1). By mid-winter (January 30, 2006), the non-cover crop treatment had 0.3°C, 0.3°C, and 0.4°C lower soil temperature at 0.1-, 0.2- and 0.4-m depths compared to the cover crop treatment (Fig. 5.4 c2). However the temperatures had a smaller difference (0.0°C - 0.2°C) for the cover crop and non-cover crop treatments during late winter and spring (Fig. 5.4 c3 and c4). On average, the cover crop treatment was consistently cooler during the fall in November 2005 and warmer during the winter (Fig. 5.4c). During the winter and early spring, it was warmer by 0.1°C to 0.4°C to a depth of 0.8 m. By April 04, 2006, the soil profile in the drier cover crop treatment was

slightly warmer (Fig. 5.4 c4) causing the top 0.2 m to start thawing earlier than in the non-cover crop treatment (Fig. 5.4 b4).

5.4.6 Variation of total soil water content with time within the same treatment

Variations of the total soil water content with time for each individual treatment were assessed for the depths up to 1.8 m from September 2005 to April 2006 (Fig. 5.6). By April 04, 2006, compared to the non-cover crop treatment, the cover crop treatment had 5.5%, 13.1%, and 10.1% lower total soil water contents at 0.8, 1.0, and 1.2 m depths, respectively (Fig. 5.6 c and d). Similar trends were observed for the native prairie grass (vegetated field) compared to the fallow (bare field) treatments (Fig. 5.6 a and b).

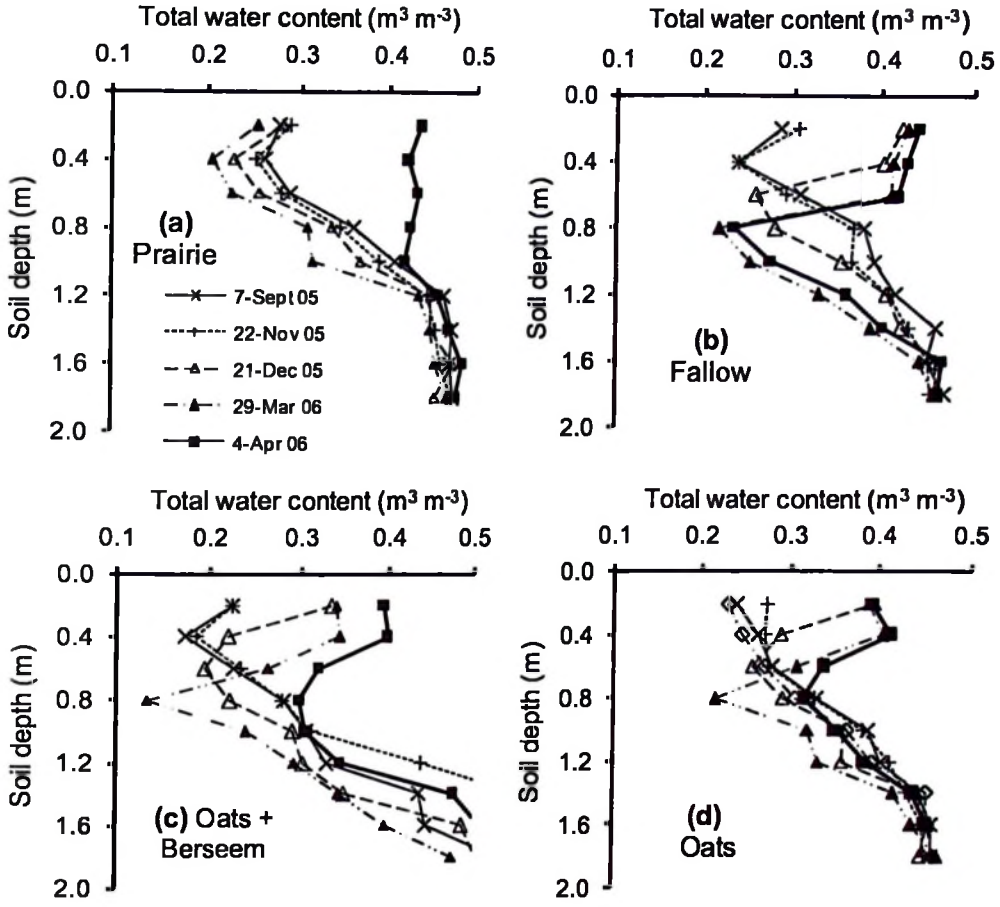

Fig. 5.6. Variation of total water content with depth within each treatment for: (a) prairie grass, (b) continuous fallow, (c) oats with berseem clover, and (d) oats alone, from September 2005 to April 2006. One measurement was taken for each treatment at each depth on each date using NMM.

The cover crop treatment being drier will require less solar heat to warm up compared to the wetter non-cover crop treatment due to the lower heat capacity of drier soil compared to the wetter soil. The cover crop treatment also had 8.8%, 12.9%, and 11.4% higher total soil water contents at 1.4, 1.6, and 1.8 m depths, respectively (Fig. 5.6

c and d). This was an indication that the cover crop treatment allowed more infiltration of the melt water into the soil profile and percolation away from the root zone.

Table 5.5. Comparison of accumulation of total soil water content in the 0.1- to 0.9-m depth for the continuous fallow and native prairie grass treatments from the late fall in December 2005 to early spring in April 2006.

		Total water content measured by NMM*		
Date	Soil depth (m)	Fallow (m^3 m^{-3})	Prairie grass (m^3 m^{-3})	Reduction** (%)
Dec 13, 2005	0.20	0.42	0.29	31.0
	0.40	0.36	0.24	33.0
	0.60	0.27	0.27	0.0
	0.80	0.31	0.33	-6.5
	Total***	0.34	0.28	17.6
Dec 21, 2005	0.20	0.42	0.28	33.3
	0.40	0.40	0.23	42.5
	0.60	0.26	0.26	0.0
	0.80	0.28	0.33	-17.9
	Total	0.34	0.28	17.6
Jan 30, 2006	0.20	0.42	0.26	38.1
	0.40	0.41	0.23	43.9
	0.60	0.26	0.25	3.8
	0.80	0.26	0.32	-23.1
	Total	0.34	0.27	20.6
Mar 29, 2006	0.20	0.43	0.25	41.9
	0.40	0.41	0.20	51.2
	0.60	0.41	0.23	43.9
	0.80	0.22	0.31	-40.9
	Total	0.37	0.25	32.4
Apr 04, 2006	0.20	0.44	0.43	2.3
	0.40	0.43	0.42	2.3
	0.60	0.42	0.43	-2.4
	0.80	0.23	0.42	-82.6
	Total	0.38	0.43	-13.2

* For each treatment, one measurement value was taken using NMM on each date and at each soil depth

** The percentage reduction is relative to the fallow as the denominator

*** Total soil water content in the depth from 0.1 m to 0.9 m.

The native prairie treatment maintained a lower total water content than the fallow within the top 1.0 m of the profile during early spring on March 29, 2006 (Table 5.5; Figs. 5.6a and 5.6b). This was the time just before the start of spring snowmelt. In their study on winter wheat cover crop, Joyce et al. (2002) also reported increased infiltration on the cover crop plots compared to the continuous fallow.

The soil temperatures within the to 0.8 m soil depth were still above zero by December 21, 2005 in the native prairie grass treatment even when the temperatures in the fallow had dropped below -3.0°C (Fig. 5.7a).

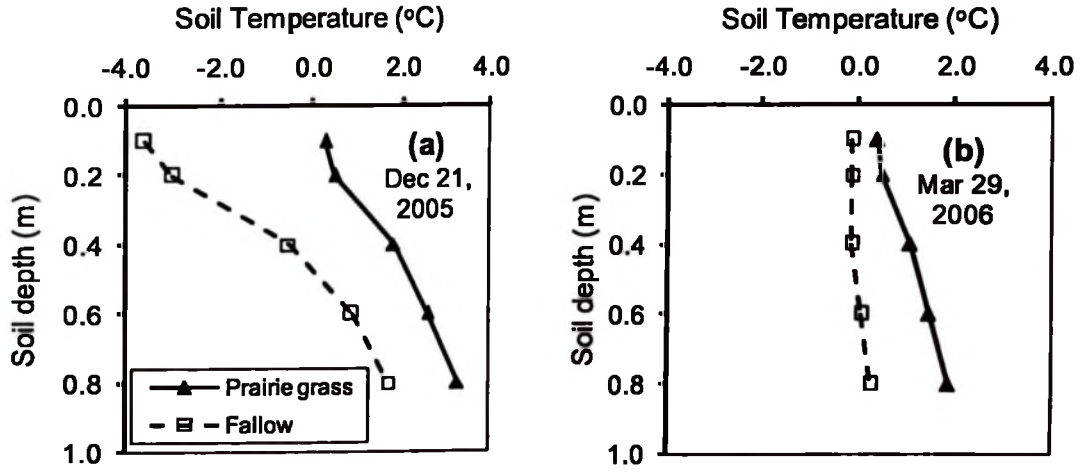

Fig. 5.7. Soil temperature variations with depth for the fallow and native prairie grass treatments during: (a) early winter on December 21, 2005 and (b) early spring on March 29, 2006.

The presence of prairie grass residues before the first snowfall (October 2005) helped to trap more snow and insulate the soil, preventing it from early freezing. During

spring, the prairie treatment was 0.5 to 1.5°C warmer than the fallow (Fig. 5.7b). The total water content in the 0.1- to 0.9-m depth increased from 0.25 $m^3 m^{-3}$ on March 29 to 0.43 $m^3 m^{-3}$ on April 04 (72% increase) in the prairie grass treatment after the start of spring snowmelt (Table 5.5; Fig. 5.6a). The increased total water content was due to infiltration that was enhanced by the prairie grass residues trapping more snow (Fig. 5.6a). In the continuous fallow, on the other hand, soil moisture in the 0.1- to 0.9-m depth increased by 12% (from 0.34 $m^3 m^{-3}$ to 0.38 $m^3 m^{-3}$) from the fall on December 13, 2005 to the spring on March 29, 2006 (Table 5.5; Fig. 5.6b). There was 3% change in the soil moisture for the 0.1 to 0.9-m layers during the early spring snowmelt (0.37 $m^3 m^{-3}$on March 29 and 0.38 $m^3 m^{-3}$on April 04) (Table 5.5). This was an indication that since the fallow had frozen to a greater depth during the winter, and had lower soil temperatures; it delayed to thaw in the top layers, preventing infiltration of the initial spring snowmelt in early April 2006.

For the oats with berseem clover, a trend similar to that of the native prairie was also observed during spring (Fig. 5.4 c and d) where an increase in the total water content was observed. The presence of vegetation before fall freeze-up helped trap snow and kept the soil warm enough to permit increased snowmelt infiltration in early spring. As the melt water deep percolated to the lower layers, the drier upper layers also warmed up. The frozen soil layers in the non-cover crop and the fallow treatments held more total water content and prevented deep percolation away from the root zone (Figs. 5.6b and 5.6d). The frozen soil layers also caused soil moisture to migrate from above and below the freezing layers towards the freezing front causing the root zone to have increasing total soil water content. The layers below the freezing front experienced a decrease in

water content due to upward moisture migration as the winter progressed (Figs. 5.6b and 5.6d). The infiltration and deep percolation that was occurring during the winter within the soil profile of native prairie and the cover crop treatments helped to reduce excess moisture within the root zone during the spring snowmelt infiltration (Figs. 5.6a, and 5.6c).

In summary, the presence of a crop cover or perennial vegetation resulted in relatively warmer soil temperature profiles (Fig. 5.4c), shallower depth of frozen soil layers (Fig. 5.4b), and reduced upward migration of soil moisture from unfrozen or partly frozen soil layers below. Hence, the reduced upward soil moisture migrations led to low accumulation of water within the root zone later in the winter (Fig. 5.4a). This phenomenon is expected to be of great advantage during spring snowmelt as the cover-cropped treatments (compared to treatments with no cover crop), will be drier and warm up earlier, thereby allowing early farm operations. These treatments will also experience less soil moisture than the non-cover crop treatments at the start of the subsequent growing season. However, in drier seasons the cover crop can have a negative impact on water availability for the main crops due to competition with the cover crop. For wetter seasons like 2006 covered in this study, the cover crop can therefore be used as a means of reducing excess soil moisture in areas receiving surplus precipitation in form of both rainfall and snow.

5.5 Summary and Conclusions

The movement and redistribution of soil moisture within the soil profile for different cropping systems were evaluated from the summer of 2005 to the spring of 2006. Soil moisture variations at different depths and different seasons were determined. The influence of a berseem clover annual cover crop in oats on soil moisture availability and crop performance within the growing season, and on infiltration, soil moisture redistribution, and soil freezing and thawing from the fall of 2005 to the spring of 2006 were also explored. Comparisons were also made for the native prairie grass against the fallow treatments. Berseem clover as an annual cover crop contributed to the reduction of excess water during the summer growing season due to increased plant water uptake, as compared to the oats without a cover crop. The total water content in the root zone (0.0- to 0.7- m depth) by August 16, 2005 was 34.6% lower in the treatment with oats and a cover crop (0.17 $m^3 m^{-3}$) compared to that of the oats alone (0.26 $m^3 m^{-3}$).

In 2005, the presence of berseem clover within the same season did not significantly affect the oats yield (1671 kg ha^{-1} for oats with cover crop against 1844 kg ha^{-1} for oats alone). However the cover crop reduced the soil moisture later in the 2005 growing season resulting in significantly lower (α=0.05) biomass yields (6146 kg ha^{-1} the combined biomass of oats and berseem clover, vs. 7327 kg ha^{-1} for oats alone). Farm management systems involving no-till and cover crop have to consider the soil moisture competition between the main crop and the cover crop, which may affect the performance of the main crop if there is less available moisture at later stages of the growing season.

During the winter, there was an increase in total soil water content for all the treatments in the upper soil layers above the freeze front and a decrease in water content

below the freeze front as the winter progressed. Compared to the cover crop treatment, the non-cover crop treatment (oats alone) had consistently higher total water content within the root zone during the winter due to upward soil moisture migration towards the frozen soil layer. By March 29, 2006, the oats with berseem clover cover crop treatment had 18.2% lower total soil water content (0.27 $m^3 m^{-3}$ vs. 0.33 $m^3 m^{-3}$ of water) in the 0.1 to 0.9-m soil depth. Soil moisture migrated upwards towards the freezing front. The cover crop treatment, compared to oats alone, had a shallower frozen soil layer (0.4 m against 0.6 m) during the spring. The lower soil moisture in the cover crop treatment enhanced early soil warming during the spring leading to earlier thawing. The relatively drier soils in the cover crop treatment also facilitated more spring snowmelt infiltration into deeper layers, thereby promoting deep percolation away from the root zone. Similar trends were also observed in the comparison of native prairie and the fallow. The native prairie grass had higher above ground standing residue compared to the fallow, and trapped more snow (0.68 m vs. 0.21 m) that insulated the ground during the winter. As a result, the native prairie accumulated less total soil water content by spring due to lack of a frozen soil layer, and had on average 1.0°C warmer soil temperature profiles during the spring.

This study suggests that areas experiencing excess soil water in the form of both rainfall and snow could use an annual cover crop such as berseem clover as a means to reduce excess moisture during the growing season. This cover crop could also be used for enhancing spring snowmelt infiltration, deep percolation, and early warming of the soil by having warmer soils during the winter, shallower depths of frozen soil layers, and less frozen water content within the root zone. This in turn, will allow earlier farm operations.

6. PREVIOUS SEASON COVER CROP EFFECTS ON SUBSEQUENT SOIL MOISTURE DISTRIBUTION AND YIELD IN THE NORTHERN GREAT PLAINS OF CANADA

6.1 Abstract

A primary factor in determining the yield potential of an agricultural crop is the availability of soil moisture during the growing season. The previous season cover crop can influence soil water content in the subsequent growing season, thereby, affecting the crop performance and yield. The influence of berseem clover (*Trifolium alexandrium*) cover crop in oats (*Avena sativa*) grown in 2005 on soil moisture redistribution and yield of canola (*Brassica napus*) grown in 2006 was investigated in Carman, Manitoba. Time domain reflectometry and neutron scattering methods were used to measure the unfrozen and total water contents, respectively. Thermocouples were used to measure soil temperature. Soil in the canola treatment that had a cover crop in the previous season (canola_CC) froze to a shallower depth of 0.6 m during the 2006 winter compared to a depth of 0.8 m in the treatment that previously had no cover (canola_NC). The canola_CC treatment thawed earlier in spring, and had lower soil moisture at the beginning and during the following growing season leading to poor growth performance. The canola_CC treatment had 28% lower soil moisture (0.16 vs. 0.22 m^3 m^{-3}) during the flowering stage in July 2006. The canola yield in 2006 was significantly lower (1.99 t ha^{-1} vs. 2.72 t ha^{-1}) in canola_CC compared to the canola_NC treatment. Depletion of soil moisture by cover crop should be taken into account when selecting a rotational crop

sensitive to soil moisture stress in the subsequent season. Reduced soil moisture can lead to negative effects on crops in drier subsequent seasons.

6.2 Introduction

The amount and distribution of soil moisture during the growing season is among the key factors for ensuring better crop performance and yields in agricultural fields (Aspinall et al. 1964; Fischer and Kohn 1966; Raper et al. 2000; Calvino et al. 2003). The presence of a cover crop in one season can affect soil water content and hence the crop performance within the same growing season (McGuire et al. 1998; Ross et al. 2001; Kahimba et al. 2008b). The residual effect of the cover crop from the previous growing season may have an impact on the response of the soil to fall freeze-up and spring thawing, and influence the redistribution of soil moisture in the beginning of the next growing season.

Advantages and disadvantages of cover crops within the same season are well documented. The advantages include reduction of excess soil water in wet seasons, addition of organic matter to the soil, promotion of nutrient recycling efficiency, and improvement of soil structure (McGuire et al. 1998; Paz et al. 1998; Snapp et al. 2005). Cover crops with a large above ground canopy such as berseem clover also help to suppress crop weeds (Ross et al. 2001), and lower soil temperatures (Kahimba et al. 2008b). Andraski and Bundy (2005) also showed increased corn yield due to increase in the amount of nitrates made available from mineralization of residues of red clover cover crop.

Cover cropping system has been practiced at the Ian N. Morrison Research Farm of the University of Manitoba located in Carman, Manitoba. The research farm has been conducting long-term crop rotation experiments of no-till farming and farming with fewer chemicals since the year 2000 (Schoofs et al. 2005). The farming with fewer chemicals study is aimed in establishing a farming practice whereby no in-crop pesticides are used during the growing season. The berseem clover cover crop (*Trifollium Allexandrium L.*) was included in the four-year rotations to investigate its suitability as a leguminous cover crop under Manitoba growing and climatic conditions (Nazarko et al. 2001; Schoofs et al. 2005; Nason 2007). Introduction of the berseem clover aimed at establishing a perennial cover crop that can suppress weeds under the no-till farming system. However, studies have not been done to investigate the residual effects of the use of berseem clover cover crop on the redistribution of soil moisture and crop performance in subsequent seasons following the cover crop. The Carman region, which is part of the Canadian prairies, receives about 60% (354 mm) of the total annual precipitation (588.8 mm) in the form of rainfall during the growing season from May to August (Environment Canada 2007). The rest of the precipitation is in the form of snow during the winter months. Hence, any significant soil moisture reduction such as the consumption by the cover crop and increased evaporative losses could potentially cause soil moisture deficit to the main crops, thereby affecting the crop growth performance and yields.

Major disadvantages of cover crops are competition for nutrients and soil moisture with the main crop, especially during drier seasons (McGuire et al. 1998). The costs associated with seeding and maintaining the cover crops and failure of some species in suppressing weeds are also among the disadvantages (Ross et al. 2001). Cover crops

such as winter wheat have been shown to deplete soil moisture and nutrients during spring, thereby lowering the summer crop yields (Ward et al. 2006). Most research has presented the impact of cover crop within the same growing season. However, research studying the residual effects of one season's cover crop on the response of the soil to freezing and thawing, as well as the soil water content and redistribution in the subsequent growing season is sparse. This paper presents data on the residual effects of cover crops.

Earlier soil thawing during the spring in seasonally frozen soils, such as in the Carman region of Manitoba, helps to ensure early farm operations and longer growing seasons. Some temperature sensitive crops such as canola cannot be seeded early in the spring if the temperature has not reached a certain threshold value. For example, temperatures below 10°C result in poor germination (Zheng et al. 1994). To take advantage of early season growing degree-days, canola (*Brassica napus*) can be seeded at temperatures as low as 3°C, though this temperature will cause a delay in seed germination (Zheng et al. 1994). Warmer soil temperatures during spring enhance soil thawing and infiltration of melt water (Cruse et al. 2001). The presence of a cover crop prior to soil freezing in the fall contributes to additional surface residue that causes a delay in soil freezing, shallower depth of the frozen soil layer, and less accumulation of total soil moisture during the winter. It also leads to earlier soil warming during the following spring (Raper et al. 2000; Kahimba and Sri Ranjan 2007, Kahimba et al. 2008b). However, earlier soil thawing and enhancement of snowmelt infiltration in the previously cover-cropped plots enhances deep percolation away from the root zone. This

leads to lower soil moisture at the end of spring snowmelt and during the following growing season (Bullock 1988).

In dryland agriculture, the relationship between crop yield and soil moisture stress can be linked to the use of cover crop in the previous season. While the cover crop is advantageous to the existing crops, the residual effect of the cover crop can influence the fall freeze-thaw behavior of the soil, and thereafter its response to spring snowmelt infiltration.

The advantages of cover crops within the growing season and the relationship between the soil moisture stress and yield during the same season are well documented. However, more information is needed on its residual effects in subsequent seasons. Therefore, the objectives of this study were to:

1) Determine the influence of a previous-season berseem clover cover crop on subsequent winter soil freezing, and spring soil thawing and warming up, and

2) Determine the soil water content and growth performance of canola as affected by berseem clover cover crop of theprevious growing season.

6.3 Materials and Methods

6.3.1 Site location and characteristics

A three-year field study was conducted from 2005 through 2007 growing seasons at the Ian N. Morrison Research Farm of the University of Manitoba, located in Carman, Manitoba (49° 30' N, 98° 02' W, and 262 m elevation above mean sea level). The Ian N. Morrison Research Farm is within the Northern Great Plains of Canada experiencing seasonal soil freezing and thawing. This area receives average annual precipitation of

588.8 mm (15-year average, 1991-2005) in the form of rain and snow (Fig. 6.1; Environment Canada 2007). The monthly mean air temperatures over the area (15-year average, 1991-2005) range from -16.2°C in January to 19.1°C in July, with mean annual air temperature of 3.4°C (Fig. 6.2; Environment Canada 2007).

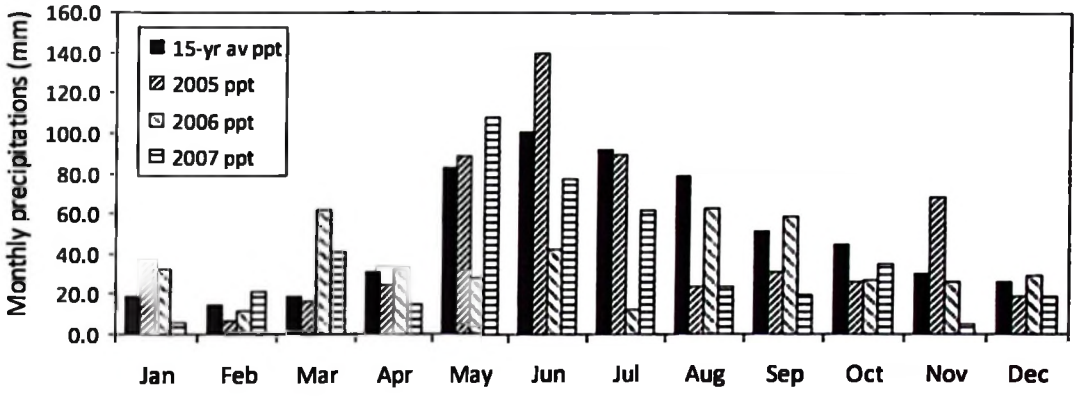

Fig. 6.1. Mean monthly precipitation at the Ian N. Morrison Research Farm during year 2005 to 2007 as compared to the 15-year average monthly precipitation.

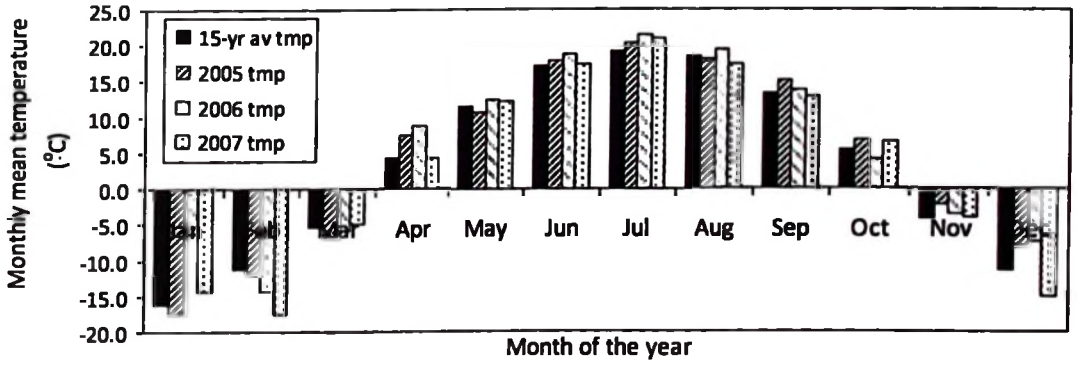

Fig. 6.2. Monthly mean temperature at the Ian N. Morrison Research Farm during year 2005 to 2007 as compared to the 15-year average monthly mean temperature.

The length of the growing season in areas experiencing seasonal soil freezing and thawing such as the Carman region in Southern Manitoba depends on the number of frost-free days (Nadler 2007). For Carman region, the frost-free days range from 119 to 126 days, with the frost-free season from May 15 to September 26 (Environment Canada 2007; Nadler 2007). The ground topography on the research field is predominantly level with average slope less than 0.5% (Mills and Haluschak 1993). Soils in the selected experimental plots were well-drained fine sandy loam, (well-drained Hibson from sub group Orthic Black). The average particle size distribution of the top 0.7 m depth was 76% sand, 8% silt, and 16% clay. The equivalent USDA soil Taxonomy is Mollisol (very fine sandy loam). The layers below had 4% sand, 44% silt, and 52% clay. The average depth to clay layer was 0.70 m (Mills and Haluschak 1993; Nason 2007).

Soil survey performed during establishment of the research site indicated that the area has the same soil types and uniform soil profiles with a depth to clay layer ranging between 0.70 and 0.75 m on an area 500 by 800 m across the selected experimental plots (Mills and Haluschak 1993). Hence, the selected experimental plots had fairly the same soil types and uniform layers along the soil profile. The top soil layers had an average saturated hydraulic conductivity of 0.29 m per day. The fine sandy loam soils were well drained with water table at 1.5 to 2.0 m during the fall and winter, and rising to within 1.0 m during the spring and summer (Mills and Haluschak 1993). The top 0.7 m of the soil had a field capacity (FC) of 0.22 to 0.25 $m^3 m^{-3}$, permanent wilting point (PWP) of 0.064 to 0.082 $m^3 m^{-3}$, and available water ranging from 15% to 17% by volume. The bottom layers from 0.7 to 1.2 m had 0.30 $m^3 m^{-3}$ FC, 0.13 $m^3 m^{-3}$ PWP, and 21% available water (Mills and Haluschak 1993).

6.3.2 Farm management practices at the Ian N. Morrison Research Farm

The Ian N. Morrison Research Farm has been conducting no-till farming experiments since the year 2000. The introduction of no-till farming and no in-crop pesticide use aimed at establishing a farm management practice of "Farming with Fewer Chemicals, FFC" (Bourgeois and Entz 1996; Nazarko et al. 2001). Crops grown in the selected experimental plots are oats (*Avena sativa L.),* linola /flax (*Linum usitatissimum*), wheat (*Triticum spp.*), canola (*Brassica napus*), and alfalfa (*Medicago sativa L.*) (MASC 2006; Nason 2007). A combination of no-till farming and use of cover crops has also been practiced at the Ian N. Morrison Research Farm (Nason 2007). Berseem clover (*Trifolium alexandrium*) cover crop (Joe Burton variety) was used in the 2005 growing season as one of the treatments in the experimental plots.

6.3.3 Field experimental set up

Six plots of an existing four-year crop rotation were used for the field experiment. The four crops in one block of the rotation were oats with berseem clover cover crop (2005) – canola (2006) – wheat (2007) – linola (2008). The second block of rotations had oats alone (2005) – canola (2006) – wheat (2007) – linola (2008). The effects of berseem clover in oats compared to oats alone on crop performance and soil moisture redistribution (within season effects) have been described in our previous paper (Kahimba et al. 2008b; chapter 5). The goal of this paper is to describe the previous season (2005) cover crop's residual effect on the canola grown in the subsequent 2006 growing season. The plot sizes in the selected field plots were 4 m wide and 12 m long. Each block was separated from the adjacent blocks by an access road 12 m wide that was

grassed to prevent erosion. The surrounding environments on the sides of the plots considered in this study were canola, wheat, fallow, and native prairie grass.

The year-round monitoring of soil moisture was performed on two treatments, each treatment being located on a single field plot of 4 m by 12 m. To minimize the effects of soil heterogeneity, the two plots were selected within the same block and close to each other, separated by a 6-m wide plot. Within each treatment three replicates of time domain reflectometry (TDR) probes, one replicate of thermocouple probes, and one replicate of NMM access tube were installed. The soil moisture measurement using TDR were replicated at three locations within the same treatment to minimize the effect of any soil heterogeneities within the plots. At each location, five TDR miniprobes were installed at 0.1 m depth and at 0.2 m interval to a depth of 0.8 m. The TDR probes measure only the unfrozen water content of the soil. Measurement precision for the TDR method using down-sized miniprobes ranges from 0.01 to 0.03 $m^3 m^{-3}$ (Persson and Haridy 2003). The neutron moisture meter (NMM) measures the total water content. For each of the three replicates of TDR measurements, one replicate of NMM measurement was taken at each depth on each date of data collection.

The NMM probe was inserted into the ground through a neutron access tube, installed at the centre of each plot, to measure the total water content at 0.2 m intervals from a depth of 0.2 to 1.8 m. Thermocouples, installed at the same depths along with the TDR probes, were used to measure the soil temperatures within the soil profile. The NMM measurement precision for water content is 0.01 $m^3 m^{-3}$ (Evett and Steiner 1995). The higher measurement precision and a wide range of literature have made the NMM method to be used as a standard measurement technique for comparing with other

methods of soil moisture measurement (Evett 2003). Principles of TDR and NMM measurement techniques are described in Topp and Davis (1985); Spaans and Baker (1995); Evett (2000a, 2003a, and 2003b); and Kahimba and Sri Ranjan (2007).

6.3.4 Data collection and analysis

Both unfrozen and total soil water contents, as well as soil temperature within the soil profile were monitored during the summer, winter, and spring. All the three measurements were taken within the same day. To minimize sampling errors during data collection, the same order of plots arrangement was followed for each date of data collection. The TDR, NMM, and soil temperature measurements were taken within approximately two hours for the two treatments. In addition, due to larger variation in soil temperature with time within the same hour during daytimes, temperatures for the two treatments were measured continuously within the same 15-25 minutes in between the soil moisture measurement times. The data collection continued from the summer of 2005 to the summer of 2007. The spring soil thawing and warming up; amount and distribution of soil water content at various stages of plant growth; oats and canola yields; and the accumulation and redistribution of soil moisture and temperature during the winter and spring of the subsequent season were compared for the previously cover-cropped and the non-cover-cropped treatments. In the 2005 season, the treatments were oats with berseem clover cover crop (oats + berseem), and oats without the cover crop (oats alone). The oats alone and the oats with berseem clover were seeded on May 12, 2005 and oats was harvested on August 08, 2005. The cover crop continued to grow until the fall in November when the ground started to be covered by snow (Nason 2007; Kahimba et al. 2008b).

In the 2006 season, canola alone was planted in both treatment plots. The 2006 treatments were canola in the previously cover-cropped treatment (canola_CC), and canola in the previously no cover crop treatment (canola_NC). The canola was seeded on May 10, 2006 and it was harvested on August 26, 2006. No other farm operations were carried out after the harvest of canola. Harvesting was done by taking two rows to a distance of 1.0 m (0.305 m^2) from the centre of each of the three replicates in one plot (Nason 2007). The yield measurements for both oats in 2005 and canola in 2006 were taken at the end of the respective growing seasons. The canola yield for each treatment was taken as an average of three replicate plots from different blocks having the same rotational scenario and receiving the same farm management practices.

6.3.5 Experimental design and statistical analysis

Two treatments each with three replicates were used in the experiment. In the first treatment, oats were seeded with the berseem clover cover crop in the 2005 season, and canola alone in the 2006 season (canola_CC). In the second treatment, oats alone were seeded in the 2005, and canola alone in the 2006 growing seasons (canola_NC). The use of the same crop and management practices (seeding time, weeding, harvesting) in all the treatments in 2006 allowed for good comparison of the residual effects of the cover crop from the 2005 crop rotational practice to the 2006 growing season. The soil moisture and soil temperature variations with depth and time within the root zone were compared for the canola_CC and canola_NC treatments. Analysis of variance (ANOVA) and LSD comparison test procedure of the SAS statistical analysis (SAS Inc. 2004) with $\alpha = 0.05$ were used to test for differences between the means of the canola yields for the 2006 growing season.

6.4 Results and Discussion

6.4.1 Soil moisture distribution during the 2006 growing season

The amount of total and unfrozen soil water content, variation in soil temperature within the soil profile, and crop performance were evaluated in the field on two treatments that had canola alone in the 2006 growing season. Experimental results were analyzed to see whether the two canola treatments in 2006 (canola_CC and canola_NC) were influenced by the two different cropping systems in 2005 (i.e., oats with berseem clover cover crop and oats alone).

Table 6.1 presents variations in total water content at each depth in the 0.1- to 0.9-m soil depth during the spring and summer from March to August 2006, and during the winter and spring from January to July 2007. At the end of winter and before the start of spring snowmelt on March 29, 2006, the canola_CC treatment had accumulated 18.2% less total water content over the winter (0.27 vs. 0.33 m^3 m^{-3}) compared to the canola_NC treatment (Table 6.1).

Table 6.1. Total water content in the 0.1- to 0.9-m soil profile for two cropping systems from March 2006 to July 2007.

Date	Soil depth (m)	Total water content measured by NMM		
		Canola_NC* ($m^3\ m^{-3}$)	Canola_CC** ($m^3\ m^{-3}$)	Reduction (%)
Mar 29, 2006	0.20	0.39	0.34	12.82
	0.40	0.40	0.35	12.50
	0.60	0.31	0.26	16.13
	0.80	0.22	0.13	40.91
	Total***	0.33	0.27	18.18
Apr 04, 2006	0.20	0.39	0.39	0.00
	0.40	0.41	0.40	3.50
	0.60	0.34	0.32	5.10
	0.80	0.32	0.30	5.50
	Total	0.37	0.35	5.41
July 11, 2006	0.20	0.20	0.17	14.85
	0.40	0.23	0.16	28.40
	0.60	0.24	0.20	16.93
	0.80	0.26	0.21	19.16
	Total	0.23	0.18	19.96
Aug 22, 2006	0.20	0.16	0.15	6.70
	0.40	0.15	0.13	16.91
	0.60	0.16	0.15	8.32
	0.80	0.18	0.14	23.89
	Total	0.16	0.14	14.21
Jan 17, 2007	0.20	0.25	0.23	5.44
	0.40	0.22	0.16	27.98
	0.60	0.18	0.16	10.50
	0.80	0.19	0.13	28.98
	Total	0.21	0.17	17.79
Feb 20, 2007	0.20	0.25	0.24	3.13
	0.40	0.23	0.17	24.92
	0.60	0.19	0.18	9.01
	0.80	0.23	0.14	40.10
	Total	0.22	0.18	19.34
Mar 27, 2007	0.20	0.24	0.30	-24.45
	0.40	0.23	0.27	-16.65
	0.60	0.20	0.28	-39.19
	0.80	0.23	0.23	0.66
	Total	0.23	0.27	-19.25
Apr 17, 2007	0.20	0.31	0.28	9.58
	0.40	0.32	0.24	24.73

Date	Soil depth (m)	Total water content measured by NMM		
		Canola_NC* (m^3 m^{-3})	Canola_CC** (m^3 m^{-3})	Reduction (%)
	0.60	0.23	0.21	9.08
	0.80	0.22	0.20	8.24
	Total	0.27	0.23	13.70
June 26, 2007	0.20	0.27	0.26	5.75
	0.40	0.27	0.21	22.21
	0.60	0.28	0.25	10.11
	0.80	0.32	0.28	12.89
	Total	0.28	0.25	12.71
July 18, 2007	0.20	0.20	0.15	23.90
	0.40	0.22	0.15	30.27
	0.60	0.21	0.17	18.67
	0.80	0.22	0.16	26.30
	Total	0.21	0.16	24.83

* Canola_CC = Canola treatment that had oats with berseem clover cover crop in 2005 and canola alone in 2006.

** Canola_NC = Canola treatment that had oats alone in 2005 and canola alone in 2006.

*** Total = total soil water content (m^3 m^{-3}) measured using NMM in the soil depth from 0.1 to 0.9 m.

In the previous study, Kahimba et al. (2008b) indicated that the treatment that had berseem clover cover crop in 2005 delayed to freeze during the fall of 2005 and was consistently warmer during the winter 2006. The treatment also had shallower depth of frozen layer that resulted in lower accumulation of total soil water content as the winter progressed (Kahimba et al. 2008b). While the canola_CC treatment maintained consistent lower total water content compared to canola_NC treatment prior to the 2006 spring snowmelt (Kahimba et al. 2008b), there was a temporary increase in soil moisture in all the treatments observed on April 04, 2006 due to spring snowmelt infiltration. The temporary increase was also observed in the spring of 2007 on March 27 (Table 6.1). From March 29 to April 04, 2006, the total soil moisture in the 0.1- to 0.9-m soil depth increased by 15.15% from 0.33 to 0.37 m^3 m^{-3} in the canola-NC treatment. It also

increased by 29.63% from 0.27 to 0.35 m^3 m^{-3} in the canola_CC treatment. The higher percent increase in the canola_CC treatment is also an indication that the treatment warmed earlier and allowed more infiltration of the melt water.

During the flowering stage in July 2006, the total soil water content in the 0.1- to 0.9-m soil depth was 20.0% lower (0.18 vs. 0.23 m^3 m^{-3}) in the canola_CC compared to the canola_NC treatment. The lower amounts of soil moisture in the treatment that had berseem clover cover crop in 2005 is attributed partly to depletion of the soil moisture by the cover crop in the previous season, as well as the differences in soil freezing depths during the winter. The shallower depths of frozen soil layer in the Canola_CC treatment (Kahimba et al. 2008b) affected water movements from unfrozen soil layers below the freeze front towards the frozen layers, leading to lower accumulation of total soil moisture during the winter of 2006 (Table 6.1).

During the winter and spring of 2007, as the winter progressed, there was a decrease in the total soil water content in the bottom layers for all the treatments prior to spring snowmelt. An increase in total soil water content was observed after the spring snowmelt in late March and early April 2007. The canola_CC treatment had consistently lower amounts of total soil water content than the canola_NC treatment during the winter of 2007 (Table 6.1). Between January and March 2007, the canola_CC treatment had 18-20% lower total water content in the 0.1- to 0.9-m soil depth compared to the canola_NC treatment. By February 20, 2007 the total water content was 19.3% lower (0.18 vs. 0.22 m^3 m^{-3}) in the canola_CC compared to the canola_NC treatment.

The variation of total soil water content for the two treatments was an indication that although both treatments had canola alone in the 2006 growing season, the residual effect of the cover crop of the previous season influenced the response of the soil to freezing and soil moisture redistribution in the subsequent season. The residual effect was experienced both in the subsequent growing season and during the following winter soil freeze-up. The increased total soil water content during the winter in the canola_NC treatment (Table 6.1) was caused by a deeper layer of frozen soil pulling more unfrozen soil water content from the unfrozen soil layers below towards the freezing front (Kahimba and Sri Ranjan 2007). During spring snowmelt, however, a temporary increase in soil moisture was observed for all the treatments due to spring snowmelt infiltration on March 27, 2007 as stated earlier, with the largest increase observed in the earlier-thawed canola_CC treatment. This was caused by earlier thawing of the canola_CC treatment that did not freeze to a greater depth and was relatively warmer than the canola_NC treatment (as explained later in section 6.4.3 and Figs. 6.5 and 6.7). However, when complete snowmelt completed and the top soil had thawed, the canola_CC treatment maintained lower soil water content in the soil profile (e.g. April 17, 2007 on Table 6.1). This was an indication that earlier thawing of deeper layers in the canola_CC treatment (Figs. 6.7 b3 and b4) facilitated more deep percolation away from the root zone, leaving the surface layers of the zone area relatively drier.

6.4.2 Variation of total water content with time from summer 2005 to summer 2007

The variation of total soil water content as a function of time in the 0.1- to 0.9-m soil depth from September 2005 to September 2007 is presented in Fig. 6.3. The 2005 season gives the within-season effects of the berseem clover cover crop, while the 2006

season presents the previous-season effects of the cover crop. The spring snowmelt for both 2006 and 2007 seasons was accompanied by a higher increase in total water content in all the treatments. The highest increase was observed in the canola_CC treatment, which had shallower depth of frozen soil layer, was much warmer during winter, and thawed earlier during spring as stated earlier (Table 6.1).

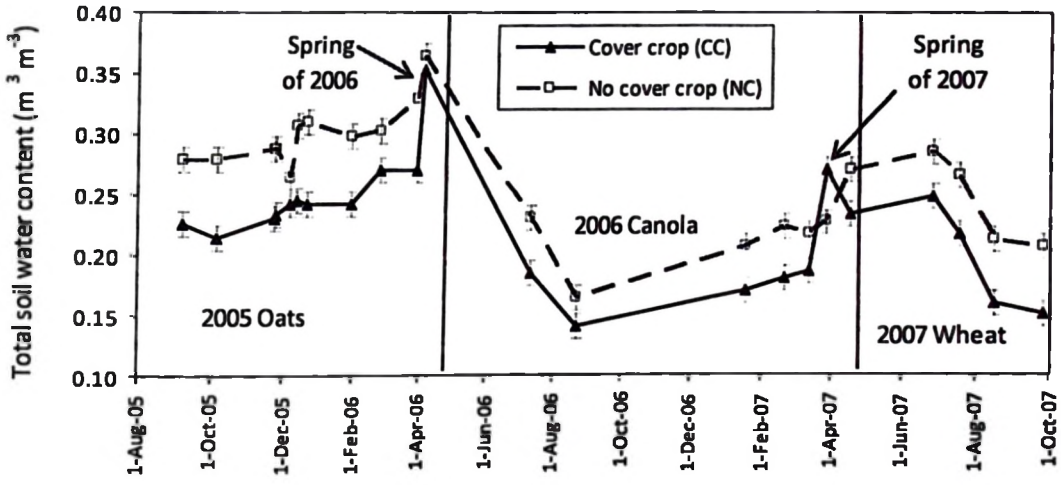

Fig. 6.3. Variations of total soil water content in the 0.1- to 0.9-m soil depth for the oats + berseem clover and oats alone treatments in the 2005/2006 season; and for canola_CC and canola_NC treatments in the 2006/2007 season. Measurements were taken using NMM.

The presence of berseem clover resulted in lower soil water content during both the 2005 and 2006 growing seasons. Similar results on reduction of soil moisture by the presence of cover crop were also reported by McGuire et al. (1998) who observed that consumption of soil water by winter wheat (*Triticum aestivum L.*) led to soil moisture deficit for crops in the subsequent growing season. The measurements in this study were taken year-round on a monthly basis (one to two observations per month) from August

2005 to September 2007. Ideally continuous measurement of soil moisture, (i.e., using data loggers left at site) would have given a much better indication of the soil moisture trends in a shorter time interval. Restrictions on the use of NMM that contain radioactive materials hindered the automation of the total soil moisture measurements. Therefore, the soil moisture and soil temperature trends over time were confirmed by repeated measurements at the same depths over several days within a year. In addition, the TDR probes had to be connected manually to individual probes for measurement, which limited their use for continuous measurement. The need for TDR instrument to be in a warm enclosure precluded their use during the winter when nighttime temperature can dip as low as -30°C.

6.4.3 Soil temperature during the 2006 growing season

The soil temperature within the top root zone depth (0.0 to 0.2 m) during the 2006 growing season was influenced by the previous season cover crop (Table 6.2, Fig. 6.4). Compared to the canola_NC treatment, soil temperature at 0.1 m depth in the canola_CC treatment was 1.5°C (8.9%) and 1.8°C (9.9%) higher during flowering (Fig. 6.4a) and maturity (Fig. 6.4b) stages, respectively. The soil temperature profile for the bottom soil layers from 0.4 to 0.8 m was almost the same with temperature differences of 0.1°C to 0.8°C (Table 6.2). The well grown canola in the canola_NC treatment (Fig. 6.5a) helped to keep the soil temperatures cooler. The better above ground canopy provided shade to the ground, hence minimizing the evaporative losses from the soil surface.

During the winter and early spring when all the treatments were covered with snow, there was no loss of soil moisture by evaporation from the soil surface. At the time of spring snowmelt, while the canola_CC treatment warmed earlier, there were no live

plants left to cause a difference in water loss by transpiration. In addition, the remaining plant residues had been suppressed by the winter snowpack, and during spring snowmelt the soil temperatures in both treatments were less than 1°C. Hence, evaporative losses from the surface would not have contributed to much of a difference in water contents on the two treatments.

Table 6.2. Soil temperature in the 0.2- to 0.8-m soil profile for two cropping systems from March 2006 to July 2007.

Soil depth (m)	Management system	Soil temperature (°C)*										
		Year 2006				Year 2007						
		Mar 29	Apr 04	July 11	Aug 22	Jan 17	Feb 20	Mar 12	Mar 27	Apr 17	June 26	July 18
0.2	Canola_CC**	0.1	0.3	17.3	18.5	-0.8	-2.5	-0.5	0.3	1.5	19.1	19.3
	Canola_NC***	0.0	0.3	16.6	18.0	-1.1	-3.6	-1.0	-0.1	0.4	19.6	18.4
	Difference****	0.1	0.0	0.7	0.5	0.3	1.1	1.0	0.4	1.1	-0.5	0.9
0.4	Canola_CC	0.2	0.3	17.0	18.9	0.4	-1.7	-0.3	0.1	0.3	18.8	18.3
	Canola_NC	0.1	0.2	16.2	18.6	-0.1	-2.9	-1.0	-0.1	-0.1	19.3	17.8
	Difference	0.1	0.1	0.8	0.3	0.5	1.2	0.7	0.2	0.4	-0.5	0.5
0.6	Canola_CC	0.3	0.3	16.5	18.2	1.1	-1.0	-0.1	0.1	0.3	17.7	17.1
	Canola_NC	0.2	0.3	15.9	17.8	1.2	-1.8	-0.8	-0.1	-0.1	18.1	16.5
	Difference	0.1	0.0	0.6	0.4	-0.1	0.8	0.7	0.2	0.4	-0.4	0.6
0.8	Canola_CC	0.9	0.8	15.6	16.9	2.0	0.2	0.3	0.3	0.6	16.1	15.8
	Canola_NC	0.6	0.6	15.3	16.8	1.9	-0.5	-0.4	0.1	0.1	16.5	15.5
	Difference	0.3	0.2	0.3	0.1	0.1	0.7	0.7	0.2	0.5	-0.4	0.3

* Soil temperature measurements were taken using digital thermocouple thermometer.

** Canola_CC = Canola treatment that had oats with berseem clover cover crop in 2005 and canola alone in 2006.

*** Canola_NC = Canola treatment that had oats alone in 2005 and canola alone in 2006.

**** Soil temperature differences between the Canola_CC and Canola_NC treatments.

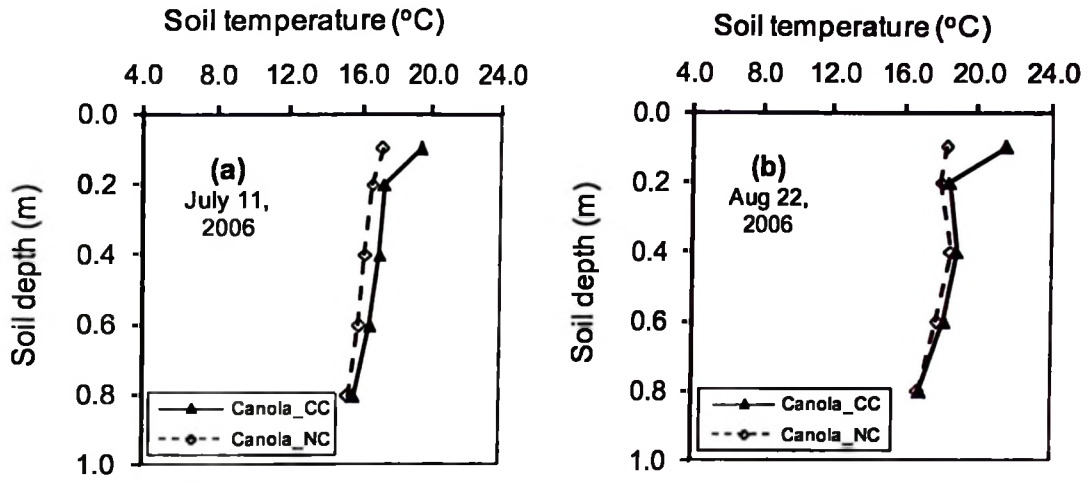

Fig. 6.4. Soil temperature variation with depth for the canola_CC and canola_NC treatments in the 2006 growing season during: (a) flowering stage and (b) maturity stage.

The canola in the canola_CC treatment had less above ground canopy cover (Fig. 6.5b), hence poor ground coverage. The better growth of the canola_NC treatment (Fig. 6.5a) is associated with the presence of higher soil water content.

Fig. 6.5. Comparison of growth performance of canola on June 26, 2006 for: (a) canola_NC and (b) canola _CC treatments.

During anthesis stage in June 2006, soil temperature in the canola_NC treatment was 20.3% cooler (18.1°C) in the top 0.2 m compared to soil temperature in the canola_CC treatment (22.7°C) at the same depth. The average soil temperature in the root zone (0.1 – 0.8 m depth) ranged from 22.7°C to 16.1°C in canola_CC, and 18.1°C to 15.5°C in canola_NC treatments (Table 6.2). Similar results on ground cooling due to increased crop cover by leguminous cover crops such as sudangrass (*Sorghum sudanese L.)* and cowpea (*Vigna unguiculata L.)* were also reported by Snapp et al. (2005).

6.4.4 Soil moisture variation with depth

The distribution of soil moisture as a function of depth during flowering and maturity stages of canola during the 2006 growing season is shown in Fig. 6.6. Since the two treatments had the same crop in 2006 receiving similar crop management practices, any difference in soil moisture distribution and crop performance could be attributed to the residual effects of the cover crop of the previous season.

The total soil moisture in the top 1.4-m depth was consistently lower in the canola_CC compared to the canola_NC treatments during both the flowering and maturity stages (Fig. 6.6 a & b). During maturity stage (Fig. 6.6b) the total soil moisture in the 0.1- to 0.9-m depth was 14.2% lower (0.14 vs. 0.16 m^3 m^{-3}) for the canola_CC compared to the canola_NC treatment (Table 6.1; Fig. 6.6b). The poor vegetative growth of canola in the canola_CC treatment can be attributed to the reduced water content within the root zone. The 2006 growing season was relatively a drier year with lower precipitation during the growing season (Fig. 6.1).

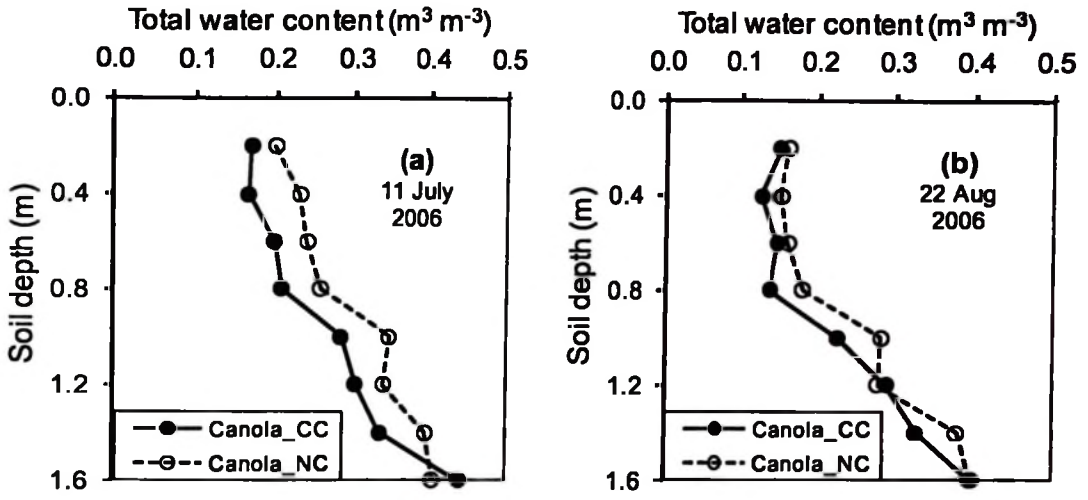

Fig. 6.6. Variations of total soil water content on the canola_CC and canola_NC treatments in the growing season during: (a) flowering stage in July 2006 and (b) maturity stage in August 2006.

The influence of the previous season cover crop was also revealed during the winter and spring of 2007 (Fig. 6.7). The canola_NC treatment accumulated more total soil water content during the winter compared to the canola_CC (Fig. 6.7 a1 and a2). Between February and March 2007, the canola_CC treatment was 0.2 to1.2°C warmer in the top 0.4 m soil depth compared to the canola_NC treatment. As a result, less water migrated upwards from the deeper unfrozen soil layers towards the freezing front. The canola_NC treatment plots froze to a greater depth and had less unfrozen water content in the root zone (Fig. 6.7 b1 and b2). The canola_NC treatment was also consistently cooler than the canola_CC along the soil profile during the winter (Fig. 6.7c).

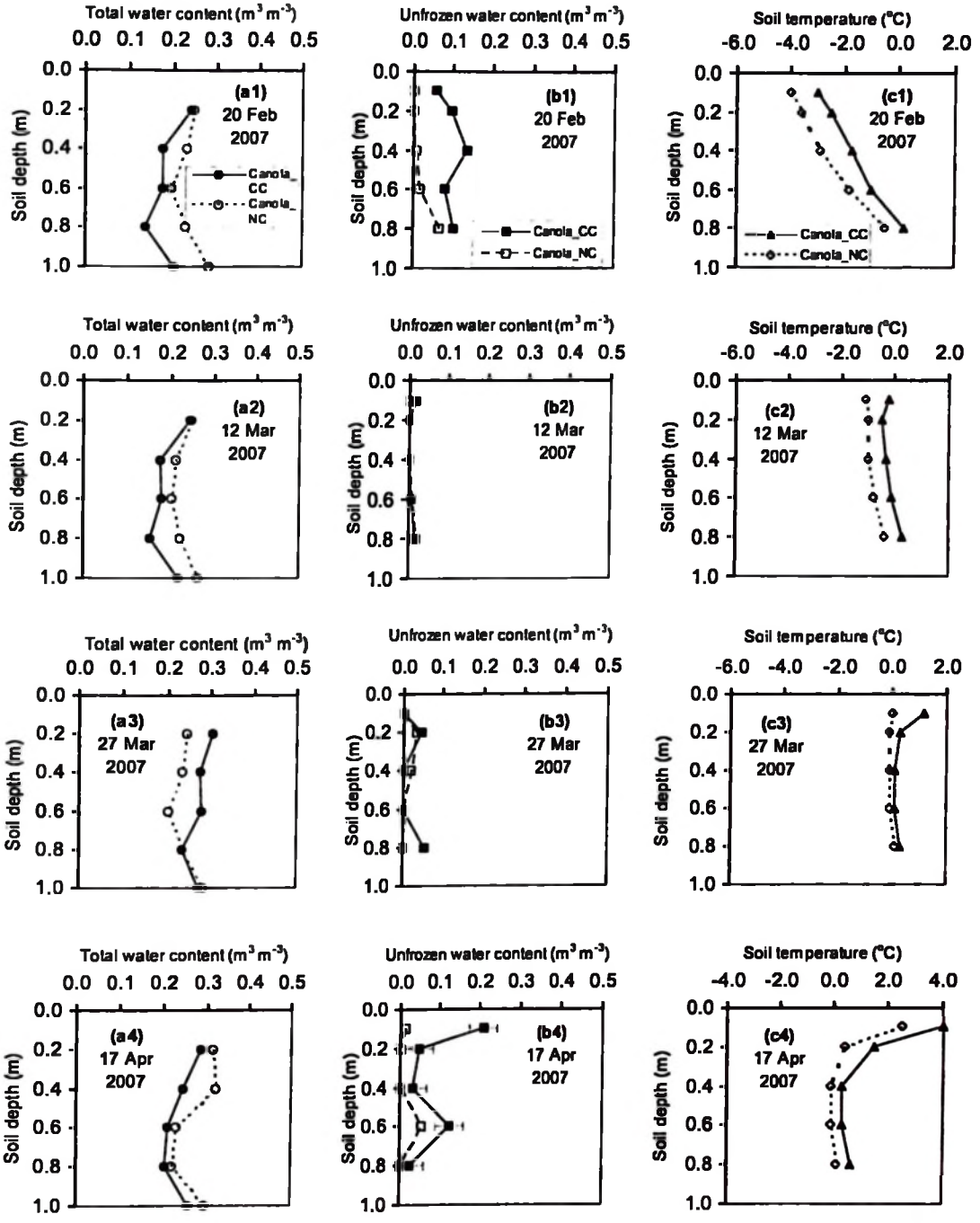

Fig. 6.7. **(a) Total (NMM) water content, (b) unfrozen (TDR) water content, and (c) soil temperature variations with depth for the canola_CC and canola_NC treatments during the winter and spring of 2007. Rows 1 to 4 in the figure indicate different sampling dates.**

During the spring of 2007 (Fig. 6.7 a3, b3, and c3) the canola_CC treatment thawed earlier allowing more infiltration of the melt-water. In the top 0.0- to 0.1-m depth, the canola_CC treatment had remained with only 29% of frozen water content (0.08 m^3 m^{-3} out of 0.28 m^3 m^{-3}), while the canola_NC treatment still had about 94% frozen water content (0.31 m^3 m^{-3} out of 0.33 m^3 m^{-3}). After snowmelt on April 17, the canola_CC treatment had remained with a total of 13.7% lower total water content (0.23 m^3 m^{-3}) than the canola_NC treatment (0.27 m^3 m^{-3}) in the 0.1- to 0.9-m soil depth (Fig. 6.7 a4; Table 6.1).

Considering the monthly precipitation, the 2005 growing season was relatively wetter than 15-year average precipitation, while the 2006 growing season was drier than the 15-year average (Fig. 6.1). From May 1 to September 30 the total amount of precipitation was 83% higher (372.6 mm) in 2005 compared to the total precipitation (203.0 mm) in the 2006 season. As a result, for drier years similar to 2006, the soil will have lower water contents to support plant growth at the beginning of the growing season resulting in poor growth performance. If the berseem clover cover crop is used in one season, consideration has to be given to rotate it with crops that need less water, especially when an agro-climatic risk assessment is performed (e.g. Nadler 2007) and the subsequent season is anticipated to be drier.

6.4.5 Cover crop influence on subsequent crop yield

The influence of the berseem clover cover crop on the oats yield in 2005 and canola yield in 2006 was compared (Table 6.2 and Fig. 6.8). Three replicate plots were used for yield measurements taken during the harvesting stage to compare the performance of the same crop (canola) under different previous cover crop treatments.

Table 6.3. Effects of previous season (2005) cover crop management system on canola yield in the subsequent (2006) season.

Management system	Total canola yield in the 2006 growing season (kg/ha)		
	Average yield	SEM*	CV**
Canola_CC	1986.3 a***	170.3	14.8
Canola _NC	2723.3 b	100.6	6.4

* SEM is standard error of measurements

** CV is the coefficient of variation

*** Means followed by a different letter in the same column are significantly different (α=0.05).

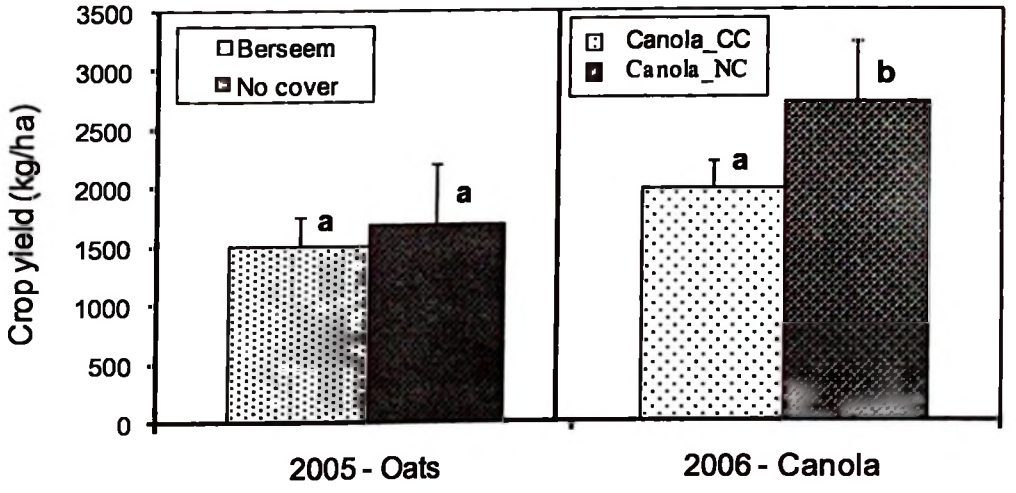

Fig. 6.8. Comparison of crop yields for oats with and without berseem clover cover crop in the 2005 growing season, and canola alone in the 2006 growing season. Error bars indicate standard errors of measurement.

Considering the effect of berseem clover cover crop in oats within the same season (Fig. 6.8), there was no significant difference ($\alpha = 0.05$) in oat yield in 2005 (1.52 t ha^{-1} for oats with berseem clover vs. 1.69 t ha^{-1} for oats alone). This is partly because 2005 was a wetter season (Fig. 6.1); hence, the reduction of soil moisture by the berseem clover cover crop could not cause significant soil moisture stress to the oats. In the 2006 growing season, however, which was drier compared to 2005 (Fig. 6.1), the canola yield was significantly lower in the canola_CC treatment (1.99 vs. 2.72 t ha^{-1}) compared to the canola_NC treatment (Table 6.3, Table 6.4, and Fig. 6.8). In addition, the presence of volunteer cover crops from the previous season could have possibly affected the germination and hence, the plant population in the canola_CC treatment.

Table 6.4. Analysis of variance showing the effects of previous season (2005) cover crop on subsequent canola yield in 2006 for the canola_CC and canola_NC treatments.

Source	DF	Total sum of squares*	Mean square	F – value**	Pr > F
Model	1	814,753.50	814,753.50	13.89	0.020
Error	4	234,663.33	58,665.83		
Corrected total	5	104,9416.83			

* Coefficient of variation (CV) = 10.29; RMSE = 242.21

** Tabular F-value: $F_{(1, 4, 0.05)} = 7.71$

In the previous study, Kahimba et al. (2008b) also found that the treatment that had berseem clover cover crop in 2005 accumulated consistently lower total soil moisture

from the fall 2005 to spring 2006. The same treatment with significantly lower yield (Canola_CC) had consistently lower soil moisture during the 2006 growing season (Table 6.1).

Therefore, the lower yields of canola in 2006 on the treatment that previously had berseem clover cover crop could be attributed to the lower total soil moisture in the soil profile by the end of winter 2006, and the consistently lower total soil moisture during the 2006 growing season.

In regions that occasionally experience dry growing seasons, crops that require less soil moisture could be the best alternatives for rotations following the cover crop. The moisture stress effect on subsequent crop yields has also been reported in the literature. Fischer and Kohn (1966) studied the effects of limited moisture to grain yield and post flowering vegetative growth of wheat crop at Wagga Wagga in southern New South Wales, Australia. They concluded that soil moisture stress especially at the time of flowering greatly affected the yield. Aspinal et al. (1964) and Calvino et al. (2003) have also reported the high correlation between soil moisture and yield. The influence of cover crop on the soil moisture and growth performance observed in this research is specific to the Carman region. Similar findings would be expected in other geographic locations that practice rotations involving cover cropping system and experience seasonal soil freezing and thawing.

The presence of cover crop can have both positive and negative effects depending on the amount of soil moisture present at the beginning of the growing season. If the subsequent growing season turns out to be wetter, the previous season cover crop would have a beneficial effect. In this experiment, the subsequent year (2006) turned out to be

drier leading to poor growth performance and lower yields due to the depletion of soil moisture by the previous cover crop.

6.5 Summary and Conclusions

This study demonstrates the influence of a previous season berseem clover cover crop on the performance canola grown in the subsequent season in terms of soil water content, crop growth performance, and yield. The study was carried out in Carman, Manitoba, which is part of the Northern Great Plains of Canada, which experience seasonal soil freezing and thawing.

During the 2006 growing season, compared to the canola_NC treatment (canola in the treatment that had no cover crop in 2005), the canola_CC treatment (canola in the treatment that had a cover crop in 2005) had consistently lower soil moisture. It had 20.0% lower (0.18 vs. 0.23 $m^3 m^{-3}$) and 14.2% lower water content (0.14 vs. 0.16 $m^3 m^{-3}$) during flowering and maturity stages, respectively. The canola_CC treatment had poor crop growth performance with smaller above ground canola biomass, causing the ground to be 4.6° C warmer than the canola_NC treatment during the anthesis stage. As a result, the canola_CC treatment, which was influenced by presence of berseem clover in the previous growing season, had significantly lower yield (1.99 vs. 2.72 t ha^{-1}) compared to the canola_NC treatment.

During the winter from January to March 2007, the canola_CC treatment had 18 to 20% lower total soil moisture in the 0.1- to 0.9-m soil depth, and it was 0.2 to 1.2°C warmer in the top 0.4 m soil depth compared to the canola_NC treatment. The canola_CC treatment froze to a shallower depth (0.6 m vs. 0.8 m) during the 2007 winter season, and

by February 2007 it had accumulated 19.3% lower total soil water content (0.18 m vs. 0.22 m) due to reduced upward migration of unfrozen water from the deeper soil layers.

During the spring of 2007, the canola_CC treatment warmed and thawed earlier compared to the canola_NC treatment. The canola_CC had accumulated low total water content during winter; hence, it needed less energy to warm up due to lower heat capacity. The earlier soil thawing in the canola_CC treatment facilitated infiltration of the melt water and percolation away from the root zone. As a result, after spring snowmelt in April 17, the canola_CC treatment had 13.7% lower total water content (0.23 vs. 0.27 m^3 m^{-3}) in the 0.1- to 0.9-m soil depth compared to the canola_NC treatment.

The soil moisture redistribution is influenced by the previous season cover crop. The presence of cover crop can have both positive and negative effects depending on the amount of soil moisture present at the beginning of the growing season. For areas experiencing seasonal soil freezing and thawing such as the Ian N. Morrison Research farm in Carman, Manitoba, the selection of the type of crop following cover crops during the subsequent growing season may be influenced by the soil moisture redistribution dynamics during the preceding fall, winter, and spring seasons.

7. MODELING SOIL TEMPERATURE, FROST DEPTH, AND SOIL MOISTURE REDISTRIBUTION IN SEASONALLY FROZEN AGRICULTURAL SOILS

7.1 Abstract

Soil freezing and thawing processes and soil moisture redistribution play a critical role in the hydrology and microclimate of seasonally frozen agricultural soils. Accurate simulations of the depth and timing of frost and the redistribution of soil water are important for ensuring early farm operations and proper choice of rotational crops. The Simultaneous Heat and Water (SHAW) model was used to predict soil temperature, frost depth, and the amount and redistribution of soil moisture in Carman, Manitoba. Model simulations were compared with three growing seasons of field data collected year-round beginning from the summer 2005 to summer 2007 in four cropping systems (oats with berseem clover cover crop, oats alone, canola, and fallow). The simulated soil temperatures compared well with measured data in all the seasons (R^2 = 0.96-0.99). The soil moisture simulations were better during the summer (*RMSE* = 9.1-12.0% of the mean) compared to the winter season (*RMSE* = 17.5-19.7% of the mean). During the winter, the SHAW model over-predicted by 0.02 to 0.10 $m^3 m^{-3}$ the amount of total soil moisture below the freeze front, and under-predicted by 0.02 to 0.05 $m^3 m^{-3}$ the soil moisture in the upper frozen layers. The model was revised to account for the reduction in effective pore space resulting from frozen water to improve the soil moisture predictions during the wintertime. After the revisions, the model performed well during the winter (*RMSE* = 13.6% vs. 17.5% in vegetated fields, and 13.8% vs. 19.7% in the fallow). The modified SHAW model could be used as a tool for predicting the soil

moisture status as a function of depth during spring thawing, and for assessing the availability of soil moisture at the beginning of the subsequent growing season.

7.2 Introduction

Soil freezing and thawing processes can influence the soil moisture availability and redistribution during the fall through spring seasons (Kennedy and Sharratt 1998; Flerchinger et al. 2006; Lin and McCool 2006). Accurate simulation of the depth and timing of frost, soil temperature, and the unfrozen and total soil water content at different times of the year is important for determining the response of the soil to thawing during spring, and the soil moisture availability at the beginning of the subsequent growing season. Knowing the soil moisture, frost depth, and soil temperature status during spring is important for ensuring early farm operations and the selection of suitable climate- and moisture-sensitive crops (Bootsma and Brown 1985; DeGaetano et al. 1995, 2000).

The scarcity of available field-measured unfrozen and total water contents and soil temperature data is a major limitation in the validation of wintertime freeze-thaw simulations. The complexity of the wintertime hydrological processes is also another factor contributing to the challenge (Kennedy and Sharratt 1998; Warrach et al. 2001; Lin and McCool 2006; Kahimba and Sri Ranjan 2007). With the advances in modeling technology, various models have been developed that deal specifically with winter soil freeze-thaw phenomena. Examples are the SHAW model (Simultaneous Heat and Water) by Flerchinger and Saxton (1989a, 1989b), SOIL (simulation model for soil water movement and heat) by Jansson (1991), CLASS (Canadian Land Surface Scheme) by Verseghy et al. (1993), FROST (Kennedy and Sharratt 1988), and SEWAB (Surface Energy and Water Balance) (Warrach et al. 2001).

moisture status as a function of depth during spring thawing, and for assessing the availability of soil moisture at the beginning of the subsequent growing season.

7.2 Introduction

Soil freezing and thawing processes can influence the soil moisture availability and redistribution during the fall through spring seasons (Kennedy and Sharratt 1998; Flerchinger et al. 2006; Lin and McCool 2006). Accurate simulation of the depth and timing of frost, soil temperature, and the unfrozen and total soil water content at different times of the year is important for determining the response of the soil to thawing during spring, and the soil moisture availability at the beginning of the subsequent growing season. Knowing the soil moisture, frost depth, and soil temperature status during spring is important for ensuring early farm operations and the selection of suitable climate- and moisture-sensitive crops (Bootsma and Brown 1985; DeGaetano et al. 1995, 2000).

The scarcity of available field-measured unfrozen and total water contents and soil temperature data is a major limitation in the validation of wintertime freeze-thaw simulations. The complexity of the wintertime hydrological processes is also another factor contributing to the challenge (Kennedy and Sharratt 1998; Warrach et al. 2001; Lin and McCool 2006; Kahimba and Sri Ranjan 2007). With the advances in modeling technology, various models have been developed that deal specifically with winter soil freeze-thaw phenomena. Examples are the SHAW model (Simultaneous Heat and Water) by Flerchinger and Saxton (1989a, 1989b), SOIL (simulation model for soil water movement and heat) by Jansson (1991), CLASS (Canadian Land Surface Scheme) by Verseghy et al. (1993), FROST (Kennedy and Sharratt 1988), and SEWAB (Surface Energy and Water Balance) (Warrach et al. 2001).

The main problem with most of the sophisticated models is that they are data intensive with longer simulation times (Warrach et al. 2001). Other models that are less data intensive such as SEWAB (Warrach et al. 2001) have the advantage of faster execution times, but they tend to oversimplify the actual processes happening in the soil leading to less accurate simulations of the real phenomena happening in the soil (Kennedy and Sharratt 1998).

In this paper, a physically based Simultaneous Heat And Water (SHAW) model was used to simulate the soil temperature, duration and timing of frost, and soil moisture redistribution from the summer through spring seasons. The SHAW model was originally developed by Flerchinger and Saxton (1989a, 1989b) to simulate heat and water flow in the canopy-snow-surface-soil system. Various components of this model have been tested for their accuracy. Examples are the simulations of evapotranspiration, ET (Flerchinger et al. 1996), model performance under various residue heights and architecture, and cover cropping system (Flerchinger et al. 2003), and simulations of within canopy surface radiation exchange (Flerchinger et al. 2006). The SHAW model has also been tested against other models. Kennedy and Sharratt (1998) compared SHAW, SOIL, Benoit, and Gusev models and concluded that the SHAW and SOIL models had better predictions of frost depth compared to the Benoit and Gusev models. Therefore, the SHAW model was selected for use in this study due to its accuracy and the inclusion of a detailed account of the soil freeze-thaw processes.

The limitations in the availability of year-round field data, especially the unfrozen and total water contents, frost depths, and soil temperature profiles, measured simultaneously, had made it difficult to extensively test the model performance in

agricultural soils experiencing seasonal soil freezing and thawing conditions as prevailing in central Canadian Prairies. Therefore, the objectives of this paper were to:

1.) Use the SHAW model to simulate the depth and timing of frost, soil temperature, and soil moisture redistribution from summer through spring seasons,

2.) Compare the SHAW model simulations for different seasons of the year against measured field data collected year-round over two years, and

3.) Revise the model hydraulic processes during soil freezing and thawing to enable better prediction of soil moisture during the winter and spring.

7.3. The Shaw model

The SHAW model simulates heat, water, and solute transfer within a one-dimensional soil profile. The heat and water movement is simulated through both the plant canopy, snow, residue cover, and the soil (Flerchinger and Pierson 1991; Flerchinger 2000). Among important features of this model is a detailed account of the snowmelt and soil freeze-thaw processes, and simulations of transpiration and transfer of water vapor through multi-species plant canopy (Flerchinger and Saxton 1989b). The model uses an energy balance approach in simulating snow and frost depths. The energy balance approach is considered to be more accurate than the temperature-driven approach in determining heat exchanges in the soil-plant- atmosphere ecosystem (Lin and McCool 2006).

The main equation in the model that accounts for surface energy balance is given as follows (Flerchinger et al. 1996; Flerchinger 2000):

$$R_n + H + L_v E + G = 0 \tag{7.1}$$

where, R_n is net all-wave solar radiation (W m^{-2}), H is sensible heat flux (W m^{-2}), L_v is latent heat of vaporization (J kg^{-1}), E is total evapotranspiration, $L_v E$ is latent heat flux (W m^{-2}), and G is soil heat flux (W m^{-2}). The Eq. 7.1 gives the interrelation between the water fluxes and energy at the soil surface.

The equation for soil water flux that takes into account the soil freezing and thawing is given as follows (Flerchinger 2000):

$$\frac{\partial \theta_l}{\partial t} + \frac{\rho_l}{\rho_l}\frac{\partial \theta_i}{\partial t} = \frac{\partial}{\partial z}\left\{K\left(\frac{\partial \varphi}{\partial z} + 1\right)\right\} + \frac{1}{\rho_l}\frac{\partial q_l}{\partial z} + U \tag{7.2}$$

where, θ_l is volumetric liquid water content (m^3 m^{-3}), θ_i is volumetric ice content (m^3 m^{-3}), ρ_i is density of ice, ρ_l is density of water, K is saturated hydraulic conductivity (m s^{-1}), t is time (s), z is soil depth (m), φ is soil matric potential (m), and U is source/sink term (m^3 m^{-3} s^{-1}). The left hand side terms in Eq. 7.2 represent the change in volumetric liquid water content and change in volumetric ice content, respectively. The right hand side terms represent the net liquid influx in a layer, net vapor influx, and a source/sink term accounting for the water extraction by roots, respectively. All the terms are in m^3 m^{-3} s^{-1}.

The unsaturated hydraulic conductivity (K) is a critical factor that determines the flow of unfrozen water in unsaturated soils. It also influences the unfrozen water flow and redistribution in freezing soils. During the winter as the soil begins to freeze, some amounts of free water are immobilized by freezing and do not participate in the flow. Hence, the freezing soil behaves as a drying soil with respect to liquid water availability

and mobility. The unsaturated hydraulic conductivity (K) is calculated in the SHAW model using the following equation (Brooks and Corey 1966):

$$K = K_s \left(\frac{\theta_l}{\theta_s}\right)^{(2b+3)} \tag{7.3}$$

where, K_s is saturated hydraulic conductivity (m s^{-1}), b is pore size distribution index, θ_l is the soil water content at a given time (m^3 m^{-3}), and θ_s is the saturated soil water content (m^3 m^{-3}). The Brooks and Corey (1966) equation is used to relate the soil moisture characteristic as follows:

$$\varphi = \varphi_e \left(\frac{\theta_l}{\theta_s}\right)^{-b} \tag{7.4}$$

where, φ_e is air entry pressure (m) and φ is soil matric potential (m).

The main assumption in the model on the relationship between matric potential and unsaturated hydraulic conductivity is that frozen soils behave like unsaturated dry soils (Flerchinger 1991; Flerchinger 2000). Hence water flow in a freezing soil will behave the same as water flow in a drying soil. Therefore, the soil moisture characteristic equation used for determining water flow in freezing soil has been assumed to behave the same as in unsaturated soils. The detailed physics of various other components of the model have been described in Flerchinger and Saxton (1989a), Flerchinger and Pierson (1981), Flerchinger et al. (1996), and Flerchinger (2000).

Since its development in 1989 and subsequent improvements, the SHAW model has been verified and used in many other researches dealing with heat, water, and solutes transfer within the soil-plant-atmosphere ecosystem (e.g. Kennedy and Sharratt 1998; DeGaetano et al. 2000; Flerchinger et al. 1996, 2003, 2006). Some of the identified

weaknesses in the SHAW model in the recent studies include over-prediction of the midday canopy temperatures due to simplified assumptions of long-wave radiation transfer within the canopy (Flerchinger et al. 2006). Examples of proposals that have been made to improve the model performance are such as improvement on the simulation of the depth and timing of frost (Kennedy and Sharratt 1998), inclusion of water budget scheme to improve simulations of frost depth (DeGaetano et al. 2000), and simulation of surface radiation exchange within canopies (Flerchinger et al. 2006).

Sensitivity analyses have also been done on some of the model components to determine model input parameters that have a larger influence on model simulations. Air temperature, initial snow depth, and lower boundary soil temperature values have a larger influence on frost depth; while soil hydraulic parameters have a smaller influence on the frost depth (Flerchinger 1991). The limited availability of winter-time field measured soil moisture, depth and timing of frost, and soil temperature data have hindered extensive verification of various components of the SHAW model simulations during the winter time (e.g. Flerchinger et al. 1996; Xiao et al. 2006). The field data on soil temperature profile and the unfrozen and total water contents collected over three seasons in the current study, will help to verify the SHAW model seasonal performance for regions experiencing seasonal soil freezing and thawing.

7.4 Materials and Methods

7.4.1 Description of the study site

The study site was at the Ian N. Morrison Research Farm of the University of Manitoba located in Carman, Manitoba (49° 30' N, 98° 02' W, 262 m elevation a.m.s.l.).

The area experiences seasonal soil freezing and thawing, with 119 to 126 frost- free days starting from May 15 to September 26 (Environment Canada 2007; Nadler 2007). The average annual precipitation over the area (15-year average, 1991-2005) is 588.8 mm (Environment Canada 2007). The 15-year mean annual temperature was 3.4°C (Environment Canada 2007). The monthly mean maximum temperatures occur in July (+19.1°C), while the monthly mean minimum temperatures (-16.2°C) occur in January (Kahimba et al. 2008b). The experimental farm has a relatively flat topography with ground slopes ranging from 0.0% to 0.5%. The surface texture of the soil at the experimental site is classified as a well-drained Hibson, with a texture class of very fine sandy loam from the sub group Orthic Black Chernozem (Mills and Haluschak 1993) or Mollisol (very fine sandy loam) in the USDA Soil Taxonomy. Soil profile over the selected experimental plots was relatively uniform with the depth to clay layer ranging between 0.70 and 0.75 m (Mills and Haluschak 1993).

7.4.2 Instrumentation and field data collection

Simulation of unfrozen water in frozen soil is a challenge in many soil moisture models simulating soil moisture movement during the winter time. This is because it is difficult to obtain data for model validations, especially during the fall freeze-up, winter, and spring snowmelt when soil water may exist in both the frozen and unfrozen states, simultaneously. Most soil moisture measurement techniques can measure either the total soil water content (e.g. Neutron Moisture Meter (NMM) and gravimetric), or the unfrozen water content (e.g. Time Domain Reflectometry (TDR)), but not both water phases simultaneously. In addition, data collection in agricultural experiments is largely confined to the growing season leading to a dearth of data during the winter time. In this

study, the unfrozen water content for different soil depths was measured using the TDR method at 0.1 m depth and at 0.2 m intervals from 0.2 m to 0.8 m. The total water content was measured using the NMM technique at 0.2 m intervals from 0.2 m to 1.8 m. The TDR method is regarded as the most practical technique for measuring liquid water content in frozen soils (Seyfried and Murdock 1996). Both techniques were used on the same day within approximately one to two hours on each date of data collection to minimize errors associated with the temperature change on the TDR measurement. The soil temperature was also measured on the same day, at the same depths of TDR measurement using a digital thermocouple thermometer with a precision of ±0.1°C. The soil moisture and soil temperature data collected from the field were used for comparison with simulations from the SHAW model.

7.4.3 Model input parameters

The SHAW model is a physically based model that has extensive data requirements. It requires initial conditions of soil temperature and soil moisture profiles at each soil depth (node), and depth of snow at the start of simulation. Other model input parameters are the general site information, weather conditions, and soil and plant parameters. The hourly weather data used in the simulation were collected from an automatic weather station located within the Ian N. Morrison Research Farm, about 300 m from the selected experimental field plots. Tables 7.1 and 7.2 give the details of soil and plants input parameters, respectively, used in this simulation. The soil parameters were obtained from the detailed soil survey performed during establishment of the field station (Mills and Haluschak 1993). Detailed descriptions of the model input parameters are presented in Flerchinger and Saxton (1989a, 1989b) and Flerchinger (2000).

Table 7.1. Soil characteristics used as input parameters for the SHAW model.

Soil characteristics	Soil depth range (m)				
	0.0-0.2	0.2-0.4	0.4-0.6	0.6-0.8	>0.8
Particle size distribution (%)					
Sand	79.00	73.00	77.00	77.00	4.00
Silt	8.00	8.00	7.00	7.00	44.00
Clay	13.00	19.00	16.00	16.00	52.00
Organic matter	3.76	2.72	1.24	1.24	0.00
Campbell's pore size distribution index	3.05	3.22	3.18	3.12	3.05
Air entry potential (m)	-0.40	-0.22	-0.21	-0.20	-0.20
Saturated hydraulic conductivity (cm/hr)	2.90	4.58	4.00	0.41	0.20
Bulk density (kg/m^3)	1250	1420	1400	1400	1310

Table 7.2. Plant characteristics used as input parameters for the SHAW model.

Plant characteristics	Farm management		
	Year 2005 - 2006		Year 2006 - 2007
	Oats with Berseem clover	Oats alone	Canola
Height of plant species (m)	1.00	1.00	1.20
Width of plant leaves (cm)	2.50	2.50	10.00
Dry biomass of plant species (kg/m^2)	0.67	0.74	0.60
Leaf area index (LAI)	3.10	3.10	3.30
Effective rooting depth (m)	0.75	0.75	0.95

The SHAW model optionally uses plant growth curves or constant plant growth parameters (no plant growth curves) if the plant growth parameters are not taken at different stages of plant growth. Accurate simulations could possibly be achieved if the

plant growth parameters are monitored. In this study, an option of constant plant growth parameters was chosen since the plant growth curves were not monitored.

The solar radiation data obtained from the automatic weather station were available only during the growing season from April to September. For the period between September and April there were no solar radiation data. Hence solar radiation data for the missing period were estimated using the SolarCalc model developed by Spokas and Forcella (1996). The SolarCalc model uses daily weather data as input parameters (maximum and minimum air temperatures (°C) and total precipitation (mm)). The model also requires inputs of year of simulation and the topographic characteristics of the area (latitude, longitude, and elevation above m.s.l). The output from the SolarCalc model is hourly incoming solar radiation (W m^{-2}). The simulated hourly incoming solar radiation was used as part of the input weather data of the SHAW model. The SolarCalc model, which was used to obtain the missing solar radiation data in this study, has the advantage that it uses limited daily weather parameters that are commonly measured in most recording weather stations (Spokas and Forcella 1996).

The field measured soil temperature data were available at 0.1, 0.2, 0.4, 0.6, and 0.8 m soil depths. The soil temperatures at depths below 0.8 m were estimated assuming that the temperature at 4.0 m depth was equal to the average annual air temperature of 3.4°C (Flerchinger et al. 1996; Environment Canada 2007). The SHAW model also requires the surface soil temperature as an input parameter at the surface node. However, in this study no probes were installed at the surface to measure the soil temperature. Hence, a procedure developed by Gupta et al. (1990) was adopted for estimating the soil surface temperature. In their study, Gupta et al. (1990) stated that the daily maximum

and minimum air temperature measured at 2.0 m height is directly proportional to the upper boundary soil temperature, depending on soil surface conditions. The hourly soil surface temperature was approximated using normalized hourly values and the maximum and minimum soil surface temperature as follows (Gupta et al. 1990):

$$T_{ot} = \Gamma_{ot}\left(T_{o\max} - T_{o\min}\right) + T_{o\min} \tag{7.5}$$

where, T_{ot} is the estimated soil surface temperature at time t, Γ_{ot} is the average normalized hourly soil surface temperature, T_{omax} is the estimated maximum soil surface temperature, and T_{omin} is the estimated minimum soil surface temperature. Hence using the proposed procedure, the daily maximum and minimum air temperatures obtained from the weather station were used to estimate the daily maximum and minimum soil surface temperatures, that were further used to estimate the hourly soil surface temperature at depth 0.0 m and time t. Details on the procedure for estimating the hourly soil temperatures at various soil depths and for different soil surface conditions are explained in Gupta et al. (1982, 1984, and 1990). The use of predicted solar radiations and surface soil temperature as input parameters in the SHAW model can possibly affect the simulations accuracy depending on the accuracy of the models that determine the hourly incoming solar radiation and the surface soil temperature.

7.4.4 The SHAW model simulations

The SHAW model was used to predict soil temperature profile, depth and timing of frost, and unfrozen and total water contents. Simulations were performed year-round from the summer of 2005 to the summer of 2007. The simulations were compared with measured field data. The model performance was assessed in three cropping systems

having oats with berseem clover cover crop and oats alone (2005-2006 season), canola (2006-2007), and a continuous fallow. The model was also used to simulate the depth and timing of frost during the winter.

The performance of the SHAW model in simulating soil moisture and soil temperature during the summer and fall when the soil is still unfrozen, against the winter when the soil is frozen and temperatures are below zero was evaluated. The ground cover effect was also evaluated for the two seasons. The predicted values of total soil water content, the soil temperature profile, and frost depth were compared with the measured values. Based on the simulations of the model for different seasons of the year, parts of the model that needed improvement were identified. Revised equations were developed that could be used to improve the SHAW model predictions to better simulate the hydrologic conditions especially during the winter when the soils are partly frozen and soil moisture exists in both frozen and unfrozen states.

In addition to predicting the year-round hydrological processes, the model was also used to assess the response of the soil to fall freeze-up and spring snowmelt under different farm management practices, and determine the soil moisture availability at the beginning of the next growing season. Proposals have been made on the potential for using the SHAW model for year-round predictions of the hydrological processes in areas such as the Ian N. Morrison research farm in Carman, Manitoba, that experience seasonal soil freezing and thawing.

7.4.5 Statistical model validations

Statistical analyses were done to assess the performance of the model for different seasons of the year. Both absolute and relative error measures (Willmott et al. 1985; (Kahimba et al. 2008a) were used to validate the model and assess the accuracy of the model simulations. The square of the Pearson's product-moment correlation coefficient $(r)^2$ or coefficient of determination (R^2) was used to measure correlations between measured and predicted water content and soil temperature. The R^2 was calculated as follows (Legates and McCabe Jr. 1999):

$$R^2 = \left[\frac{\sum_{i=1}^{n}(M_i-\bar{M})(P_i-\bar{P})}{\sqrt{\left[\sum_{i=1}^{n}(M_i-\bar{M})^2\right]\left[\sum_{i=1}^{n}(P_i-\bar{P})^2\right]}}\right]^2 \quad (7.6)$$

where, M_i and P_i are the measured and predicted values, respectively; n is the total number of observations; and $\bar{M}$ and $\bar{P}$ are the means of the measured and predicted values, respectively. The R^2 values range between 0.0 and 1.0, with values close to 1.0 indicating better correlation (Spokas and Forcella 2006).

The index of agreement, (d) also measures the correlation between the measured and simulated values. It was calculated as follows:

$$d = 1.0 - \left[\frac{\sum_{i=1}^{n}(M_i-P_i)^2}{\sum_{i=1}^{n}(|P_i-\bar{M}|+|M_i-\bar{M}|)^2}\right] \quad (7.7)$$

where, M_i and P_i are the measured and predicted values, respectively; n is the total number of observations; and $\bar{M}$ and $\bar{P}$ are the means of the measured and predicted values, respectively. The value of d ranges between 0.0 and 1.0, with values close to 1.0 indicating better model agreement (Spokas and Forcella 2006).

While the R^2 and d give better indications of the degree of agreement between the measured and the predicted values, they may not be better indicators of the model accuracy, since they do not account for proportional differences in the measured and the predicted values; and they can easily be biased by extreme values (Willmott et al. 1985; Legates and McCabe Jr. 1999). Hence, the relative error measures need to be supplemented with absolute error measures (Spokas and Forcella 2006; (Kahimba et al. 2008a).

Considering the absolute error measures, the root mean square error (*RMSE*) was calculated as shown in Eq. 7.8 below (Legates and McCabe Jr. 1999):

$$RMSE = \sqrt{\frac{1}{n}\sum_{i=1}^{n}(M_i - P_i)^2} \quad (7.8)$$

where, n is number of observations, M_i is measured soil moisture, and P_i is predicted soil moisture. When expressed as a percentage of the mean, a *RMSE* (%) value of 10 is regarded as a reasonable accuracy for most agricultural experiments (Tarpley 1979). The mean absolute error (*MAE*) gives the weighted average of the absolute value of errors. A better model performance is when the *MAE* is close to zero. The *MAE* was calculated as shown in Eq. 7.9 below (Legates and McCabe Jr. 1999):

$$MAE = \frac{1}{n}[\sum_{i=1}^{n}|M_i - P_i|] \quad (7.9)$$

where variables in Eq. 7.9 have the same definitions as in Eq. 7.8.

The mean bias error (*MBE*) gives the uniformity of errors distribution. It assists in determining whether the model is overestimating or underestimating the measured

values. A value close to zero indicates that the errors are evenly distributed, while a negative value of $M_i - P_i$ indicates underestimation. The *MBE* was calculated as follows:

$$MBE = \frac{1}{n}\sum_{i=1}^{n}(M_i - P_i) \tag{7.10}$$

where variables in Eq. 7.10 have the same definitions as in Eq. 7.8. The absolute error measures have the advantage that they are less influenced by outliers, and they take into account the proportional and additive differences between the measured and the predicted values (Legates and McCabe Jr. 1999). They also give a better indication of model accuracy since they can be expressed in the same units of the measured data (Tarpley 1979; Spokas and Forcella 2006).

7.5 Results and Discussion

7.5.1 Year-round simulations of soil moisture in different cropping systems

The SHAW model was used to predict soil moisture in a vertical soil profile at depths from 0.0 to 1.8 m. The simulations were performed for different cropping systems from the summer of 2005 to the summer of 2007. Comparison was made between the simulated total soil moisture and field measured soil moisture taken using the neutron scattering method. In the 2005 growing season the treatments used in the simulations were oats with berseem clover cover crop and oats alone representing simulations on vegetated fields, and a continuous fallow representing simulations on bare grounds. In the 2006 growing season simulations were compared with measured values from plots that had canola alone and a continuous fallow. A complete water balance using the SHAW model was not performed due to lack of measured data on evapotranspiration and root water uptake.

Summary of the statistical analysis for the year-round simulations from August 2005 to September 2007 is presented in Table 7.3. On average the model performed well in vegetated plots (R^2 = 0.76-0.99, d = 0.91-0.99, *MBE* = 0.02-0.04 $m^3\ m^{-3}$, and *RMSE* = 8.82-19.54%) compared to the continuous fallow. The corresponding statistical values for the continuous fallow were R^2 = 0.63-0.74, d = 0.86-0.93, *MBE* = 0.04-0.05 $m^3\ m^{-3}$, and *RMSE* = 11.91-18.35%, respectively.

Table 7.3. The SHAW model statistical analysis for the measured and predicted total soil moisture and soil temperature during the 2005-2007 seasons.

			Statistical parameters							
				Relative error measures*		Absolute error measures**				
Year	Parameter	Farm management	N	R^2	d	MAE	MBE	ME	RMSE	RMSE (%)
2005/2006	Total soil moisture (m^3 m^{-3})	Oats+berseem	77	0.90	0.99	0.02	0.00	0.07	0.03	8.82
		Oats alone	97	0.66	0.87	0.04	-0.03	0.09	0.05	14.11
		Fallow	98	0.74	0.93	0.04	-0.01	0.09	0.05	11.91
	Soil Temperature (°C)	Oats+berseem	72	0.96	0.98	0.49	-0.45	1.80	0.65	31.65
		Oats alone	91	0.96	0.98	0.55	-0.55	1.70	0.73	42.60
		Fallow	88	0.96	0.99	0.34	-0.01	2.10	0.58	36.41
2006/2007	Total soil moisture (m^3 m^{-3})	Canola	110	0.76	0.91	0.04	-0.02	0.13	0.06	20.74
		Fallow	107	0.63	0.86	0.05	-0.03	0.11	0.06	18.35
	Soil Temperature (°C)	Canola	106	0.99	1.00	0.80	-0.76	4.30	1.20	14.00
		Fallow	110	0.99	1.00	0.80	-0.32	4.80	1.28	13.12

* The parameters are: N = number of observations, R^2 = coefficient of determination, and d = index of agreement.

** The parameters are: *MAE*= mean absolute error, *MBE* = mean bias error, *ME* = maximum error, and *RMSE* = root mean square error.

The variation with depth of the simulated and measured total soil moisture from 0.0 to 1.8 m soil depth on vegetated fields (oats with berseem clover) for the 2005 season is presented in Fig. 7.1. During February and March 2006 the model over-predicted the total soil moisture just below the freeze front by 0.02 to 0.05 $m^3 m^{-3}$ and under-predicted the total soil moisture above the freeze front by 0.01 to 0.04 $m^3 m^{-3}$ (Figs. 7.1c and 7.1d).

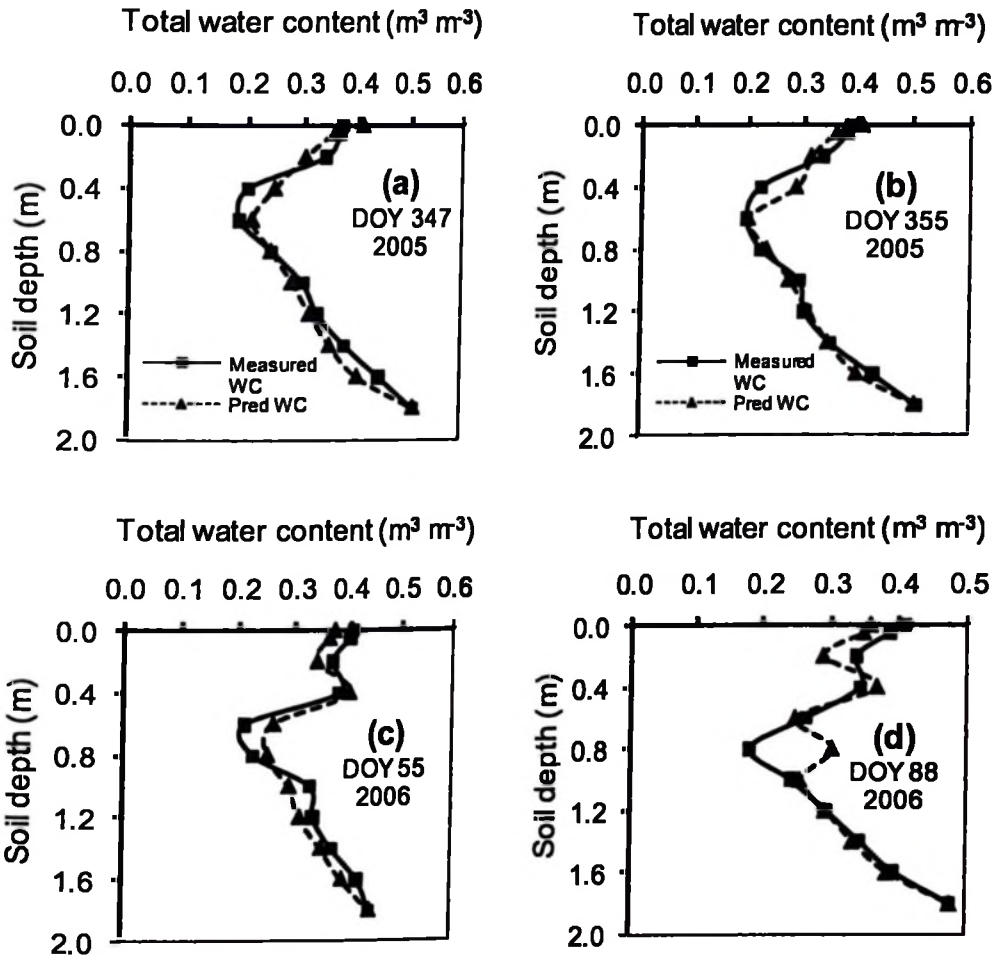

Fig. 7.1. Measured and predicted total soil water contents at different soil depths in the oats + berseem clover cover crop treatment during: (a and b) the fall in 2005 and (c and d) winter and spring in 2006.

The model simulated the soil moisture, in the unfrozen layers below 1.2 m, fairly well during all the seasons. For the continuous fallow (Fig. 7.2), the over-prediction below the freeze front was observed at 0.8 m soil depths, and under-prediction in the top 0.5 m soil depth. In the previous study, Kahimba et al. (2008b) presented the soil freezing patterns indicating that the depth of freeze front could be indicated by the region of zero soil moisture measured by TDR, which comes in line with lowest total soil moisture measured by NMM. In this case from Fig. 7.2a and 7.2b, by March 29 (DOY 88), 2006 the freeze front in the fallow was about 0.8 m deep (Fig. 7.2).

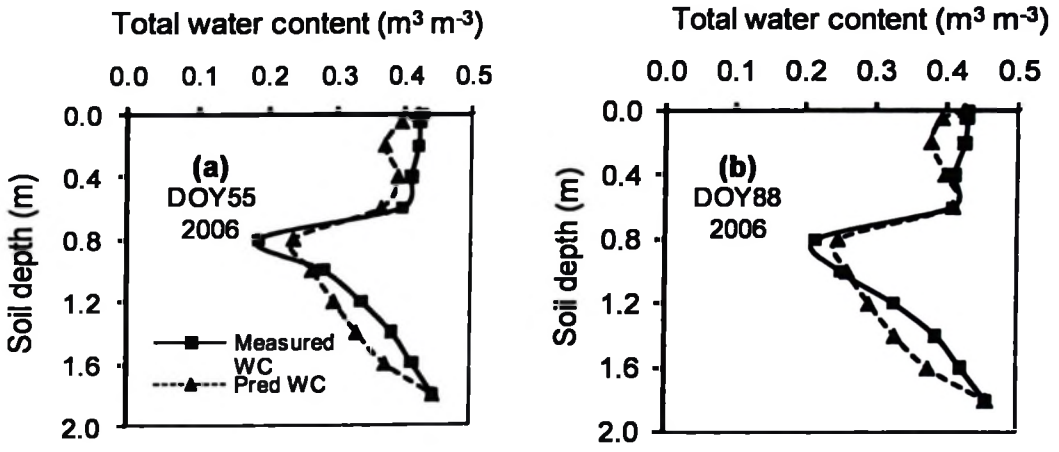

Fig. 7.2. Measured and predicted total soil water contents at different soil depths in the fallow during: (a) winter on February 24, 2006 and (b) early spring on March 29, 2006. The measured total water contents (WC) were taken using NMM method.

The model over-predicted the total soil moisture below the freeze front by 0.04 to 0.11 $m^3 m^{-3}$ in the fallow treatment. The over-prediction below the freeze front on winter months was an indication that the model allowed less soil moisture migration from below the freeze front towards the frozen soil layer as the freeze front advanced downwards.

The lesser upward migration was also a cause for the lower amount of the simulated total water content in the frozen soil layers above the freeze front.

7.5.2 Soil temperature simulations on different cropping systems

The performance of the model for simulating soil temperature profile was also evaluated on different cropping systems. The model preformed well on all the cropping systems during the two simulation years. Figure 7.3 presents the variation with depth of the simulated and measured profile soil temperature from 0.0 to 1.8 m soil depth for the vegetated fields (oats with berseem clover) and the continuous fallow.

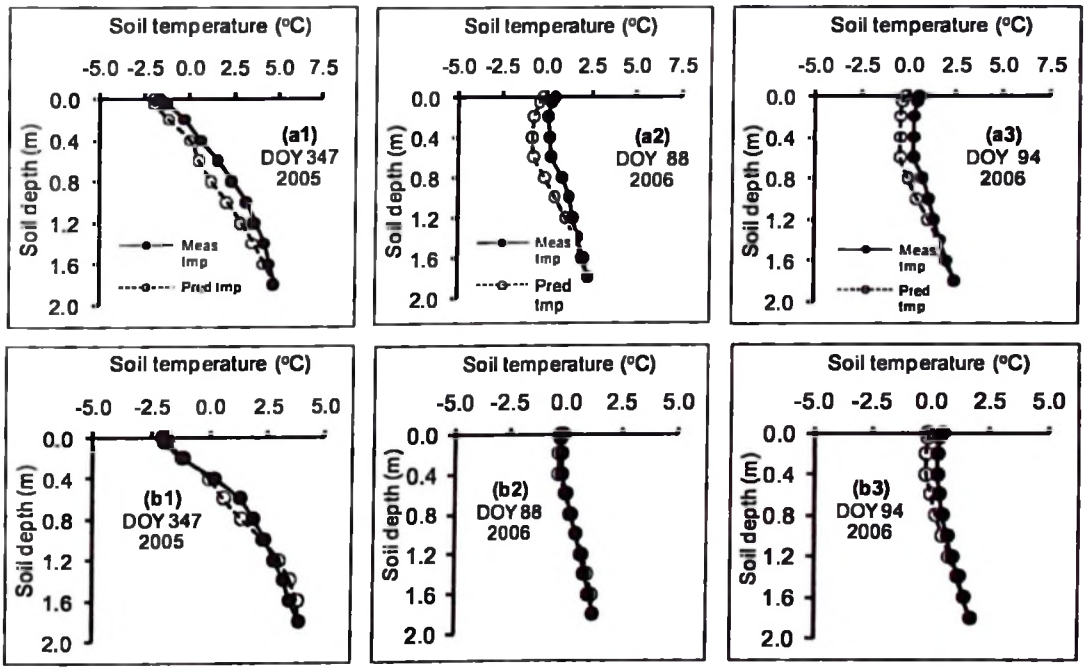

Fig. 7.3. Measured and predicted soil temperature at different soil depths: (a) in the oats + berseem clover cover crop and (b) in the fallow treatment. The measurements on (a1) and (b1) were during the fall; (a2) and (b2) during winter; and (a3) and (b3) during spring.

The R^2 for the soil temperature predictions ranged between 0.96 and 0.99 on both the vegetated fields and the fallow (Table 7.1). The mean absolute error ranges were from 0.5 to 0.8°C and from 0.3 to 0.8°C for the vegetated fields and the continuous fallow, respectively (Table 7.1). The mean bias error (*MBE*) ranged between -0.45 and -0.76°C for the vegetated fields, and between -0.01 and -0.32°C for the fallow. The negative values of *MBE* was an indication that on average the SHAW model slightly underestimated the actual soil temperature profile on both vegetated fields and the fallow (Table 7.1 and Fig. 7.3). Comparing the vegetated fields against the continuous fallow, the ground cover conditions did not affect the accuracy of the model in simulating the soil temperature at different soil depths. The soil temperature is less affected by the plant parameters such as root water uptake and root length compared to the water content.

7.5.3 Comparison of summer and winter model simulations

A comparison was made between the SHAW model simulations of the summer and winter hydrological processes. Statistical analysis was performed to assess the accuracy of the model both during the summer when the soil was unfrozen and during the winter when the soil was frozen and temperatures were below zero. Table 7.4 presents summary of statistical analysis of the model performance in simulating soil moisture and soil temperature during the summer compared to winter for vegetated plots and continuous fallow. Comparison was made for a total of 55 to 118 days in which physical measurements of soil moisture and soil temperature were performed in the field.

Table 7.4. Comparison of the summer and winter SHAW model predictions of soil moisture and soil temperature on vegetated plots and continuous fallow treatments in the 2005-2007 seasons.

			Statistical parameters							
				Relative error measures*		Absolute error measures**				
Farm Management	Parameter	Season of simulation	N	R^2	d	MAE	MBE	ME	RMSE	RMSE (%)
Vegetated plots	Total soil moisture ($m^3\ m^{-3}$)	Summer	118	0.90	0.97	0.02	-0.02	0.08	0.04	12.01
		Winter	116	0.67	0.89	0.04	-0.02	0.16	0.06	17.54
	Soil Temperature (°C)	Summer	113	0.99	1.00	0.50	-0.44	2.50	0.80	8.68
		Winter	110	0.91	0.90	0.66	-0.66	2.10	0.82	N/A***
Continuous Fallow	Total soil moisture ($m^3\ m^{-3}$)	Summer	64	0.92	0.97	0.02	-0.02	0.07	0.03	9.05
		Winter	109	0.52	0.84	0.05	0.00	0.20	0.07	19.72
	Soil Temperature (°C)	Summer	55	1.00	1.00	0.50	-0.30	2.30	0.68	6.84
		Winter	109	0.98	0.99	0.66	-0.02	1.20	0.34	N/A

* The parameters are: N = number of observations, R^2 = coefficient of determination, and d = index of agreement.

** The parameters are: *MAE*= mean absolute error, *MBE* = mean bias error, *ME* = maximum error, and *RMSE* = root mean square error.

*** Not applicable during the winter when the soil mean temperature is close to zero.

7.5.3.1 Soil moisture simulations. The accuracy of the SHAW model in simulating soil moisture was better in the summer when the soil was unfrozen compared to winter when the soil was frozen and temperatures are below zero (Table 7.4). Statistical evaluations indicated that the range in model performance during the summer were R^2 = 0.90-0.92; d = 0.97; and *RMSE* = 9.1-12.0%. During the winter the ranges were R^2 = 0.52-0.67; d = 0.84-0.89; and *RMSE* = 17.54-19.72%. Based on the *RMSE* value of 10% (Tarpley 1979), the model performed fairly well during the summer compared to during the winter. In their study, DeGaetano et al. (1995) also noted that the presence of vegetations and crop residue increases the complexity of the winter soil freezing and thawing processes.

The seasonal model accuracy of soil moisture predictions also varied depending on the ground cover condition. Figure 7.4 presents the scatter plots that compare the performance of the model on vegetated fields against continuous fallow during the summer and winter seasons. The results indicated that, during the summer, better model performance was observed in the fallow compared to the vegetated fields (R^2 = 0.92 vs. 0.90; and *RMSE* = 9.1% vs. 12.0%) (Fig. 7.4 a1 and b1; Table 7.4). The difference between vegetated fields and the fallow in the summer model simulations could be associated with the uncertainties associated with estimation of plants physical parameters and growth performance such as the measurements of leaf area index, plants biomass and root lengths on the vegetated treatments.

The continuous fallow treatment had poor model simulations during the winter (R^2 = 0.52 vs. 0.67) compared to vegetated treatments (Fig. 7.4 a2 and b2).The poor simulations in the fallow could be attributed to deeper layer of frozen layer compared to vegetated fields, hence greater migration of the unfrozen water towards the freeze front.

In summary, The SHAW model had better simulations during the summer than during winter regardless of ground conditions. Considering the ground cover effects, better simulations of soil moisture during the summer were observed in the fallow compared to vegetated fields, while during the winter the fallow performed more poorly than the vegetated fields.

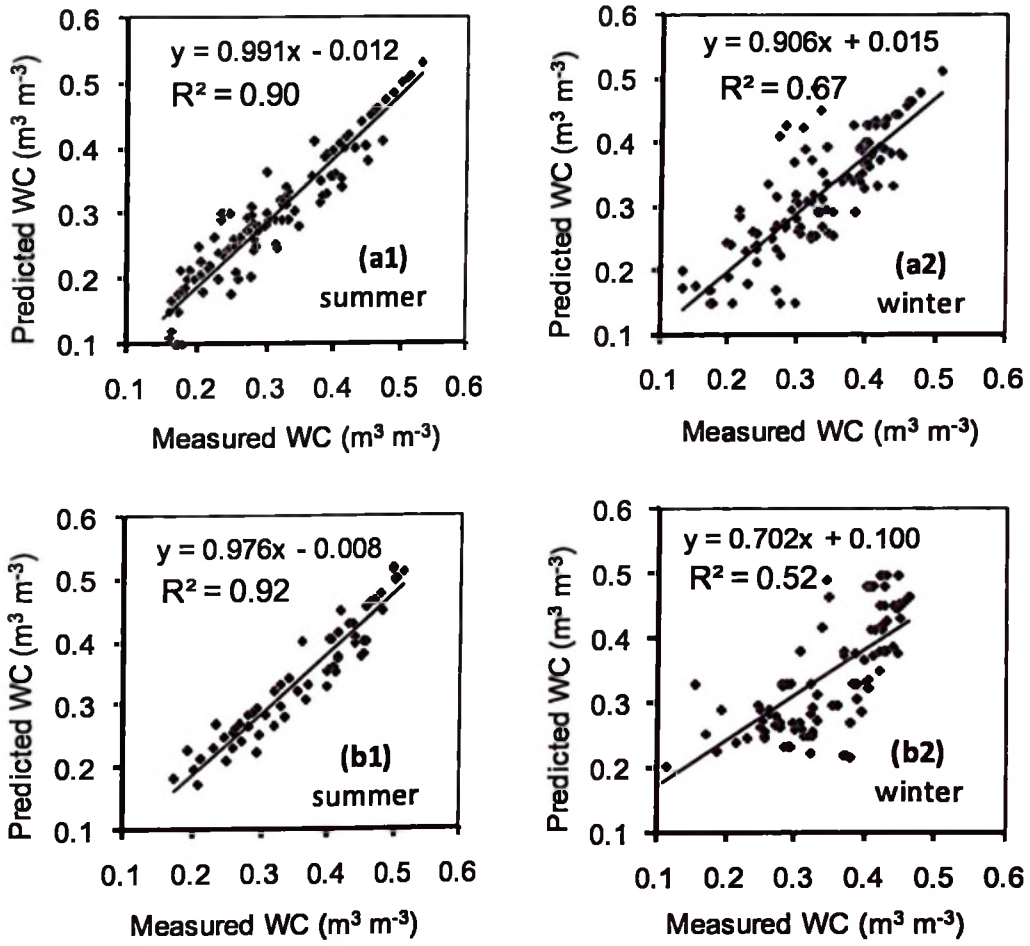

Fig. 7.4. Scatter plots of estimated versus measured total soil moisture during the summer of 2005 and winter 2006 for: (a) vegetated fields (oats with berseem clover cover crop) and (b) continuous fallow treatments.

The poor model simulation on the fallow compared to vegetated fields during the winter indicated that the over-estimation of total soil moisture below the freeze front and under-estimation above the freeze front was more magnified in the fallow, since the bare fields (i.e. fallow) froze to a greater depth and had most of the soil moisture below the freeze front migrate towards a thicker frozen soil layer above (Kahimba et al. 2008b). Hence, if there are errors in predicting the soil moisture migrations due to freeze front, the errors will be magnified on the deeper frozen soil layers as observed in fallow.

The over-predictions of total soil moisture just below the freeze-front could be attributed to the SHAW model assumption (Eq. 7.2) that the unsaturated hydraulic conductivity (K) of drying soil is similar to the K of freezing soil (Flerchinger 2000). In a freezing soil, however, part of the pore space is occupied by frozen water making the effective porosity available for unfrozen water movement to be smaller than in a drying soil. Hansson et al. (2004), while incorporating the heat and water flow algorithms under subzero conditions in the HYDRUS-1D model, they also assumed that soil freezing has the same effects as soil drying. Better simulations of soil moisture below the freeze front was obtained only for short durations of 24 h. However, for longer durations (50 h) the HYDRUS-1D model also over-predicted the soil moisture below the freeze front with unclear reasons (Hansson et al. 2004). The ice content of freezing soil should be taken into account and the total porosity of the frozen soil should be reduced by the amount equivalent to the ice content during the derivation of equations for water flow in freezing soils. Details of the proposal for algorithm modifications are presented in section 7.5.4 below.

7.5.3.2 Soil temperature simulations. Comparisons were also made on model performance in simulating soil temperature during the summer and winter on different ground cover conditions (Table 7.4, Fig. 7.5).

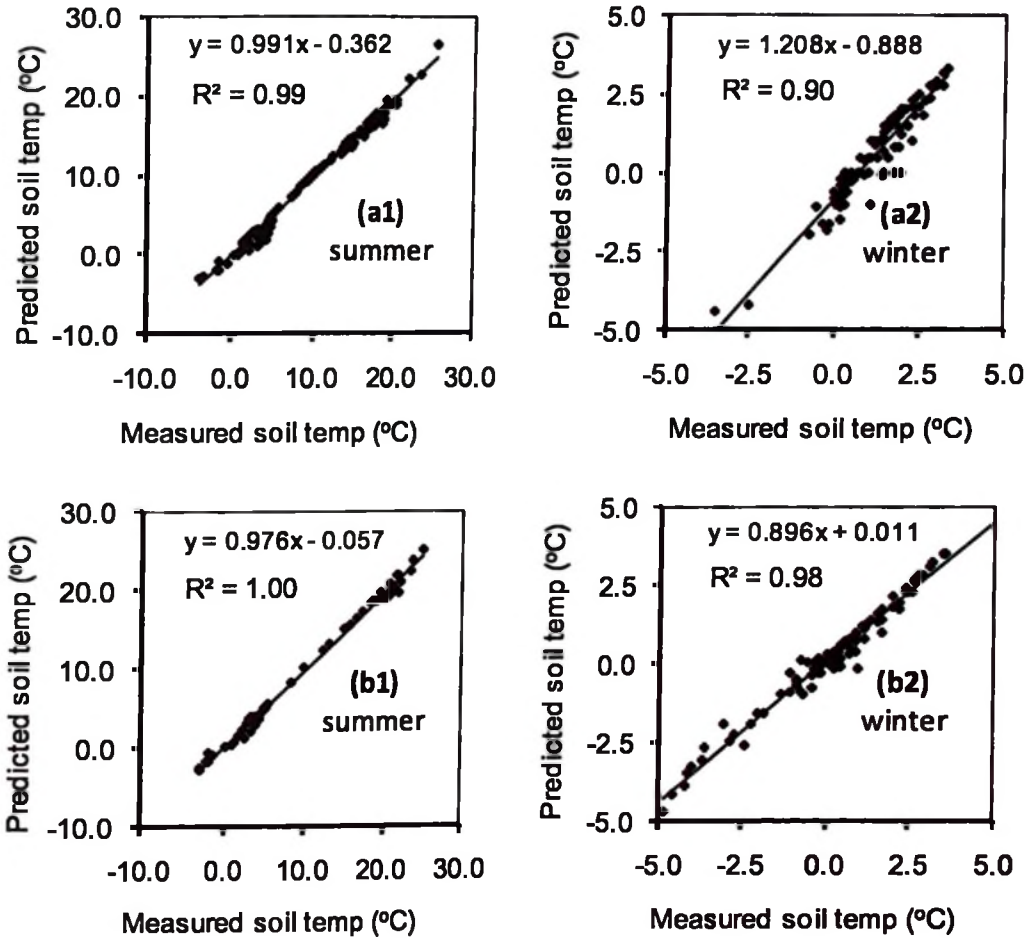

Fig. 7.5. Scatter plots of estimated versus measured soil temperature profile during the summer of 2005 and winter 2006 for: (a) vegetated fields (oats with berseem clover cover crop) and (b) continuous fallow.

Considering the summer against winter simulations, the soil temperature simulations were not affected by season or ground cover for both cases of vegetated and non-vegetated treatments. However, the *MBE* range of -0.02 to -0.66 on all the treatments

indicated a consistent small underestimation of the modeled temperatures compared to the measured soil temperatures, both during the summer and winter seasons (Table 7.4, Fig. 7.3, Fig. 7.5).

During the summer, the R^2 value was 0.99 and *MAE* was 0.5°C on vegetated fields, and 1.00 and 0.5°C, respectively, on the fallow. During the winter, the R^2 and *MAE* values were 0.90 and 0.5°C on vegetated fields, and 0.98 and 0.66°C on the fallow, respectively (Fig. 7.5, Table 7.4). Eitzinger et al. (2000), while validating an improved daily soil temperature sub model, commented that soil temperature deviations of less than 1.0°C indicated a good agreement between the modeled and measured values. The statistical results obtained using the SHAW model indicate that the model performed well and the soil temperature simulation algorithms in the model were not affected by the formation of ice in the soil matrix, as observed in the soil moisture simulations (Table 7.3).

7.5.4 Proposed revisions to the SHAW model

7.5.4.1 Water flow mechanisms in freezing soils. As stated earlier, the SHAW model assumes that a freezing soil behaves similar to a drying unsaturated soil. Hence, water flow in a freezing soil will behave the same as water flow in a drying soil (Flerchinger 1991; Flerchinger 2000). However, considering the role of ice particles in the soil matrix, compared to a drying soil, the water content that is converted to ice in a freezing unsaturated soil continues to remain in the soil matrix. The ice content of a freezing soil is expected to affect the pore size distribution and reduce the effective soil porosity that is available for flow of the unfrozen water, thereby affecting the unsaturated hydraulic conductivity (i.e. frozen water acts as additional 'solids' in the soil matrix). This implies

that contrary to the assumption in the original SHAW model, the soil moisture redistribution in a drying soil may be different from the redistribution in a freezing soil due to the reduction in the frozen soil's effective porosity and pore size distribution.

The assumption that water flow in a freezing soil is similar to water flow in a drying soil leads to the assignment of a lower unsaturated hydraulic conductivity as the soil freezes, and hence, lower migration of liquid water from the unfrozen layers below the freeze front towards the frozen layers above. Seyfried and Murdock (1996), using wintertime simulations, found that an over-estimation of total soil moisture below the freeze front could be a result of most models assuming the unfrozen water in frozen soils to be independent of the total water contents, hence unrealistically estimating the amount of unfrozen water in frozen soils.

To minimize the errors in the SHAW model prediction of soil moisture during the winter, modifications have been proposed to the original equations (Eq. 7.3 and Eq. 7.4 above) used in the SHAW model for relating the soil moisture characteristics and calculating the unsaturated hydraulic conductivity of a freezing soil. The modifications involve the reduction of saturated water content by the amount of ice content in the denominator of Eq. 7.10 as follows:

$$K = K_s \left(\frac{\theta_l}{\theta_s - \theta_i}\right)^{(2b+3)} \tag{7.10}$$

where, K is the unsaturated hydraulic conductivity, K_s is saturated hydraulic conductivity (m s^{-1}), b is pore size distribution index, θ_l is the unfrozen soil water content at a given time (m^3 m^{-3}), θ_i is the ice content at a given time (m^3 m^{-3}) and θ_s is the saturated soil water content (m^3 m^{-3}). As the soil freezes, both the numerator and the

denominator of Eq. 7.10 decrease by the same amount to account for the frozen water. Therefore, as the water continues to freeze the decrease in the ratio and hence the unsaturated hydraulic conductivity will not be as fast as it was presented in the original SHAW model. The Brooks and Corey (1966) equation is used to relate the soil moisture characteristic as follows:

$$\varphi = \varphi_e \left(\frac{\theta_l}{\theta_s - \theta_l}\right)^{-b} \tag{7.11}$$

where, φ_e is air entry potential (m) and φ is soil matric potential (m).

Table 7.5. Comparison of winter model predictions of soil moisture on vegetated plots and continuous fallow treatments using the original and the revised SHAW models in the 2005-2007 seasons.

Farm	Management	SHAW Model type	Statistical parameters							
				Relative error measures*		Absolute error measures**				
			N	R^2	d	MAE	MBE	ME	RMSE	RMSE (%)
Vegetated	plots	Original	116	0.67	0.89	0.04	-0.02	0.16	0.06	17.54
		Revised	116	0.78	0.94	0.03	-0.01	0.11	0.05	13.56
Continuous	Fallow	Original	109	0.52	0.84	0.05	0.00	0.20	0.07	19.72
		Revised	109	0.71	0.91	0.03	0.00	0.17	0.05	13.75

* The parameters are: N = number of observations, R^2 = coefficient of determination, and d = index of agreement.

** The parameters are: *MAE*= mean absolute error, *MBE* = mean bias error, *ME* = maximum error, and *RMSE* = root mean square error.

The Eqs. 7.10 and 7.11 were incorporated in the original source code of the SHAW model and simulations of soil moisture during the winter were performed using the revised SHAW model. Table 7.5 presents a summary of statistical comparisons of wintertime soil moisture predictions using the original and the revised SHAW models. The scatter plots of the measured and predicted soil moisture pooled from the 2006 and 2007 winter seasons are presented in Fig. 7.6.

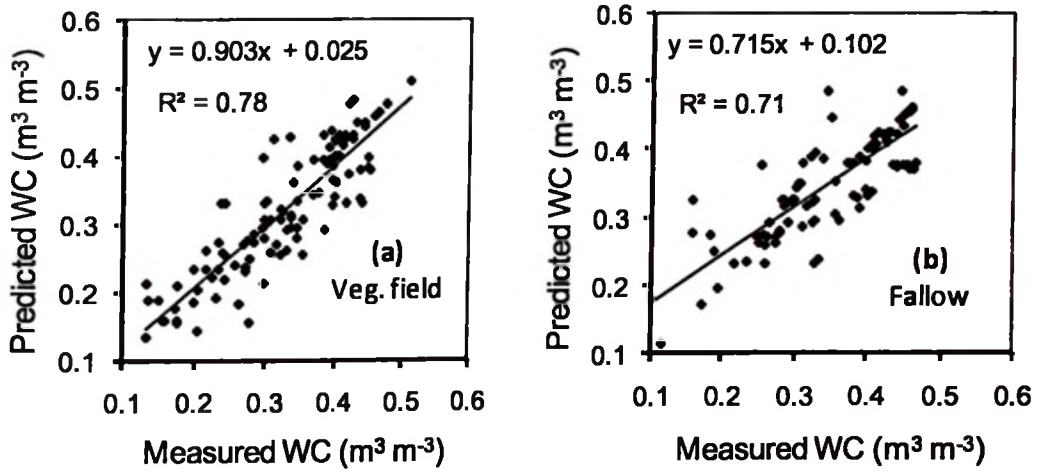

Fig. 7.6. Scatter plots of the measured vs. estimated soil moisture, predicted using the revised SHAW model during the winter of 2006 and 2007 for: (a) vegetated fields (oats with berseem clover cover crop) and (b) continuous fallow treatments.

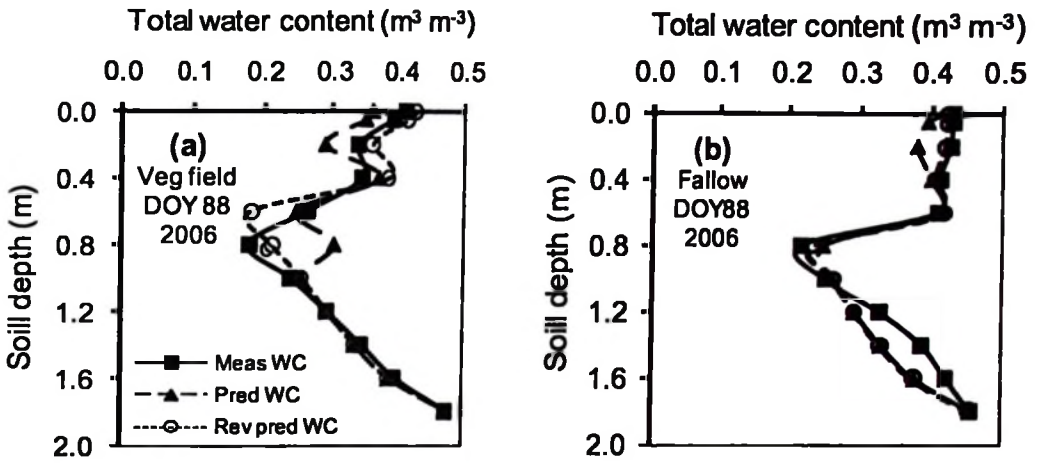

Fig. 7.7. Comparison of predicted soil water content from the original and revised (rev) SHAW model for: (a) vegetated fields (oats with berseem clover cover crop) and (b) continuous fallow treatments on March 29, 2006.

Improvement in the predictions were observed both in the vegetated field (R^2 = 0.78 vs. 0.67; *RMSE* = 13.56% vs. 17.54%) and in the fallow (R^2 = 0.71 vs. 0.52; *RMSE* = 13.75% vs. 19.72%) (Table 7.5 and Fig. 7.6). Improvements were also observed at specific depths of freeze front and on the under-prediction of total soil moisture above the freeze front (Fig. 7.7). On March 29, 2006, the differences in total soil moisture on the vegetated field (Fig. 7.7a) and on the fallow (Fig. 7.7b) were 0.01 to 0.04 m^3 m^{-3} both below and above the freeze front.

Using the proposed equations, when the soil is frozen and the ice content is above zero, the unsaturated hydraulic conductivity of the freezing soil will be higher than in the original model, and more water will move from the unfrozen soil layers below the freezing front towards the frozen soil layers above. The upward water migration from

below the freeze front will lead to lower soil moisture below the freeze front and higher moisture content above the freeze front as the winter progresses. Hence, the use of the proposed equations (Eq. 7.10 and Eq. 7.11) to account for the decrease in the effective porosity of the soil due to additional 'solid' ice improved the wintertime simulations.

Jin and Sands (2002) also observed poor simulations of DRAINMOD model in simulating wintertime hydrologic processes. Modifications of the unsaturated hydraulic conductivity and infiltration rate, taking into account the ice content of the soil, helped to improve the simulations of the DRAINMOD model (Jin and Sands 2002). Studies on soil moisture migrations due to freezing were also performed by Nassar et al. (2000). However, this study was limited to laboratory soil columns, and did not involve comparison with actual field measurement of unfrozen and total water contents.

7.5.4.2 Calculation of the solar azimuth angle in the SHAW model. The total incoming solar radiation is separated in the SHAW model into the direct and diffuse radiation. To account for the solar radiation calculations, the algorithm in the subroutine *SOLAR* of the original source code involved calculation of the sun's angle from the due north (the solar azimuth angle) using the following sine equation (Flerchinger 2000):

$$AZM = \sin^{-1}\{-\cos(\delta) \times \sin(h_s)/\cos(\alpha)\} \quad (7.12)$$

where, AZM is the solar azimuth angle, δ is the sun declination, h_s is the sun's hour angle at present time, and α is the solar altitude angle. The sine algorithm failed to calculate the AZM values on April 12 at 0700 h for both the 2006 and 2007 simulation years. The hourly simulations of the executable file generated from the source code were stopping on DOY 102 and hour 0600. The simulations were being performed on northern

region located at 49.5°N, 98.02 °W, and 262 m a.m.s.l. To overcome this problem the cosine algorithm for calculating the solar azimuth angle was used as shown in Eq. 7.13 below (Allen et al. 2002):

$$AZM = \cos^{-1}\left\{\frac{\sin(\alpha)\times\sin(\Phi)-\sin(\delta)}{\cos(\alpha)\times\cos(\Phi)}\right\} \quad (7.13)$$

where, Φ is the latitude of the area. Other parameters are similar to those of Eq. 7.12. The cosine algorithm allowed the simulation past the DOY 102, 0700 h without failure. The 0700 h on April 12 at this Northern latitude is the approximate time of sunrise with an azimuth at sunrise of positive angle greater than 90°. The inverse sine function may incorrectly give angles between 0 and ±90 even for values that were supposed to be more than 90°, since both the sine of angles above 90 (90°-180°) and below 90 (0°-90°) are positive. The returned angles between -90° and +90° causes failure of the inverse sine function to distinguish between the north and south Azimuths. The inverse cosine function on the other hand returns angles between 0° and 180°, but does not distinguish between east and west azimuths (G. N. Flerchinger, Research Hydraulic Engineer, Northwest Watershed Research Centre, USDA-ARS, Boise, ID, personal communication, May 19, 2008). Hence, the cosine-based *SUBROUTINE SOLAR* was revised further to account for the East-West azimuths correction of the inverse cosine function (G. N. Flerchinger, personal communication, May 19, 2008).

7.5.5 Simulations of frost depth

The SHAW model was used to simulate the frost depth, and the accumulation of snow at the soil surface. The predicted values of frost depth were compared with the measured values obtained between the fall of 2005 and spring of 2006 from both the

original and the revised codes. Figure 7.8 presents a comparison between the predicted frost depths using the original and the revised SHAW models. The predicted values were compared against the observed values for the vegetated fields and the continuous fallow. The SHAW model better predicted the depth and timing of frost on vegetated fields compared to the fallow. Using the original SHAW Model, the differences between the measured and predicted frost depths ranged between 0.02 to 0.15 m (overestimation) in oats with berseem clover (Fig. 7.8a), while it was -0.04 to -0.25 m on the fallow (Fig. 7.8b). The model underestimated the depth of freeze front in the fallow treatment. Better predictions of frost depth were observed using the revised model compared to the original model.

The underestimation of frost depth in the fallow could also be a result of problems associated with predictions of soil moisture in a freezing soil as stated earlier. Using the revised code, the predicted frost depth compared well with the measured depth. The differences in the oats with berseem clover treatment ranged between 0.02 to 0.05 m. In the fallow, the maximum difference was reduced to -0.09 m. A poor simulation of one component of the hydrological processes such as the redistribution of soil moisture or snow depth in a freezing soil can lead to inaccurate simulation of other related parameters such as the depth and advancement of the soil frost (Kennedy and Sharratt 1998).

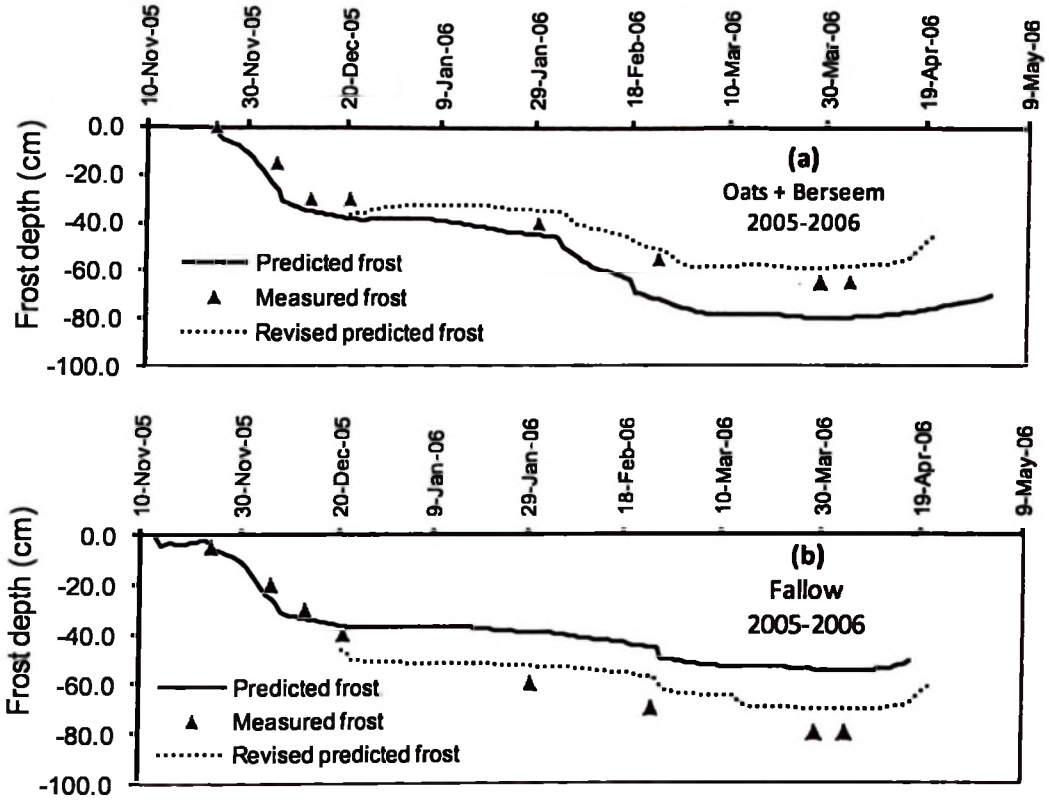

Fig. 7.8. Comparison of the measured and simulated frost depths from the original and revised Simultaneous Heat and Water (SHAW) models for: (a) vegetated fields (oats with berseem clover cover crop) and (b) continuous fallow treatments in the 2005-2006 seasons. Time Domain Reflectometry (TDR) measurements were used to determine the measured frost depth.

7.5.6 Year-round predictions of soil moisture

The year-round simulations performed using the revised SHAW model gave an indication of the soil moisture status and redistribution during the fall freeze-up, winter, and spring snowmelt. Figure 7.9 presents the soil moisture predictions at different depths

in the oats with berseem clover cover crop and the oats alone treatments from the fall in September 2005 through the summer in July 2006.

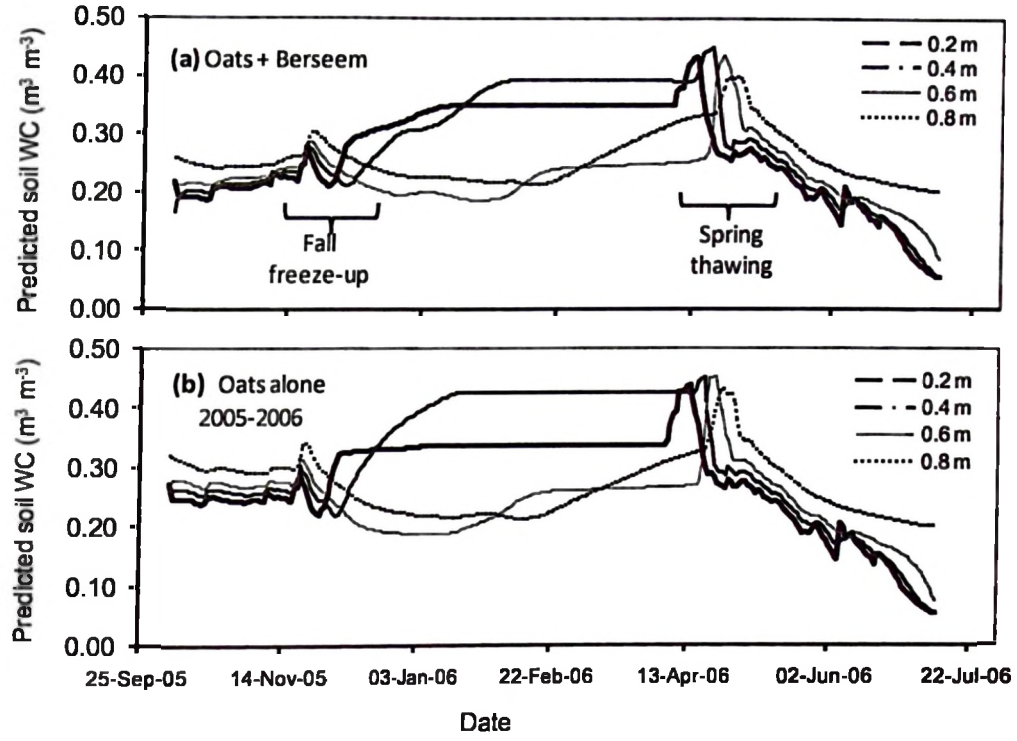

Fig. 7.9. Revised SHAW model predictions of total soil moisture at 0.2- to 0.8-m soil depths in: (a) oats with berseem clover cover crop and (b) oats alone treatments during the 2005 – 2006 season.

A sharp increase in total soil moisture during the fall in mid to late November and early December indicated infiltration from early snowmelt when the soil was still unfrozen (Figs. 7.9a and 7.9b). A similar rise was observed during spring snowmelt and soil thawing in late March and early April 2006. The simulations also gave an indication of the soil moisture status at various depths at the beginning of the growing season between May and June after the spring snowmelt. For example on May 1, 2006, the predicted total soil moisture at 0.2, 0.4, 0.6 and 0.8 m soil depths were 0.26, 0.29, 0.30

and 0.39 for the previous oats with berseem clover cover crop and 0.27, 0.31, 0.32, and 0.41 for the previous oats alone treatment, respectively (Fig. 7.9). The predicted total soil moisture in the 0.1 to 0.9 m soil depth was 5% lower (0.31 vs. 0.33 $m^3 m^{-3}$) in May 2006 in the previous cover crop treatment compared to the previous oats alone treatment. Results on lower soil moisture during spring on previous cover crop treatment compared to previous no cover treatment have also been reported in our previous studies on the influence of previous season cover crop (chapter 5 and 6; Kahimba et al. 2007).

Based on the results of this study, the SHAW model gave a very good indication of the soil temperature and soil moisture status during fall freeze up and spring soil thawing. The model also gave an indication of the available soil moisture at the beginning of the next growing season. The SHAW model is a multidisciplinary model that simulates many other hydrological processes. Hence, more validations under different weather conditions need to be done to assess the effect of the proposed changes on other components of the model. With the proposed improvements for winter soil moisture simulations in the original source code, the SHAW model could be used as a better tool for predicting year-round hydrological processes in seasonally frozen agricultural soils.

7.6. Summary and Conclusions

A physically-based Simultaneous Heat and Water (SHAW) model was used for simulating year-round hydrologic processes in seasonally frozen agricultural soils. The model was used to predict the soil temperature, amount and redistribution of profile soil moisture, and the depth and timing of frost at the Ian N. Morrison Research Farm of the University of Manitoba in Carman, Manitoba. The simulated soil temperature compared well with the measured data, with model efficiency ranging from 0.96 to 0.99. The accuracy of the model on soil temperature predictions were not affected by ground covers during both the summer and winter seasons.

The soil moisture predictions were affected by both the ground cover conditions and season of the year. Better simulations of soil moisture were observed during the summer and fall seasons when soil was unfrozen (R^2 = 0.90-0.92; *RMSE* = 9.1-12.0%) compared to winter to spring times when the soil was frozen/partly frozen (R^2 = 0.52-0.67; *RMSE* = 17.5-19.7%). During the summer the model showed better simulations of soil moisture in the fallow (R^2=0.92; *d*=1.0; *RMSE*=9.1) compared to the vegetated treatments (R^2 = 0.90; *d*=0.97; *RMSE*=12.0%). During the winter, better simulations of soil moisture were observed in the vegetated treatment, which had shallower depth of frozen soil layer (R^2 = 0.67 vs. 0.52; *RMSE* = 17.5 vs. 19.7) compared to the continuous fallow treatment, which had a deeper layer of frozen soil. The SHAW model over-predicted by 0.02 to 0.10 $m^3 m^{-3}$ the amount of total soil moisture below the freeze front and under-predicted by 0.02 to 0.05 $m^3 m^{-3}$ the soil moisture in the upper frozen layers. Exclusion of the ice content of freezing soil in the SHAW model equations used for relating the soil moisture characteristic to the unsaturated hydraulic conductivity of

freezing soil were identified as potential sources of errors that led to poor performance of the soil moisture predictions during the winter. New equations were proposed that account for the reduced effective porosity of the soil due to ice content of a freezing soil. Using the revised equations the wintertime soil moisture simulations were improved for both the vegetated fields (R^2 = 0.78 vs. 0.67; *RMSE* = 13.56% vs. 17.54%) and in the fallow (R^2 = 0.71 vs. 0.52; *RMSE* = 13.75% vs. 19.72%).

The SHAW model was used to predict the depth and timing of frost. Better simulations of frost depth were observed in the vegetated treatment of oats with berseem clover cover crop (difference 0.02 – 0.10 m) compared to the fallow. The model under-predicted the frost depth in the fallow by 0.04 to 0.25 m during the winter of 2006. After the revisions, the difference in maximum frost depth was reduced to 0.05 m instead of 0.1 m in the vegetated fields, and 0.09 instead of 0.25 m in the fallow. The model was also used to predict soil moisture status at the beginning of the subsequent growing season. By May 1, 2008 the total soil moisture in the 0.1 to 0.9 m soil depth was 5% lower (0.31 vs. 0.33 $m^3 m^{-3}$) in the previous cover crop treatment compared to the previous oats alone treatment.

This paper presents the potential for using the SHAW model as a tool for predicting year-round hydrological processes such as soil moisture, soil temperature, and depth and timing of frost in seasonally frozen agricultural soils. It also presents areas of the model that need improvement for better simulations of winter time soil moisture, and how the revised model could potentially be used to predict the soil moisture status as a function of depth during spring thawing, and the availability of soil moisture at the beginning of the growing season.

8. CONCLUSIONS

1. Time domain reflectometry (TDR) miniprobes (probe lengths 30-50 mm) are more practical for field soil moisture measurements at depth intervals of 100 mm or less. Calibration of the TDR miniprobes for field measurement needs to be done along with the type and length of the extension cable to be used in the field. For each probe rod length, diameter, and wire (rod) configuration, different cable types will give a different optimum extension cable length. For the miniprobes 1.6 mm diameter, 35 mm long, and 3-wire configuration used in this study, the optimum length of the RG-58 50 Ω coaxial cable was found to be 40.0 m.
2. The accuracy of the TDR method in the field is affected by variation in soil temperature. Therefore, field measurements of soil moisture using TDR need to be adjusted to account for temperature effects. In this study, a temperature calibration method was developed for making temperature correction of the field-measured TDR soil moisture.
3. The TDR method is one of the most accurate and practical methods of measuring unfrozen soil water content in frozen and partly frozen soils. A combination of TDR and neutron moisture meter (NMM), which measures total water content, enabled partitioning of the total water content into frozen and unfrozen states. The two methods combined together give a practical way of studying field soil moisture during the fall through spring seasons in seasonally frozen agricultural soils.
4. Cover crop farm management practices have both agronomic and hydrologic advantages and disadvantages. Cover crops such as berseem clover when planted

with the main crop in the same season, will help to reduce excess soil moisture that would otherwise affect the performance and yield of the main crop. However if there is less available root-zone soil moisture, especially later in the growing season, the cover crop will compete with the main crop for available moisture causing soil moisture stress. The soil moisture stress will affect crop growth performance later in the season.

5. The residual effects of cover crop planted during spring influence response of the soil to freeze-thaw during fall freeze-up. The effects also influence soil moisture redistribution during winter, and thereafter, the response of the soil to spring thawing. Compared to non-cover-cropped plots, soils in cover-cropped plots will have less moisture at the onset of fall freeze-up. It will also have milder winter soil temperatures, freeze to a shallower depth, and accumulate less total soil moisture during the winter. As a result, the cover-cropped plots will thaw earlier in spring and allow more percolation of melt water below the root zone.
6. The residual effects of berseem clover cover crop of one season affect soil moisture availability at the beginning of the subsequent growing season. If the subsequent season turns out to be drier, the residual effect of the previous season cover crop will cause lower soil moisture during the next growing season. The reduced soil moisture will potentially cause poor growth performance resulting in a significantly lower crop yield during the subsequent season. Therefore, crop rotation management involving cover crop should consider soil moisture availability for main crop and the cover crop to avoid soil moisture stresses associated with presence of cover crops.

7. The Simultaneous Heat and Water (SHAW) model was used to simulate year-round hydrologic conditions in seasonally frozen agricultural soils. While the model simulated soil water content and soil temperature during the summer well, simulations of soil moisture were less accurate during the winter when the soil was frozen. Generally the model over estimated soil moisture below freeze front and underestimated the soil moisture above the freeze front. The main contributing factor was identified to be an assumption that water flow in freezing soil is similar to water flow in drying soil, without accounting for the reduction in porosity of freezing soil due to frozen water. Presence of ice affects unfrozen water movement in a freezing soil. Hence, equations for unsaturated hydraulic conductivity and soil moisture characteristic of freezing soil have to take into account the space occupied by freezing (ice) water.
8. During the summer better accuracy of the SHAW model was observed in a fallow compared to vegetated fields. This could be attributed to cumulative errors associated with establishment of plants' physical characteristics such as LAI, biomass, and rooting depths. During the winter, the fallow experienced the highest overestimation of soil moisture below the freeze-front compared to vegetated fields. This was also because the bare field (fallow) froze to a greater extent with more ice content in the soil profile than the vegetated fields. Hence, more water migrated from unfrozen to a thicker frozen soil layer in the fallow compared to the vegetated fields.
9. In this study, areas of the model that needed improvement were identified and the model source code was modified to account for decreased effective porosity of the

soil due to presence of ice content in freezing soil. The amended equations were incorporated in the water flux algorithms of the SHAW program source code to account for water migrations above and below the freeze front during the winter. The revised SHAW model could be used as a better management tool for predicting available soil moisture, soil temperature, and depth and timing of frost in areas such as the Ian N. Morrison Research farm of the University of Manitoba in Carman, Manitoba, that experience seasonal soil freezing and thawing.

10. The revised SHAW model was used to predict year-round hydrologic parameters, response of the soil to spring thawing, and soil moisture availability at the beginning of the subsequent growing season. Therefore, the SHAW model could be used as a better tool for studying year-round hydrologic processes in areas such as the Northern Great Plains of Canada, experiencing seasonal soil freezing and thawing.

9. RECOMMENDATIONS FOR FUTURE RESEARCH

The following are the recommendations for future work

1. The TDR miniprobes used in the field were permanently placed into the soil and stayed in place year-round from summer in August 2005 to September 2007. Long-term performance of field-installed TDR miniprobes needs to be assessed. This could involve assessment of physical damage to probes, coaxial cable embedded in the soil, and thermocouples. In addition, areas experiencing seasonal soil freezing and thawing are subject to frost heave during winter freeze-up. The frost heave effects over repeated years may result in vertical displacement of field installed TDR miniprobes. The NMM measurement depths are defined and updated with respect to existing ground level. Assessment needs to be done on changes in vertical depth of the probe location over time due to frost heave. This may involve taking profile leveling during first installation from a permanent bench mark to the probes locations, and repeating the level measurement every year after soil thawing to track if there are significant vertical changes in the probes' positions.
2. The 35-mm TDR miniprobes and the RG-58 50 Ω coaxial cable used in this experiment were calibrated in the laboratory to establish optimum extension cable length for given probe rods diameter and configuration. Future research on this aspect needs to consider other types of probe rods diameters and configurations, and different types of cable lengths.
3. Using TDR multiplexers that connects multiple probes and data loggers for continuous measurement of soil moisture will be a better way to study real-time

situations in the field, compared to measurements at specific dates and times. The real time data acquisition accompanied with remote sensing will also help to remotely acquire data that are continuous or at a fixed defined interval. Such kind of data acquisition system will minimize costs of field visit and difficulties associated with winter field accessibility to different areas of the field.

4. Avoiding field accessibility during the winter by remote data acquisition can also allow the use of experimental designs that involve treatments from multiple blocks and multiple replications for all the parameters. This will help avoid the limitation of having to design an experiment that is limited to an area, and with replications that allow manual data acquisition within the same day.
5. Different types of cover crop need to be used in order to generalize the influence of cover crop and establish exceptions based on the varieties of the cover crop used. In this study berseem clover (*Trifolium alexandrium* L.) cover crop was used. The assessment of the crop performance may also need to consider other aspects of plant growth such as root length and biomass, timing of flowering and maturity, and grains quality as affected by soil moisture availability and the use of cover crop.
6. More replicates need to be done on each block instead of doing replications within each treatment in the same blocks. This could be achieved if TDR probes are multiplexed to facilitate more data collection within a single day.
7. Further verification of the revised SHAW model needs to be done on other locations with different weather conditions. The verification sites should experience seasonal soil freezing and thawing.

8. The SHAW model simulates many other hydrologic parameters. Further study needs to be done to determine how the revisions made on the winter-time soil moisture simulations might affect other hydrologic parameters that are simulated by the model. Examples are evapotranspiration, salts and vapor flux, root water uptakes, leaf water potential, and the surface energy balance.

REFERENCES

Allen, R.G., L.S. Preira, D. Raes and M. Smith. 2002. Crop Evapotranspiration: Guidelines for computing crop water requirements. FAO Irrigation and Drainage Paper No. 56. Rome, Italy: FAO, Water Development and Management Unit.

Amer, S.A., T.O. Keefer, M.A. Weltz, D.C. Goodrich and L.B. Bach. 1994. Soil moisture sensors for continuous monitoring. *Water Resources Bulletin* 30: 69-83.

Andraski, T.W. and L.G. Bundy. 2005. Cover crop effects on corn yield response to nitrogen on an irrigated sandy soil. *Agronomy Journal* 97(4): 1239-1244.

Aspinall, D., P.B. Nicholls and L.H. May. 1964. The effects of soil moisture stress on the growth of barley. I: Vegetative development and grain yield. *Australian Journal of Agricultural Research* 15(5): 729-745.

Baker, J.M. 2001. Infiltration into frozen soils. In *International Symposium on Snowmelt Erosion and Related Problems.* Oslo, Norway. March 28-30.

Baker, J.M. and R.R. Allmaras. 1990. System for automating and multiplexing soil moisture measurement by time-domain reflectometry. *Soil Science Society of America Journal* 54(1): 1-6.

Bargar, B., J.B. Swan and D. Jaynes. 1999. Soil water recharge under uncropped ridges and furrows. *Soil Science Society of America Journal* 63(5): 1290-1299.

Blonquist, J.M. Jr., S.B. Jones and D.A. Robinson. 2005. Standardizing characterization of electromagnetic water content sensors: Part 2. Evaluation of seven sensing systems. *Vadose Zone Journal* 4(4): 1059-1069.

Bonfil, D. J., I. Mufradi, S. Klitman and S. Asido. 1999. Wheat grain yield and soil profile water distribution in a no-till arid environment. *Agronomy Journal* 91(3): 368–373.

Bootsma, A. and D.M. Brown. 2002. Freeze protection methods for crops. Factsheet. Ottawa, ON: Ministry of Agriculture, Food and Rural affairs. http://www.omafra.gov.on.ca/english/crops/facts/85-116.html (2008/02/22).

Boquet, D.J., R.L. Hutchinson and G. A. Breitenbeck. 2004. Long-term tillage, cover crop, and nitrogen rate effects on cotton: Yield and Fiber Properties. *Agronomy Journal* 96(5): 1436-1443.

Bourgeois, L. and M.H. Entz. 1996. Influence of previous crop type on yield of spring wheat. Analysis of commercial field data. *Canadian Journal of Plant Science* 76(3): 457-459.

Brendan, H.G. 2003. Comparison of techniques for measuring the water content of soil and other porous media. Unpublished M.Sc. thesis. New South Wales, Australia: Department of Agricultural Chemistry and Soil Science, University of Sydney.

Brooks, R.H. and A.T. Corey. 1966. Properties of porous media affecting fluid flow. *Journal of Irrigation and Drainage* 92(1): 61-88.

Bullock, M.S., W.D. Kemper and S.D. Nelson. 1988. Soil cohesion as affected by freezing, water content, time and tillage. *Soil Science Society of America Journal* 52(3): 770-776.

Calvino, P.A., F.H. Andrade and V.O. Sadras. 2003. Maize yield as affected by water availability, soil depth, and crop management. *Agronomy Journal* 95(2): 275-282.

Campbell Scientific, Inc. 2001. Reducing TDR probe rod length to improve water content measurements in soils with high electrical conductivity. Logan, UT: Campbell Scientific Inc, Application note (435) 753-2342.

Cavers, C. and J. Heard. 2001. Managing crops for excess water stress. In *Proceedings 2nd Annual Manitoba Agronomists Conference*, 27-32. Winnipeg, Manitoba: University of Manitoba.

Charbeneau, J.R. 2000. *Groundwater Hydraulics and Pollutant Transport.* Upper Saddle River, NJ: Prentice Hall, Inc.

Cruse, R.M., R. Mier and C.W. Mize. 2001. Surface residue effects on erosion of thawing soils. *Soil Science Society of America Journal* 65(1): 178-184.

Dabney, S.M. 1998. Cover crop impacts on watershed hydrology. *Soil and Water Conservation* 53(3): 207–213.

Dabney, S.M., J.A. Delgado and D.W. Reeves.2001. Using winter cover crops to improve soil and water quality. *Communications in Soil Science and Plant Analysis* 32(7&8): 1221–1250.

Dahan, O., E.V. McDonald and M.H. Young. 2003. Flexible time domain reflectometry probe for deep vadose zone monitoring. *Vadose Zone Journal* 2(2): 270-275.

DeGaetano, A.T., D.S. Wilks and M.D. Cameron. 1996. A physically based model for soil freezing in humid climates using air temperature and snow cover data. *Journal of Applied Meteorology* 35(6): 1009-1027.

DeGaetano, A.T., M.D. Cameron and D.S. Wilks. 2000. Physical simulation of maximum seasonal soil freezing depth in the United States using routine weather observations. *Journal of Applied Meteorology* 40(3): 546-555.

Deutsch, A., G. Arjavalingam, C.W. Surovic and A.P. Lanzetta. 1994. Performance limits of electrical cables for intrasystem communication. *International Business Machines Journal of Research Development* 38 (6): 659-673.

Eitzinger, J.W., J. Patron and M. Hartman. 2000. Improvement and validation of a daily soil temperature sub model for freezing/thawing periods. *Soil Science* 165(7): 525-534.

Entz, M.H., V.S. Baron, P.M. Carr, D.W. Meyer, S.R. Smith Jr. and W.P. McCaughey. 2002. Potential of forages to diversify cropping systems in the Northern Great Plains. *Agronomy Journal* 94(2): 240-250.

Environment Canada. 2007. Canadian Climate Normals 1991-2005. http://www.climate.weatheroffice.ec.gc.ca/Welcome_e.html (2007/12/15).

Ess, D.R., D.H. Vaughan and J.V. Perumpral. 1988. Crop residue and root effects on soil compaction. *Transactions of the ASAE* 41(5): 1271-1275.

Evett, S.R. 1994. TDR-temperature arrays for analysis of field soil thermal properties. In *Proceedings of the Symposium on Time Domain Reflectometry in Environmental, Infrastructure, and Mining Applications*, 320-327. Evanston, IL. September 7-9.

Evett, S.R. 2000a. Some aspects of time domain reflectometry (TDR), neutron scattering (NS), and capacitance methods of soil water content measurement. In *International Atomic Energy Agency Symposium* 59(1137): 5-49. Vienna, Austria: International Atomic Energy Agency.

Evett, S.R. 2000b. The TACQ computer program for automatic time domain reflectometry measurements: I. Design and operating characteristics. *Transactions of the ASAE* 43(6): 1939 – 1946.

Evett, S.R. 2000c. The TACQ computer program for automatic time domain reflectometry measurements: II. Waveform interpretation methods. *Transactions of the ASAE* 43(6): 1947 – 1956.

Evett, S.R. 2003a. Soil water measurements by neutron thermalization. In *Encyclopedia of Water Science,* ed. B. A. Stewart and T. A. Howell, 889-893. New York, NY: Marcel Dekker, Inc.

Evett, S.R. 2003b. Soil water measurement by time domain reflectometry. In *Encyclopedia of Water Science,* eds. B.A. Stewart and T.A. Howell, 894-898. New York, NY: Marcel Dekker, Inc.

Evett, S.R. and J.L. Steiner. 1995. Precision of neutron scattering and capacitance type soil water content gauges from field calibration. *Soil Science Society of America Journal* 59(4): 961-968.

Evett, S.R., J.P. Laurent, P. Claude and C. Hignett. 2002. Neutron scattering, capacitance, and TDR soil water content measurements compared on four continents. In *Proceedings 17th World Congress of Soil Science Symposium* 59(1021): 1–10. Bangkok, Thailand. August 14–21.

Fernandez, D.P., A.R.H. Goodwin, E.W. Lemmon, J.M.H. Levelt Sengers and R.C. Williams. 1997. A formulation for the static permittivity of water and steam at temperatures from 238 to 873 K at pressures up to 1200 MPa, including derivatives and Debye-Hückel coefficients. *Journal of Physical and Chemical Reference Data* 26(4): 1125-1166.

Fischer, R.A. and G.D. Kohn. 1966. The relationship of grain yield to vegetative growth and post-flowering leaf area in the wheat crop under conditions of limited soil moisture. *Australian Journal of Agricultural Research* 17(3): 281-295.

Flerchinger, G.N. 1991. Sensitivity of soil freezing simulated by SHAW model. *Transactions of the ASAE* 34(6): 2381-2389.

Flerchinger, G.N. 2000. The simultaneous heat and water (SHAW) model: Technical documentation. Technical Report NWRC 2000-09. Boise, Idaho: USDA Agricultural Research Service, Northwest Watershed Research Centre. [Online] available: http://www. Nwrc.ars.usda.gov/download/shaw/ShawDocumentation [November 15, 2007].

Flerchinger, G.N. and K.E. Saxton. 1989a. Simultaneous heat and water model of a freezing snow-residue-soil system I: Theory and development. *Transactions of the ASAE* 32(2): 565-571.

Flerchinger, G.N. and K.E. Saxton. 1989b. Simultaneous heat and water model of a freezing snow-residue-soil system II. Field verification. *Transactions of the ASAE* 32(2): 573-578.

Flerchinger, G.N. and F.B. Pierson. 1991. Modeling plant canopy effects on variability of soil temperature and water. *Agricultural Forest Meteorology* 56(3): 227-246.

Flerchinger, G.N., C.L. Hanson and J.R. Wright. 1996. Modeling evapotranspiration and surface energy budgets across a watershed. *Water Resources Research* 32(8): 2539-2548.

Flerchinger, G.N., T.J. Sauer and R.A. Aiken. 2003. Effects of crop residue cover and architecture on heat and water transfer at the soil surface. *Geodema* 116(1-2): 217-233.

Flerchinger, G.N., W. Xiao and Q. Yu. 2006. Evaluation of the SHAW model for within-canopy radiation exchange. ASABE Paper No. 062011. Portland, Oregon: ASABE.

Fuller, R. and T. Blankenship. 2002. *Building a Cisco Wireless LAN*, 1st Edition, Rockland, MA: Syngress Publishing, Inc.

Gong, Y., Q. Cao and Z. Ssun. 2003. The effects of soil bulk density, clay content and temperature on soil water content measurement using time-domain reflectometry. *Hydrological Processes* 17(18): 3601-3614.

Gray, D.M., D.I. Norum and J.M. Wigham. 1973. Infiltration and the physics of flow of water through porous media. In *Handbook on the Principles of Hydrology*, ed. D.M. Gray, 5.1-5.58. Port Washington, NY: Water Information Centre, Inc.

Grønsten, H.A. 2001. Runoff event simulation using WEPP on two Norwegian arable soils. *International Symposium on Snowmelt Erosion and Related Problems.* Oslo, Norway. March 28-30.

Guaraglia, D.O., J.L. Pousa and L. Pilan. 2001. Predicting temperature and heat flow in a sandy soil by electrical modeling. *Soil Science Society of America Journal* 65(4): 1074–1080.

Gupta, S.C., J.K. Radke, W.E. Larson and M.J. Shaffer. 1982. Predicting temperatures of bare-and residue-covered soils from daily maximum and minimum air temperatures. *Soil Science Society of America Journal* 46(2): 372–376.

Gupta, S.C., W.E. Larson and R.R. Allmaras. 1984. Predicting soil temperature and soil heat flux under different tillage-surface residue conditions. *Soil Science Society of America Journal* 48(2): 223–232.

Gupta, S.C., J.K. Radke, J.B. Swan and J.F. Moncrief. 1990. Predicting soil temperatures under a ridge-furrow system in the U.S. Corn Belt. *Soil & Tillage Research* 18(2): 145-165.

Hansson, K., J. Simunek, M. Mizoguchi, L. Lundin and M. van Genuchten. 2004. Water flow and heat transport in frozen soil: Numerical solution and freeze-thaw applications. *Vadose Zone Journal* 3(2): 693-704.

Heimovaara, T.J. 1993. Design of triple-wire time domain reflectometry probes in practice and theory. *Soil Science Society of America Journal* 57(6): 1410-1417.

Herkelrath, W.N. and G.N. Delin. 1999. Long term monitoring of soil moisture in a harsh climate using reflectometer and TDR probes. In *Proceedings of the Second International Symposium and Workshop on Time Domain Reflectometry for Innovative Geotechnical Applications,* 262-272. Evanston, Illinois: Infrastructure Technology Institute, Northwestern University.

Hillel, D. 2004. *Introduction to Environmental Soil Physics.* Amsterdam, Holland: Elsevier Academic Press.

Hook, W.R. and N.J. Livingston.1996. Errors in converting time domain reflectometry measurements of propagation velocity to estimates of soil water content. *Soil Science Society of America Journal* 59(1): 35-41.

Hubscher, R.A., D. Or, J.M. Wraith and B. Smith. 1996. Win_TDR users guide. Version 1.0. Logan, Utah: Plants, Soils and Biometeorology Department, Utah State University.

Hymer, D.C., M.S. Moran and T.O. Keefer. 2000. Soil water evaluation using a hydrologic model and calibrated sensor network. *Soil Science Society of America Journal* 64(1): 319 –326.

Janowicz, R.J, D.M. Gray and J.W. Pomeroy. 2003. Spatial variability of fall soil moisture and spring snow water equivalent within a mountainous sub-arctic watershed. *In Proceedings of the 60th Eastern Snow Conference,* 127-139. Sherbrooke, QC. June 4-6.

Jansson, P.E. 1991.SOIL: simulation model for soil water movement and heat conditions. Report 165. Uppsala, Sweden: Swedish University of Agricultural Science, Department of Soil Science.

Jin, C.X. and G.R. Sands. 2003. The long-term field-scale hydrology of subsurface drainage systems in a cold climate. *Transactions of the ASAE* 46(4): 1011-1021.

Jones, S.B. and D. Or. 2002. Thermal and geometrical effects on bulk permittivity of porous mixtures containing bound water. *Journal of Non-Crystalline Solids* 305(1-3): 247-254.

Jones, S.B., J.M. Wraith and D. Or. 2002. Time domain reflectometry measurement principles and applications. *Hydrological Processes* 16(1): 141–153.

Joyce, B.A., W.W. Wallender, J.P. Mitchell, L.M. Huyck, S.R. Temple, P.N. Brostrom and T. C. Hsiao. 2002. Infiltration and soil water storage under winter cover cropping in California's Sacramento valley. *Transactions of the ASAE* 45(2): 315-326.

Jurry, W.A., W.R. Gardner and W.H. Gardner. 1991. *Soil Physics,* 5th Edition. New York, NY: John Wiley & Sons Inc.

Kahimba, F.C. and R. Sri Ranjan. 2007. Soil temperature correction of field TDR readings obtained under near freezing conditions. *Canadian Biosystems Engineering* 49: 1.19 - 1.26.

Kahimba, F.C., R. Sri Ranjan and M. Krishnapillai. 2007a. Impact of cable lengths on the accuracy of dielectric constant measurements by time domain reflectometry. *Canadian Biosystems Engineering* 49: 1.11-1.18.

Kahimba, F.C., R. Sri Ranjan, J. Froese and M. Entz. 2007b. Previous season cover crop effects on soil moisture distribution and yield in the subsequent season. In *Proceedings of the American Society of Agricultural and Biological Engineers (ASABE) Annual International meeting.* Minneapolis, MN, USA: June 17-20. (Paper No. 072262).

Kahimba, F.C., P.R. Bullock, R. Sri Ranjan, and H.W. Cutforth. 2008. Evaluation of the SolarCalc model for simulating hourly and daily incoming solar radiation in the Northern Great Plains of Canada. *50th CSBE/SCGAB Annual Conference.* Paper No. CSBE08143. Vancouver, BC. July 13 -16.

Kahimba, F.C., R. Sri Ranjan, J. Froese, M. Entz and R Nason. 2008. Cover crop effects on infiltration, soil temperature and soil moisture distribution in the Canadian prairies. *Applied Engineering in Agriculture* 24(3): 321-333.

Kane, D.L. and E.F. Chacho. 1990. Frozen ground effects on infiltration and runoff. In *Cold Regions Hydrology and Hydraulics, Technical Council on Cold Regions Engineering Monograph,* ed. W.L. Ryan and R.D. Crissman, 259-300. Reston, VA: American Society of Civil Engineers.

Kelly, S.F., J.S. Selker and J.L. Green. 1995. Using short soil moisture probes with high-bandwidth time domain reflectometry instruments. *Soil Science Society of America Journal* 59(1): 97-102.

Kennedy, I. and B. Sharratt. 1998. Model comparisons to simulate soil frost depth. *Soil Science* 163(8): 636-645.

Lane, P.N.J., D.H. Mackenzie and A.D. Nadler. 1995. Field and laboratory calibration and test of TDR and capacitance techniques for indirect measurement of soil water content. *Australian Journal of Soil Research* 40(3): 555 – 555.

Legates, D.R. and G.J. McCabe Jr. 1999. Evaluating the use of "goodness-of-fit" measures in hydrologic and hydro climatic model validation. *Water Resources Research* 35(1): 233–241.

Lin, C. and D.K. McCool. 2006. Simulating snowmelt and soil frost depth by an energy budget approach. *Transactions of the ASABE* 49(5): 1383-1394.

Logsdon, S.D. 2000. Effect of cable length on time domain reflectometry calibration for high surface area soils. *Soil Science Society of America Journal* 64(1): 54-61.

Long, D.S., J.M. Wraith and G. Kegel. 2002. A heavy-duty time domain reflectometry soil moisture probe for use in intensive field sampling. *Soil Science Society of America Journal* 66: 396-401.

Lunardini, V.J. 1988. Freezing soil with an unfrozen water content and variable thermal properties. CRREL Report 88-2. Hanover, NH: U.S. Army Cold Regions Research Laboratory.

Luo, L., A. Robock, K.Y. Vinnikov, A. Schlosser and A.G. Slater. 2002. Effects of frozen soil on soil temperature, spring infiltration, and runoff: Results from the PILPS 2(d) experiment at Valdai, Russia. *Journal of Hydrometeorology* 4(2): 334-351.

Marshall, T.J. and J.W. Holmes. 1988. *Soil Physics* 2nd Edition. Cambridge, UK: Cambridge University Press.

MASC. 2006. Regional varieties and yield. Manitoba Management Plus Program (MMPP). Winnipeg, MB: Manitoba Agricultural Services Corporation. Available at: http://www.mmpp.com. Accessed 10 October 2006.

McGuire, A.M., D.C. Bryant and R.F. Denison. 1998. Wheat yields, nitrogen uptake, and soil moisture following winter legume cover crop vs. fallow. *Agronomy Journal* 90(3): 404-410.

Mills, G.F. and P. Haluschak. 1993. Soils of the Carman Research Station. Special report series No. 93-1. Winnipeg, MB: Manitoba Soil Survey Unit and Manitoba Land Resource Unit.

Miyazaki, T. 2006. *Water Flow in Soils*, 2nd edition. Boca Raton, FL: Taylor & Francis Group.

Mojid, M.A., G.C.L. Wyseure and D.A. Rose. 2003. Electrical conductivity problems associated with time-domain reflectometry (TDR) measurement in geotechnical engineering. *Geotechnical and Geological Engineering* 21: 243–258.

Nadler, A.J. 2007. An agro climatic risk assessment of crop production on the Canadian Prairies. M.Sc. thesis. Winnipeg, Manitoba: University of Manitoba, Department of Soil Science.

Nason, R.S.M. 2007. Resource use of annual, cover crop, and perennial cropping systems, as well as the native grass system. M.Sc. thesis. Winnipeg, Manitoba: University of Manitoba, Department of Plant science.

Nassar, I.N., R. Horton and G.N. Flerchinger. 2000. Simultaneous heat and mass transfer in soil columns exposed to freezing/thawing conditions. *Soil Science* 165(3): 208-216.

Nazarko, O., R. Van Acker, M. Entz and G. Martens. 2001. Pesticide-Free Production: A participatory research case study. In *Proceedings 2nd Manitoba Agronomists Conference*, 235. Winnipeg, Manitoba: University of Manitoba.

Nielsen, D.C., M.F. Vigil, R.L. Anderson, R.A. Bowman, J.G. Benjamin and A.D. Halvorson. 2002. Cropping system influence on planting water content and yield of winter wheat. *Agronomy Journal* 94(5): 962–967.

Or, D. and J.M. Wrath. 1999. Temperature effects on bulk dielectric permittivity measured by time domain reflectometry: A physical model. *Water Resources Research* 35(2): 371 – -383.

Or, D., S.B. Jones, J.R. VanShaar, S. Humphries and L. Koberstein. 2004. WinTDR soil analysis software version 6.1- Users guide. Soil physics group research report. Department of Plants, Soils, and Biometeorology, Utah State University, Logan, UT.

Osborne, S.L., W.E. Riedell, T.E. Schumacher and D.S. Humburg. 2003a. Use of cover crops to increase corn emergence and field trafficability. Soil/Water Research, Progress Report, 2-39. Brookings, SD: USDA-ARS.

Osborne, S.L., W.E. Riedell, D.S. Humburg and T.E. Schumacher. 2003b. Cover crops to consider. In *Proceedings South Dakota No-Till Association, Sioux Falls*, 17-23. Pierre, SD: South Dakota No-Till Association.

Paz, J.O., W.D. Batchelor, T.S. Colvin, S.D. Logsdon, T.C. Kaspar and D.L. Karlen. 1998. Analysis of water stress effects causing spatial yield variability in soybeans. *Transactions of the ASABE* 41(5): 1527-1534.

Pepin, S., N.J. Livingstone and W.R. Hook. 1995. Temperature-dependent measurement errors in the time domain reflectometry determinations of soil water. *Soil Science Society of America Journal* 59(1): 38-43.

Persson, M. and R. Berndtsson. 1998. Texture and electrical conductivity effects on temperature dependency in time domain reflectometry. *Soil Science Society of America Journal* 62(4): 887-893.

Persson, M and S. Haridy. 2003. Estimating water content from electrical conductivity measurements with short time-domain reflectometry probes. *Soil Science Society of America Journal* 67(2): 478-482.

Pierce, C.E., C. Blaine, F. Huang and C.H. Dowding. 1994. Effects of multiple crimps and cable length on reflection signatures from long cables. In *Proceedings of the International Symposium on Time Domain Reflectometry in Environmental Infrastructure, and Mining Applications*, 540–554. Evanston, IL. Sept 7-9.

Raper R.L., D.W. Reeves, C.H. Burmester and E.B. Schwab. 2000. Tillage depth, tillage timing, and cover crop effects on cotton yield, soil strength, and tillage energy requirements. *Applied Engineering in Agriculture* 16(4): 379-385.

Reddy, K.N. 2001. Effects of cereal and legume cover crop residues on weeds, yield, and net return in soybean (glycine max). *Weed Technology* 15(4): 660-668.

Robinson, D.A, S.B. Jones, J.M. Wraith, D. Or and S.P. Friedman. 2003a. A review of advances in dielectric and electrical conductivity measurements in soils using time domain reflectometry. *Vadose Zone Journal* 2(4): 444-475.

Robinson, D.A., M. Schaap, S.B. Jones, S.P. Friedman and C.M.K. Gardner. 2003b. Considerations for improving the accuracy of permittivity measurement using

TDR: Air-water calibration, effects of cable length. *Soil Science Society of America Journal* 67(1): 62-70.

Ross, P.J. 2003. Modeling soil water and solute transport – fast, simplified numerical solutions. *Agronomy Journal* 95(6): 1352-1361.

Ross, S.M., J. R. King, R.C. Izaurraldeb and J.T. O'Donovanc. 2001. Weed suppression by seven clover species. *Agronomy Journal* 93(4): 820-827.

Sainju, U.M. and B.P. Singh. 2001. Tillage, cover crop, and kill-planting date effects on corn yield and soil nitrogen. *Agronomy Journal* 93(4): 878-886.

SAS Institute Inc. 2004. Statistical analysis system (SAS) software version 9.1.2, Cary, NC: SAS Institute, Inc.

Schoofs, A., M.H. Entz, R.C. Van Acker, J.R.T. Martens and D.A. Derksen. 2005. Agronomic performance of Pesticide Free Production under two crop rotations. *Renewable Agriculture and Food Systems* 20(2): 91-100.

Seyfried, M. 2004. Determination of unfrozen water in frozen soil using dielectric techniques: Effects of temperature, ice and measurement frequency. In *American Geophysical Union, Eos Transactions* v. 17, pp 85. Washington, Washington D.C: American Geophysical Union.

Seyfried, M.S. and M.D. Murdock. 1996. Calibration of time domain reflectometry for measurement of liquid water in frozen soils. *Soil Science* 161(2): 87-98.

Seyfried, M.S. and M.D. Murdock. 2001. Response of new soil water sensor to variable soil water content and temperature. *Soil Science Society of America Journal* 65(1): 28-34.

Snapp, S.S., S.M. Swinton, R. Labarta, D. Mutch, J.R. Black, R. Leep, J. Nyiraneza and K. O'Neil. 2005. Evaluating cover crops for benefits, costs and performance within cropping system niches. *Agronomy Journal* 97(1): 322-332.

Spaans, E.J.A. and J.M. Baker. 1995. Examining the use of time domain reflectometry for measuring liquid water content in frozen soil. *Water Resources Research* 31(12): 2917-2926.

Spokas, K. and F. Forcella. 2006. Estimating hourly incoming solar radiation from limited meteorological data. *Weed Science* 54: 182-189.

Sri Ranjan, R. and C.J. Domytrak. 1997. Effective volume measured by TDR miniprobes. *Transactions of the ASAE* 40(4): 1059 – 1066.

Stahli, M., P.E. Jansson and L.C. Lundin. 1999. Soil moisture redistribution and infiltration in frozen sandy soils. *Water Resources Research* 35(1): 95-103.

Tardif, R. 2002. Notes on soil moisture sensor calibration and temperature correction. NCAR/RAP. http://www.rap.ucar.edu/staff/tardif/Documents/NCAR_doc/soil_moisture_calib.pdf_ (2006/02/28).

Tarpley, J.D. 1979. Estimating incident solar radiation at the surface from geostationary satellite data. *Journal Applied Meteorology* 18(9): 1172-1181.

Tektronix, Inc. 1998. Service manual, 1502B metallic time-domain reflectometer, 070-6267-04. Beaverton, OR: Tektronix, Inc.

Topp, G.C. and J.L. Davis. 1985. Measurement of soil water content using TDR: A field evaluation. *Soil Science Society of America Journal* 49(1): 19-24.

Topp, G.C., J.L. Davis and A.P. Annan. 1980. Electromagnetic determination of soil water content: measurements in coaxial transmission lines. *Water Resources Research* 16(3): 574-582.

Topp, G.C., J.L. Davis and A.P. Annan.1982. Electromagnetic determination of soil water content using TDR: II. Evaluation of installation and configuration of parallel transmission lines. *Soil Science Society of America Journal* 62(4): 865-873.

Topp, G.C., J.L. Davis and A.P. Annan. 2003. The early development of TDR for soil measurements. *Vadose Zone Journal* 2(4): 492-499.

Troxler. 2001. Manual of operation and Instruction for model 4300 depth moisture gauge. Research Triangle Park, NC: Troxler Electronic Laboratories Inc.

Unger, P.W. and M.F. Vigil. 1998. Cover crop effects on soil water relationships. *Journal of Soil and Water Conservation* 53(3): 200–207.

Vanclooster, M., C. Gonzalez, J. Vanderborght, D. Mallants and J. Diels. 1994. An indirect calibration procedure for using TDR in solute transport studies. In *Proceedings International Symposium on Time Domain Reflectometry in Environmental Infrastructure, and Mining Applications,* 215–226. Evanston, IL. Sept. 7-9.

Vanderborght, J., R. Kasteel, M. Herbst, M. Javaux, D. Thiery, M.Vanclooster, C. Mouvet and H. Vereecken. 2005. A set of analytical benchmarks to test numerical models of flow and transport in soils. *Vadose Zone Journal* 4(1): 206-221.

Verseghy, D.L., N.A. McFarlane and M. Lazare. 1993. CLASS – A Canadian land surface scheme for GCMS, II. Vegetation model and coupled runs. *International Journal of Climatology* 13: 347-370.

Ward, J.K., F.J. Arriaga, K.S. Balkcom, T.S. Komecki, J.S. Bergtold, A.J. Price and R.L. Raper. 2006. Effects of conservation systems on soil moisture and productivity in cotton. ASABE Paper No. 061038. Portland, Oregon: ASABE.

Warrach, K., H.T. Mengelkamp and E. Raschke. 2004. Treatment of frozen soil and snow cover in the land surface model SEWAB. *Theoretical and Applied Climatology* 69(1/2): 23-37.

Warrick, A.W. 2002. *Soil Physics Companion*. Boca Raton, Florida: CRC Press LLC.

Weast, R.C. 1986. *Handbook of Chemistry and Physics*, 67th edition. Boca Raton, Florida: CRC Press LLC.

Willmott, C.J., S.G. Ackleson, R.E. Davis, J.J. Feddema, K.M. Klink, D.R. Legates, J. O'Donnel and C.M. Rowe. 1985. Statistics for the evaluation and comparison of models. *Journal of Geophysical Research* 90(C5): 8995-9005.

Winslow, C.J., E.R. Hunt Jr., S.C. Piper. 2001. A globally applicable model of daily solar irradiance estimated from air temperature and precipitation data. *Ecological Modelling* 143(3): 227-243.

Wraith, J.M. and D. Or. 1999. Temperature effects on soil bulk dielectric permittivity measured by time domain reflectometry: Experimental evidence and hypothesis development. *Water Resources Research* 35(2): 361-369.

Xiao, W., Q. Yu, G.N. Flerchinger and Y. Zheng. 2006. Evaluation of SHAW model in simulating energy balance, leaf temperature, and micrometeorological variables within a maize canopy. *Agronomy Journal* 98(3): 722-729.

Xiaozu, X., J.L. Oliphant and A.R. Tice. 1987. Factors affecting water migration in frozen soils. CRREL Report 87-9. Hanover, NH: U.S. Army Cold Regions Research Laboratory.

Zegelin, S.J., I. White and G.F. Russell. 1992. A critique of the time domain reflectometry technique for determining field soil-water content. In: Eds Topp et

al. Advances in measurement of soil physical properties: Bringing theory into practice. *Soil Science Society of America* special publication No. 30: 187-208.

Zheng, G.H., R.W. Wilen, A.E. Slinkard and I.W. Gusta. 1994. Enhancement of canola seed germination and seedling emergence at low temperature by priming. *Crop Science* 34(6): 1589-1593.

Zuzel, J.R. and J.L. Pikul Jr. 1987. Infiltration into seasonally frozen agricultural soil. *Journal of Soil and Water Conservation* 42: 447-450.

APPENDICES

Appendix A: Raw data used for laboratory water calibration of TDR miniprobes that were used for field installation and data collection at the Ian N. Morrison Research Farm in Carman, Manitoba.

Cable ID	Cable length (m)	Program	Probe length (m)	TDR* K-value	TDR θ_v** ($m^3\ m^{-3}$)	Callib Temp (°C)	Actual K-Value	Actual θ_v ($m^3\ m^{-3}$)	K-value error	K-value sq. error	θ_v error ($m^3\ m^{-3}$)	θ_v sq. error ($m^3\ m^{-3}$)
1	2.0	TDR20	0.0350	80.560	0.978	19.3	80.621	0.980	-0.061	0.004	-0.001	0.00000
2	2.0	TDR20	0.0346	80.512	0.977	19.4	80.584	0.979	-0.071	0.005	-0.002	0.00000
3	2.0	TDR20	0.0351	80.634	0.980	19.3	80.621	0.980	0.013	0.000	0.000	0.00000
4	2.0	TDR20	0.0350	80.470	0.976	19.3	80.621	0.980	-0.151	0.023	-0.004	0.00001
5	2.0	TDR20	0.0352	80.538	0.978	19.3	80.621	0.980	-0.083	0.007	-0.002	0.00000
7	2.0	TDR20	0.0351	80.858	0.985	19.3	80.621	0.980	0.238	0.057	0.006	0.00003
9	2.0	TDR20	0.0350	80.458	0.976	19.2	80.658	0.980	-0.200	0.040	-0.005	0.00002
11	2.0	TDR20	0.0350	80.830	0.985	19.2	80.658	0.980	0.172	0.029	0.004	0.00002
12	2.0	TDR20	0.0352	80.886	0.986	19.2	80.658	0.980	0.228	0.052	0.006	0.00003
14	2.0	TDR20	0.0349	80.848	0.985	19.2	80.658	0.980	0.191	0.036	0.005	0.00002
15	2.0	TDR20	0.0352	80.779	0.983	19.4	80.584	0.979	0.195	0.038	0.005	0.00002
16	2.0	TDR20	0.0352	80.695	0.981	19.2	80.658	0.980	0.037	0.001	0.001	0.00000
18	2.0	TDR20	0.0350	80.932	0.987	19.2	80.658	0.980	0.274	0.075	0.007	0.00005
21	2.0	TDR20	0.0350	80.719	0.982	19.2	80.658	0.980	0.061	0.004	0.001	0.00000
23	2.0	TDR20	0.0350	80.367	0.973	20.0	80.362	0.973	0.005	0.000	0.000	0.00000
24	2.0	TDR20	0.0347	80.930	0.987	19.2	80.658	0.980	0.272	0.074	0.007	0.00004
25	2.5	TDR25	0.0350	80.648	0.980	19.5	80.547	0.978	0.101	0.010	0.002	0.00001
26	2.5	TDR25	0.0350	80.460	0.976	19.4	80.584	0.979	-0.124	0.015	-0.003	0.00001
27	2.5	TDR25	0.0350	80.773	0.983	19.4	80.584	0.979	0.190	0.036	0.005	0.00002
28	2.5	TDR25	0.0350	80.415	0.975	19.5	80.547	0.978	-0.131	0.017	-0.003	0.00001
29	2.5	TDR25	0.0350	80.575	0.978	19.6	80.510	0.977	0.066	0.004	0.002	0.00000
30	2.5	TDR25	0.0350	80.627	0.980	19.4	80.584	0.979	0.043	0.002	0.001	0.00000
31	2.5	TDR25	0.0349	80.527	0.977	19.4	80.584	0.979	-0.057	0.003	-0.001	0.00000
32	2.5	TDR25	0.0349	80.383	0.974	19.5	80.547	0.978	-0.164	0.027	-0.004	0.00002
33	2.5	TDR25	0.0349	80.756	0.983	19.4	80.584	0.979	0.172	0.030	0.004	0.00002
34	2.5	TDR25	0.0350	80.327	0.972	19.9	80.399	0.974	-0.071	0.005	-0.002	0.00000
35	2.5	TDR25	0.0348	80.579	0.979	19.5	80.547	0.978	0.032	0.001	0.001	0.00000

Cable ID	Cable length (m)	Program	Probe length (m)	TDR* K-value	TDR θ_v** ($m^3\ m^{-3}$)	Callib Temp (°C)	Actual K-Value	Actual θ_v ($m^3\ m^{-3}$)	K-value error	K-value sq. error	θ_v error ($m^3\ m^{-3}$)	θ_v sq. error ($m^3\ m^{-3}$)
36	2.5	TDR25	0.0348	80.480	0.976	19.4	80.584	0.979	-0.104	0.011	-0.003	0.00001
37	2.5	TDR25	0.0350	80.669	0.981	19.6	80.510	0.977	0.159	0.025	0.004	0.00002
41	2.5	TDR25	0.0349	80.481	0.976	19.7	80.473	0.976	0.008	0.000	0.000	0.00000
43	2.5	TDR25	0.0349	80.369	0.973	19.8	80.436	0.975	-0.067	0.004	-0.002	0.00000
44	2.5	TDR25	0.0350	80.380	0.974	19.9	80.399	0.974	-0.019	0.000	0.000	0.00000
45	2.5	TDR25	0.0348	80.795	0.984	19.6	80.510	0.977	0.285	0.081	0.007	0.00005
47	2.5	TDR25	0.0351	80.581	0.979	19.8	80.436	0.975	0.145	0.021	0.004	0.00001
50	2.5	TDR25	0.0349	80.582	0.979	19.6	80.510	0.977	0.072	0.005	0.002	0.00000
51	2.5	TDR25	0.0350	80.404	0.974	19.9	80.399	0.974	0.005	0.000	0.000	0.00000
54	2.5	TDR25	0.0350	80.265	0.971	19.8	80.436	0.975	-0.171	0.029	-0.004	0.00002
55	2.5	TDR25	0.0350	80.601	0.979	19.5	80.547	0.978	0.054	0.003	0.001	0.00000
58	2.5	TDR25	0.0350	80.726	0.982	19.8	80.436	0.975	0.290	0.084	0.007	0.00005
59	2.5	TDR25	0.0350	80.596	0.979	19.7	80.473	0.976	0.123	0.015	0.003	0.00001
60	2.5	TDR25	0.0350	80.625	0.980	19.8	80.436	0.975	0.189	0.036	0.005	0.00002
61	3.0	TDR30	0.0355	80.821	0.984	18.4	80.955	0.988	-0.134	0.018	-0.003	0.00001
62	3.0	TDR30	0.0352	80.581	0.979	19.9	80.399	0.974	0.182	0.033	0.004	0.00002
63	3.0	TDR30	0.0353	80.416	0.975	19.6	80.510	0.977	-0.094	0.009	-0.002	0.00001
64	3.0	TDR30	0.0353	80.376	0.974	20.0	80.362	0.973	0.014	0.000	0.000	0.00000
65	3.0	TDR30	0.0351	80.354	0.973	20.0	80.362	0.973	-0.007	0.000	0.000	0.00000
66	3.0	TDR30	0.0355	80.757	0.983	18.4	80.955	0.988	-0.198	0.039	-0.005	0.00002
67	3.0	TDR30	0.0353	80.514	0.977	20.0	80.362	0.973	0.152	0.023	0.004	0.00001
68	3.0	TDR30	0.0351	80.722	0.982	18.4	80.955	0.988	-0.233	0.054	-0.006	0.00003
69	3.0	TDR30	0.0351	80.726	0.982	18.4	80.955	0.988	-0.229	0.052	-0.006	0.00003
70	3.0	TDR30	0.0349	81.083	0.991	18.4	80.955	0.988	0.128	0.016	0.003	0.00001
71	3.0	TDR30	0.0353	80.617	0.979	20.0	80.362	0.973	0.255	0.065	0.006	0.00004
72	3.0	TDR30	0.0355	80.511	0.977	20.0	80.362	0.973	0.149	0.022	0.004	0.00001
73	3.0	TDR30	0.0352	81.131	0.992	18.4	80.955	0.988	0.176	0.031	0.004	0.00002
74	3.0	TDR30	0.0351	80.509	0.977	19.6	80.510	0.977	-0.001	0.000	0.000	0.00000
75	3.0	TDR30	0.0353	80.272	0.971	20.0	80.362	0.973	-0.090	0.008	-0.002	0.00000
76	3.0	TDR30	0.0353	80.350	0.973	20.0	80.362	0.973	-0.012	0.000	0.000	0.00000

Cable ID	Cable length (m)	Program	Probe length (m)	TDR* K-value	TDR θ_v** ($m^3\ m^{-3}$)	Callib Temp (°C)	Actual K-Value	Actual θ_v ($m^3\ m^{-3}$)	K-value error	K-value sq. error	θ_v error ($m^3\ m^{-3}$)	θ_v sq. error ($m^3\ m^{-3}$)
77	3.0	TDR30	0.0352	80.919	0.987	18.4	80.955	0.988	-0.036	0.001	-0.001	0.00000
78	3.0	TDR30	0.0353	80.224	0.970	20.0	80.362	0.973	-0.138	0.019	-0.003	0.00001
79	3.0	TDR30	0.0352	80.515	0.977	20.0	80.362	0.973	0.153	0.023	0.004	0.00001
80	3.0	TDR30	0.0350	80.350	0.973	19.6	80.510	0.977	-0.160	0.025	-0.004	0.00001
80	3.0	TDR30	0.0351	80.989	0.989	18.4	80.955	0.988	0.034	0.001	0.001	0.00000
81	3.0	TDR30	0.0352	80.299	0.972	20.0	80.362	0.973	-0.063	0.004	-0.002	0.00000
82	3.0	TDR30	0.0356	80.659	0.980	20.0	80.362	0.973	0.297	0.088	0.007	0.00005
83	3.0	TDR30	0.0353	80.171	0.969	20.0	80.362	0.973	-0.191	0.036	-0.005	0.00002
84	3.0	TDR30	0.0351	80.793	0.984	18.4	80.955	0.988	-0.162	0.026	-0.004	0.00002
	N			**66**								
	Mean			**80.595**	**0.979**		**80.566**	**0.978**	**0.029**		**0.001**	
	Std deviation			**0.213**	**0.005**		**0.185**	**0.005**	**0.149**		**0.004**	
	RMSE								**0.151**		**0.004**	
	RMSE (%)								**0.188**		**0.377**	
	Max error								**0.297**		**0.007**	
	Mean absolute error								**0.127**		**0.003**	

* The TDR K-value is the dielectric constant of de-iodized liquid water measured using TDR cable tester at a specified temperature

** The TDR water content derived using TDR-measured K-values and the Topp's model (Topp et al. 1980).

Appendix B: Calibration of TDR miniprobes for water content measurements using laboratory soil columns.

S/No.	Cable ID	Cable length (m)	Oven dry θ_v * ($m^3 m^{-3}$)	TDR θ_v** ($m^3 m^{-3}$)	Error (TDR-Oven)	Absolute error	Square error
1	1	2.0	0.418	0.414	-0.003	0.003	1.18E-05
2	14	2.0	0.433	0.445	0.012	0.012	1.43E-04
3	9	2.0	0.440	0.435	-0.004	0.004	1.84E-05
4	11	2.0	0.439	0.449	0.010	0.010	9.44E-05
5	5	2.0	0.424	0.429	0.004	0.004	1.74E-05
6	12	2.0	0.428	0.422	-0.006	0.006	3.09E-05
7	15	2.0	0.431	0.440	0.009	0.009	8.41E-05
8	16	2.0	0.437	0.419	-0.018	0.018	3.18E-04
9	20	2.0	0.415	0.416	0.001	0.001	9.67E-07
10	4	2.0	0.393	0.390	-0.003	0.003	1.08E-05
11	8	2.0	0.406	0.412	0.006	0.006	3.25E-05
12	10	2.0	0.395	0.392	-0.003	0.003	1.01E-05
13	17	2.0	0.394	0.381	-0.012	0.012	1.51E-04
14	19	2.0	0.379	0.368	-0.011	0.011	1.31E-04
15	21	2.0	0.414	0.406	-0.008	0.008	6.32E-05
16	33	2.5	0.440	0.447	0.007	0.007	4.90E-05
17	41	2.5	0.411	0.417	0.006	0.006	3.12E-05
18	30	2.5	0.473	0.454	-0.019	0.019	3.46E-04
19	47	2.5	0.465	0.452	-0.014	0.014	1.95E-04
20	54	2.5	0.455	0.458	0.004	0.004	1.26E-05
21	43	2.5	0.460	0.454	-0.006	0.006	3.66E-05
22	25	2.5	0.422	0.422	0.000	0.000	1.13E-07
23	29	2.5	0.395	0.386	-0.009	0.009	8.34E-05
24	37	2.5	0.409	0.415	0.006	0.006	3.53E-05
25	55	2.5	0.405	0.407	0.003	0.003	6.54E-06
26	64	3.0	0.440	0.457	0.017	0.017	2.81E-04
27	83	3.0	0.474	0.466	-0.009	0.009	7.51E-05
28	70	3.0	0.468	0.448	-0.020	0.020	3.87E-04
29	72	3.0	0.461	0.451	-0.010	0.010	9.46E-05
30	80	3.0	0.471	0.451	-0.020	0.020	3.83E-04
31	67	3.0	0.461	0.445	-0.016	0.016	2.49E-04
32	62	3.0	0.400	0.388	-0.012	0.012	1.40E-04
33	69	3.0	0.417	0.424	0.007	0.007	5.04E-05
34	71	3.0	0.405	0.411	0.006	0.006	3.47E-05
35	76	3.0	0.412	0.406	-0.006	0.006	3.71E-05

S/No.	Cable ID	Cable length (m)	Oven dry θ_v * ($m^3 m^{-3}$)	TDR θ_v** ($m^3 m^{-3}$)	Error (TDR-Oven)	Absolute error	Square error
36	78	3.0	0.422	0.427	0.005	0.005	2.13E-05
N					**36**		
Mean			**0.428**	**0.425**	**-0.003**		
Std deviation					**0.010**		
RMSE					**0.010**		
RMSE (%)					**2.357**		
Max error					**0.020**		
Mean absolute error (MAE)					**0.009**		
R^2					**0.863**		

* Oven dry θ_v is the water content measured using the standard thermo-gravimetric method and converted to volumetric water content using bulk density of the soil samples.

** The sample soil water content was measured using TDR method.

Appendix C: Measured and actual dielectric constant (K_a) of water for different extension cable lengths. The data were used for determining the influence of cable lengths on the accuracy of TDR measurements.

Phys. Cable length (m)	Electr cable length (m)	Measured K-value	Measured θ_v ($m^3\ m^{-3}$)	Average meas K-value	Average θ_v ($m^3\ m^{-3}$)	Temp (°C)	Actual K-value	Actual θ_v ($m^3\ m^{-3}$)	K-value error	θ_v error ($m^3\ m^{-3}$)	% dev of θ_v
2.50	3.00	80.42	0.975	80.48	0.976	19.8	80.44	0.975	0.047	0.001	0.114
		80.46	0.976								
		80.28	0.971								
		80.77	0.983								
4.50	5.61	80.39	0.974	80.29	0.971	20.0	80.36	0.973	-0.074	-0.002	-0.178
		80.41	0.974								
		80.35	0.973								
		80.01	0.965								
7.05	8.74	80.22	0.970	80.20	0.969	19.9	80.40	0.974	-0.196	-0.005	-0.471
		80.46	0.976								
		79.86	0.961								
		80.27	0.971								
9.55	11.95	81.62	1.004	80.50	0.977	19.8	80.44	0.975	0.061	0.001	0.148
		80.93	0.987								
		79.62	0.956								
		79.82	0.960								
12.85	16.16	80.44	0.975	80.53	0.977	20.0	80.36	0.973	0.167	0.004	0.404
		81.39	0.999								
		80.27	0.971								
		80.02	0.965								
17.40	21.52	80.40	0.974	80.44	0.975	20.0	80.36	0.973	0.082	0.002	0.197
		81.16	0.993								
		79.28	0.948								
		80.93	0.987								
19.90	24.91	80.41	0.974	80.53	0.977	20.3	80.25	0.971	0.284	0.007	0.686
		80.47	0.976								

Phys. Cable length (m)	Electr cable length (m)	Measured K-value	Measured θ_v ($m^3 m^{-3}$)	Average meas K-value	Average θ_v ($m^3 m^{-3}$)	Temp (°C)	Actual K-value	Actual θ_v ($m^3 m^{-3}$)	K-value error	θ_v error ($m^3 m^{-3}$)	% dev of θ_v
		81.01	0.989								
		80.24	0.970								
30.00	37.79	81.66	1.005	80.51	0.977	20.5	80.18	0.969	0.337	0.008	0.812
		80.85	0.985								
		79.44	0.951								
		80.11	0.967								
40.00	49.95	81.76	1.008	80.37	0.973	19.7	80.47	0.976	-0.104	-0.003	-0.252
		80.32	0.972								
		79.40	0.951								
		80.00	0.964								
50.35	62.86	77.42	0.906	79.61	0.955	20.3	80.25	0.971	-0.641	-0.015	-1.519
		80.28	0.971								
		82.06	1.016								
		78.68	0.934								
70.00	87.91	76.14	0.880	77.92	0.917	21.0	79.99	0.964	-2.078	-0.047	-4.731
		80.14	0.968								
		81.44	1.000								
		73.94	0.837								

Appendix D: The SHAW model input data files on the continuous fallow treatment for the 2005-2006 seasons at the Ian N. Morrison Research Farm in Carman, Manitoba (data for one out of four treatments on one season have been taken as example of the SHAW model input data files).

Table D-1: List of the SHAW model input/output files for the continuous fallow treatment

0	0	0										
CRMF05.SIT												
CRMF05.WEA												
CRMF05.MOI												
CRMF05.TMP												
12	1	12	12	24	12	12	12	0	12	0	0	1
OUTF05.OUT												
PROFLF05.OUT												
TEMPF05.OUT												
MOISTF05.OUT												
MATRCF05.OUT												
ENERGF05.OUT												
WCBALF05.OUT												
WFLOWF05.OUT												
ROOTXF05.OUT												
FROSTF05.OUT												
SALTSF05.OUT												
SOLUTF05.OUT												

Table D-2: Total soil moisture at depths from 0.0 to 1.8 m.

			Soil depths (m)										
JDAY*	**JHR**	**JYR**	**0.00**	**0.05**	**0.20**	**0.40**	**0.60**	**0.80**	**1.00**	**1.20**	**1.40**	**1.60**	**1.80**
279	12	2005	0.23	0.25	0.33	0.27	0.32	0.40	0.43	0.48	0.50	0.51	0.52
326	12	2005	0.21	0.24	0.33	0.26	0.32	0.41	0.40	0.45	0.47	0.50	0.50
340	12	2005	0.50	0.50	0.47	0.30	0.29	0.36	0.40	0.45	0.45	0.50	0.51
347	12	2005	0.44	0.44	0.42	0.36	0.27	0.31	0.35	0.41	0.41	0.45	0.46
355	12	2005	0.42	0.42	0.42	0.40	0.26	0.28	0.35	0.41	0.42	0.46	0.46
30	12	2006	0.42	0.42	0.42	0.41	0.26	0.26	0.32	0.39	0.41	0.46	0.45
55	12	2006	0.43	0.42	0.42	0.41	0.40	0.19	0.28	0.36	0.38	0.44	0.44
88	12	2006	0.43	0.43	0.43	0.41	0.41	0.22	0.25	0.33	0.39	0.44	0.46
94	12	2006	0.45	0.45	0.44	0.43	0.42	0.23	0.27	0.36	0.40	0.47	0.46
192	12	2006	0.29	0.29	0.27	0.23	0.27	0.28	0.32	0.37	0.38	0.42	0.42

* JDAY is the day of the year, JHR is the hour of the day, and JYR is the year of simulation.

Table D-3: Soil temperature at depths from 0.0 to 1.8 m.

			Soil depths (m)										
JDAY	**JHR**	**JYR**	**0.00**	**0.05**	**0.20**	**0.40**	**0.60**	**0.80**	**1.00**	**1.20**	**1.40**	**1.60**	**1.80**
228	12	2005	14.7	20.0	24.5	24.5	24.6	24.7	24.2	23.5	22.5	21.2	20.0
238	12	2005	12.8	18.0	18.3	18.6	18.6	18.2	17.6	16.8	16.0	15.0	14.1
279	12	2005	10.0	13.0	12.3	8.3	5.0	3.8	3.7	3.7	3.6	3.6	3.6
326	12	2005	10.5	11.8	12.0	10.6	9.4	8.3	7.5	7.0	6.7	6.4	6.1
340	12	2005	-2.9	-2.7	-1.9	1.1	2.6	3.5	4.0	4.4	4.8	5.2	5.6
347	12	2005	-2.0	-1.9	-1.2	0.2	1.3	1.9	2.4	2.8	3.2	3.5	3.9
355	12	2005	-3.7	-3.6	-3.0	-0.5	0.9	1.7	2.2	2.6	2.9	3.2	3.5
30	12	2006	-1.0	-0.8	-0.4	0.2	0.7	1.2	1.6	2.0	2.4	2.7	3.1
55	12	2006	-2.8	-2.7	-2.2	-1.0	0.0	0.7	1.2	1.6	2.0	2.4	2.8
88	12	2006	-0.2	-0.2	-0.1	-0.1	0.1	0.3	0.5	0.7	0.9	1.1	1.3
94	12	2006	0.5	0.4	0.3	0.3	0.4	0.5	0.7	0.9	1.2	1.4	1.7
192	12	2006	24.3	24.0	21.9	21.7	20.8	19.6	18.3	17.2	16.3	15.2	14.1

Table D-4: Site characteristics of the experimental fields

CARMAN 2005-06: PLOT52 - FALLOW, NO VEGETATIONS (Hourly simulations)												
279	12	2005	192	2006								Line A
49	30	0.50	0.00	12.50	262.00							Line B
0	0	0	11	0	0.001	1	0	0	0	1	0	0	Line C
2.0	2.0	0.5											Line D
0.0	0.15												Line E
0	0	0.225	1.00										Line G
0.00	3.05	-0.4	2.90	1250.0	0.5	79.00	8.00	13.00	3.76				Line J
0.05	3.05	-0.4	2.90	1250.0	0.5	79.00	8.00	13.00	3.76				Line J-1
0.20	3.22	-0.22	4.58	1420.0	0.5	73.00	8.00	19.00	2.72				Line J-2
0.40	3.18	-0.21	4.00	1400.0	0.5	77.00	7.00	16.00	1.24				Line J-3
0.60	3.18	-0.21	4.00	1400.0	0.5	77.00	7.00	16.00	1.24				Line J-4
0.80	3.05	-0.20	0.41	1310.0	0.5	4.00	44.00	52.00	0.00				Line J-5
1.00	3.05	-0.20	0.41	1310.0	0.5	4.00	44.00	52.00	0.00				Line J-6
1.20	3.05	-0.20	0.20	1310.0	0.5	4.00	44.00	52.00	0.00				Line J-7
1.40	3.05	-0.20	0.20	1310.0	0.5	4.00	44.00	52.00	0.00				Line J-8
1.60	3.05	-0.20	0.20	1310.0	0.5	4.00	44.00	52.00	0.00				Line J-9
1.80	3.05	-0.20	0.20	1310.0	0.5	4.00	44.00	52.00	0.00				Line J-10
													Line J-11

Table D-5: Weather data*

Julian Day	Hour of day	Year	Air temp (°C)	Wind speed (mph)	Rel. humidity (%)	Total ppt (in)	Snow density** (g/cm^3)	Solar rad (W/m^2)
179	0	2005	12.90	2.46	104.20	0.000	0.000	0.00
179	1	2005	12.29	2.56	104.60	0.000	0.000	0.00
179	2	2005	12.86	3.23	104.50	0.000	0.000	0.00
179	3	2005	12.80	3.16	104.00	0.000	0.000	0.00
179	4	2005	13.02	4.90	103.00	0.000	0.000	0.00
179	5	2005	12.98	4.80	103.00	0.000	0.000	0.00
179	6	2005	13.07	6.43	102.50	0.000	0.000	3.01
179	7	2005	13.53	5.07	101.30	0.000	0.000	40.98
179	8	2005	13.91	3.50	101.10	0.000	0.000	95.10
179	9	2005	14.76	6.67	98.40	0.000	0.000	158.10
179	10	2005	15.44	6.27	94.30	0.000	0.000	291.00
179	11	2005	16.01	4.55	93.90	0.000	0.000	315.00
179	12	2005	16.25	3.85	93.40	0.000	0.000	343.10
179	13	2005	16.46	4.54	94.50	0.000	0.000	296.00
179	14	2005	16.78	3.80	92.90	0.000	0.000	309.00
179	15	2005	17.65	5.64	91.70	0.000	0.000	370.20
179	16	2005	18.13	6.34	89.70	0.000	0.000	520.20
179	17	2005	18.33	5.36	87.70	0.000	0.000	433.20
179	18	2005	18.62	5.13	88.30	0.000	0.000	227.00
179	19	2005	18.56	5.86	89.60	0.000	0.000	217.20
179	20	2005	18.31	4.59	90.40	0.000	0.000	171.20
179	21	2005	17.20	3.03	96.70	0.000	0.000	104.90
179	22	2005	16.00	3.37	101.00	0.000	0.000	12.70
179	23	2005	16.13	3.96	101.20	0.000	0.000	0.02
180	0	2005	16.17	5.69	100.20	0.000	0.000	0.00
180	1	2005	16.15	5.78	99.40	0.000	0.000	0.00
180	2	2005	15.80	7.23	100.00	0.000	0.000	0.00
180	3	2005	15.56	8.11	100.40	0.000	0.000	0.00
180	4	2005	15.48	4.67	101.30	0.000	0.000	0.00
180	5	2005	15.25	5.27	102.90	0.000	0.000	0.00
180	6	2005	15.25	5.62	103.30	0.000	0.000	1.04
180	7	2005	15.53	8.05	103.60	0.031	0.000	4.52
180	8	2005	15.60	8.24	104.80	0.126	0.000	3.35
180	9	2005	15.66	7.16	106.00	0.496	0.000	2.12
180	10	2005	15.71	9.92	106.30	0.409	0.000	2.73
180	11	2005	15.81	12.61	105.90	0.126	0.000	20.57
180	12	2005	15.97	11.30	104.90	0.000	0.000	78.60
180	13	2005	16.19	11.32	103.80	0.000	0.000	138.90
180	14	2005	16.24	10.05	103.40	0.008	0.000	37.27

Julian Day	Hour of day	Year	Air temp (°C)	Wind speed (mph)	Rel. humidity (%)	Total ppt (in)	Snow density** (g/cm^3)	Solar rad (W/m^2)
180	15	2005	16.10	10.02	103.60	0.000	0.000	49.70
180	16	2005	16.26	9.68	103.20	0.000	0.000	67.13
180	17	2005	15.85	9.84	105.20	0.016	0.000	56.16
180	18	2005	15.62	7.86	105.60	0.000	0.000	48.68
180	19	2005	15.73	6.79	105.60	0.000	0.000	34.08
180	20	2005	15.73	6.32	105.30	0.016	0.000	16.18
180	21	2005	15.52	5.63	105.60	0.024	0.000	6.07
180	22	2005	15.32	6.94	106.00	0.063	0.000	1.06
180	23	2005	14.93	7.76	106.20	0.087	0.000	0.00
181	0	2005	14.41	8.30	106.50	0.134	0.000	0.00
181	1	2005	14.15	9.67	106.60	0.071	0.000	0.00
181	2	2005	13.94	10.31	106.40	0.039	0.000	0.00
181	3	2005	13.63	11.65	106.40	0.039	0.000	0.00
181	4	2005	13.51	12.60	106.20	0.102	0.000	0.00
181	5	2005	13.39	14.47	106.10	0.079	0.000	0.00
181	6	2005	13.45	14.97	106.10	0.079	0.000	1.06
181	7	2005	13.62	15.13	104.10	0.047	0.000	13.35
181	8	2005	13.53	15.31	104.40	0.039	0.000	29.17
181	9	2005	13.68	15.93	104.20	0.024	0.000	66.13
181	10	2005	13.89	16.74	100.70	0.000	0.000	118.90
181	11	2005	14.47	15.97	96.20	0.000	0.000	122.00
181	12	2005	15.08	16.97	91.70	0.000	0.000	162.80
181	13	2005	15.79	16.89	88.30	0.000	0.000	187.40
181	14	2005	17.21	18.45	81.00	0.000	0.000	309.70
181	15	2005	18.02	18.54	74.70	0.000	0.000	681.00
181	16	2005	17.85	15.59	76.10	0.000	0.000	643.10
181	17	2005	18.33	11.74	78.80	0.000	0.000	406.70
181	18	2005	18.91	10.54	77.20	0.000	0.000	486.90
181	19	2005	19.03	9.57	75.30	0.000	0.000	422.30
181	20	2005	18.55	6.56	77.50	0.000	0.000	263.40
181	21	2005	16.91	3.44	86.00	0.000	0.000	117.80
181	22	2005	14.43	1.93	97.40	0.000	0.000	17.80
181	23	2005	12.58	0.79	103.80	0.000	0.000	0.05
182	0	2005	11.73	2.29	105.00	0.000	0.000	0.00

* Three-day out of 365-day weather data have been selected as example of the hourly input weather data used in the SHAW model.

** A value of 0.000 on snow density allows the model to calculate the respective snow density values.

Julian Day	Hour of day	Year	Air temp (°C)	Wind speed (mph)	Rel. humidity (%)	Total ppt (in)	Snow density** (g/cm^3)	Solar rad (W/m^2)
180	15	2005	16.10	10.02	103.60	0.000	0.000	49.70
180	16	2005	16.26	9.68	103.20	0.000	0.000	67.13
180	17	2005	15.85	9.84	105.20	0.016	0.000	56.16
180	18	2005	15.62	7.86	105.60	0.000	0.000	48.68
180	19	2005	15.73	6.79	105.60	0.000	0.000	34.08
180	20	2005	15.73	6.32	105.30	0.016	0.000	16.18
180	21	2005	15.52	5.63	105.60	0.024	0.000	6.07
180	22	2005	15.32	6.94	106.00	0.063	0.000	1.06
180	23	2005	14.93	7.76	106.20	0.087	0.000	0.00
181	0	2005	14.41	8.30	106.50	0.134	0.000	0.00
181	1	2005	14.15	9.67	106.60	0.071	0.000	0.00
181	2	2005	13.94	10.31	106.40	0.039	0.000	0.00
181	3	2005	13.63	11.65	106.40	0.039	0.000	0.00
181	4	2005	13.51	12.60	106.20	0.102	0.000	0.00
181	5	2005	13.39	14.47	106.10	0.079	0.000	0.00
181	6	2005	13.45	14.97	106.10	0.079	0.000	1.06
181	7	2005	13.62	15.13	104.10	0.047	0.000	13.35
181	8	2005	13.53	15.31	104.40	0.039	0.000	29.17
181	9	2005	13.68	15.93	104.20	0.024	0.000	66.13
181	10	2005	13.89	16.74	100.70	0.000	0.000	118.90
181	11	2005	14.47	15.97	96.20	0.000	0.000	122.00
181	12	2005	15.08	16.97	91.70	0.000	0.000	162.80
181	13	2005	15.79	16.89	88.30	0.000	0.000	187.40
181	14	2005	17.21	18.45	81.00	0.000	0.000	309.70
181	15	2005	18.02	18.54	74.70	0.000	0.000	681.00
181	16	2005	17.85	15.59	76.10	0.000	0.000	643.10
181	17	2005	18.33	11.74	78.80	0.000	0.000	406.70
181	18	2005	18.91	10.54	77.20	0.000	0.000	486.90
181	19	2005	19.03	9.57	75.30	0.000	0.000	422.30
181	20	2005	18.55	6.56	77.50	0.000	0.000	263.40
181	21	2005	16.91	3.44	86.00	0.000	0.000	117.80
181	22	2005	14.43	1.93	97.40	0.000	0.000	17.80
181	23	2005	12.58	0.79	103.80	0.000	0.000	0.05
182	0	2005	11.73	2.29	105.00	0.000	0.000	0.00

* Three-day out of 365-day weather data have been selected as example of the hourly input weather data used in the SHAW model.

** A value of 0.000 on snow density allows the model to calculate the respective snow density values.

Appendix E: The SHAW model source code modifications to account for solar azimuth angle calculations and reduced soil saturation due to ice content in freezing soils.

Code E-1. Modified subroutine SOLAR that calculates the solar azimuth angle based on the inverse cosine function. (The additions are presented in BOLD, and deletion of the original code have been written as comments in italic fonts preceded with C*).

```
C**********************************************************************
C
      SUBROUTINE SOLAR (DIRECT,DIFFUS,SUNSLP,ALTITU,SUNHOR,ALATUD,SLOPE,
     >                  ASPECT,HRNOON,HAFDAY,DECLIN,HOUR,NHRPDT)
C
C     THIS SUBROUTINE SEPARATES THE TOTAL RADIATION MEASURED ON THE
C     HORIZONTAL INTO THE DIRECT AND DIFFUSE ON THE LOCAL SLOPE.
C
C**********************************************************************
      COMMON /TIMEWT/ WT,WDT,DT
      COMMON /SWRCOE/ SOLCON,DIFATM,DIFRES,SNOCOF,SNOEXP
      INTEGER HOUR
C
C**** CHECK IF SUN HAS RISEN YET (OR IF IT HAS ALREADY SET)
      IF (SUNHOR .LE. 0.0) THEN
        DIRECT=0.0
        DIFFUS=0.0
        RETURN
      END IF
      SUNRIS=HRNOON - HAFDAY/0.261799
      SUNSET=HRNOON + HAFDAY/0.261799
C
C*C**** CALCULATE HOUR ANGLE AT WHICH THE SUN WILL BE DUE EAST/WEST IN
C*C     ORDER TO ADJUST AZIMUTH ANGLE FOR SOUTHERN AZIMUTHS
C*C     -- SIN(AZIMUTH) TELLS YOU ONLY THE EAST/WEST DIRECTION - NOT
C*C     WHETHER THE SUN IS NORTH/SOUTH.
C*C      IF (ABS(DECLIN).GE.ABS(ALATUD)) THEN
C*C        LATITUDE IS WITHIN THE TROPICS (EQUATION WON'T WORK)
C*       HRWEST=3.14159
C*       ELSE
C*        HRWEST=ACOS(TAN(DECLIN)/TAN(ALATUD))
C*     END IF
C*

C**** SUM UP VALUES AND FIND AVERAGE SUN POSITION FOR TIME STEP
      SINAZM=0.0
      COSAZM=0.0
      SUMALT=0.0
      COSALT=0.0
      SUNMAX=0.0
      DO 10 IHR=HOUR-NHRPDT,HOUR
        THOUR=IHR
C
C****   DETERMINE THE GEOMETRY OF THE SUN'S RAYS AT CURRENT TIME
      HRANGL=0.261799*(IHR-HRNOON)
```

```
      IF (THOUR .GT. SUNRIS  .AND.  THOUR .LT. SUNSET) THEN
C       SUN IS ABOVE HORIZON -- CALCULATE ITS ALTITUDE ABOVE THE
C       HORIZON (ALTITU) AND ANGLE FROM DUE NORTH (AZMUTH)
        SINALT=SIN(ALATUD)*SIN(DECLIN)
     >       + COS(ALATUD)*COS(DECLIN)*COS(HRANGL)
        ALTITU=ASIN(SINALT)
C
C*        AZM = ASIN(-COS(DECLIN)*SIN(HRANGL)/COS(ALTITU))

        AZM = ACOS((SIN(ALTITU)*SIN(ALATUD)
     >       - SIN(DECLIN))/(COS(ALTITU)*COS(ALATUD)))
C
C*      CORRECT AZIMUTH FOR SOUTHERN ANGLES
C*        IF (ALATUD-DECLIN .GT. 0.0) THEN
C*C         NORTHERN LATITUDES   (HRANGL=0.0 AT NOON)
C*          IF (ABS(HRANGL).LT.HRWEST) AZM=3.14159-AZM
C*         ELSE
C*C          SOUTHERN LATITUDES
C*          IF (ABS(HRANGL).GE.HRWEST) AZM=3.14159-AZM
C*        END IF

C       PUT AZIMUTH IN THE CORRECT QUADRANT DEPENDING ON TIME OF DAY
C       (HRANGL=0.0 AT NOON)
        IF (HRANGL.LT.0.0) THEN
         AZM=3.14159-AZM
         ELSE
         AZM=3.14159+AZM
        END IF
C       SUM CONDITIONS TO GET AVERAGE ALTITUDE AND AZMUTH
C       (OBTAIN AVERAGE BY SUMMING VECTOR COMPONENTS)
        SUN=SOLCON*SINALT
        SUMALT=SUMALT+SUN*SINALT
        COSALT=COSALT+SUN*COS(ALTITU)
        SINAZM=SINAZM+SUN*SIN(AZM)
        COSAZM=COSAZM+SUN*COS(AZM)
        SUNMAX=SUNMAX+SUN
      END IF
C
  10 CONTINUE
C
C**** DETERMINE AVERAGE SOLAR RADIATION, AVERAGE ALTITUDE AND AZIMUTH OF
C    THE SUN AND ANGLE ON LOCAL SLOPE
     IF (SUNMAX .EQ. 0) THEN
       ALTITU=0.0
       SUNSLP=0.0
      ELSE
       ALTITU=ATAN(SUMALT/COSALT)
       AZMUTH=ATAN2(SINAZM,COSAZM)
       SUNMAX=SUNMAX/(NHRPDT+1)
       SUNSLP=ASIN( SIN(ALTITU)*COS(SLOPE)
     >       + COS(ALTITU)*SIN(SLOPE)*COS(AZMUTH-ASPECT))
     END IF
C
C**** SEPARATE THE SOLAR RADIATION INTO DIRECT AND DIFFUSE COMPONENTS
     IF (ALTITU .LE. 0.0) THEN
C    SUN IS BELOW THE HORIZON - ALL RADIATION MUST BE DIFFUSE
```

```
      DIFFUS=SUNHOR
      DIRECT=0.0
      RETURN
    END IF
    TTOTAL=SUNHOR/SUNMAX
C   LIMIT TOTAL TRANSMISSIVITY TO MAXIMUM (DIFATM) WHICH WILL
C   CAUSE TDIFFU TO BE 0.0
    IF (TTOTAL .GT. DIFATM) TTOTAL = DIFATM
    TDIFFU=TTOTAL*(1. - EXP(0.6*(1.-DIFATM/TTOTAL)/(DIFATM-0.4)))
    DIFFUS=TDIFFU*SUNMAX
    DIRHOR=SUNHOR-DIFFUS
C
C**** NOW CALCULATE THE DIRECT SOLAR RADIATION ON THE LOCAL SLOPE
    IF (SUNSLP .LE. 0.0) THEN
C     SUN HAS NOT RISEN ON THE LOCAL SLOPE -- NO DIRECT RADIATION
      DIRECT=0.0
    ELSE
      DIRECT=DIRHOR*SIN(SUNSLP)/SIN(ALTITU)
C     IF THE SUN'S ALTITUDE IS NEAR ZERO, THE CALCULATED DIRECT
C     RADIATION ON THE SLOPING SURFACE MAY BE UNREALISTICALLY LARGE --
C     LIMIT DIRECT TO 5*DIRHOR (THIS IS APPROXIMATELY THE CASE WHEN
C     THE SUN IS 10 DEGREES ABOVE THE HORIZON AND THE SLOPING SURFACE
C     IS PERPENDICULAR TO THE SUN'S RAYS
      IF (DIRECT .GT. 5.*DIRHOR) DIRECT=5.*DIRHOR
    END IF
C
    RETURN
    END
C ***************************************************************************************
```

NB: The revised subroutine SOLAR with the proposed inverse cosine function on the AZM equation was sent to Dr. Gerald Flerchinger and he revised the quadrant of the Azimuth angle depending on time of the day (G. Flerchinger, personal communications, May 19, 2008).

Code E-2. **Modified subroutine MATVLC that relates volumetric liquid water content and matric potential, taking into account the ice content of freezing soil.**

(The corrections to the original code are presented in BOLD fonts).

```
C***********************************************************************
C
      SUBROUTINE MATVLC (I, MAT, VLC, DLDM, VIC, ICES)
C
C     THIS SUBROUTINE DEFINES THE RELATION BETWEEN THE VOLUMETRIC
C     LIQUID CONTENT AND THE MATRIC POTENTIAL. THE SUBROUTINE IS DIVIDED
C     INTO THREE PART, AND THE OUTPUT DEPENDS ON WHICH PART IS CALLED
C          MATVL1 : THE MATRIC POTENTIAL IS CALCULATED FROM MOISTURE
C          MATVL2 : THE MOISTURE CONTENT IS CALCULATED FROM MATRIC
C          MATVL3 : THE DERIVATIVE OF MOISTURE CONTENT WITH RESPECT
C                TO MATRIC POTENTIAL IS CALCULTED.
C             I = NODE NUMBER
C
C***********************************************************************
      COMMON /SLPARM/ B(50),ENTRY(50),RHOB(50),SAT(50),SATK(50),
     >          NSALT,SALTKQ(10,50),VAPCOF(50),VAPEXP(50),
     >             SAND(50),SILT(50),CLAY(50),OM(50)

      REAL MAT, VLC, DLDM, VIC(50)
          INTEGER  ICES(50)
C*************************************************
          ENTRY MATVL1 (I, MAT, VLC, DLDM, VIC, ICES)
C
C     DETERMINE THE MATRIC POTENTIAL FROM THE MOISTURE CONTENT
C
C     CHECK IF THERE IS ICE CONTENT IN THE SOIL MATRIX
C     NO ICE CONTENT IF ICESDT(I) IS LESS THAN 1.
C     VICDT(I) IS THE VOLUMETRIC ICE CONTENT IN THE FROZEN/PARTLY
C     FROZEN SOIL LAYER (I)
C
C
       IF (ICES(I) .EQ. 0) THEN
C                 NO ICES PRESENT
        MAT=ENTRY(I)*(VLC/SAT(I))**(-B(I))
       ELSE
C                 ICES PRESENT
                      IF (SAT(I)-VIC(I) .LT. 0.13)       VIC(I)= SAT(I)-0.13
                            MAT=ENTRY(I)*(VLC/(SAT(I)-VIC(I))**(-B(I)))
       ENDIF
       RETURN
C****
      ENTRY MATVL2 (I, MAT, VLC, DLDM, VIC, ICES)
C
C     DETERMINE THE MOISTURE CONTENT FROM THE MATRIC POTENTIAL
C
C     CHECK IF THERE IS ICE CONTENT IN THE SOIL MATRIX
C
      IF (ICES(I) .EQ. 0) THEN
C                 NO ICES PRESENT
```

```
                IF (ENTRY(I) .GT. MAT) THEN
                VLC=SAT(I)*(MAT/ENTRY(I))**(-1./B(I))
                ELSE
                        VLC=SAT(I)
                END IF
     ELSE
                        IF (ENTRY(I) .GT. MAT) THEN
          IF (SAT(I)-VIC(I) .LT. 0.13)     VIC(I)= SAT(I)-0.13
                            VLC=(SAT(I)-VIC(I))*(MAT/ENTRY(I))**(-1./B(I))
                ELSE
                VLC=SAT(I)-VIC(I)
                END IF

     END IF
     RETURN
C****
     ENTRY MATVL3 (I, MAT, VLC, DLDM, VIC, ICES)
C
C    DETERMINE THE DERIVATIVE OF THE MOISTURE CONTENT WITH RESPECT
C    TO MATRIC POTENTIAL
     IF (MAT .GT. ENTRY(I)) THEN
       DLDM=-VLC/B(I)/ENTRY(I)
      ELSE
       DLDM=-VLC/B(I)/MAT
     END IF
          RETURN
C****
     END
```

NB: The additional parameters VICDT and ICESDT were revised accordingly in the calling functions of the main program.

SPE
S602
:S
K33

2008